THE GEOLOGIC HISTORY OF MARS

James W. Head[1], Michael H. Carr[2], *[1]Department of Geological Sciences, Brown University, Providence, R.I. 02912 USA; 2U. S. Geological Survey, Menlo Park, CA 94025 USA. Contact: james_head@brown.edu.*

Introduction: Our current understanding of the geologic history of Mars (Fig. 1) provides insight into a number of outstanding questions that need to be addressed in future Mars exploration missions. Here we review the general themes in our current understanding of the geologic history of Mars [1] and identify a list of key questions that will help to guide future exploration planning.

Current Understanding of the Geologic History of Mars: Mars accumulated and differentiated into crust, mantle and core within a few tens of millions of years of Solar System formation. Formation of the Hellas basin, which has been adopted as the base of the Noachian period, is estimated to have occurred around 4.1 to 3.8 Gyr ago, depending on whether or not the planet experienced a late cataclysm. Little is known of the pre-Noachian period except that it was 1) characterized by a magnetic field, and 2) subject to numerous large basin-forming impacts, probably including one that formed the global dichotomy. The Noachian period, which ended around 3.7 Gyr ago, was characterized by high rates of cratering, erosion, and valley network formation. During the Noachain, most of the Tharsis rise (volumetrically) formed and surface conditions were at least episodically such as to cause widespread production of hydrous weathering products such as phyllosilicates. The precise environment of origin of the phyllosilicates (surface alteration by water, deep groundwater circulation, impact-energy related, all of the above?) is not well understood, however. Extensive sulfate deposits accumulated late in the era. Average erosion rates in the Noachian, though high compared with later epochs, fell short of the lowest average terrestrial rates. The record suggests that the warmer, wetter conditions necessary for fluvial activity were met only occasionally, such as might occur if caused by large impacts or volcanic eruptions.

At the end of the Noachian, rates of impact, valley formation, weathering, and erosion all dropped precipitously but volcanism continued at a relatively high average rate throughout the Hesperian, resulting in the resurfacing of at least 30% of the planet. Large water floods (the outflow channels) formed episodically, possibly leaving behind large bodies of water, perhaps even forming a sea or ocean in the northern lowlands lasting for an unknown duration. The major canyon system formed. The observations suggest that the change at the end of the Noachian suppressed most aqueous activity at the surface other than large floods, and resulted in growth of a thick cryosphere. However, the presence of discrete sulfate rich deposits, sulfate concentrations in soils, and the occasional presence of Hesperian valley networks indicate that water activity did not decline to zero.

After the end of the Hesperian around 3 Gyr ago the pace of geologic activity slowed further. The average rate of volcanism during the Amazonian was approximately a factor of ten lower than in the Hesperian and activity was confined largely to Tharsis and Elysium. The main era of water flooding was over, although small floods (such as at Cerberus Fossae) occurred episodically until geologically recent times. Canyon development was largely restricted to formation of large landslides. Erosion and weathering rates remained extremely low. The most distinctive characteristic of the Amazonian is formation of features that have been attributed to the presence, accumulation, and movement of ice. Included are the polar layered deposits, glacial deposits on volcanoes, ice-rich veneers at high latitudes, and a variety of landforms in the 30-550 latitude belts, including lo-bate debris aprons, lineated valley fill and concentric crater fill. Pedestal craters record the presence of thick mantles of mid-to high-latitude ice deposits at many times throughout the Amazonian. Most of the gullies on steep slopes also formed late in this era. The rate of formation of the ice-related features and the gullies probably varied as changes in obliquity affected ice stability relations. Collapse of the CO2 atmosphere may have occurred from time to time in the Amazonian. The current configuration of spinaxis/orbital parameters (and thus climate-related deposits) is almost certainly not typical of the Amazonian as a whole.

Lessons for Future Exploration: The advent of the international Mars exploration program during the last two decades has brought untold new knowledge of, and perspectives on, the geologic history of Mars. It has also raised important new questions [2], which form the basis of future research and mission planning. Among the outstanding questions are: What is the history of the magnetic field? What is the history of water on Mars, its total abundance, and its acquisition (accretion, degassing) and loss with time? What was the nature of the Noachian climate? Was it warm and wet, cold

*) All the abstracts are the original authors' versions

*and wet, or some combination that changed with time? Was Noachian valley network formation episodic or continuous? Were there oceans in the northern lowlands in the Noachian? What factors caused changes in the Noachian climate? Was there a late heavy bombardment and, if so, what were its consequences? How did the seemingly pervasive aqueous formation of Noachian crustal rocks occur and over what time scales? What caused the change in surface chemistry and water flux at the end of the Noachian? When did the major canyons of Valles Marineris form and how, and at what rate did they evolve? Are the sediments on the floor of the canyons Noachian, or later, in age, and how did they originate? Were there extensive lakes in the canyons and if so, how were they related to outflow channel formation? Were outflow channels catastrophic or episodic, and how much water and sediment were emplaced in the northern lowlands (ponds, lakes or seas)? What was the fate of the outflow channel effluent? What caused the change from phyllosilicate to sulfate deposits around the Noachian-Hesperian boundary? When did Mars become characterized by a global cryosphere and how much groundwater remains today in the subsurface? How has the thickness and latitudinal distribution of the cryosphere changed with time? What was the flux of volcanism during the Hesperian; was it a steady decline from the Noachian, or a peak related to the emplacement of Hesperian ridged plains? Why was volcanism centralized to the Tharsis and Elysium regions? What is the spin-axis/orbital parameter history of Mars and how has this controlled the distribution of volatiles in the surface and subsurface? Under what atmospheric and astronomical parameter conditions do tropical mountain glaciers, mid-latitude glaciers, and large circumpolar ice caps form and what do these deposits tell us about the climate history of Mars? What it the age of the current polar ice deposits and why do they apparently differ? What is the origin of the north polar basal unit? How long does it take to form the individual polar layers and what processes of deposition and sublimation are involved? Answering these fundamental questions requires the sophisticated, multidiscipline approach that is necessary for developing an in-depth understanding of the geologic history of Mars. Reaching this new understanding requires a robust future international Mars exploration program.

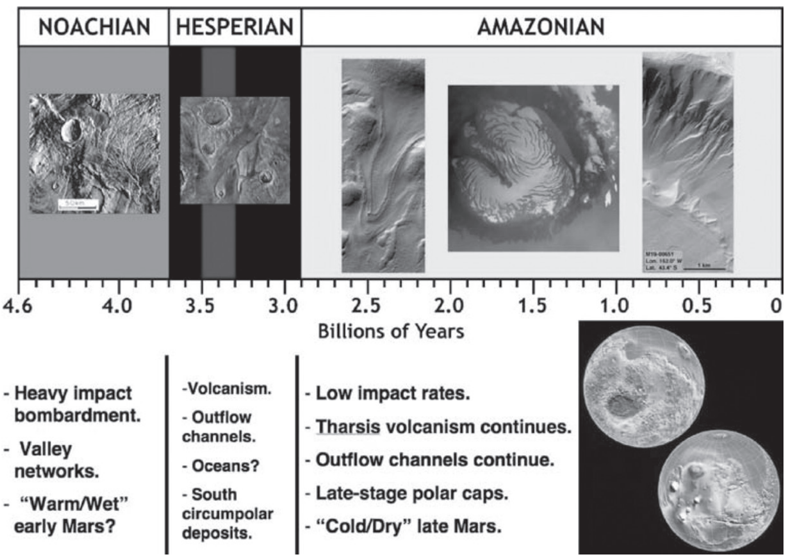

Fig. 1. Geologic history of Mars.

References: [1] Carr, M. H. and Head, J. W., 2010. Geologic history of Mars, Earth and Planetary Science Letters 294,185–203. [2] Head, J.W., 2007. The geology of Mars: New insights and outstanding questions, In: Chapman, M., (Ed), The Geology of Mars: Evidence from Earth-Based Analogs, Cambridge University Press, 2007, pp. 1-46.

EPISODICITY OF VOLCANIC AND FLUVIAL PROCESSES ON MARS

G. Neukum[1], A.T. Basilevsky[1,2], and the HRSC Team, *[1]Freie Universitaet Berlin, Malteserstr., 74-100, Haus D, 12249 Berlin Germany; [2]Vernadsky Institute, Kosygin Str., 19, 119991 Moscow, Russia. Contact: gerhard.neukum@fu-berlin.de*

We have investigated 12 typical regions on Mars (Figure 1) in detail with respect to their geologic evolution through time on the basis of detailed geologic mapping and determining age relationships through crater counting techniques using imagery.

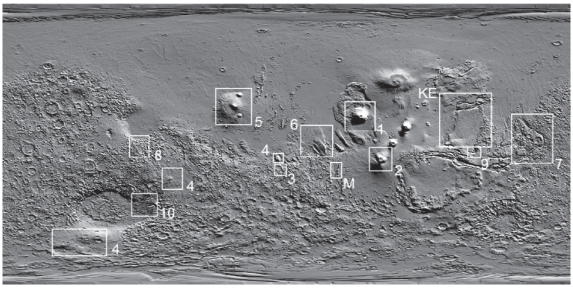

Fig. 1. Regions of this study.

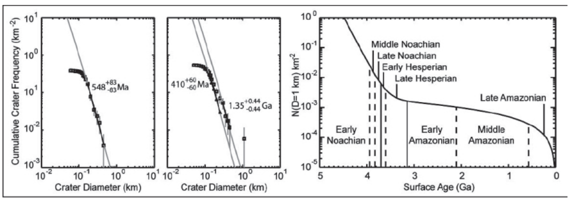

Fig. 2. Crater counting methodology

New data in combination with previously obtained data have been analyzed by way of a refined method of cratering age extraction that also gives fine details of periods of resurfacing (Figure 2).

We have found that there has been volcanic and fluvial/glacial geologic activity on the Martian surface at all times from >4 Ga ago until present. This activity shows episodic pulses in intensity of both volcanic and fluvial/glacial processes at ~3.8–3.3 Ga, 2.0–1.8 Ga, 1.6 to 1.2 Ga, ~800 to 300 m.y., ~200 m.y., and ~100 m.y., and a possible weaker phase around ~2.5–2.2 Ga ago (Figure 3). In between these episodes, there was relative quiescence of volcanic and/or fluvial/glacial activity. The episodes we find on the Martian surface in the crater frequency analyses of HRSC, MOC and THEMIS data coincide with some age groups of the Martian meteorites (~1.3 Ga, ~600–300 m.y., ~170 m.y.). It appears that the surface activity expressions and their episodicity are related to the interior evolution of the planet when convection in the asymptotic stationary state changes from the so-called stagnant-lid regime to an episodic behavior. Similarities in episodic behavior are found for the other terrestrial planets: Venus, the Earth's moon, and the Earth itself suggesting a common general relationship in the evolutionary tracks.

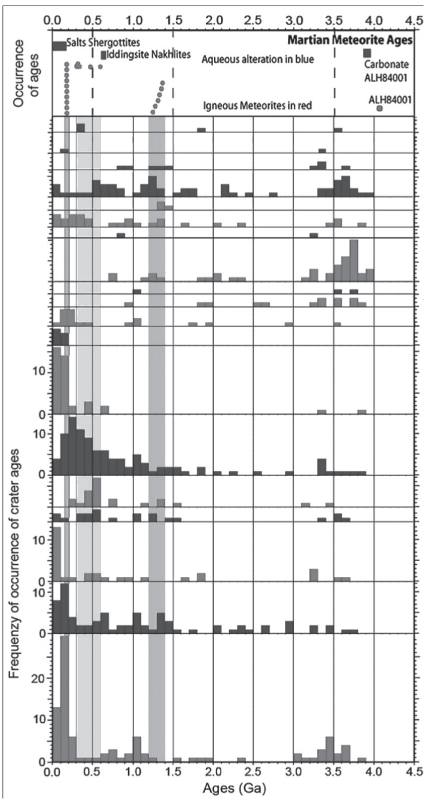

Fig. 3. Top – ages of Martian meteorites. Main part of the figure are crater age determinations of volcanic (red) and fluvial activities. 1 – Dao / Niger fluvial, 2 - Juventae Chasma fluvial, 3 - Libia Montes fluvial, 4 - Iani / Tiu / Ares fluvial, 5 – Medusae Fossae volcanic, 6 – Elysium volcanic, 7 – Highland paterae fluvial, 8 – Highland paterae volcanic, 9 – Gusev fluvial, 10 – Gusev volcanic, 11 – Arsia Mons volcanic, 12 – Olympus Mons fluvial, 13 – Olympus Mons volcanic, 14 – Mangala Valles fluvial, 15 – Mangala Valles volcanic, 16 - Echus fluvial, 17 – Echus volcanic, 18 – Kasei Valles region fluvial, 19 – Kasei Valles region volcanic. Numbers in this figure do not correspond numbers in Figure 1.

IMPACT CRATERING ON MARS

B. A. Ivanov, *Institute for Dynamics of Geospheres, RAS, 119334, Moscow, Russia. Contact: baivanov@idg.chph.ras.ru*

Introduction: Impact cratering on Mars is an important natural process created major landforms at the surface and, possibly, new minerals by shock heating and following hydrothermal activity in impact craters. Ongoing bombardment of Mars is now recorded instrumentally [1-7]. In the geological past larger impact craters played an important role of “hot spot” generators locally activated the volatile-bearing crust. Observations and their analysis and modeling allow us reveal more and more details of Martian geologic history.

“New” small impact craters: Repetitive imaging of Mars by various spacecraft revealed 20 potential “new” impact sites [1]: impact craters with documented time periods of formation, assuming that the appearances of dark spots correspond to crater formation. During the first ~6,000 orbits HiRISE was targeted to the same sites and confirmed 19 of these as pristine impact locations. By summer 2010 data from ~18,000 MRO orbits had been released and processed increasing the number of recognized “new” craters by a factor of 10. To date >140 new impact sites have been discovered (mostly by CTX) and confirmed by HiRISE imaged craters in the diameter range from 2.4 to 53 m. Within accuracy of formation date recognition the bombardment rate is almost constant in time with a possible slight variations from aphelion to perihelion in Mars orbital position ([6], predicted in [7]).

Clusters and Mars/Moon comparison. About 90 recognized to date new impacts formed multiple craters (pairs, triplets, clusters), proving that the considerable part of meteoroids are enough fragile to be fragmented in the tiny Martian atmosphere. In ~40 new impact sites we observe strewn fields of >10 individual craters. In 4 cases 500 to 3000 individual craters are recognized, In 6 cases strewn fields include >100 craters with D>2m. The presence of clustered impacts sufficiently changes the production function of size-frequency distribution (SFD) used to compare Martian and lunar crater chronology (Fig. 1).

The comparison of lunar and Martian cratering records in the comparable diameter range proves the approximate (factor of 3) correctness of earlier theoretical predictions [7, 8]. Further analysis will allow us to improve the Mars/Moon cratering rate ratio.

Shock wave footprints. In 3 cases of multiple impacts we see dark arcs (“scimitars”, “parabolas”,) as relatively narrow curved strips extended well beyond the halo area [5].

In these three cases we find parabolic features (exampled in Fig. 2) which may be treated as surface records of atmospheric shock wave interaction. To verify the idea the model of expanding hemispheric air shock waves is applied to find the theoretical curves of shock wave crossing. In all cases reasonably small (ms-range) assumed delay of smaller impacts vs. the main impact results in a good fit to observed “parabolic” geometry. In all cases smaller craters should be formed later than the main crater - in accord with the simple idea that smaller fragments are stronger decelerated after the

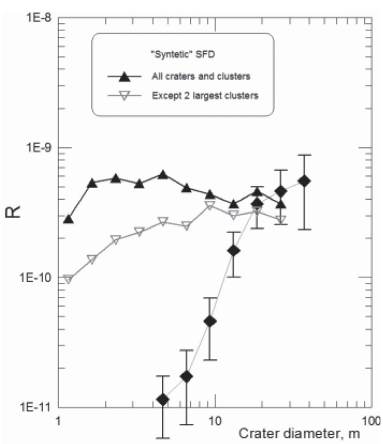

Fig. 1. R-plot of “new” craters (diamonds) based on their effective diameters $D_{eff}=(SD_i^3)^{1/3}$ for clusters in comparison with the size-frequency distribution of all individually recognizable craters (triangles). Black upward triangles are for all “new” impacts; open downward triangles show the R-plot after excluding the two most populated clusters.

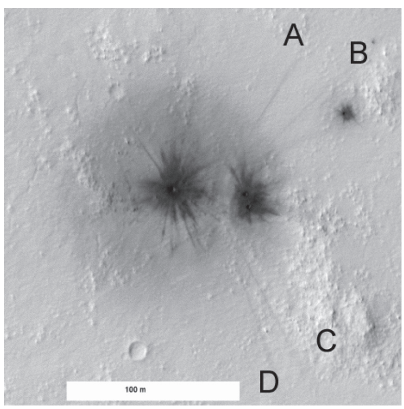

Fig. 2. PSP_008045_2020. Multiple impacts resulted from the projectile atmospheric breakup (D_{eff}*=5m,* totally 5 individual craters are visible). Parabolas A, B, C, and D extend ~100 m from the center. The most dark areas around individual craters are formrd by ejecta deposition. Less contrasting wide haloes extend ~60 crater radii.

breakup and reach surface a bit later. The direct modeling of atmospheric deceleration well fit the assumed time delay derived from the parabola geometry.

The physical mechanism of enhanced dust removing along shock wave intersection lines may include both the interference of positive/negative pressure phases in crossing shock fronts and the atmospheric vortex origin behind the crossing line.

These observations constrain the surface structure of Martian surface in dusted areas. The presence of wide dark haloes and shock wave–related arcs witness in favor of thin (few mm) bright dust cover which may be relatively easy removed by transient events.

Impact related hydrothermal activity: The recognition of water bearing minerals (phyllosilicates, serpentine deposits [9-11]) put forward the problem of low-temperature hydrothermal metamorphism. Too hot rocks in just formed impact craters, as speculated, can destroy some of these minerals. For this reason our analysis of impact cratering on Mars includes the numerical modeling of impact crater formation in H_20/rock mixture as a target. The model demanded the large volume of preparation work including development of 9-phase equation of state for H_20 (water +8 ices) [12]. Another technical problem is finding of pressure/temperature equilibrium between rock and H_20 in each mixed computational cell.

Numerical model results. Resulted modeling allows us to construct the initial conditions for the start of hydrothermal circulation just after the crater formation. For the beginning the model assumes H_20-filled porosity with 20 vol% at the surface exponentially decreased into depth and vanishing near 8 km depth [13]. Modeling shows that for relatively small craters (20 to 30 km in diameter) a lot of water is trapped in the central uplift. Being immediately vaporized from the surface, water at depths of ~1 km is in supercritical state due to lithostatic pressure (Fig. 3). Temperatures below H_20 critical temperature (~650K or ~380°C) are prevailed in the central uplift what looks as an evidence in favor of the following low-temperature hydrothermal circulation. The model data can be used as initial conditions for the further circulation modeling instead of recently published “home-made” quazi-analytical models [9, 14].

Super critical salt deposition. The formation of relatively hot water-bearing fragmented rocks in central peaks of impact craters (Fig. 3) demands the discussion about brine behavior at the start of hydrothermal circulation. The first portion of circulating H_20 is porous water, possibly brine, in the permeable crust uplifted by impact. In supercritical state solubility dramatically decreased resulting in fine particle formation and salt deposition (e.g. [15-17]). Hence removing of hot water from permeable central uplift may result in early salt deposition. Later circulation water may react with these early deposits and ambient rocks at lower temperatures. The idea should be tested in future when the accurate starting conditions will be included into hydrothermal circulation modeling.

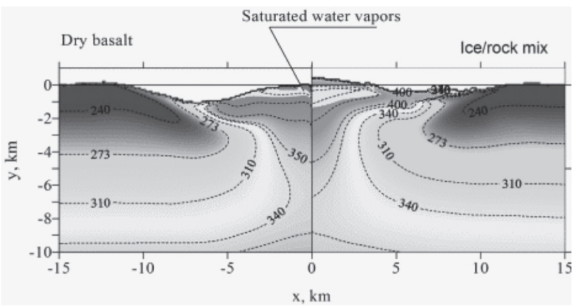

Fig. 3. Comparison of thermal field under just formed impact crater on Mars (D~25 km). Left panel shows isotherms (labeled in K) for dry basalt target. Right panel illustrates model cratering in ice/rock mixed target. Blue zones near the center have p-T conditions where H20 is in the form of saturated vapors below critical temperature of ~650K. Super-critical zone is located above.

Acknowledgements: The work is supported by PGG contract # NNX08AM21G. I am in debt to my permanent collaborators H.J. Melosh, A.S. McEwen, and B. Pierazzo for motivation and discussion. HiRISE and CTX scientific teams continue their marvelous work on the new Mars vision.

References: [1] Malin M.C. et al. (2006) Science, 314, 1573-1577. [2] Ivanov B.A., H.J. Melosh, and A.S. McEwen (2008) LPS XXXIX, Abstract #1402. [3] Ivanov B.A., H.J. Melosh, and A.S. McEwen (2008) 3d EPSC (Münster), Abstract #EPSC2008-A-00340. [4] Ivanov B.A., H.J. Melosh, and A.S. McEwen (2009) LPS XXXX, Abstract #1410. [5] Ivanov B.A., H.J. Melosh, and A.S. McEwen (2010) LPSC XXXXI, Abstract #2020. [6] Daubar, I.J. et al. (2010) LPSC XXXXI, Abstract #1978. [7] Ivanov, B.A. (2001) Space Sci. Rev., 96, 87-104. [8] Hartmann, W.K. (2005) Icarus, 174, 294-320. [9] Fairen, A.G. et al. (2010) Proc. Nat. Acad. Sci., 107 (27), 12095-12100. [10] Ehlmann, B.L. et al. (2009) JGR, 114, E00D08. [11] Ehlmann, B.L. et al. (2010) GRL, 37, 06201. [12] Ivanov B.A. (2005) LPSC XXXVI, Abstract #1232. [13] Clifford, S.M. (1993) JGR, 98, 10,973–11,016. [14] Barnhart, C.J., F. Nimmo, and B.J. Travis (2010) Icarus, 208, 101-117. [15] Petersen, R.C. (1986) J. Am.Chem. Soc. 108, 2100-2102. [16] Bermejo, M.D., and M.J. Cocero (2006) AIChE Journal, 52 (11), 3933-3951. [17] Furukawa, Y., H. et al. (2007) EPSL, 158, 543-549.

THE DISTRIBUTION OF ASH FROM ANCIENT EXPLOSIVE VOLCANOES ON MARS

L. Kerber[1], J.W. Head[1], J.B.Madeleine[2], L. Wilson[3], F. Forget[2] , *[1]Brown University Department of Geological Sciences. 324 Brook Street, Providence, RI 02912, [2]Laboratoire de Météorologie Dynamique du CNRS, Université Paris 6, Paris, [3]Lancaster Environment Centre, Lancaster University Lancaster LA1 4YQ, UK. Contact : Laura_Kerber@brown.edu.*

Introduction: Extensive friable layered deposits (FLDs) were identified in early images of Mars and are distinguished by their easily eroded surfaces, which form dunes, yardangs, and etched terrain. Fine-grained deposits include the equatorial Medusae Fossae Formation, the Electris deposits, and the Arabia deposits, as well as some deposits in Hellas and Argyre and layered and pitted deposits near the poles [1]. These deposits display a variety of morphologies and differ greatly in the cohesiveness and fineness of their layering. Many of the deposits appear to drape unconformably over topography, suggesting deposition by airfall [see 2]. Theories for the origins of these friable layered deposits include ancient reworked aeolian material, paleo-(and current) ice and dust deposits, ignimbrites, and ashfall [3-9]. The fine texture of the deposits and the ubiquitous presence of dust on Mars make the composition difficult to determine using spectral data. The deposits are easily eroded and moved by the wind, making them difficult to date accurately using craters [9].

In order to test the likelihood that these friable units are composed of volcanic ash, we combined a model for plinian eruptions into the Martian atmosphere [10] with a global circulation model (GCM) [11] in order to simulate the transport of the ash from the vent into the plume and finally to its emplacement on the surface. Simulations were run for major volcanoes using the modern martian atmosphere at present obliquity (Figs. 1-3). The vent elevation used for each volcano was the current volcano height, resulting in a range of resultant tephra fall-out heights, generally between 5 and 35 km. Erupted mass was distributed into six grain-size bins based on the theoretical grain-size distribution calculated by Wilson and Head [10]. Each simulation was run for one year followed by a half a year to allow particles to fall out of suspension. This was done to simulate the cumulative effect of many discrete eruptions over long periods of time.

Results: Powerful eruptions with high plumes or from eruptions from high altitude vents disperse material more widely (e.g., the Tharsis Montes, Fig. 2). Additionally, due to the strong seasonal westerly winds at the latitudes of the volcanoes, the bulk of the pyroclastic material erupted from a volcano would be emplaced to the east of its source. The dispersal of ash from Apollinaris Patera coincides well with the Medusae Fossae Formation [12], and ash from Syrtis Major could provide some material for the eastern Arabia Terra etched terrain [3,4], but there is no obvious volcanic source for fine-grained layered deposits near Meridiani Planum. Similar comparisons can be made between the simulated ash extents and the boundaries of the other FLDs to assess the probability that they are volcanic.

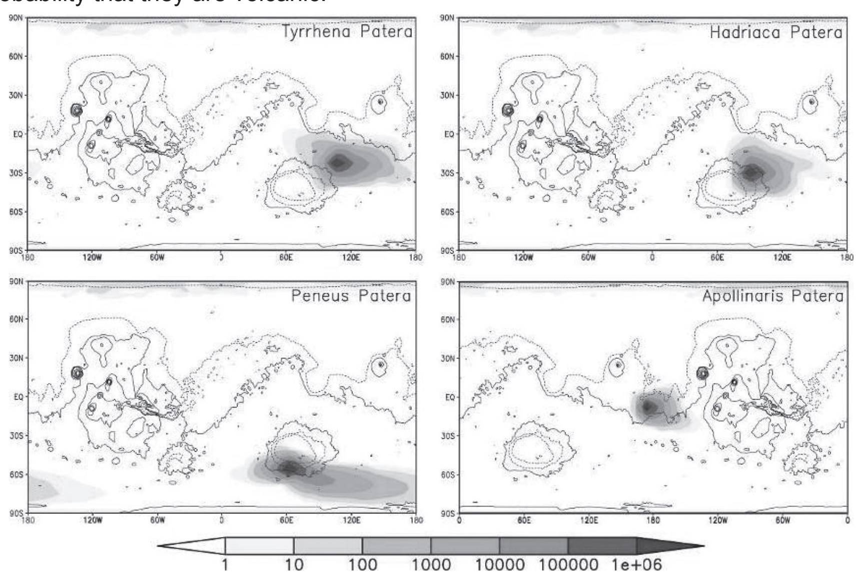

Figure 1. Ash distributions for highland paterae in kg/m2.

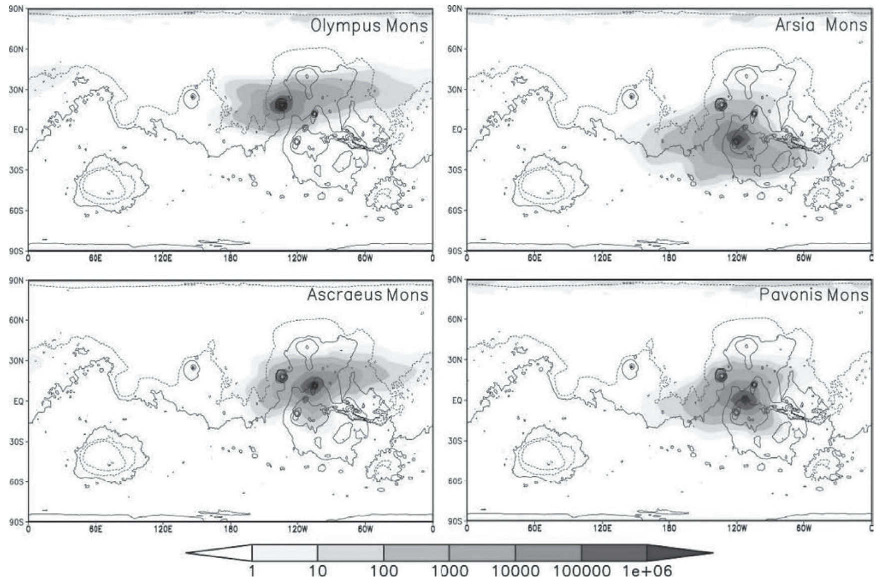

Figure 2. Ash distributions from the Tharsis volcanoes in kg/m2.

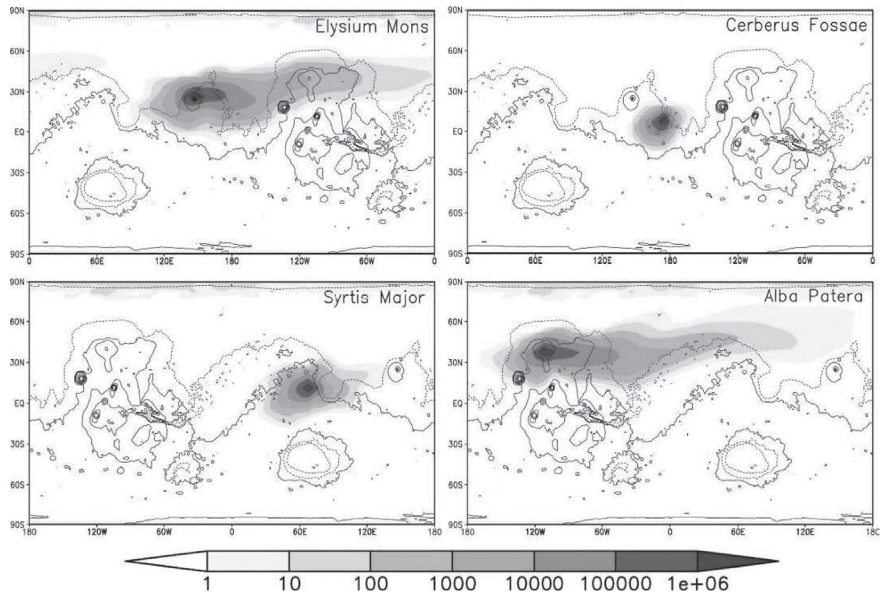

Figure 3. Ash distributions from other major volcanic centers on Mars in kg/m2.

References: [1] Tanaka K.L. (2000) Icarus 144, 254-266. [2] Sakimoto, S.E.H., et al. (1999) JGR 104, E10 24,141-22,154. [3] Greeley, R. and Guest J.E. (1987) USGS Map I-1802-B. [4] Scott D.H. and Tanaka K.L. (1986) USGS Map I-1802-A. [5] Scott D.H. and Tanaka K.L. (1982) JGR, 87, 1179–1190. [6] Bradley, B.A. et al. (2002) JGR 107, E8. [7] Hynek, B.M. et al. (2003) JGR 108, E9 5111. [8] Head J.W. and Kreslavsky M.A. (2004) LPSC XXXV, Abstract #1635. [9] Schultz, P.H. and A.B. Lutz (1988) Icarus 73, 91-141. [10] Wilson, L. and J.W. Head (2007) JVGR 163, 83-97 [11] Forget, F. et al. (1999) JGR 104, 24,155-24,176. [12] Kerber, L. et al., (2009) LPSC XL, Abstract 2176.

HEND: RESULTS AND NEW QUESTIONS AFTER 9 YEARS ON THE MARTIAN ORBIT

I. G. Mitrofanov, *Institute for Space Research, Profsojuznaja 84/32, 117997 Moscow, Russia. Contact: imitrofa@space.ru*

Introduction: High Energy Neutron Detector (HEND) arrived to Mars in October 25, 2001, onboard NASA's Mars Odyssey. Since that time, HEND successfully operates on the Martian orbit providing continuous data stream for neutron emission from the Mars surface. Analysis of this data has allowed to get new scientific results about the nature of Mars, and to understand new questions about the red planet, which should be studied in future. In this talk I will address to these subjects.

Five main results of HEND investigation: (1) HEND measured global distribution of water in the shallow subsurface of Mars, which manifested large content of water 10 – 60 wt% in the regolith above the latitudes of 60° at south and at north (Figure 1).

(2) HEND found two areas at equatorial latitudes with rather high content of water 7 – 10 wt% in the soil, Arabia and Medusae Fossae.

(3) HEND measured seasonal deposition of carbon dioxide over the high latitude surface around poles, and this data allowed to measure mass of these deposits at different latitudes.

(4) HEND determined neutron component of Martian radiation environment over the glob on the planet, which is important hazard factor for future manned missions to Mars.

(5) HEND measured large number of strong Solar Flares and Solar Particle Events (SPEs). This data allowed build the first interplanetary frame of observations of the active Sun from different directions.

Questions for addressing in future studies: (1) HEND, as long-living instrument on the Martian orbit, will allows to study the general picture of seasonal circulation and condensation of the Martian atmosphere. This data will allow to test the dynamic model of the atmosphere, and to test the possibility of slow trends of the Martian climate.

(2) Future measurements shall also address the question of presently existing global transport of water on the Mars. Several Martian years of observations will allow to test this question, and, if supported by data, to measure the quantity of water flux over the planet.

(3) Operating in parallel with another instruments in LEO (BTN on International Space System), on the Moon orbit (LEND on NASA's Lunar Reconnaissance Orbiter) and in the interplanetary space (MGNS on ESA's BepiColombo), HEND will provide data for "stereoscopic vision" of the active Sun during the incoming cycle of solar activity.

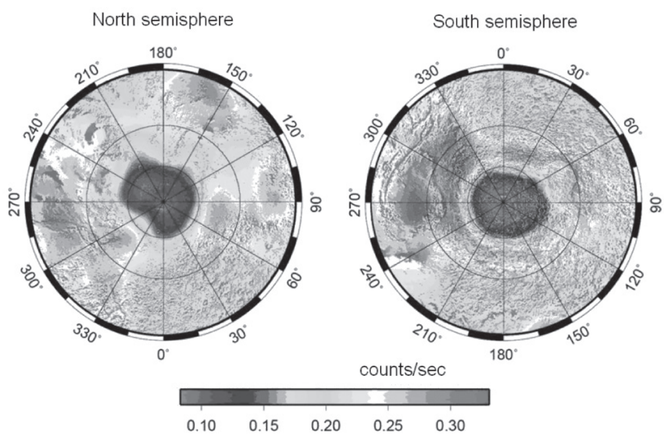

Fig. 1: Map of neutron emission from the Martian surface (in counts/sec). Blue color corresponds to high content of water > 5 wt%

MARS EXPRESS: MISSION STATUS REPORT AND SCIENTIFIC HIGHLIGHTS

O. Witasse[1], *[1]European Space Agency, Noordwijk, The Netherlands. Contact: owitasse @ rssd.esa.int*

Mars Express is the first European mission to orbit another planet in our Solar System. The spacecraft was launched on 2 June 2003 from the Baikonur Cosmodrome aboard a Soyuz-Fregat vehicle, for an originally approved mission of 2.5 years. In addition to global studies of the surface, subsurface, atmosphere and upper atmosphere of Mars at unprecedented spatial, spectral and temporal resolution, the unifying theme of the mission is the search for water in its various states everywhere on the planet. Dedicated flybys of Phobos are regularly planned, in order to gain new data on the mysterious moon. The overall impact of the mission has been (and still is) very high and is best illustrated by the number of articles (almost 500) published in international scientific journals.

The presentation will include a status report on the project, spacecraft and instruments performances. The status of the archive will also be discussed. Scientific highlights will be presented. A selection of scientific achievements is given below:

- The discovery of phyllosilicates by the OMEGA imaging spectrometer, in both hemispheres, indicates that long standing bodies of water formed early in the history of Mars. This allows the study of the past habitability of Mars. The relative abundance of liquid water on the surface through time, as well as its climate history, have been derived from the detection and mapping of alteration minerals.

- Methane has been detected by the PFS spectrometer, indicating that the planet is either biologically or geologically active.

- Tropical and equatorial glacial landforms have been identified by the high- resolution camera, as well as possible glaciers active just a few hundred thousand years ago.

- The MARSIS radar measurements tell us that the Polar Layered Deposits consist of nearly pure water ice. Maps of H_2O ice and CO_2 ice in the polar regions have been produced by OMEGA.

- Volcanism on Mars may have persisted until recent times (Olympus Mons caldera being only 100 Ma old) and could still be active near the North Pole. Several outbursts of volcanism may have occurred throughout Martian history.

- The solar wind penetrates deeper into the Martian atmosphere (down to 250 km) than previously thought, according to the ASPERA data. The current rate of escape of energetic ions is relatively low.

- The SPICAM spectrometer detected auroras, created by energetic electrons impacting the atmosphere over regions controlled by the crustal magnetic field.

- The existence of a transient ionospheric layer, due to meteors burning in the atmosphere, has been identified in radio-occultation data.

- Investigations at Phobos are very successful: as example, let us mention the sharpest images of Phobos ever acquired, the most accurate estimate of the mass, the detection of backscattered solar wind protons, and the computation of very precise ephemerids.

- Very high-altitude CO_2 clouds have been detected and are being studied by all atmospheric instruments.

- SPICAM discovered that the upper atmosphere density is controlled by dust content.

MARS: INTERNAL CONSTITUTION. ON HYDROGEN IN THE MARTIAN CORE

V. N. Zharkov[1], [1]*Institute of Physics of the Earth, B.Gruzinskaya 10 Moscow, Russia. Contact: zharkov@ifz.ru*

The idea of the origin of the terrestrial planets from planetesimals oxidized to varying degrees was discussed by Dreibus and Waenke (1989). The composition of the Earth and Mars is considered to be a certain mixture of component A and B.

Component A. This substance is highly reduced. Iron and all siderophile elements are in the metal state, and even silicon is partially metallic. Protobodies consisting of the A component filled the feeding zone of the forming Earth.

Component B. This substance is highly oxidized and contains all elements, including volatiles, with abundances like those in meteorites of class C1. Iron and all siderophile and lithophile elements are present mainly as oxides. Component B constituted the protobodies in the zone of the contemporary asteroidal belt.

Dreibus and Waenke (1989) concluded from their estimates of the bulk composition of Mars that component A and B are mixed in this planet in the ratio 60:40, whereas the ratio 85:15 was reported for the Earth. In was inferred that the accretion of Mars was almost homogeneous, in contrast to the chemically inhomogeneous accretion of the Earth.

At present, a commonly adopted opinion is that Jupiter was the first among the planets to be formed (Zharkov, 1993). Owing to a strong gravitational field, young Jupiter strewed the remaining protobodies from its feeding zone. These protobodies, as well as resonant interactions, destroyed the feeding zone of the planet, which could be formed in the asteroidal belt, and substantially reduced the number of protobodies in the feeding zone of growing Mars, thus slowing down its growth. As a result, Mars acquired a mass an order of magnitude smaller than could be attained without the influence of Jupiter. It is Jupiter's effect that is responsible for the two- component model of the formation of terrestrial planets.

In the planetary interior, the conditions for the dissolution of hydrogen in iron arise under high pressures and temperatures. The source of hydrogen is the reaction $Fe + H_2O \rightarrow FeO + H_2$.

As gas pressure grows, hydrogen starts dissolving in iron: $Fe + (x/2)H_2 \rightarrow FeH_x$.

The pressure at the center of Mars, according to the available models, is less than 450 kbar. Hydrogen dissolves in iron at relatively low pressures. Particularly, the molecular ratio H/Fe ≈ 0.2- 0.4 is attained near the melting point at pressures as small as several tens of kilobars, and the ratio H/Fe ≈ 1 is attained at moderate temperatures and pressures of ~70 kbar. The dissolution of hydrogen in iron reduces the density and appreciably lowers the melting point. We summarize the experimental data on the system Fe-S-H and advance arguments in favor of the presence of hydrogen in the core, estimate the influence of hydrogen on the physical parameters of the core.

The oxidized component B, mentioned at the beginning of the abstract, is assumed to have a composition equivalent to that of carbonaceous chondrites of class C1. The water content attains in such bodies ~7.3 wt %. Ahrens *et al.* (1989) studied in laboratory conditions the question as to what are the shock pressures at which the minerals containing volatiles (CO_2, H_2O, and SO_2) begin to lose them. They found that consolidated minerals start losing volatiles at shock pressures within the range 30-50 GPa. Such shock pressures are achievable when the impactor has a velocity of ~2-3 km/s, colliding with a target of the same material. Consequently, the dehydration of planetesimals that belong to component B begins when the radius of growing proto-Mars is $r \sim 0.4R$ and attains 75% at $r = R$ (R being the radius of Mars).

To estimate the mass of H_2 that can be buried in the interior of growing proto-Mars, we put r ≈ 0.5R and $\rho \approx 3.5 g/cm^3$. Then one easily obtains $\sim 2.4 \times 10^{23}$g of hydrogen. The mass of the iron-nickel (of $Fe_{0.9}Ni_{0.1}$) core comprises in model DW $\sim 1.2 \times 10^{26}$g. Therefore, if all the buried hydrogen ultimately becomes a constituent of the Martian core, we obtain the composition $(Fe_{0.9}Ni_{0.1})_{0.9}H_{0.1}$, where the subscripts mean molecular fractions. This estimate can be considered the lower bound for the hydrogen content in the Martian core. Under the assumption that component B has the same composition as C1 chondrites (~7.3 wt % of H_2O), we produced in the process of the accumulation of Mars is $\sim 2 \times 10^{24}$g of H_2. Thus, the upper bound for the hydrogen content in the iron core of Mars, not achievable in practice, is

$$\frac{N_{Fe}}{N_H} = \frac{1.2 \times 10^{26}}{56 \times 2 \times 10^{24}} \sim \frac{1.2}{1.12} \sim 1.07 \Rightarrow \mathrm{FeH}\cdot$$

The estimates given above were obtained with the data on water content of about 7.3 wt. % in C1 chondrites from the paper by Dreibus and Waenke (1989). If one takes into account recent estimates of water countent (Lodders and Fegley, 1998) the estimates of hydrogen content in the Martian core should be increased by a factor of 2.5-3. Then, the estimates of hydrogen in the core as $H_{0.5}$ and $H_{0.7}$ look quite reasonable. Zharkov(1996) found that addition of the molecular concentration x=0.1 of hydrogen to the iron core of Mars reduces its density by about 0.16 g/cm^3.

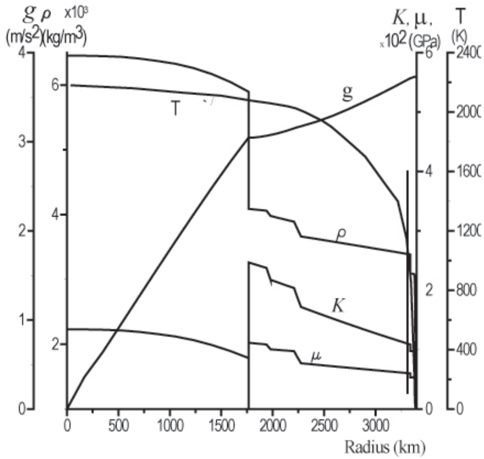

Fig.1

The distribution of density ρ, gravity g, temperature T, bulk modulus K and the rigidity μ as a function of radius through the planet for the trial M7-3 model.

Hydrogen and other possible admixtures (Ni, S) have also a considerable effect on reducing the melting point of the Martian iron core.

Coefficients determining the drop of the melting point of iron caused by the dissolution of admixture atoms in iron (Fukai, 1992)

Admixture atoms	Ni	H	S
$-\dfrac{dT_m}{dx}$, 10^3K	1	2	3

Table 1

Table 1 presents the estimated values of the derivatives $-\dfrac{dT_m}{dx}\times(10^3 K)$ and their molecular concentrations in the iron core of Mars. It is easy to estimate on the basis of these derivatives the possible drop of the melting point of iron under the conditions of the Martian core for the expected trial composition $Fe_{0.9}Ni_{0.1}S_{0.2}H_{0.5}$. We found it to be -$\Delta T_m$= (0.1+3×0.22+2×0.5)×10^{3}K ~ 1700K. In model DW, the molecular concentration of sulfur is equal to 0.22. This estimate implies that the Martian core in the liquid state and most likely have not the inner core. Also may suppose, that generation of a early magnetic field of Mars was by the cooling from the surface of the Martian core.

In the paper (Zharkov et al.,2009) have constructed a set of interior structure models. The models satisfying the moment of inertia and the elastic Love number k_2^s : the interval of values for the normalized mean moment of inertia I/MR_0^2 = 0.3647 – 0.3663 and the interval of the corresponding elastic Love numbers k_2^s= 0.148±0.009 (Konopliv et al.,2006), M is the mass of Mars, R_0 is the mean radius. The trial model of Mars is shown in the Figure. Its parameters are: the crustal density is 3g cm^{-3}, the crustal thickness is 70 km, the iron number of mantle's silicates Fe# = 22 (Fe# is the atomic ratio $Fe^{2+}/(Fe^{2++}$ Mg) multiplied by 100), the radius of core is 1766 km, the pressure at core-mantle boundary is 19.6 GPa, the bulk content of Fe in the planet is 27.3wt.%, I/MR_0^2 is 0.3658, k_2^s is 0.151, weight ratio Fe/Si is 1.71.

References: Ahrens, T.J., O'Keefe, J.D., Lange, M.A., 1989. Formation of atmospheres during accretion of the terrestrial planets. In: Attreya, S.K., Pollack, J.B., Matthews M.S.(Eds.). Origin and Evolution of Planetary and Satellite Atmospheres. Univ. Arizona Press, pp.328-385.

Dreibus G., Waenke, H., 1989. Supply and loss of volatile constituents during the accretion of terrestrial planels. L.S..,pp.268-288.

Fukai.Y., Some Properties of the Fe – H System at High Pressure and Temperatures, and Their Implications for the Earth's Core High-Pressure Research: Application to Earth and Planetary Sciences, Syono.Y. and Manhnani.M.H.,Eds.,Tokyo:Terra, Washington,D.C.: Am. Geophys. Union,1992,pp.373 – 385.

Konopliv,A.S., Yoder,C.F., Standish,E.M., Yuan,D.-N., Sjorgen,W.L., 2006. A global solution for Mars static and seasonal gravity, Mars orientation, Phobos and Deimos masses, and Mars ephemeris. Icarus 182, 23 – 50.

Zharkov,V.N., Gudkova,T.V., Molodensky,S.M. 2009. On models of Mars' interior and amplitudes of forced nutations. 1. The effects of deviation of Mars from its equilibrium state on the flattening of the core-mantle boundary. Phys. Earth Planet. Inter.172, 324 – 334.

Lodders, K., Fegley, B., 1998. The Planetary Scientist's Companion. Oxford University Press.

Zharkov, V.N.,1996. The internal structure of Mars: a key to understanding the origin of terrestrial planets. Solar Syst. Res. 30,456-465.

Zharkov, V.N., 1993. The role Jupiter in the formation of planets. Geophys. Monogr. 74, IUGG, Am.Geophys. Union 14, 7-17.

IMPORTANCE OF COORDINATED ORBITAL AND LANDED OBSERVATIONS FOR MARS SCIENCE

R. E. Arvidson, *Washington University in St. Louis, MO, USA.*
Contact: arvidson@wunder.wustl.edu

Introduction: This abstract focuses on examples from landed and orbital observations that show the synergy associated with coordinated observations and how joint analysis of the data sets allows us to better understand the nature and origin of the surface of Mars. Emphasis is placed on understanding aqueous processes.

Phoenix Lander: The Phoenix Lander touched down on the ejecta deposit of Heimdal crater just before the beginning of the northern hemisphere summer season and conducted observations with the Mars Reconnaissance Orbiter (MRO) through the late summer [1]. In fact the selection of the landing site was heavily influenced by the observations from Odyssey THEMIS and GRS/NS spectrometer data that predicted the depth to icy soil and by CTX and HiRISE data that allowed finding a landing site with an acceptably low abundance of rocks and relatively low slopes [2]. Icy soil was found at the depth pre-dicted from analysis of the orbital data [3], and ob-servations toward the end of the summer from orbit and Phoenix showed snowfall and water ice frost development [4].

Spirit Rover: Spirit has been exploring the Inner Basin in the Columbia Hills for much of its mission, including documenting the volcaniclastic deposits associated with Home Plate and associated sulfate and opaline silica deposits formed in aqueous envi-ronments [5] (Fig. 1). During a drive south Spirit drove onto the side of the ~8 m wide Scamander crater and became embedded in sulfate-rich sands. An extensive measurement campaign was imple-mented while analyses, tests, and simulations were underway to determine the best extrication proce-dures. The data show that Spirit excavated through sulfate enriched crusts within the crater and exposed deeper sulfate-rich sands (Fig. 2). These deposits are interpreted to have formed via aqueous processes while Home Plate was active. Subsequent downward translocation of the more soluble ferric sulfates are inferred to have occurred during later periods asso-ciated with solid-state green house warming under modest snow covers during periods of high spin axis obliquity. None of these aqueous deposits was de-tected from orbital data before Spirit's wheels unco-vered them. The lesson is that Mars is even more diverse and has an even richer history of aqueous processes than indicated from analysis of orbital data [6].

Opportunity Rover: Opportunity has traversed over 21km across ancient sabkha and aeolian sulfate deposits in Meridiani Planum, including detailed measurements in the ~800 m wide Victoria crater [7]. Coordinated observations between Opportunity, OMEGA on Mars Express and MRO CRISM, CTX, and HiRISE have been crucial to the development of a self-consistent model for the properties and origin of both bedrock and the ubiquitous aeolian ripples that cover much of the surface. Drive path planning over the ripples has depended heavily on HiRISE images to avoid large ripples with soft soils. CRISM data show that the bedrock is anhydrous, and when combined with Opportunity data, we now understand it is a consequence of a thin coating or dehydration rind dominated by iron oxides. Analysis of CRISM data for the rim of the Endeavour, a pre-sabkha cra-ter, shows the presence of phyllosilicates [8]. Hy-drated sulfate deposits are exposed in the sedimenta-ry deposits adjacent to the rim [8]. These results are being used to help define where on the rim Opportu-nity will make its "land fall" (Figs. 3-4).

References: [1]. Smith, P. et al. 2009. H_2O at the Phoenix Landing Site, *Science*, 3 July 2009, 325: 61-64 doi: 10.1126/science.1172768.
[2] Arvidson, R. E. et al. 2008. Phoenix Landing Site Selection and Characteristics, *J. Geophys. Res.*, 113, E00A03 doi: 10.10292077JE003021.
[3] Arvidson, R. E. et al. 2009. Results from the Mars Phoenix Lander Robotic Arm Experiment, *J. Geophys. Res.*, doi:10.1029/2009JE003408.
[4] Cull, S. et al. 2010. The Seasonal Ice Cycle at the Mars Phoe-nix Landing Site: II. Post-Landing CRISM and Ground Observa-tions, *J. Geophys. Res.*, doi: 10.1029/2009JE003410.
[5] Arvidson, R. E. et al. 2010. Spirit Mars Rover Mission: Overview and Selected Results from the Northern Home Plate Winter Haven to the Side of Scamander Crater, *J. Geophys. Res.* 2010je003633, in press.
[6] Murchie, S. L. et al. 2009. A Synthesis of Martian Aqueous Mineralogy After One Mars Year of Observations From the Mars Reconnaissance Orbiter, *J. Geophys. Res.*, 114, E00D06, doi: 10.1029/2009JE003342.
[7] Squyres, S. W, et al. 2009. Exploration of Victoria Crater by the Mars Rover Opportunity, *Science*, 324: 1058-1061, doi: 10.1126/science.1170355.
[8] Wray, J. J. et al. 2009. Phyllosilicates and sulfates at Endea-vour Crater, Mars, *Geophys. Res. Lett.*, 36, 21, doi: 10.1029/2009GL040734.

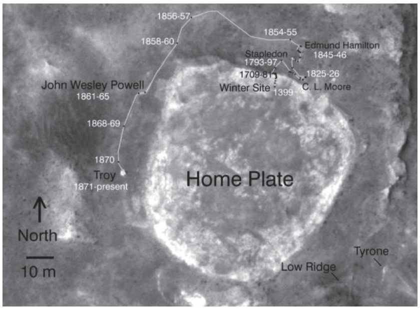

Fig. 1: HiRISE subframe showing Home Plate with sites and traverses overlain from the third win-ter campaign site on the northern slopes of Home Plate to embedding of Spirit at Troy. Times in sols for selected locations are shown, along with place names for areas highlighted in this paper. Spirit is the white feature located in Troy. The area called the sidewalk is located to the southeast of Spirit. Low Ridge is where Spirit spent its second winter. Sul-fate-bearing soils and opaline silica deposits were found by Spirit to surround Home Plate. HiRISE image ESP_0013499_1650_red.

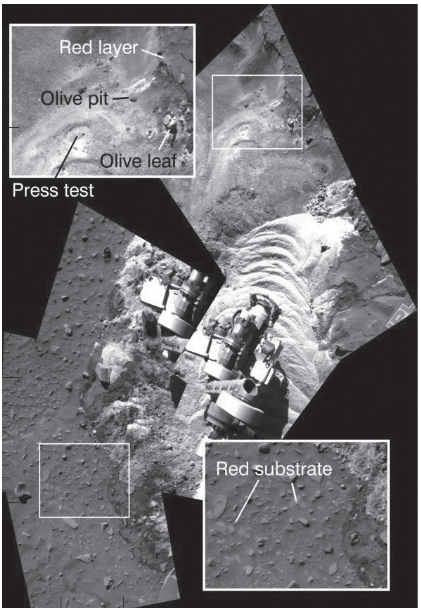

Fig. 2: Pancam false color mosaic from sols 2163 and 2177 showing Ulysses disturbed soils excavated during the last ten backwards extrication drives. Note “sand waves” excavated by the left front wheel. The brightness and color indicate that these newly exposed deposits are also sulfate-rich, providing further evidence that the floor of Scamander crater is underlain by these materials. The IDD instruments block part of the newly excavated soil exposures.

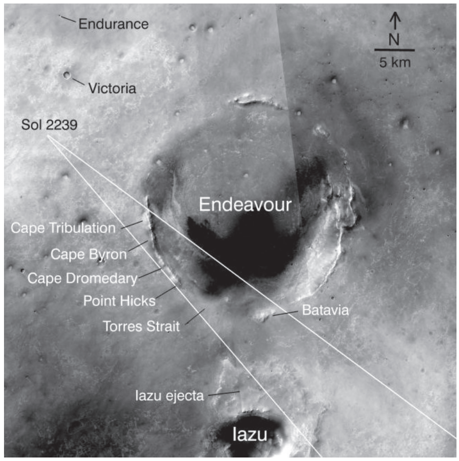

Fig. 3: MRO Context Imager mosaic showing the location of Opportunity on sol 2239 when Pancam was used to acquire a super resolution image of a portion of the Endeavour crater rim. Angular cover-age of the Pancam data is shown, along with rim segment names. CRISM data show that the rim ex-poses phyllosilicates and hydrated sulfate layered deposits are evident adjacent to the rim [8].

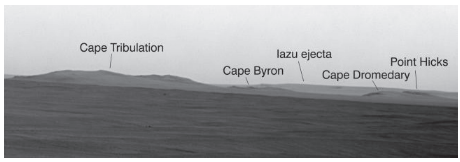

Fig. 4: Opportunity Pancam super resolution ob-servation of a portion of Endeavour’s rim acquired on sol 2239. Cape Tribulation, based on CRISM data, shows evidence for phyllosilicate exposures [8].

MÖSSBAUER MINERALOGY AT MERIDIANI PLANUM AND GUSEV CRATER: SUMMARY OF 6 YEARS OF OPERATIONS AND RECENT RESULTS FROM THE MER MÖSSBAUER SPECTROMETER

G. Klingelhöfer[1], R. Morris[2], B. Bernhardt[4], I. Fleischer[1], C. Schröder[4], D. Rodionov[1,5], M. Blumers[1], J. Maul[1], J. Girones Lopez[1], P. Lechner[6], L. Strüder[7], *[1]Institut für Anorganische und Analytische Chemie, Universität Mainz, Germany, [2]NASA/JSC, Houston, USA, [3]Eberhard Karls Universität, Tübingen,Germany, [4]von Hoerner&Sulger GmbH,Schwetzingen, Germany, [5]Space Research Institute IKI, Moscow, Russia; [6]PNSensor, München, Germany; [7]MPI für extraterrestrische Physik, Garching, Germany. Contact: klingel@mail.uni-mainz.de*

Introduction: The Miniaturized Mössbauer Spectrometer MIMOS II is part of the Athena science payload onboard NASA's twin Mars Exploration Rovers "Spirit" and "Opportunity". In January 2004, the first in situ extraterrestrial Mössbauer spectrum was received from the Martian surface [1,2]. At the present time (September 2010) both Mössbauer Spectrometers on board of MER rovers continue to collect scientific data. Both spectrometers are operational after more than 6 years of work. Acquired dataset approaches number of 500 for each rover.

Meridiani Planum. MER-B "Opportunity": Afte a long traverse of more than 8 km across the plains of Meridiani covered by sedimentary rock layers with jarosite and other sulfates, millimeter sized spherules made out of hematite, and basaltic sands, Opportunity arrived at Victoria crater spending nearly two years of its mission exploring this area. Victoria is an impact crater about 800 meters in diameter that lies roughly 5 km south of Opportunity's landing site (Eagle Crater). At Victoria, Opportunity traversed about 30% of the way around the crater, documenting eolian cross-stratification exposed in the crater walls, and then descended into the crater. Opportunity exited Victoria crater on sol 1634 of its mission, and began a long southward traverse toward Endeavour crater (large crater, approximately 20 km in diameter).

During its traverse, Opportunity encountered three "cobbles" found to be iron meteorites, named "Block Island". "Shelter Island" and "Mackinac Island". Another iron meteorite has been found in January 2005 (named "Heat Shield Rock") [3,4]. "Heat Shield Rock" and "Block Island" have been investigated in details (see [6]). Mössbauer spectra obtained on "Heat Shield Rock" and "Block Island" are dominated by iron-nickel phases, with contributions from schreibersite and/or cohenite. Another interesting target on Opportunity's traverse to Endurance crater was an -30 cm tall rock named "Marquette Island". The major iron-bearing minerals are olivine and pyroxene. Most of the total rock Fe is contained in olivine. A small amount of the total rock Fe is contained in nanophase ferric oxide (Fig.1). A Mössbauer magnetic sextet (e.g. magnetite, maghemite or hematite) has not been detected. "Marquette Island" is tentatively interpreted as an ejecta block from some distant crater.

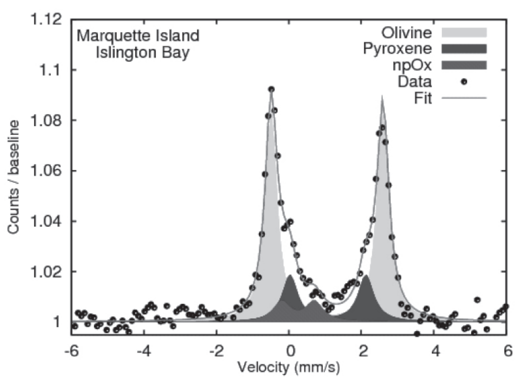

Fig.1. Mössbauer spectrum from the target Islington Bay (on Marquette Island). dominated by olivine with contributions from pyroxene and nanophase ferric oxide.

Gusev Crater. MER-A "Spirit": After exploring the planes of Gusev Crater which are dominated by basaltic rocks and soil not exhibiting significant weathering signatures, Spirit explored the Columbia Hills about 2 km away from the landing site. In the Columbia Hills the Mössbauer instrument identified Minerals like goethite (Fe-Hydroxid) which are mineralogical evidence for aqueous alteration processes in this area in the past. Also Spirit and its instruments detected clear evidence of hydrothermal processes active there in the past.

Recent Results – Carbonates in the Columbia Hills: Decades of speculation about a warmer, wetter Mars climate in the planet's first billion years call upon a denser CO_2-rich atmosphere than at present. Such an atmosphere should have led to the formation of outcrops rich in carbonate minerals, for which evidence has been sparse.

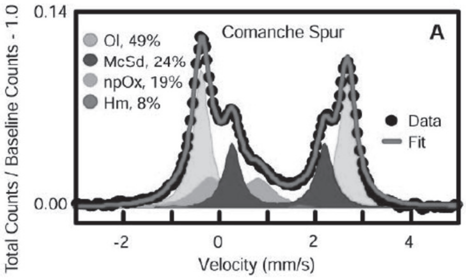

Fig. 2. Comanche Spur Mössbauer spectrum [composite of Horseback and Palomino targets. Ol = Fe^{2+} in olivine; McSd = Fe^{2+} in Mg-Fe carbonate; npOx = Fe^{3+} in nanophase ferric oxide; and Hm = Fe^{3+} in hematite (from [5]).

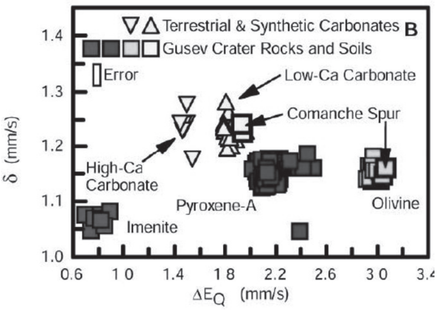

Fig. 3. Mössbauer doublet identification diagram showing Gusev crater rocks and soils and terrestrial and synthetic Fe-bearing carbonates (from [5]).

Using the Mars Exploration Rover (MER) Spirit, we have now identified outcrops rich in Mg-Fe carbonate (16 to 34 wt.%) in the Columbia Hills of Gusev crater. Its composition approximates the average composition of the carbonate globules in Martian meteorite ALH 84001. The Gusev carbonate probably precipitated from carbonatebearing solutions under hydrothermal conditions at near neutral pH in association with volcanic activity during the Noachian era [5].

MIMOS IIA with XRF capability: The new instrument MIMOS IIA originally developed for the ESA ExoMars mission (now 2018) will use newly designed Si-Drift detectors [7] with circular geometry (SDD) allowing high resolution X-ray fluorescence spectroscopy in parallel to Mössbauer measurements. The new detector system has been optimized for the special backscatter geometry of the miniaturized Mössbauer spectrometer. The ring is formed by four segments, each of them carrying 2 SDDs with integrated FET. The main goal of the new detector system design was to combine high energy resolution at high counting rates and large detector area while making maximum use of the area close to the collimator of the 57Co Mössbauer source. The active area per SDD segment is 2x45 mm^2.

The energy resolution at 5.9 keV is < 280 eV at room temperature and 131 eV FWHM at –40°C. This performance will increase the signal to noise ratio (SNR) and reduce the integration time of Mössbauer measurement by a factor of 10 (see also Fig. 5).

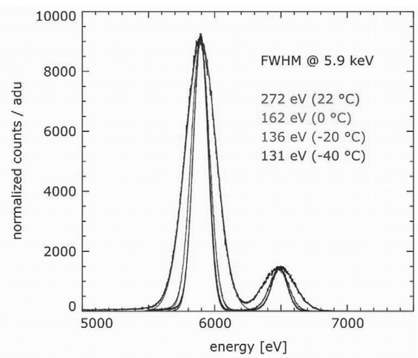

Fig. 4. Spectra of an Fe55 source recorded with the new SDD module [8].

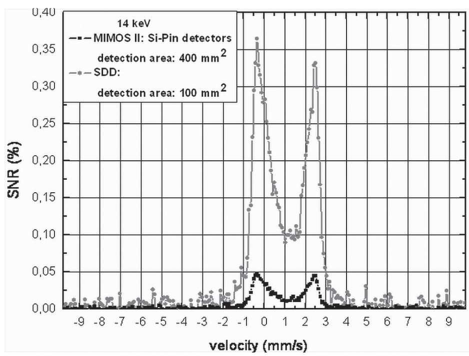

Fig. 5. Comparison of SNR of 14.41 keV backscatter Mössbauer spectra obtained with fully equipped MER instrument MIMOS II (black) and partially equipped MIMOS IIA instrument (only 1 detector segment; red) [8].

References: [1] Morris R.V. et al. (2004) Science, 305, 833-836 ;
[2] Klingelhoefer G. et al. (2004) Science 306, 1740-1745; [3] Fleischer et al., Meteoritics&Planet. Sci. (2010) submitted, [4] Schröder et al. (2008), JGR 113. E06S22; [5] Morris et al. (2010) Science, 329, 421-424; [6] Fleischer et al., this symposium.
[7] P. Lechner et al., Nucl. Instr. and Meth. A 377 (1996), 346-35. [8] M. Blumers et al., Nucl. Instr. and Meth. A (2010), doi: 10.1016/j.nima.2010.04.07

THUMBPRINT TERRAINS IN ISIDIS PLANITIA, MARS: CHARACTERISTICS AND MODES OF FORMATION

M.A. Ivanov[1,2], H. Hiesinger[2], F.J. Hielscher[2], G. Erkeling[2], and D. Reiss[2];
[1]Vernadsky Institute, RAS, Moscow, Russia, mikhail_ivanov@brown.edu; [2]Muenster Univ., Muenster, Germany.

Introduction: The floor of the Isidis basin is the largest region of thumbprint terrain (TPT) on Mars [1]. Currently, we are geologically mapping a broad region centered over Isidis Planitia (1-27°N - 75103°E, [2]). We conduct the mapping using all available image data from the coarse (THEMIS-IR) to the finest (HiRISE) resolution that allows integration of features of different scales into a self-consistent model of geologic history of the mapped region. Because TPT is one of the most intriguing landforms on Mars, which characterizes the majority of the Isidis floor, we apply our mapping results and observations to test a variety of models proposed for the formation of TPT.

Models of TPT formation: A review of models proposed for the formation of TPT reveals that they fall into four categories: (I) glacial, (II) deformational, (III) volcanic/volcano-glacial, and (IV) sedimentary/mud volcanism. The principal features of TPT that these models try to explain are either coned ridges or cones with central depression or individual cones.

Glacial models: Models of the first category consider features of TPT as pure glacial landforms related to either retreat of glacier [3-5] or its advance [1,6-11]. The main features that motivated these models are arcuate ridges of TPT that resemble, for example, moraines of the terrestrial glaciers. The cones that constitute most of the ridges of TPT drew less attention but in some models are considered as ice-cored mounds [4-6].

Deformational models: Another model consider ridges as the most important feature of TPT and explains them as remnants of huge mud flows that have formed a mud lake on the floor of Isidis Planitia [12]. The cones of the ridges are not considered in this model.

Volcanic models: Cones of TPT are the key features in the models of this category. They explain the cones as either pure volcanic features (e.g., cinder cones) [13] or as the result of interaction of hot magma/lava with water/ice-bearing materials. The later models consider two possibilities. (1) Heating from above due to superposition of hot lavas onto wet/icy sediments. This caused formation of pseudocraters and rootless cones [14-19]. The most important feature in these models is the similarity of the crater diameter/basal diameter ratio of pseudocraters in Iceland and the cones of TPT on Mars [16]. (2) The second possibility is the heating of wet/icy materials from below by magmatic intrusions [20-22], for example, by shallow sills from Syrtis Major [22]

Mud volcanism: Models of this category consider the cones of TPT but explain then as sedimentary or mud volcanoes instead of traditional volcanic features. The motivation of these models is the apparent lack of specific volcanic landforms other than the cones (clear volcanic constructs, lava flows, tubes, etc.) in the regions where TPT occurs. One group of these models proposes subsurface accumulations of gases (e.g., CO_2 in the form of gas-hydrates) as a driving agent of mud volcanism. Sudden release of gas may lead to explosive, CO_2 — driven eruptions [23-24]. The other group of mud volcanism models considers burial of wet/liquid sediments by thick layer of younger materials. The overburden pressure of the superposed materials causes eruption of the liquefied sediments from the deeper horizons [25-28].

Characteristic features of TPT in Isidis: TPT in Isidis Planitia displays several important features that are suggestive of the mode of origin of this terrain. (1) During geological mapping of the Isidis Planitia region, we defined a single unit of coned plains (HApc) that makes up the majority of the floor of Isidis Planitia [2]. In the mosaics of medium- to high-resolution images (THEMIS-vis, HRSC), a sharp contact outlines the unit of coned plains almost circumferentially. The cones and coned ridges (chains of cones) that define the TPT occur almost exclusively within the unit HApc. (2) Our crater counts within unit HApc display three ages, ~3.6, ~3.1, and ~1.8 Ga. (3) Isolated cones or short chains consisting of 2-3 coalesced cones represent the absolute majority of structures within the unit HApc [17,19,29]. Almost any cone displays a large summit depression but there is no evidence for flows of material emanating from the cones. (4) Isolated cones and small chains of cones preferentially populate the central region of the basin floor whereas longer chains of cones tend to occur at the periphery of the floor [18,29]. (5) In the very high-resolution HiRISE images, unit HApc consists of two major components: a) darker plains (basal unit) and b) lighter cones. Relatively small amounts of dune-forming sands cover both components. (6) Large and fresh impact craters on the floor of Isidis Planitia expose the deeper horizons that underlie the basal unit of the coned plains and, thus, TPT. These horizons appear as roughly layered rocks with specific spurand-gully pattern of erosion, which is typical of thick stacks of lava flows elsewhere on Mars. (7) Walls of small impact craters display interiors of the basal unit. Its upper portion represents a homogeneous mass of rocks and boulders (from the resolution limit and up to 10-15 m in diameter) that usually show no evidence for layering. (8) Some small impact craters expose contacts of the basal unit and the cones. Fine-grained (no rocks or boulders are seen at the highest HiRISE resolution, 26 cm/px) material of the cones superposes the basal unit. (9) The surface of the cones is typically peppered with small, rimless, rounded pits that are from a few meters to several tens of meters in diameter. The majority of the pits are rounded and almost circular but some of them (especially the largest) are angular and display a hummocky texture inside. The pits occur exclusively on the surface and walls of the cones and are absent within the surrounding basal unit.

Synthesis: The specific features of TPT permit us to constrain a rather wide range of models proposed for the formation of this terrain. First of all, the fact that the isolated cones and their smaller groups/chains are the predominant features of TPT in Isidis strongly favors the volcanic category of models of their formation, leaves little room for the glacial models, and is inconsistent with the deformational models. Fine-scale details of the cones further disfavor the glacial models of formation of TPT. In places where impact craters expose the interiors of cones, HiRISE images show that the basal unit does not underlie the entire cone, which would be expected if the cones represent ice-cored mounds, drop-moraines or other landforms left behind a retreating glacier. The fine-grained texture of the interiors of the cones is different from the rocky texture of the basal unit, which is poorly consistent with the variety of models explaining TPT as push moraines formed as a glacier advanced. Thus, the volcanic class of models (including mud volcanism) appears to be more likely for the formation of TPT in Isidis. Morphologic characteristics of the basal unit put additional constraints on the range of volcanic models. In all high-resolution images (HiRISE, CTX, MOC, HRSC, THEMIS-vis) available for the floor of the Isidis basin, there is no evidence for lava flows either on the surface or in the cross-sections (walls of impact craters) of the basal unit, which appears as a homogenous mass of rocks and boulders. This suggests that the basal unit was not emplaced as a sequence of lava flows and is not consistent with the requirements of the volcanic models considering formation of the cones of TPT as pseudocraters and/or rootless constructs due to heating of wet/icy sediments from above [e.g., 14].

The large crater diameter/basal diameter ratio for the cones, the apparently homogenous fine-grained texture of their bodies, and the lack of flows emanating from the cones collectively suggest that they likely formed due to explosive eruptions of fine-grained material rather than by effusive eruptions of lava. The lack of flows is, however, consistent with effusive mud volcanism because flows of mud could be more easily eroded after their emplacement.

The other feature that plays an important role in the assessment of the models of TPT formation is the presence of small rimless pits on the cones. The pits occur on their surface and are absent in the basal unit; some larger pits have angular shape. This strongly suggests a genetic link between the pits and cones and excludes an explanation of the pits as impact craters. The size of the pits (from a few meters up to tens of meters) is inconsistent with them to be voids of gas bubbles especially if the cones formed by explosive eruptions of disintegrated material. We propose that the pits represent marks of former pieces of ice delivered to the surface during (and due to) formation of the cones. This interpretation implies that the cones formed in cold environments and constrains the range of the models to the process of mud volcanism.

Conclusions: The results of our geological mapping of the region of Isidis Planitia have shown that TPT in this region forms a specific geologic unit that probably formed near the Hesperian/Amazonian boundary (~3 Ga). The main features of TPT in Isidis are small cones [17,19,29] of fine-grained material superposed on a roughly textured basal unit. The morphologic and morphometric characteristics of the cones are poorly consistent with the glacial models of their emplacement and suggest mud volcanism (effusive or explosive) as the principal mechanism of formation of the cones and, hence, TPT. A variety of processes may have been responsible for mobilization of material for mud volcanism [28] but the presence of volatile-rich sediments on the floor of the Isidis basin appears to be mandatory.

References: 1) Lockwood, J.F. et al., LPSC-23, 795, 1992; 2) Ivanov, M.A. et al., LPSC,-41, #1294, 2010; 3) Carr, M. H. and G. Schaber, JGR, 82., 4039, 1977; 4) Lucchitta, B.K., Icarus, 45, 264, 1981; 5) Rossbacher, L.A. and S. Judson, Icarus, 45, 39, 1981; 6) Guest, J.E. et al, JGR, 82, 4111, 1977; 7) Grizzaffi, P. and P. H. Schultz, Icarus, 77, 358, 1989; 8) Scott, D.H. and J.R. Underwood, PLPS, 21, 627, 1991; 9) Kargel, J.S. and R.G. Strom, Geology, 20, 3, 1992; 10) Kargel, J.S. et al., JGR, 100, 5351, 1995; 11) Pomerantz, W.J. and J.W. Head, LPSC-34, #1277, 2003; 12) Jons, H-P., LPSC-18, 470, 1987; 13) Plescia, J.B., NASA Tech. Mem., 82385, 263, 1980; 14) Frey, H, et al., JGR, 84, 8075, 1979; 15) Frey, H., and M. Jarosewich, JGR, 87, 9867, 1982; 16) Frey, H., LPSC-17, 239, 1986; 17) Rohkamp, D. et al., EPSC, #A00502, 2008; 18) Pithawala, T.M. and R.R. Ghent, LPSC-39, #1465, 2008a; 19) Hiesinger, H. et al., EGU, #EGU2009-7812, 2009; 20) Chapman, M.G., Icarus, 109, 393, 1994; 21) Bridges, J.C. et al., JGR, 108, 5001, 2003; 22) Pithawala, T.M. and R.R. Ghent, EPSC, #A00583, 2008b; 23) Hoffman, N. et al, LPSC-32, #1493, 2001; 24) Ori, G. et al., LPSC-32, #1539, 2001; 25) Davis, P.A. and K.L. Tanaka, LPSC26, 321, 1995; 26) Tanaka, K.L., JGR, 102, 4131, 1997; 27) Tanaka, K.L. et al., JGR, 108, 8043, 2003; 28) Skinner, J.A. and A. Mazzini, MPG, 26, 1866, 2009; 29) Hielscher, F.J.et al., LPSC-41, #2394, 2010.

SOME ASPECTS OF THE MARTIAN ATMOSPHERIC VARIATIONS AS SEEN FROM MARS6 ODYSSEY GRS

C. d'Uston[1], **O. Gasnault**[1], [1]*CESR, 9 Avenue du colonel Roche Toulouse, France. Contact: lionel.duston@CESR.fr*

Introduction: Mars Odyssey orbiter carried a gamma-ray spectrometer, GRS, to measure the intensities of gamma-ray lines produced by the chemical elements in the material of the Martian surface [1]. For some lines, the intensity depends on the GCR flux which trigger the cascade of nuclear reactions; for all lines, the gamma photons emitted at the Martian surface must propagate through the atmosphere to reach the instrument, and in this travel part of their flux is attenuated as a function of both atmospheric composition and thickness.

The measured intensities are very low and require long integration times for a reliable evaluation, typically of the order of a day. As the goal is to map these intensities across the surface of Mars in order to elaborate the maps of elemental abundances, this integration time is reached after several months of orbiting around Mars. During this period of time, several conditions may have varied particularly the intensity of the galactic cosmic rays which trigger the gamma emissions and the thickness of the atmosphere that follows the seasonal cycle [2].

Analysis of the observations: Here, we report on the variations which were found in the intensities of the recorded gamma-ray fluxes over more than one Martian year. Besides the works related to atmospheric variations already published by T. Prettyman on the variations of the CO2 frost thickness over the polar caps [3], and by A. Sprague on the Ar content of the atmosphere [4], two other characteristics of the recorded spectra are examined.

The first is the intensity of the K line which doesn't depend on the GCR flux so that its time variations are associated with the changes in atmospheric attenuation as shown in Figure 1; in this figure, the K line intensity at 1.4 MeV is measured in the mid latitude band during each Martian season, and the atmospheric transmission coefficient at that energy is derived from the Forget Mars Global Circulation Model (FGCM). It is seen that the two graphs show a very good correlation.

However, to follow the detail of this variation in the different regions of Mars, the intensity of the K line is not large enough when integrated over limited areas during each Martian season. This work takes advantage of the relatively large count rate in the continuum component of the recorded measurements; then the second approach to the monitoring of the atmospheric is the level of the continuum in the range from 0.2MeV to 0.3 MeV; in this part, the spectrum doesn't contain lines which could influence significantly the counting statistics.

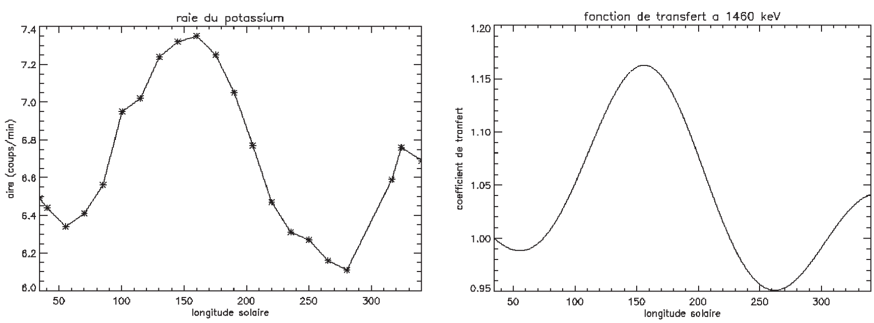

Fig. 1 : The top panel shows the evolution of the K line countrate as a function of solar longitude as recorded in the mid latitude band; the bottom panel shows the corresponding evolution of the transmission factor through the atmosphere for this line.

The measured continuum component is due to several contributions: some are locally produced in the spacecraft and in the instrument itself; some are due to the detection of charged particles and neutrons from different sources but are negligible in this energy range; a large part results partly from the scattering of the gamma as they propagate within the surface materials toward the surface and then through atmosphere

In a given region with a certain mineral condition composition, the changes in the production rate are due to possible variations of the galactic cosmic ray (GCR) flux), and to variations of the atmospheric characteristics. This is illustrated in figure 2 which covers ~1.5 Martian year; in this figure where several typical regions of Mars are examined, a general trend is the increase of the counting rates after Ls 200 which is related to the increase of the cosmic ray flux.

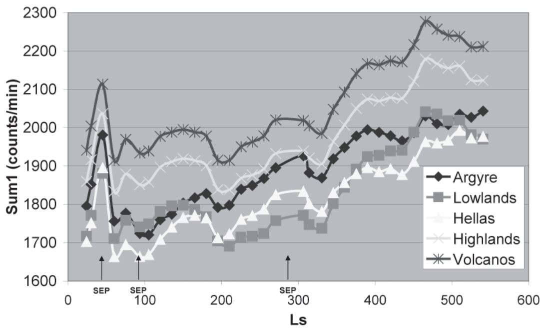

Fig. 2: Count-rate of the low energy continuum registered over different regions of Mars versus solar longitude.

In order to see the possible variations due to atmospheric seasonal changes, these observations have been normalized to the equatorial band observations, and are then presented compared to the equivalently normalized relative pressure variations predicted by the FGCM; this is illustrated in figure 3 for the Hellas basin region and for all the successive Martian years as a function of the solar longitude. It shows a remarkable anticorrelation that reproduces itself each year; this clearly corresponds to an atmospheric effect as the thicker the atmosphere the lower the intensity of recorded counts.

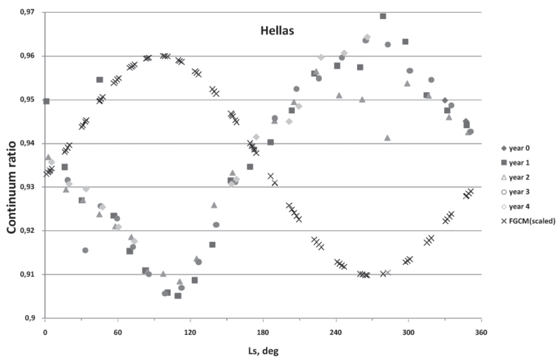

Fig. 3

This remarkable observation is made evident since the attenuation effects are more sensitive in the regions with thicker atmosphere like in Hellas basin or Argyre basin and in the northern lowlands; In the latter the phasing of this oscillating behaviorur is opposite as the relative variations in the north are opposed to those in the south. It is also observed that the amplitude of the count-rate variation is less in the elevated regions like over the volcanoes as the change of transparency is then much less, and there may be more influence of short term variations.

This work is ongoing and more quantitative study is now addressed to examine the possibility of providing measured effects to check the Martian GCM as they may become useful to predict regional conditions for future exploration missions.

References: [1] Boynton et al., (2004), Space Sci. Rev., 110, 37–83.

[2] Forget et al. Haberle, et al., J. Geophys. Res., 104(E4), 8957– 8974.
[3] Kelly et al., J. Geophys. Res. VOL. 111, E03S07, doi:10.1029/2006JE002678, 2006 [printed 112(E3), 2007]
[4] Sprague et al., J. Geophys. Res. VOL. 112, E03S02, doi:10.1029/2005JE002597, 2007

CLOUDS ON MARS: THEIR ROLE IN PAST AND CURRENT CLIMATE

F. Montmessin, *LATMOS/CNRS, 11 bd d'Alembert, 78280 Guyancourt, France. Contact:franck.montmessin@latmos.ipsl.frx*

Mars harbors a variety of cloudy phenomena resulting from the seasonal activity of water vapor and carbon dioxide in the atmosphere. Water ice clouds are mostly observed during two specific seasons: (i) during northern spring/summer in the equatorial region when Mars orbits near aphelion (as first identified by Clancy et al., 1996) and (ii) during fall and winter of both hemispheres favored by the cold temperature prevailing in these regions. Due to their relatively low coverage (10-15%) compared to terrestrial (60%) and Venusian (>95%) standards, water ice clouds have long been considered as a minor manifestation of Mars' climate. With growing understanding of the Mars water cycle, it has however come clearer that Mars clouds play a major role in regulating water migration about the planet. For instance, it has been acknowledged that cloud presence in the northern spring/summer imposes a prominent handedness on the annually averaged cross-equatorial flow of water, biasing budget towards a net accumulation in the north where the major surface reservoir of ices are observed. Similar cloud advection-related phenomena are known to affect water return towards the poles during fall/winter, eventually deciding of the mean atmospheric water content outside the polar regions. While the effect of water ice clouds on the radiative balance of the planet has not been evaluated yet on a global scale, it can be anticipated, considering the usual scheme of Cloud Radiative Forcing prevailing on the Earth, that Martian water ice clouds, being rather thin and elevated, will tend to warm the surface of Mars. In addition to water ice, ice clouds condensing out of the main atmospheric constituent, CO_2, are also known to form. Suspected to exist in the polar regions as thick, low-lying, probably convective layers, they have been just discovered in the equatorial mesosphere of Mars. Their influence on current Mars climate appear essentially tied to their seasonally modulating effect of the surface frost properties in the polar regions. However, when Mars possessed a denser atmosphere, the presence of such clouds may have been a major actor to raise surface temperatures to above the triple-point of water, providing conditions conducive for running liquid water.

MODERN CLIMATE AND HYDROLOGICAL CYCLE OF MARS

A.V.Rodin[1,2], A.A.Fedorova[2], N.A.Evdokimova, A.V.Burlakov, O.I.Korablev
[1]Moscow Institute of Physics and Technology, Russia; [2]Space Research Institute, Russia. Contact: Alexander.Rodin@phystech.edu

Introduction: More than decade of successful spacecraft exploration of Mars along with theoretical efforts have substantially changed our view on its modern climate. Continuous monitoring of atmospheric temperatures, water vapor, CO2 and H2O clouds and precipitation, dust loading in the atmosphere carried out in different spectral ranges from UV to far infrared, has provided a detailed picture of the Martian climate cycle. The discovery of widespread subsurface ice inventories and large amounts of bound water in the upper regolith layer actualized a long-discussed question on water exchange between the atmosphere and planet's solid surface. This exchange, as well as the distribution of tracers, including water vapor and ice, is in turn affected by the dynamical state of the atmosphere and radiative properties of aerosols. These processes have been studied interactively by means of a complex Mars climate model based on the GFDL's GCM.

Data sets: We considered data on IR spectral sounding of the Martian atmosphere, including results of the first systematic monitoring of the Mars water cycle performed by MAWD experiments onboard Viking orbiters[1], MGS/TES and Mars Express/SPICAM data; hyperspectral images in the visible to NIR spectral range provided by Mars Express/OMEGA experiment. We also refer to publications based on the results of MRO/CRISM and MCS experiments.

The model: General Circulation Model of the Martian atmosphere is based on GFDL's FMS dynamical core, working in sigma coordinates with horizontal resolution 1.2°´1°[2]. The model takes into account the Martian topography and surface thermal inertia, interactively includes dust and water ice cloud microphysics, aerosol optical properties, and water vapor diffusion in the regolith. Dust injection from the surface assumed to be due to dust devils parameterized by threshold value of thermal contrast between the surface and lower model layer. The intensity of suface dust sources is the only external parameter of the model, tuned so as dust opacity reached realistic values. The model has been run for more than 20 Martian years in order to equilibrate water cycle, and the results were side-by-side compared with observations.

Results: Modeling of the Martian water cycle reliably reproduces well known features, which evidently have the dynamical nature, such as the prominent tropical cloud belt forming in the aphelion season in the ascending branch of the Hadley cell and the winter tropical water vapor maximum that forms in the same latitudes during the South hemisphere summer.

At the same time, both models and observations demonstrate significant zonal modulation in water vapor concentration and location of clouds, with zonal wavenumbers changing from 1 to 3 according to season. Zonal variations correlating with those in the atmospheric water, have been observed in the seasonal frost deposits and the microphysical properties of persistent ice in the North polar cap. Moreover, symmetric zonal structure is found in the distribution of bound water in the upper regolith layer. Detailed modeling of hydrological processes points out that such modulation reflects changing wave structure of the zonal circulation that may be caused by barotropic instability in the circumpolar vortex[3]. As wave transport contributes to seasonal meridional migration of water, these finding suggest that the hydrological cycle of Mars is strongly linked with wave dynamics of the atmosphere. Dominated with essentially low wavenumbers due to the excessive static stability of dusty troposphere, this dynamics provides an interesting example of highly coherent atmospheric control over planetary climate.

Conclusions: GCM simulations suggest that atmospheric dynamics plays a critical role in the Martian hydrological cycle, with strong contribution of wave transport to the seasonal migration of water. Communication between the atmosphere and regolith takes place mainly in the form of ice condensation/sublimation rather than hydration/dehydration.

References: Fedorova A. A., Rodin A.V., Baklanova I.V.: MAWD observations revisited: seasonal behavior of water vapor in the Martian atmosphere. Icarus, Vol. 171, pp. 54-67, 2004
Wilson R.J., Banfield D., Conrath B.J., Smith M.D.: Traveling waves in the Northern Hemisphere of Mars. Geophysical Research Letters, Vol. 29, Issue 14, pp. 29-1, CiteID 1684, DOI 10.1029/2002GL014866, 2002.
Barbosa Aguiar A. C., Read P. L., Wordsworth R. D. et al. A laboratory model of Saturn' North polar Hexagon // Icarus. 2010. V. 206. P. 755-763.

The work has been supported by RFBR grant 10-02-01206-a.

THE INTERCONNECTED NATURE OF THE MARTIAN METHANE, ORGANICS, OXIDANTS, ISOTOPES, AND PROSPECTS FOR SAM/MSL

Sushil K. Atreya[1], Paul R. Mahaffy[2], *[1]Univ. of Michigan, Ann Arbor, MI 48109-2143 USA, [2]GSFC, Greenbelt, MD 20771 USA. Contact:atreya@umich.edu, paul.r.mahaffy@nasa.gov*

The only organic molecule ever reported to have been detected on Mars is methane [1, 2,3], in the atmosphere. No organics have yet been positively identified in the planet's surface, which seems puzzling considering the rain of exogenous organic material over eons even if Mars lacked indigenous organic material. Oxidants may be at work [4]. Two types of oxidants have been identified – peroxide and perchlorate. While the former can destroy organics directly and the simpler organic molecules such as methane indirectly by its products, superoxides, hydoperoxy and hydroxyl radicals [5], perchlorate is an inefficient oxidizer but could become potent following mineral processing in the surface, though less likely. The origin of methane on Mars is unknown. Current models predict either a geologic or biologic origin [6], but the current observations lack the needed information for discriminating between the two. The determination of methane and the organics on Mars, together with precision measurements of carbon isotopes is a key objective of the Sample Analysis at Mars Suite of instruments on the 2011 Mars Science Laboratory, Curiosity [7,8]. Life as we know it is deficient in heavy carbon, but the carbon isotopes provide only one constraint to the scenario of habitability of Mars. It is only through the measurement of many other related light isotopes, trace species, and the mineralogical and geological context that one can expect to understand the potential for life on Mars, now or in the past [6]. Many of these investigations are planned on the 2011 Mars Science Laboratory, and additional data are expected from future missions including the NASA-ESA 2016 Trace Gas Orbiter. [<http://www.umich.edu/~atreya> to download author's pdf's]

Bibliography: [1]Krasnopolsky, V.A., Maillard, J.P., Owen, T.C., 2004. Detection of methane in the Martian atmosphere: evidence for life? Icarus 172, 537-547.

[2]Formisano V. et al., 2004. Detection of Methane in the Atmosphere of Mars, Science, 306, 1758.

[3]Mumma M. et al., 2009. Strong Release of Methane on Mars in Northern Summer 2003, Science 323,1041.

[4]Oyama, V.I., Berdahl, B.J., Carle, G.C., 1977. Preliminary findings of Viking gas-exchange experiment and a model for Martian surface-chemistry. Nature 265 110-114.

[5]Atreya S.K. et al., 2006. Oxidant Enhancement in Martian Dust Devils and Storms: Implications for Life, and Habitability, Astrobiology 6, 439-450. [2]Delory G. et al., p451-460, ibid.

[6]Atreya S.K. et al., 2007. Methane and Related Trace Species on Mars: Origin, Loss, Implications for Life, and Habitability, Planet Space Sci., 55, 358-369.

[7] Mahaffy, P.R., 2009. Sample Analysis at Mars: Developing Analytical Tools to Search for a Habitable Environment on the Red Planet, Geochem. News 141, October issue.

[8]Webster, C.R., Mahaffy, P.R., 2010. Determining the local abundance of Martian methane and its $^{13}C/^{12}C$ and D/H isotopic ratios for comparison with related gas and soil analysis on the 2011 Mars Science Laboratory (MSL) Mission, Planet Space Sci., in press.

SUPRATHERMAL C, N, AND O ATOMS IN THE MARS UPPER ATMOSPHERE

V. I. Shematovich, *Institute of Astronomy RAS, 48 Pyatnitskaya str., 119017 Moscow, Russian Federation. Contact: shematov@inasan.ru*

Introduction: Solar forcing on the Martian upper atmosphere via both UV absorption and atmospheric sputtering results in the formation of an extended neutral corona populated by the suprathermal (hot) H, C, N, and O atoms (Nagy et al., 1990; Lammer and Bauer, 1991; Hodges 2000; Nagy et al., 2001; Chaufray et al., 2008; Valeille et al., 2009). The hot corona, in turn, is altered by the inflow of solar wind and local pick-up ions onto the Martian exobase which can affect the long-term evolution of the atmosphere (Johnson and Luhmann, 1998).

Modeling: The kinetics and transport of hot heavy — C, N, and O, — atoms in the transition region (from thermosphere to exosphere) of the Martian upper atmosphere are discussed. Reactions of dissociative recombination of the ionospheric ions CO_2^+, CO^+, O_2^+, and N_2^+ with thermal electrons in Martian ionosphere are the main photochemical sources of hot heavy atoms. The CO and N_2 dissociation processes are also the important sources of the suprathermal C and N atoms. Suprathermal atoms are formed in such exothermic photochemical reactions with an excess of kinetic energy up to a few eV and their energy is lost in the elastic and inelastic collisions with ambient thermal atmosphere gas. Detailed calculations of formation, collisional kinetics and transport of hot heavy atoms in transitional region (from thermosphere to exosphere) of upper atmosphere of Mars are presented. These calculations were conducted using the stochastic model of the hot planetary corona (Shematovich, 2004). Kinetic energy distribution functions of hot atoms were calculated using the differential cross sections for collisions of hot C, N, and O atoms with ambient atmosphere. For example, in the Figure 1 the calculated energy distribution functions of the suprathermal O atoms in the upper atmosphere of Mars at low solar activity level are shown (Krestyanikova and Shematovich 2005, 2006). It has been found that exosphere is populated by substantial amount of hot heavy atoms, mainly atomic oxygen, with kinetic energies less than escape energy 2 eV, i.e., hot extended corona is formed. Comparison with the previous models shows that the developed model is characterized by higher escape fluxes and higher abundances in the outer regions of the Martian upper atmosphere (Krestyanikova and Shematovich 2006).

Recent observations of the atomic hydrogen emission in the Ly-α line by the SPICAM instrument onboard Mars Express spacecraft show the presence of hot and thermal fractions of atomic hydrogen in the extended corona at Mars (Chaufray et al., 2008). Collisional coupling between light hydrogen and hot heavy atoms is considered in the given model as an important additional source of the suprathermal hydrogen atoms in the corona.

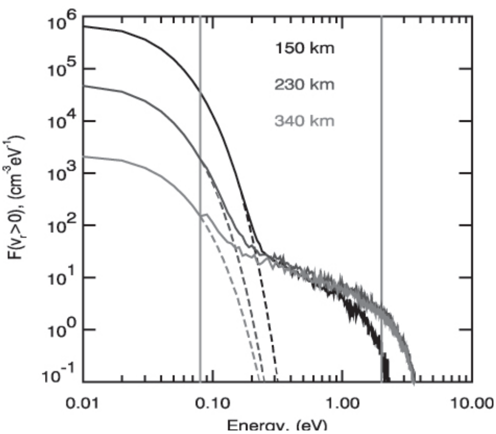

The suprathermal H, C, N, and O atoms are the important constituents of the extended neutral corona and should be taken into account in the space studies of the Martian environment. The input of exothermic photochemistry (with a dominant role of dissociative recombination of the molecular ions) into the water loss rate from Mars was estimated and its important role in the evolution of the Martian atmosphere is discussed.

This work is supported by the Russian Foundation for Basic Research projects No. 08-02-00263 and 09-02-91002-ANF.

References: Chaufray J.Y., Bertaux J.L., Leblanc F., Quemerais E., Icarus, 195, 598, 2008; Hodges R.R., J. Geophys. Res., 105, 6971, 2000; Johnson R.E. and Luhmann J.G., J. Geophys. Res. 103, 3649, 1998; Krestyanikova M.A. and Shematovich V.I., Solar System Res., 39, 22, 2005; Solar System Res. 40, 384, 2006; Lammer, H. and Bauer, S.J., Planet. Space Sci., 41, 1819, 1991; Nagy A.F., J. Kim, and T. E. Cravens T.E., Ann. Geophys., 8, 251, 1990; Nagy A.F., Lemon L.W., Fox J.L., and Kim J., J. Geophys. Res., 106, 21565, 2001; Shematovich V.I., Solar System Res., 38, 28, 2004; Valeille A. et al., J. Geophys. Res., 114, E11006, 2009

LOOKING FOR MARTIAN LIFE

L. V. Ksanfomality, *Space Research Institute, Russian Academy of Sciences, Profsoyuznaya ul. 84/32, Moscow, 117810 Russia*

The development of the concept that the Solar system is a representative planetary system in the Galaxy is a consequence of the fact that, before the 10th decade of the twentieth century, the Solar system remained the only known object of its kind with at least one habitable planet. As a result, studies of the evolution of the known planets produced a certain stereotype in theoretical investigations. The planet Mars was considered as the first candidate for possible search of life. This paper is focused on the study of the Martian physical conditions. The habitable planet should possess narrow intervals of many physical parameters that are required for the advent of amino-nucleic-acid form of life, its evolution and existence. Liquid water and temperature range are very important for them. Although the presence of liquid water on the Martian surface is usually thought to be impossible because of low pressures and low mean temperatures, there is sufficient number of lowlands on Mars where pressure exceeds the critical value required for the existence of liquid water. The extended narrow gullies on slopes with tributaries were formed, as it is supposed, by recent water streams that end with a thin stream, and disappear at the valley or crater floor. Photosynthesis is the only process that satisfies almost all the demands in energy of the Earth's biota. If the Martian life exists (or once existed), does it use the photosynthesis in its energy conversion? Are there any special restrictions?

PLASMA POPULATIONS IN THE TAIL OF INDUCED MAGNETOSPHERE

O.Vaisberg, *Space Research Institute, Profsoyuznaya 84/32, Moscow 117997, Russia. Contact: olegv@iki.rssi.ru*

Missions to Mars from 1970th Soviet orbiters to currently working Mars Express and Venus Express satellites of Mars and Venus provided important details on the structure and processes of induced magnetosphere. The magnetospheres of planets with dense atmospheres but without global magnetic fields are formed due to asymmetric mass loading of the solar wind flow in the vicinity of planet. The cavity in the solar wind flow is formed by solar wind magnetic flux tubes loaded with heavy planetary ions. This cavity forms almost impenetrable obstacle to the solar wind flow and causes formation of the bow shock. Solar wind plasma leaves loaded flux tubes along magnetic field direction. Planetary ions accelerated within dayside plasma-magnetic fill external part of the tail, forming ion population 1. Nightside ionosphere is the source of low energy flow in the tail, ion population 2. There are two accelerated populations: hot ion population in the central current sheet (population 3), and cold fast ion fluxes in the current sheets at the tail boundary (population 4). Observational characteristics of these populations and their origins are discussed.

MARTIAN PLASMA ENVIRONMENT. UNSOLVED QUESTIONS

E. Dubinin, *Max-Planck-Institute for Solar System Research, Katlenburg-Lindau, Germany*

Although Mars Global Surveyor and Mars Express have provided us with a wealth of in-situ and remote sensing data on the space environment at Mars, a lot of unresolved problems still remain. Among them are the existence of hot oxygen corona, physics of plasma boundaries (MPB, PEB, ionopause), polar wind and aurora on Mars, mini-magnetospheres and reconnection, origin of large-amplitude electromagnetic coherent structures et al. The presentation will focus on these open questions.

MODELS FOR MARS AND PHOBOS RADIATION ENVIRONMENTS

G. De Angelis[1], Ts. P. Dachev[2], J.V. Semkova[2], S. Maltchev[2], B. Tomov[2], Yu. Matviichuk[2], R. Koleva[2], V. Benghin[3], I. Chernykh[3], V. Shurshakov[3], V. Petrov[3], A. Zacharov[4], N. M. Khamidullina[5], Y. Uchihori[6], H. Kitamura[6], N. Yasuda[6] , *[1]ISS, Rome, Italy; [2]Solar-Terrestrial Influences Institute, Bulgarian Academy of Sci. (STIL-BAS), Sofia, Bulgaria; [3]Institute of Biomedical Problems, Russian Academy of Sci. (IMBP-RAS), Moscow, Russia; [3]Institute of Space Research, Russian Academy of Sci. (IKI-RAS), Moscow, Russia; [5]Lavochkin Association, Khimki, Moscow Region, Russia; [6]National Institute of Radiological Sciences, Chiba, Japan. Contact: gianni.deangelis@iol.it*

Introduction: The radiation protection is one of the two NASA highest concerns priorities [1]. In view of manned missions targeted to Mars [2], for which radiation exposure is one of the greatest challenges [3], it is fundamental to determine particle fluxes and doses at any time and at any location and elevation on and around Mars [4]. With this goal in mind, models of radiation environment induced by Galactic Cosmic Rays (GCR) and Solar Particle Events (SPE) on Mars and Phobos have been developed [5]. The work is described [6] as incoming cosmic ray [7-9] and solar events [5-6] primary particles rescaled for Mars conditions then transported through the atmosphere down to the surface. Models have been developed for the surface of the satellites Phobos, in the framework of the LIULIN-PHOBOS investigation that will be onboard the PHOBOS-GRUNT mission by RKA.

Physical Environments: The Mars atmosphere structure has been modeled in a time-dependent way [10-11], the atmospheric chemical and isotopic composition over results from Viking Landers [12-13]. The surface topography has been reconstructed with a model based on Mars Orbiter Laser Altimeter (MOLA) data at various scales [14]. Mars regolith has been modeled based on orbiter and lander spacecraft data from which an average composition has been derived [4-6]. The subsurface volatile inventory (e.g. CO_2 ice, H_2O ice), both in regolith and in the seasonal and perennial polar caps, has been modeled vs. location and time [15-16]. Models for both incoming GCR and SPE particles are those used in previous analyses as well as in NASA radiation analysis engineering applications, rescaled at Mars conditions [4-6]. Preliminary models have been developed for the surface of the Martian satellites Phobos. Models first developed for the Earth Moon [6,17-20] have been first adapted to the Phobos physical environment [21-23] then Mars-rescaled time-dependent primary particles fluxes [4-9] have been transported through. The lunar surface and subsurface has been modeled as regolith and bedrock, with structure and composition taken from the results of landers as well as from groundbased radiophysical measurements ([17-20]). After modifications, these lunar-like body surface models are used to develop models for the surfaces of Martian satellites Phobos [6]. This is the first model of the Phobos radiation environment, to be tested with the LIULIN-PHOBOS experiment. Particle transport computations were performed with a deterministic (HZETRN) code [24] adapted for planetary surfaces geometry and human body dose evaluations [4]. The results differ from those obtained with simplified models of the Martian atmosphere (single composition, single thickness, no time dependence) and with a regolith-only (no-volatiles) surface model [25]. Other results, obtained with GEANT-4 Monte Carlo code [26-27], also show doses lower than these.

References: [1] O'Keefe, S. (2002), http://www.spaceflightnow.com/news/n203/27okeefe

[2] Cucinotta F.A. et al. (2001) Radiat. Res., 156, 682-688. [3] Hoffman S. J. and Kaplan D. L. (1997) NASA SP-6107. [4] De Angelis G. et al. (2004) Adv. Space Res., 34, 1328-1332. [5] De Angelis G. et al. (2006) Radiat.Meas.., 41, 1097-1102. [6] De Angelis G. et al. (2007) Nucl.Phys. B, 166, 184-202. [7] Badhwar G. D. et al. (1994) Radiat. Res., 138, 201-208. [8] Badhwar G. D. and O'Neill P. M. (1996) Adv. Space Res., 17, 7-17. [9] Wilson J. W. et al. (1999) NASA TP-209369. [10] Justus C. G. and D. L. Johnson (2001) NASA TM-2001-210961. [11] Justus C. G. et al. (1996) NASA TM-108513. [12] Owen T. K. et al. (1977) JGR, 82, 4635-4639. [13] Levine J. S. (1985) The Photochemistry of Atmospheres, Academic Press, New York. [14] Smith D. E. et al. (1999) Science, 284, 1495-1503. [15] Christensen P. R. and Zurek R. K. (1984) JGR, 89, 4587-4596. [16] James P. B. et al. (1987) Icarus, 71, 298-305, 1987. [17] De Angelis G. et al. (2002) J. Radiat. Res., 43, 41-45. [18] De Angelis G. et al. (2002) Proc.Lunar Plan. Sci. Conf. XXXIII, pp. 1417-1418. [19] De Angelis G. et al. (2007) Nucl.Phys. B, 166, 169-183. [20] De Angelis G. et al. (2005) SAE-2005-01-2831, pp. 1-11. [21] Kuzmin R.O et al. (2003) Sol. Syst. Res., 37, 266-281. [22] Simonelli D.P et al. (1993) Icarus, 103, 49-61. [23] Simonelli D.P et al. (1998) Icarus, 131, 52-77. [24] Wilson J. W. et al. (1995) NASA TP-3495. [25] Saganti P. B. et al. (2004) Space Scie. Rev., 110, 143-156. [26] Dartnell L. et al. (2007) Biogeosciences, 4, 545-558. [27] Dartnell L. et al. (2007) Geophys. Res.Letters, 34, L02207.

THE INTERNAL STRUCTURE AND THE ORIGIN OF PHOBOS

P. Rosenblatt[1], A. Rivoldini[1], S. Le Maistre[1], V. Dehant[1], *[1]Royal Observatory of Belgium, Avenue Circulaire, 3, B-1180 Brussels, Belgium. Contact :rosenb@oma.be*

Introduction: Several past and present missions to Mars have provided new information regarding its moons, Phobos and Deimos, but the question about the origin of these two small bodies remains unanswered. The surface measurements and the tidal evolution of their orbital motion around Mars have led to contradictory scenarios about their origin: asteroid capture versus in situ formation scenarios. The Phobos-Grunt mission will address this open issue by revealing the true nature of Phobos' surface. This mission also offers the unique opportunity to probe the interior of this small body, therefore to reveal the true nature of its interior. The way to probe Phobos' interior consists in precisely estimating the three principal moments of inertia of the body from the precise measurements of geodetic observables: the amplitude of the forced libration (rotation rate variations in longitude) and of the second-order C_{20} and C_{22} coefficients of the gravity field. As the principal moments of inertia are related to the internal mass distribution, their precise estimation can be used to constrain models of Phobos' interior. In this paper, we present such models based on our current knowledge of the bulk density and of the forced libration of Phobos. We assume different sets of plausible constituent materials composing the interior of Phobos. Then, we seek the probability density function over the possible distribution of these materials in the volume of Phobos and the predicted range of values for the geodetic observables. We discuss the constraints on Phobos' interior structure, which can be brought by the current density and libration amplitude values as well as those, which could be added by the measurements of the gravity field coefficients.

Bulk density, porosity and origin of Phobos: The density of Phobos has been recently re-estimated with a high precision as 1876 +/- 20 kg/m^3 [1-2]. This low density is comparable to the density of many low-albedo carbonaceous asteroids. The density of these asteroids is lower than the density of their meteorite analogs, which can be explained by a large amount of porosity (or voids) in their interior [3]. The bulk porosity inside Phobos is computed by taking into account a large range of probable material analogue to Phobos' material. Indeed, recent Phobos' spectra collected by the CRISM/MRO [4] and OMEGA/MEX [5] cameras seem to indicate a subdued signature either of carbonaceous or of silicate components. We find a porosity range of 25% to 45% depending on the chosen analogue material (Fig. 1). This suggests a loosely consolidated or 'gravitational aggregate' structure for the interior of Phobos. Such internal structure is supported by the large impact crater Stickney. Indeed, large craters on small bodies would require a large porosity in their interior in order to absorb the energy of a large impact without destroying the body [6].

Such large porosity inside Phobos provides new constraints on the capture scenario. It has been shown that the tidal evolution of Phobos orbit is too slow to change an initial elliptical orbit in the ecliptic plane into its current near-circular orbit in Mars' equatorial plane [7]. The tidal evolution of the orbit of a highly porous body may be accelerated [8] but an unlikely tidal dissipation rate into Phobos would be required to account for its current orbit [7]. Moreover, a highly porous body is less resistant to the tidal torques exerted by Mars preventing it to orbit too close to Mars. Therefore, the initial elliptical orbit of such a body could not be circularized by the drag effect in the primitive Martian atmosphere as proposed by [9]. On another hand, the high porosity is in agreement with re-accretion of material blasted into Mars' orbit as proposed in [10]. As the largest debris bodies re-accrete they form a core of large boulders with large spaces of voids. The smaller debris re-accrete later, but do not fill the gaps left between the boulders [6]. This scenario depends, however, on a Phobos formed of material from Mars. An alternative scenario would imply an impact of an early moon in Mars orbit with an asteroid [11]. A large porosity inside Phobos is consistent with re-accretion early in its history, thus providing additional support for in situ formation models.

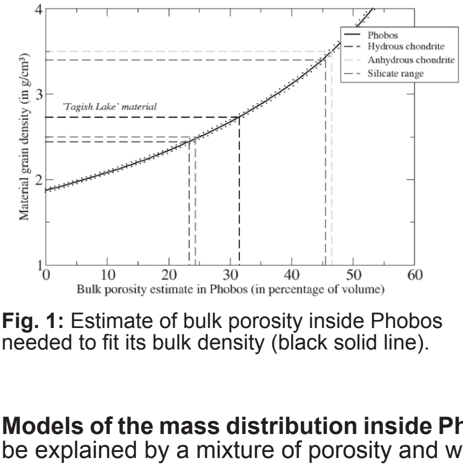

Fig. 1: Estimate of bulk porosity inside Phobos needed to fit its bulk density (black solid line).

Models of the mass distribution inside Phobos: The low density of Phobos can also be explained by a mixture of porosity and water ice [12-13]. However, the relative pro-

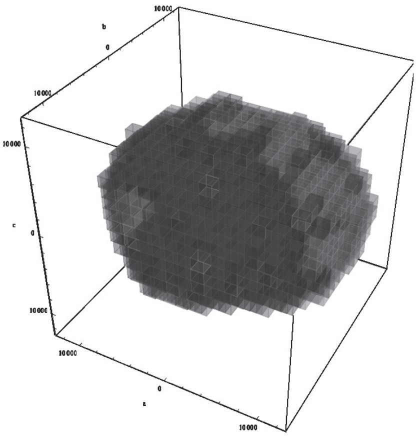

Fig. 2: Model of internal mass distribution, which fits the density and the libration amplitude of Phobos. The volume of the body has been discretized as cubes with assumed density of either a rock sample (red color), or porous-rock (green color) or water ice (blue color). See text for details.

portion of porosity and water ice cannot be determined from the average density alone. The forced libration has also been estimated as -1.24 +/- 0.15 degrees [14]. Although the error bar of this new value encompasses the value of -1.1 degrees expected from the Phobos shape with homogeneous internal mass distribution, it may indicate a heterogeneous mass distribution inside Phobos. In order to gain information about the interior structure of Phobos, we have built a model for the internal mass distribution. We have then used the average density and the libration amplitude of Phobos to infer a probability function over the interior mass distribution for different sets of plausible constituent materials.

We have developed models of Phobos' interior by discretizing its volume into 2626 cubes of equal volume (1300x1300x1300 m^3). Each cube can have the density of three kinds of material: 3100 kg/m3 for rock material, or 1350 kg/m^3 for porous-rock material or 940 kg/m^3 for water ice. The number of cubes of each density value has been fixed, given the measured density of Phobos and assuming a bulk porosity of 10%. The corresponding water ice content is 21% of the mass of Phobos. Given this number of cubes setting, we have determined the probability density functions of Phobos' principal moments of inertia and libration amplitude from a large set of random interior material distributions. As expected, the estimated values of the principal moments of inertia and libration amplitude are close to those of a homogeneous interior mass distribution (i.e. the cubes of different density are well mixed in the volume). However, the mean value of the estimated libration amplitude is different from the measured value, suggesting a Phobos interior mass distribution that deviates from homogeneous distribution. In order to allow for non homogeneous mass distribution inside Phobos, we have introduced in our models a smoothing parameter that, depending on its value, favours the accumulation of clusters of cubes of same density. Simulated sets of interior models show estimated libration values, which fit the observed value, for smoothing parameter values favoring clusters of intermediate size (Fig .2).

We have also considered sets of models with different porosity and water ice content in order to study our ability to better constrain Phobos' interior from its observed mass and libration amplitude values. We have considered smoothing parameter values favoring the formation of clusters of intermediate size and determined the probability density functions of interior mass distribution. The distribution of the estimated libration amplitude is very similar for different porosity values, showing that the observed libration amplitude alone cannot constrain the porosity inside Phobos. The mean value of the estimated C20 gravity field coefficient departs from the homogeneous value for larger porosity values, thus for lower water ice content, showing that a precise measurement of the gravity field of Phobos could provide additional constraints in its interior structure. In particular, the determination of the water ice content inside Phobos would provide a strong constraint on its origin. Indeed, water ice content is a key parameter for constraining the formation of solar system bodies and for the tidal evolution of the orbit of Phobos since water ice can significantly increase the tidal dissipation in its interior. The C_{20} coefficient could be obtained from the Mars Express Radio-Science experiment (MaRS) at very close flybys and the C_{22} coefficient from the radio-tracking data of the future Phobos-Grunt mission, due to launch in 2011, when it will co-orbit Phobos at a distance as close as 45 km. In addition, the Phobos-Grunt tracking data, when landed on Phobos' surface, could be used to improve the determination of the forced libration.

References: [1] Andert T.P. et al. (2010), Geophys. Res. Lett., 37(L09202). [2] Rosenblatt et al. (2010), EPSC2010, abstract #652. [3] Britt D.T. et al. (2002) in asteroids III, 485-500. [4] Murchie S.L. et al. (2008) LPSC, 39, Abstract #1434. [5] Gondet B. et al. (2008) LPSC, 39, Abstract #1832. [6] Richardson D.C. et al. (2002) in asteroids III, 501-515. [7] Mignard, F. (1981), Royal Astr. Soc. Mon. Not., 194, 365-379. [8] Goldreich P. and Sari R., Astrophys. J., 691, 54-60. [9] Sasaki, S. (1990), LPSC 21, 1069. [10] Craddock R.A. (1994), LPSC 25, 293. [11] Peale S.J. (2007), in treatise of geophysics, vol. 10, 465-508. [12] Murchie S. et al. (1991) J. Geophys. Res., 96, 5925-5945. [13] Avanesov G. et al. (1991) Planet. & Space Sci., 39, 281-295. [14] Willner K. et al. (2009), Earth Planet. Sci. Lett., in press.

A color version of this abstract can be found at: ftp://omaftp.oma.be/pub/astro/Rosenblatt.P/MS2010/

PHYSICAL LIBRATIONS OF PHOBOS: MODERN STATUS AND PERSPECTIVES

A. Gusev, *Kazan federal university, Kremlevskaya str, 18, Kazan, Russia. Contact: Alexander.Gusev@mail.ru*

Introduction: Phobos images show, that this skew field have the wrong form which can be approximately approximated an ellipsoid which sizes for a Phobos make 13,00 x 11,39 x 9,07 km (Willner et al, 2010), the major axis of an ellipsoid of the moon is directed to Mars, and it are rotated synchronously round Mars. A moon orbit practically circular with radius-vector 9.375 km. The orbital plane of the moon is close to an equatorial plane of Mars and is inclined under an angle of 240 to an ecliptic plane. A cycle time of a Phobos round of Mars is 7 h. 39 min.   Phobos is located well inside the corotation radius of 5.9 Martian radii, and Deimos is just outside this radius. The tides raised on Mars thus cause Phobos to be spiraling toward Mars and Deimos to be spiraling away. One of the most interesting characteristics of a Phobos are a physical librations.The Phobos has the big amplitude physical librations among known synchronously rotating a moons of planets of Solar system.

Modern status of Phobos librations: In the report will be presented the review of Phobos physical librations. We give the basic parameters of the Phobos's rotation and some scientific problems to be solved with the help of the scientific instruments installed on the spacecraft "Phobos-Grunt". Measurement of the Phobos's libration parameters will allow to study features of rotation of this insignificant body for definition of its internal structure and of its dissipation evolution in future. Yoder (1982) has calculated the dissipation in the Phobos accounting for both the tidal dissipation caused by the eccentric orbit and that caused by the forced libration of the very asymmetric satellite. This libration has an amplitude of 3.9° (Duxbury & Callahan 1981, Yoder 1982) and causes twice the tidal dissipation in Phobos that would occur if Phobos were nearly axially symmetric in the same eccentric orbit. Both the dissipation in Phobos and that in Mars from tides raised by Phobos damp the eccentricity. Even though Phobos is in a synchronous orbit around Mars, a free libration can be observed due to the varying angular speeds along an elliptical orbit. Phobos pronounced non-spherical body interacts with the gravitational field of Mars causing a large forced libration, a superimposed sinusoidal oscillation. Principal cause of it is that fact, that period of a free libration of this moon (~10 hour.) it is close to period of orbit rotation (~7,7 hour.). On exact measurements of amplitude of a libration it is possible to determine a Phobos moment of inertia that is important for mass distribution researches (interior structure) of Phobos. The free libration period could be better constrained by an estimate of dynamical ellipticity from a more accurate determination of the shape of Phobos along with an accurate measure of its physical libration amplitude.

Physical libration of Phobos: On average Phobos shows always the same face to Mars, with its axis of greatest inertia X directed towards the planet. Because the smallest moments of inertia of Phobos A and B are not equal, the moon is subjected to a restoring torque so that Phobos can theoretically freely oscillate around the direction of Mars (free physical libration in longitude). Really, because the orbit of Phobos around Mars is eccentric, the axis of greatest inertia of Phobos is forced to oscillate around the equilibrium position (forced physical libration in longitude). The plane XY of the equator of figure of Phobos almost coincides with its orbital plane. The axis of smallest inertia Z is forced to follow closely the pole of the orbit while maintaining a finite angle between the two axes (forced physical libration in latitude). In addition, the axis Z can oscillate freely around the equilibrium position (free physical librations in latitude). There are two latitudinal normal modes: Chandler-like free wobble and a free nutation of its spin axis relative to its mean position (Borderies & Yoder ,1990). Probably the free modes are small in amplitude to be detected by ranging to a lander. However, for the Moon these free modes have enough great values of amplitudes (3^2 x 8^2). For Phobos the forced librations in longitude may reach 100 to 300 m in rotational displacement and will be easily detectable with a 10 m ranging system of "Phobos-Grunt" mission. For describing of longitudinal physical libration of Phobos the parameter dynamical ellipticities $\alpha = (C-B)/A$; $\beta = (C-A)/B$; $\gamma = (B-A)/C$, where $A<B<C$ are three normalized principal moments of inertia (MOI), is very important. The predicted amplitude of physical libration (APL) is $\tau = 2e/[1-(1/3\gamma)]$ (Peale,1977), where e is the orbit eccentricity (0.015 for Phobos). Given the shape and the uniform density, MOI can be computed by direct integration. However, a simpler and more enlightening alternative is to use the gravitational coefficients: $B-A = 2\sqrt{5}\, C_{22}/\sqrt{3}$ and $C = (T-2\sqrt{5}\, C_{20})/3$, where $T = A+B+C$, in the principal axes. A numerical integration yields $T = 1.258$ (compared with 1.2 for a uniform spheres, which is the lower bound for a homogeneous body). Given the values of C_{20} and C_{22} it has been found $A = 0.355$, $B = 0.414$, $C = 0.489$ (compared with 0.4

for a uniform sphere). Substituting of MOI into g, it has been estimated γ = 0.12 and APL τ = 0.970 (Chao & Rubincam, 1989), within the rather large standard deviation of the observed value 0.78 ± 0.40 (Duxbury,1989). It must be pointed out that t is rather sensitive to the density distribution. A more accurate observation of a longitudinal and latitudinal physical librations amplitudes will provide useful constrains on the Phobos density profile.

Semi-numerical series for Phobos physical libration (Chapront-Touze, 1990) was computed by using three recent sets of Phobos inertial parameters. The importance of second order for arguments whose frequencies to the free libration frequencies is emphazed. Phobos figure give rise to a noticeable contribution to the mean motion of pericenter while contributions of Deimos' and Mars nutation to the mean motion of pericenter and node and contributation of Phobos figure to the mean motion of node are negligible. The largest periodic terms induced by Phobos' figure, by Deimos and by Mars' nutation amount respectively to about 800, 50, 30 meters, in rectangular coordinates. They are below the present level of accuracy of observations but must be taken into account in a precise theory in view of future space mission.

The main purpose of Borderies & Yoder (1990) research was a describing of model for nonlinear forced physical librations which includes all terms greater than 5 cm in amplitude. This theory is numerically evaluated using estimates of Phobos gravity field derived from Duxbery (1989) sixth degree and order, harmonic expansion model for its topography using 98 surface control points from Duxbury & Callahan (1989). The free latitude librations of Phobos are similar to free precession and free wobble.To lowest order, the free precession frequency is $2/3\beta n$ in an inertial frame while theapproximate wobble frequency is $2\sqrt{\alpha\beta}n$ in a body fixed frame, where n is mean motion of Phobos.

There exist several additional meter sized periodical librations in longitude. The latitude libration is dominated by the forced precession of Phobos figure axis with the precession of Phobos orbital plane. The relative obliquity of Phobos' z body axis relative to the orbit normal and other periodic signatures is small to usefully constrain a or b.

The last dynamical model of Phobos librations (Jacobson, 2010, AJ) included the figure acceleration due to a librating of Phobos; it determined the amplitude of the forced libration. Jacobson also took into account the secular acceleration of Phobos due to the tide that it raises on Mars and estimated the Martian tidal quality factor Q. In modeling the acceleration induced by the Phobos's figure, Jacobson assume that Phobos is in synchronous rotation with its pole normal to its orbit plane and its prime meridian librating about the sub-Mars direction (i.e., a libration in longitude); the libration in latitude is ignored. JPL planetary ephemeris DE421 (Folkner et al. 2008) provides the positions and GMs of the Sun, Moon, and planets. The Love number, gravity field, and orientation of Mars are from Konopliv et al. (2006). The Phobos quadrupole field gravitational harmonics (J_2 and C_{22}) in the figure acceleration are from Borderies &Yoder (1990)

For comparison purposes, Jacobson (2010) includes the libration amplitude observed optically from Viking 1 images by Duxbury & Callahan (1989) and the amplitude and periapsis rate from the analytical work of Borderies & Yoder (1990). Numerically integrated orbits take into account the effects of the Phobos quadrupole field, Phobos longitude libration, and the tide raised on Mars by Phobos. The author obtained estimates of the amplitude of the Phobos-forced libration angle and of the Martian tidal quality factor. The amplitude of physical librations (APL) is 1.03 +/- 0.220. For comparisons, by Chao & Rubincam (1989) for the APL gave 0.970; by Duxbury & Callahan (1989) the APL has 0.81+/- 0.50 and for Borderies & Yoder (1990) the APL is 1.190.

Subsequent studies of the residuals of the control points of Phobos (Willner et al, 2010), indicates: 1) moments of inertia along the principal axes are A = 0.3615, B = 0.4265, C = 0.5024 and the amplitude of 1.2° for the force libration. The observed amplitude differs slightly from the amplitude of 0.8 +/- 0.3° observed and computed by (Duxbury,1991), but is in well agreement with the amplitude of 1.2° derived from a topographic model (Borderies & Yoder,1990).

Perspectives. Essential improvements in our knowledge of Phobos orbit, shape, rotation, librations, and interior geochemical composion are expected, when a high-precision images and tracking data from spacecraft, captured in Phobos orbit, become possible (Phobos – Grunt project, 2011y). The importance of high-precision orbit determination for investigations in radio-science and planetary research, for example, such as physical librations, is well-known (Gusev, 2008). The interest in high-precision ILR to Mars is motivated by: i) studies of Martian interior – via the range's sensitivity to Mars precession, nutations, polar motion; ii) planetary science – via improvement of basic dynamical model parameters for the solar system; iii) tests of relativistic gravitation (Turyshev, 2010).

DYNAMICS OF GROOVE FORMATION ON PHOBOS BY EJECTA FROM STICKNEY CRATER: PREDICTIONS AND TESTS

James W. Head[1], Lionel Wilson[2], *[1]Department of Geological Sciences, Brown University, Providence, RI 02912 USA; [2]Environmental Sciences Division, Lancaster University, Lancaster LA14YQ, UK. Contact: james_head@brown.edu*

Summary: Numerous theories have been proposed for the formation of grooves on Phobos, and no single explanation is likely to account completely for the wide variety of morphologies and orientations observed. One set of grooves is geographically associated with the impact crater Stickney. As a possible explanation for the characteristics of this type of groove set, we test the hypothesis that these grooves were formed by ejecta clasts which left Stickney at velocities such that they were able to slide, roll, and/or bounce to distances comparable to observed groove lengths (of the order of one-quarter of the circumference of Phobos), partly crushing the regolith and partly pushing it aside as they moved. We show that this mechanism is physically possible and is consistent with the sizes, shapes, lengths, linearity and distribution of some of the grooves for plausible values of the material properties of both the regolith and the ejecta clasts. Because the escape velocity from Phobos varies by more than a factor of two over the surface of the satellite, it is possible for ejecta clasts to leave the surface again after generating grooves. We make predictions on the surface characteristics and distribution of such grooves and their deposits on the basis of this model and make predictions that can be compared with the model.

Discussion and Analysis: A variety of models have been proposed for the formation of the grooves and crater chains detected on Phobos including 1) original primary layering, 2) drag forces generated during capture of the satellite, 3) tidal distortion 4) impact fracturing, and 5) impact fracturing accompanied by degassing, or 6) impact fracturing accompanied by regolith drainage or 7) followed by regolith drainage, 8) ejecta emplacement and secondary cratering associated with the Stickney event, 9) ejecta from craters on Mars impacting Phobos, and 10) multiple origins.

Two factors caused us to reassess theories: 1) continuing analysis of high resolution images of linear tracks on the Moon formed by rolling and bouncing boulders has shown that these features show many similarities to grooves on Phobos; 2) continued study of the formation of impact craters on very small bodies such as asteroids and the satellites of Mars underlines the unusual and often counterintuitive nature of the cratering process and the resulting ejecta emplacement patterns. Ejection velocities associated with the vast majority of the material forming crater deposits on the Moon are sufficient to cause this material to exceed escape velocity on asteroids and Phobos and Deimos, and thus to leave the impacted body. The only ejecta remaining on the impacted body in these cases is likely to be the least shocked and latest material excavated at very low velocities (e.g., below escape velocity); ejecta from Stickney-sized craters on Phobos will look and behave much differently, with emphasis on the low-velocity emplacement of ejecta blocks, perhaps similar to the tracks from rolling and bouncing blocks observed on the Moon.

We explore the consequences of assuming that the grooves were formed by ejecta clasts with diameters of the order of 100 m which left Stickney at velocities such that they were able to roll or bounce to distances of the order of one quarter the circumference of Phobos, partly crushing the regolith and partly pushing it aside as they moved. Using basic soil mechanics relationships and estimates of regolith material properties, we calculated the range of sizes of the boulders that would be responsible for the observed grooves. We then considered the motions of clasts ejected from the 10 km diameter crater Stickney which just fail to reach escape velocity in the Phobos environment. We show that groove formation by these clasts is physically possible and that the sizes, shapes, lengths, linearity and distribution of some grooves are consistent with plausible values of the material properties of both the regolith and the ejecta clasts. We also show that there are several possibilities for the fate of these clasts. Some of the clasts will be abraded and diminished in size during their traverse before coming to rest. Because the escape velocity from Phobos varies by more than a factor of two over the surface of the satellite, it is also possible for some of the clasts to leave the surface again after generating grooves. The paths of all primary crater ejecta clasts produced on Phobos must be considered in terms of the total gravity field of both Phobos and Mars. We thus draw a distinction between super-orbital, orbital and suborbital ejecta.

Ejecta leaving the surface of Phobos at speeds greater than its escape velocity (3 to 8 m/s, depending on the position on the surface and the direction of launch) but less than the escape speed from the Mars system (a few km/s) are termed orbital. These clasts are potentially available to re-impact the Phobos surface at speeds similar to those at which they were launched and at elevations to the horizontal of order 45 degrees, thus producing craters with a wide range of sizes, some of which would not be distinguishable from primary impact craters. Ejecta leaving at even higher velocities (super-orbital ejecta) may be regarded as part of the general solar system meteoroid flux and neglected in terms of future impacts with Phobos. Sub-orbital clasts are those having an ejection velocity less than the escape velocity from PhoGROOVES ON PHOBOS: J. W. Head and L. Wilson bos alone. Such clasts are projected from near the edge of the crater cavity. They are excavated by stress waves having small stress amplitudes and stress gradients, and so will tend to be relatively coarse, relatively more coherent, and to be ejected at low speeds and at low elevation angles. There are expected to be very strong correlations between the sizes and the horizontal and vertical velocity components of such ejecta clasts.

For example, calculations show that clasts with sizes of the order of a few tens of meters may re-impact the surface at ranges of a few to 20 km. If such clasts disturb ten times their own mass of the surface on impact they may excavate secondary features up to 100 m in size. The peak stress induced in such an impacting clast will be of order 0.1 bar, and it will not survive the re-impact intact unless its strength is greater than this value. Most consolidated silicate rocks have strengths in the range of tens to a hundred bars and are thus likely to survive reimpact. If an ejecta clast does survive, it may continue on an escape path if the re-impact is at a grazing angle and the local escape velocity at the point of first contact is less than that at the initial launch point. Alternatively, it may lose enough energy to cause it to follow a non-escape path subsequently, thus bouncing one or more times. The number of bounces, the spacing between the contacts, and the ultimate fate of the ejecta clast again depend critically on the elastic properties of the ejecta clast and the surface (which, depending on the size of the clast, may effectively be an assemblage of relatively small regolith particles, a mixture of clast sizes approaching that of the impacting clast, or another single clast supported by a regolith matrix). Of even more interest are sub-orbital ejecta clasts leaving the crater cavity at speeds of 3 to 8 m/s (i.e., just below, or essentially at, the local escape velocity) and at elevation angles close to zero. These clasts will travel out of the crater, over the crater rim crest and onto the crater rim in the terminal stages of the cratering event and may slide, roll, or bounce along the surface, producing a groove-like disturbance of the pre-existing surface with a width smaller than, or similar to, their own diameter.

Summary of Predictions and Tests from the Analysis: To provide a basis for comparison with new data from spacecraft missions we summarize the predictions and tests from our model. 1) General distribution of ejecta: The low gravity and escape velocity of Phobos mean that the vast majority of ejecta clasts will leave the satellite; remaining fragments will have undergone the least amount of impact-related stress and will be preferentially the largest clasts involved in the cratering process. 2) Block excavation and the crater interior: These last blocks leaving the crater interior will not only be relatively large but will also depart at low velocities and low elevation angles. Many of them are likely to be dislodged from the crater floor in the final stages of the event and spread outward from the crater interior up the walls and out over the rim. Depending on their point of origin, these boulders could easily form tracks in the crater interior, continuing up the crater wall and out over the rim. 3) Morphology and structure of the grooves: Groove widths: The widths of grooves should be comparable to the size range of blocks shown to be capable of producing grooves on Phobos by this mechanism. The radii of the ejecta clasts required to produce grooves 100 m wide would lie in the range ~80 to 140 m, with larger grooves requiring proportionally larger clasts. Groove width-to-depth ratios: Consideration of the vertical forces acting on clasts shows that groove-like depressions with depth-to-width ratios in the range 0.05 to 0.17 are expected if the regolith cohesive strength is similar to or, more likely, a factor of 10 smaller than, that of the lunar regolith. Groove lengths: Ejecta clasts with radii in excess of ~100 m launched at speeds in the range 3 to 6 m/s are able to travel to distances of 10 to 30 km even if the regolith strength is near the upper end of the range implied by the groove shapes and is thus comparable with the strength of the lunar regolith. Groove morphology: Rolling and bouncing boulders could produce linear grooves (if the boulder is relatively rounded and rolling), chains of isolated craters (if the boulder is bouncing and leaving the ground between bounces), chains of connected craters (if the boulder is bouncing and not leaving the ground between bounces), or linear grooves with associated pits (if the boulder is rolling and bouncing and not leaving the surface). Change in groove morphology with distance: Monotonic decrease in velocity of rolling boulders, and any change in the size and morphology of the boulder will result in variations in groove morphology with range. In addition, when allowance is made for the influence of the non-spherical shape of Phobos on the motion of ejecta clasts, it is found that the speed of a clast may increase again after an initial decrease. These factors should result in changes of morphology along groove paths, as gravity, velocity and local topography vary. In addition, since the escape velocity from Phobos varies by more than a factor of two over the surface, this allows the possibility of ejecta clasts leaving the surface even after they have already generated grooves 10 to 20 km long. In this latter case, a change in morphology from coalesced pits, to isolated pits (where the boulder bounced several times as it increased velocity), to no groove at all (downrange of its launch point), might be predicted. Groove linearity: Grooves produced by the mechanism described here would be linear and would not be expected to deviate measurably from their path over the vast majority of their traverse. Even where preexisting topography was encountered (an older impact crater for example), a simple analysis shows that the combination of the forward velocity and the observed slopes is such that boulder tracks would deviate laterally from their forward path by no more than a few meters. 4) Map pattern distribution of grooves: Any preexisting structural or stratigraphic fabric will tend to dictate the exit directions of large boulders from the crater cavity, in contrast to the more radially symmetrical, shock-dominated distribution of ejecta leaving the cavity at earlier stages. Therefore, boulders ejected from Stickney in the terminal stages of the cratering event at very low velocities could easily produce distinctive, non-symmetrical ejecta patterns reflecting substrate heterogeneities.

These predictions thus from the basis for assessing and testing the theory of groove formation by the low-velocity ejection of boulders from craters such as Stickney.

ORIGIN OF THE PHOBOS GROOVES

T.C. Duxbury[1], and the LROC and HRSC Teams, [1]*George Mason University, Fairfax, VA, USA. Contact: tduxbury@gmu.edu*

Recent high resolution lunar images by NASA's Lunar Reconnaissance Orbiter have shown linear features on the lunar surface that have a similar morphology to some of the groove patterns on Phobos. The lunar "grooves" were created by boulders ejected during crater formation. These rolling boulder trails follow the local topography, are as long as many kilometers and cross other boulder trails, looking similar to the grooves on Phobos. However, the boulders are still on the lunar surface at the end of the boulder trails, typically at a local low elevation area. Since there are no boulders at the ends of the similar trails on Phobos, the boulders could have left the surface since the ejected speed is tens of meters / second, more than the escape speed, even with energy expended while rolling on the surface.

Many questions are raised that can be addressed via comparative planetology by analyzing the HRSC images of Phobos,and the LROC images and the LOLA altimetry of the moon:

What was the original orientation of Phobos with respect to Mars at the time of the Stickney impact? Possibly the impact was near the anti-Mars side, allowing the boulders to roll toward Mars and make it easier to lift off of the surface. The Stickney impact could have changed the moments of inertia, forcing Phobos to reorient to its current rotational state.

Since there are a significant number of grooves, can these be related to Phobos being a rubble pile of Mars ejecta providing a large source of boulder material to be ejected at crater impact?

What are the widths / depths of the grooves?

What would have been the sizes of the ejected boulders?

Can Phobos mass / regolith information be extracted from the groove morphology?

Does the comparative analyses support rolling boulders creating some of the grooves on Phobos?

The Russian Phobos Sample Return Mission will add to the data that can be used for this comparative analyses.

NEW SURVEY OF THE GROOVES OF PHOBOS, FROM MARS EXPRESS IMAGES

John B. Murray, *Dept. of Earth and Environmental Sciences, The Open University, Milton Keynes MK7 6AA, Great Britain. Contact: j.b.murray@open.ac.uk*

Introduction: A new map of the grooves on Phobos is presented, based on recent images from Mars Express as well as earlier data. This new survey has conclusively demonstrated that the lineaments observed on the surface of Phobos are different in several respects from all other lineaments on planets, satellites and other solid solar system bodies. There are several different families of grooves, every family consisting of parallel planar lineaments covering one hemisphere only. Each family is centred at a different location on the leading hemisphere of Phobos, with the result that an area about 12 km wide around the trailing apex of Phobos is completely devoid of grooves.

Many hypotheses have been put forward to explain these curious features, but there is as yet no general consensus on their origin. These theories fall into two groups: that they are caused by secondary impact, or that they are fractures. The secondary impact ideas include proposals that they are secondary crater chains either from Stickney, at 10 km the largest impact crater on Phobos, or from impacts on Mars, or that they are the tracks of rolling boulders ejected from Stickney. The fracture hypotheses suggest that they are fractures caused by the Stickney impact, or by tidal forces, or by drag forces during capture, or by re-opening of drag force fractures caused by the Stickney event.

Each of these ideas is examined in the light of the new evidence. The geographical distribution and orientation of the grooves, and their relative ages and cross-cutting relationships allow us to discount the fracture hypotheses altogether. The tiny gravitational field, the geographical distribution and the topography of Phobos are similarly at odds with the Stickney secondary cratering and rolling boulder theories. Only the idea that they are secondary impact crater chains from primary impacts on Mars fits all the observations.

The implications of this idea, in the form of information on Phobos' regolith, interior, and its formation and past orbital history are presented, as well as details of the impact process in relation to the ejection of material from large impact events early in crater excavation.

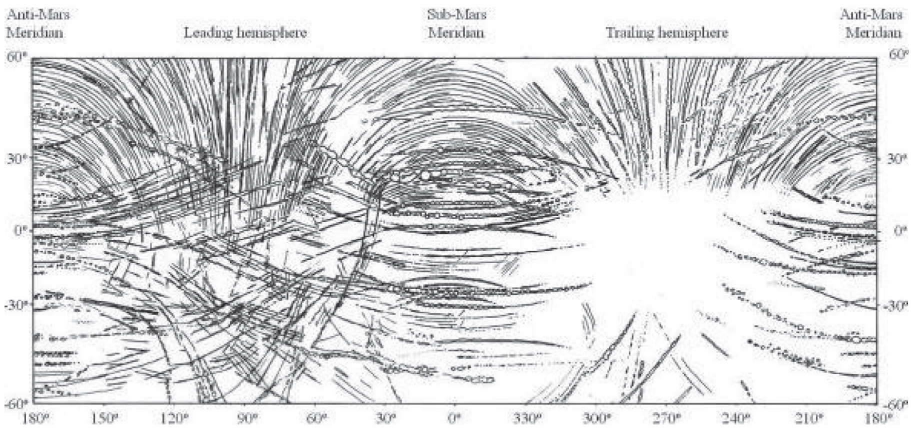

PHOBOS ORIGIN: A REAPPRAISAL

J-P. Bibring, *Institut d'Astrophysique Spatiale, Orsay, France.*
Contact:bibring@ias.u-psud.fr

The visible and near infrared spectra of Phobos, acquired both from the Earth and in Mars orbit, are totally distinct from those of Mars, whatever the martian surface unit mapped. Phobos spectra are essentially featureless, resembling those of dark asteroids considered parent bodies of primitive meteorites. This has long been considered suggesting that Phobos is a captured asteroid — as would Deimos be, for similar reasons.

From a dynamical standpoint, this assumption implies a complex scenario: the capture requires a huge loss of energy, for example through an impact on a third body. It would most likely lead to an ecliptic and excentric orbit, while the present one is circular and equatorial. Moreover, the scenario should be generic enough to have also worked for Deimos, of much lower mass. Altogether, it is highly unlikely (1).

Alternative scenarios for the origin of Phobos and Deimos can be advocated. We shall review and discuss them, on the basis of the data acquired, primarily from the hyperspectral imager OMEGA/Mars Express, with a special emphasis on the most promising one: Phobos and Deimos would originate from re-accretion in a disk formed by an early giant impact on Mars, similarly to the Earth Moon. The primitiveness of these small bodies would merely come from their size, small enough to have precluded further differentiation. Phobos would thus be in part made of Martian material.

The upcoming Phobos Grunt mission, both with its in situ measurements and the follow-on analyses on returned samples, compared to the in situ analyses of MSL, should severely constrain the Phobos origin, and open new avenues to the understanding of the early stages of solar system evolution.

References: [1] Peale S.J.: Origin and Evolution of the Natural Satellites, Ann. Rev. Astron. Astrophys. 37, 533-602, 1999

ORIGIN OF THE MARTIAN MOONS: INVESTIGATING THEIR SURFACE COMPOSITION

P. Vernazza[1], F. Cipriani[1], C. Dukes[2], D. Fulvio[2], K. T. Howard[3], O. Witasse[1], R. Brunetto[4], G. Strazzulla[5], R. P. Binzel[6], P. A. Bland[7], R. Baragiola[2]. *[1]ESA, ESTEC, NL. Contact: pierre.vernazza@esa.int. [2]Univ. of Virginia, USA. [3]NHM London, UK. [4]ESAC, Spain. [5]Obs. of Catania, Italy. [6]MIT, USA. 7IRAC, Imperial College London, UK.*

Introduction: The origin of the Martian moons hasn't been solved yet and is one of the most intriguing puzzles of the inner solar system. The three proposed scenarios for the origin of the moons are the following: 1) Capture of two distinct outer main belt asteroids 2) Formation in place (The Moons accreted in their present position) 3) Origin as Mars impact ejecta. Dynamicists argue that the present orbits of Phobos and Deimos could not be produced following capture, and so they must have originated near Mars at 1.5 AU, where the satellites are found today. However, every observable physical property (albedo, VNIR reflectance ...) indicates that the Martian satellites once resided in the outer belt (~3 AU), suggesting the objects must be captured [1]. Providing new constraints on the composition of the moons would bring us very close to the solution of this long standing issue.

Phobos and Deimos share similar visible-near infrared (0.4-2.5 µm) spectra suggesting that they have a similar surface composition. However, it appears that Deimos' spectrum is redder than any Phobos' spectrum. Further, a strong color difference is observed on Phobos itself: the spectrum covering the bright crater Stickney is much bluer than any spectrum scanning other regions of Phobos. Can these color differences be explained by space weathering [e.g., 2, 3]? Or is a variation of the surface composition the cause of the observed slope differences?

We found two meteorites, Tagish Lake and WIS 91600, whose spectra match Phobos' blue spectrum (crater Stickney) but not Phobos' redder spectra, nor Deimos spectrum. We plan to test if space weathering processes are the cause of the strong color difference observed between Phobos's blue region (crater Stickney) and other parts of Phobos and Deimos. Said differently, we plan to test if space weathering processes can redden and darken the initially WIS 91600- or Tagish Lake-like spectrum of a fresh Phobos surface (Phobos blue; supposing the latter surface is fresh), transforming its appearance to that of a Phobos red or a Deimos spectrum. If not, this would imply that both meteorites differ in composition from the martian moons.

To test this hypothesis, we started reproducing in the laboratory the effects of the solar wind ion irradiation on both meteorites. Such experiments were conducted at the Observatory of Catania (Italy) and at the University of Virginia (USA). Furthermore, a modal analysis of WIS 91600 was conducted at NHM, London (UK) in the same way as previously done for Tagish Lake [4]. We will present the results of these experiments and their immediate implications.

References: [1] Burns J. A. 1992. in Mars, 1283-1301. [2] Chapman, C. R 2004. Annual Review of Earth and Planetary Sciences 32, 539-567. [3] Vernazza et al. 2009. Nature 458, 993-995. [4] Bland, P. A. et al., 2004. Meteoritics & Planetary Science 39, 3-16.

PHOBOS DTM AND COORDINATE REFINEMENT FOR PHOBOS-GRUNT MISSION SUPPORT.

K. Willner[1], J. Oberst[1,2], F. Scholten[2], M. Wählisch[2], T. Roatsch[2], H. Hoffmann[2], K.-D. Matz[2], *[1]Technische Universität Berlin, Department of Geodesy and Geoinformation Science, Berlin, Germany, [2]German Aerospace Center (DLR), Institute of Planetary Research, Berlin-Adlershof , Germany.*
Contact: konrad.willner@tu-berlin.de / Fax: +49-30-314 21973

Abstract: Images obtained by the High Resolution Stereo Camera (HRSC) during recent Phobos flybys were used to update the global digital terrain model (DTM) of Phobos and to study the proposed new landing site area of the Russian Phobos-Grunt mission [1]. The current version of the DTM has a lateral resolution of 100 m per pixel and a ray intersection accuracy of ±15 m. Images covering the Phobos Grunt landing site were registered to the control point network to establish coordinate control for the landing site area [7]. A map was produced enabling mission planers and scientists to extract accurate body-fixed coordinates of features in the Phobos Grunt landing site area.

Introduction: The European Mars Express spacecraft is moving in a highly elliptical (11,000km at apo-apsis) orbit that reaches beyond the low equatorial (6000km above the surface), nearly circular orbit of Phobos [3,4]. Hence, Mars Express is currently the only spacecraft orbiting Mars to carry out Phobos flybys on a regular basis. In March of this year, the orbit of MEX was specifically adjusted to provide a series of Phobos flybys, as close as 110 km. The flybys were intended for radio science investigations and for studies of the prime target area of the Phobos-Grunt Sample Return Mission (PhSRM). Currently a landing site location between 210° to 240° W and 0° to 30° N [1] is discussed.

Results: The HRSC successfully imaged Phobos during three close flybys (orbits 7915, 7926, and 7937) with the nadir, stereo and photometric channels. Images from each of these, taken under identical illumination conditions, are suitable for photogrammetric stereo analysis, specifically for the automated matching algorithms [3]. Resolutions ranged from 4.4m/pixel to 19 m/pixel in the nadir and stereo channels. Further observations were dedicated to color imaging at reduced resolution. Images of these flybys cover the area from the North-Western rim of Stickney to approx. 230° West longitude and North Pole to Equator, covering the proposed landing site for the PhSRM. The previously available global digital terrain model for Phobos [6] has been only weakly controlled in the new observed areas.

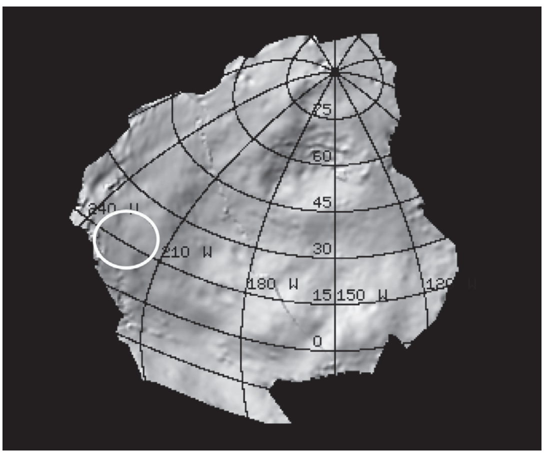

Fig. 1: Shaded DTM computed at a lateral resolution of 100 m per pixel. Relative height accuracies are better than 20 m. The proposed landing site area for the PhSRM [1] is marked.

Images obtained during the recent flybys were used to significantly refine the existing DTM. In a first step the exterior orientation information of all images of one flyby were adjusted and tied to the control point network [5,7]. Then, to prepare for the automated matching process, images are pre-rectified using a preliminary DTM derived from the global shape model [7] to minimize parallaxes between images. This significantly reduces the search area for conjugate points [2] and the number of matching outliers.

We derived a DTM with a resolution of 100m per pixel (Fig 1). The relative height accuracy, representing the remaining uncertainty of the ray intersections, is on average

10m, but not higher than 20m. We derived controlled ortho-rectified images of the Phobos-Grunt landing site that can be used to determine accurate body fixed coordinates of surface features. Different representations, such as perspective views (Fig. 2), allow us to judge the overall topography and to study the safety of the proposed Phobos-Grunt landing site area.

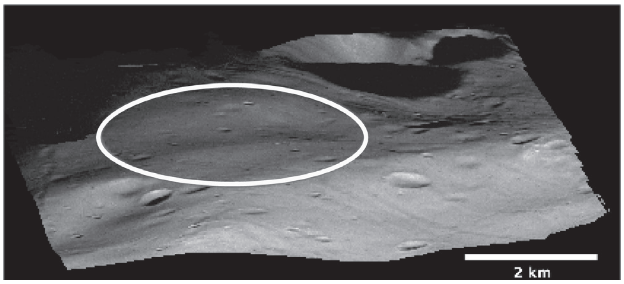

Fig. 2: Perspective view for portions of the derived DTM. The proposed landing site area for the Phobos-Grunt lander [1] is marked.

Outlook: While the derived DTM represents geometric heights, studies are currently under way to also compute dynamic height for Phobos from gravity, centrifuge, and tidal forces. With new image data from Mars Express scheduled to arrive, we expect further improvements to our DTM to be presented at the time of the conference. An update of the global digital image mosaic and atlas [6] will also be prepared.

References: [1] Basilevsky, A. T. and Shingareva, T. V.: The selection and characterization of the Phobos-Soil landing sites, Solar System Research, Vol. 44, pp. 3843, Feb. 2010.

[2] Gwinner, K., Scholten, F., Spiegel, M., Schmidt, R., Giese, B., Oberst, J., Heipke, C., Jaumann, R., and Neukum, G.: Derivation and Validation of High-Resolution Digital Terrain Models from Mars Express HRSC-Data, PE&RS, Vol. 75(9), pp. 11271142, Sept. 2009.

[3] Jaumann, R., Neukum, G., Behnke, T., Duxbury, T. C., Eichentopf, K., Flohrer, J., Gasselt, S. v., Giese, B., Gwinner, K., Hauber, E., Hoffmann, H., Hoffmeister, A., Köhler, U., Matz, K.-D., Mc-Cord, T. B., Mertens, V., Oberst, J., Pischel, R., Reiss, D., Ress, E., Roatsch, T., Saiger, P., Scholten, F., Schwarz, G., Stephan, K., Wählisch, M., and the HRSC Co-Investigator Team: The high-resolution stereo camera (HRSC) experiment on Mars Express: Instrument aspects and experiment conduct from interplanetary cruise through the nominal mission, Planetary and Space Science , Vol. 55, pp. 928-952, May 2007.

[4] Oberst, J., Schwarz, G., Behnke, T., Hoffmann, H., Matz, K.-D., Flohrer, J., Hirsch, H., Roatsch, T., Scholten, F., Hauber, E., Brinkmann, B., Jaumann, R., Williams, D., Kirk, R., Duxbury, T., Leu, C., and Neukum, G.: The imaging performance of the SRC on Mars Express, Planetary and Space Science, Vol. 56, pp. 473-491, Mar. 2008.

[5] Spiegel, M.: Kombinierte Ausgleichung der Mars Express HRSC Zeilenbilddaten und des Mars Global Surveyor MOLA DGM, Dissertation, Technische Universität München, Fakultät für Bauingenieurund Vermessungswesen, 2007.

[6] Wählisch, M., Willner, K., Oberst, J., Matz, K.-D., Scholten, F., Roatsch, T., Hoffmann, H., Semm, S., and Neukum, G.: A new topographic image atlas of Phobos, E&PSL, Vol. 294, pp. 547-553, 2010.

[7] Willner, K., Oberst, J., Hussmann, H., Giese, B., Hoffmann, H., Matz, K.-D., Roatsch, T., and Duxbury, T.: Phobos control point network, rotation, and shape, E&PSL, Vol. 294, pp. 541-546, 2010.

PHOTOMETRIC PROPERTIES OF THE PHOBOS' REGOLITH BASED ON THE PHOBOS MISSION DATE

L. Ksanfomality, *Space research institute, Moscow*

Results of Phobos spectrophotometry in the range 0.3-3 mcm are presented. are based on data obtained by means of the spectrophotometer KRFM on board of the PHOBOS spacecraft in 1989 and other studies. Phobos' reflectivity has little in common with that in papers published before the PHOBOS mission. There is some evidence of conflict with ground-based spectroscopy data published earlier. The KRFM results do not agree with reflectivity features of carbonaceous chondrites and does not permit unique identification with any other type of meteoritic material. In the 300-600 nm spectral range, a wide variety of the reflectivity features was observed to be connected with details of relief. Together with photometric properties results of mid-infrared measurements (thermal emission) are presented, made by the same KRFM instrument. The mid-infrared profiles and theoretical models are compared.

A REVISED UV ALBEDO SPECTRUM OF PHOBOS OBTAINED WITH SPICAM ON MARS EXPRESS

J.L. Bertaux, F. Montmessin, E. Quémerais and A. Rebérac *LATMOS/IPSL, CNRS/INSU, Univ. Versailles St-Quentin, 11 Bd d'Alembert, 78280 Guyancourt, France. Contact: jean-loup.bertaux@latmos.ipsl.fr*

Introduction: We present a revised spectral albedo of Phobos, collected in the UV (190-310 nm) with SPICAM during several encounters of Mars Express with Phobos, for the last 6 years, and with recent very close flybys (closest approach ~120 km from the Phobos surface for SPICAM) executed in February and March 2010. The SPICAM instrument on board Mars Express was used at almost all encounters of Mars Express with Phobos, in order to retrieve the albedo spectrum and try to determine the composition of its soil. Early results in the UV range (180-310 nm) were reported at DPS in 2004 by Perrier et al. (2004). Since then, we revised the absolute calibration (derived from UV stars), and take into account some stray light which needs to be subtracted from observed spectrum before dividing by the solar flux.

The various spectra show no obvious sign of shape variation on Phobos, a very low albedo, and a peak in the range 265-295 nm. Some comparisons with laboratory spectra of meteoritic material and mineral samples will be shown. Comparisons with OMEGA in the visible and near IR will be useful to determine the surface material of Phobos, probably a mixture of bulk material and of interplanetary dust material.

COMPOSITIONAL IMPLICATIONS OF THE COLOR OF PHOBOS

C. M. Pieters, *Brown University, Providence, RI 02912 USA.*
Contact: Carle_Pieters@brown.edu

The character and origin of Phobos remain a mystery. Is this small moon of Mars related to the family of primitive small bodies with orbits concentrated between Mars and Jupiter? Is it a rubble pile of material excavated from Mars by one or more large impacts? Is it a complex multi-layered object of material with diverse origins? Whatever the answer turns out to be, Phobos certainly holds the key to understanding many processes active in the inner solar system.

Other than direct measurement of its composition, principal constraints to evaluate the origin of Phobos come from measurements of the density and the spectral properties of its surface. The most recent bulk density estimate for Phobos is 1876 ± 20 kg/m3 implying a porosity of ~30% even for primitive materials (Andert et al., 2010). The density constraint eliminates coherent rock as the primary constituent of Phobos, but it leaves a wide range of physical and chemical options for creating the low density.

A highly significant result from Phobos-2 is that all optical systems (ISM, VSK, KRFM) noted two principal terrain types based on measured color, one distinctively “red” and the other relatively “blue” or flatter. The “blue” unit was associated with terrain near the large crater Stickney, which also happens to be located on the leading edge as the moon orbits Mars. Although the data were at relatively low spatial resolution, this color and general geology distinction led to a popular hypothesis that the two terrains might be different forms of the same material, with the “red” terrain being “blue” material that has been substantially altered in the space environment. Similar “spaceweathering” trends are observed on the Moon and (most likely) on “S-type” asteroids. Alternatively, the more dominant ‘red’ unit might represent highly primitive asteroidal material.

The suite of modern instruments that are now orbiting Mars provide an additional pulse of new information about Phobos. They are all designed primarily for Mars observations, but several have used opportunities passing Phobos to acquire additional data. The new higher resolution imagery has been a particularly valued asset for further morphological analyses of perplexing surface features such as the grooves. Small amounts of high spectral resolution data (OMEGA, CRISM), continue to find it difficult to detect the presence of any mafic minerals or hydrated species (e.g., Gondet et al., 2008).

The high spatial resolution color data from Mars Express (ESA MEX website) and from HiRISE, (e.g., Thomas et al., 2010) however, open issues previously unimagined earlier. The new color data are fully consistent with the two color unit bulk properties observed earlier at low resolution, but details seen at higher spatial resolution (Fig. 1) indicate that the relation between the two types of terrain is far more complex than originally suspected. Spatial diversity can be seen at all scales. Apparent movement of material can be seen away from the leading edge high. Stratigraphic relations between the two types of material is also unclear. Erosional or depositional processes may both be active.

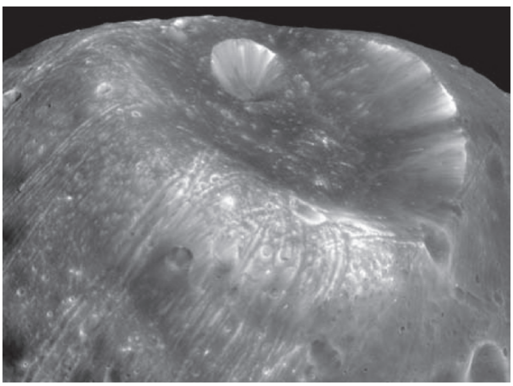

Fig. 1: HiRISE color image of Stickney crater on the leading edge of Phobos. Colors are enhanced to illustrate the “red” and “blue” different units. The spatial and stratigraphic relations between these two types of material is complex. [NASA image]

These new color data expand the concept that two distinct types of material exist on Phobos. Is one derived from the other? Is one local and the other foreign? Has one cycled through processes active in this environment more than the other? Was Phobos formed heterogeneous from two basic constituents?

This Mars-facing side of Phobos has been studied more thoroughly because most sensors have imaged the body from inside Phobos' orbit. Very little color data exist for the anti-Mars side of Phobos, where Phobos-Grunt is to land, The detailed geology of this site and its relation to the diversity seen on the Mars-facing side and the leading edge are thus poorly known. Mars Express is currently the only spacecraft that can collect valuable new color data for this region in preparation for Phobos-Grunt activities.

References: Andert, T. P., P. Rosenblatt, M. Pätzold, B. Häusler, V. Dehant, G. L. Tyler, and J. C. Marty (2010), Precise mass determination and the nature of Phobos, Geophys. Res. Lett., 37, L09202, doi:10.1029/2009GL041829. ESA Mars Express Blog for Phobos: http://webservices.esa.int/blog/blog/7 Gondet, B, J-P. Bibring, Y. Langevin, F. Poulet, S. Murchie and the OMEGA Science team (2008) Phobos observations by the OMEGA/Mars Express hyperspectral imager, LPSC abstract #1832. Thomas, N., et al., (2010) Spectral Heterogeneity on Pho bos and Deimos: HiRISE Observations and Comparisons to Mars Pathfinder Results, LPSC abstract #2595.

COMPOSITIONAL INTERPRETATION OF PFS/MEX AND TES/MGS THERMAL INFRARED SPECTRA OF PHOBOS

M. Giuranna[1], T. L. Roush[2], T. Duxbury[3], R. C. Hogan[4], C. Carli[5], A. Geminale[1], V. Formisano[1], [1]*Istituto di Fisica dello Spazio Interplanetario INAF-IFSI, Roma, Italy;* [2]*NASA Ames Research Center, Moffett Field, California;* [3]*Jet Propulsion Laboratory, California Institute of Technology, Pasadena, California;* [4]*Bay Area Environmental Research Institute, Moffett Field, California; 5Isituto di Astrofisica Spaziale e Fisica cosmica INAF-IASF, Roma, Italy. Contact: marco.giuranna@ifsi-roma.inaf.it*

Introduction: The origin of the Martian satellites presents a puzzle of long standing. The satellites of Mars have VNIR spectra similar to outer belt asteroids, suggesting that they were captured [2]. However, dynamicists have had a difficult time explaining their capture from the outer asteroid belt, preferring them to be objects that formed near their current solar distance [2]. It has even been suggested that Phobos is ejecta from a large basin-forming impact on Mars, perhaps the last survivor of a once-larger population [3]. These various scenarios lead to vastly different compositions for Phobos, with associated implications for early Martian history. Addressing the composition of Phobos will help constrain theories of its formation.

Dataset: TES is a Michelson interferometer operating from 1700 to 200 cm^{-1} (~6 to 50 μm) with spectral resolutions of 6.25-12.5 cm^{-1} [4], [5]. PFS [6] LW Channel operates in the range 250–1700 cm^{-1} (5.9–40 μm) [7]. The spectral resolution is ~1.3 cm^{-1}. Both TES and PFS had several opportunities to observe Phobos. At these wavelengths, both instruments can detect the fundamental vibrational modes of materials. The number, position, intensity, and shape of which are dependent upon the atomic masses, inter-atomic force fields, and molecular geometry, providing a sensitive means of determining mineralogy. A linear combination of 3 black bodies is used to perform a least squares fit of the observed radiance. Using these results as inputs, an upper hull is fit to the radiance maxima. Emissivity values are produced by dividing the measured radiance by the hull.

Results: *Surface temperatures.*The minima and maxima surface temperatures derived by PFS range from 130-160 K and 290-353 K, respectively. These results are in good agreement with the minimum (night, 140 K) and maximum (day, 300 K) brightness temperatures of the satellite surface derived from Viking orbiter measurements [8]. Using Earth-based observations, [9] derived a Phobos surface temperature of 320-340 K. From the observations presented here, only those for PFS orbit 6906 approach these values. Here the heliocentric distance is ~1.388 AU, very similar to that during [9] (1.38-1.39), and the derived surface temperatures are consistent with those reported by [9].

We also compare our results with the results of the numerical modeling of the thermal regime of Phobos' surface regolith layer (on seasonal time scales) in [10]. There is a general good agreement, as our derived temperatures are mostly within the range of predicted diurnal temperatures on the Phobos surface, and the variation of surface temperature as predicted by the model is also reproduced by our results (Fig. 1).

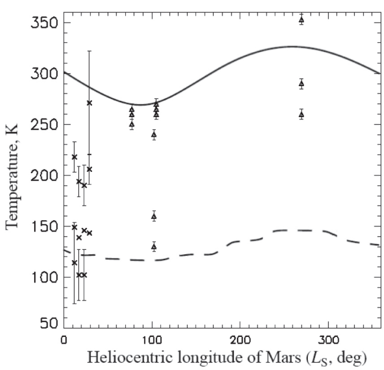

Fig. 1: Comparison of PFS (triangles) and TES (×) derived temperatures with calculated seasonal variations of the maximum (solid line) and minimum (dashed line) diurnal temperatures on the Phobos surface from [10].

Surface composition. Our compositional interpretation of thermal emission data relies upon several digital spectral libraries, containing measured emissivity for a variety of materials (TES library), spectra of terrestrial rocks, lunar materials, and various meteorites reflectivities (ASTER and RELAB spectral libraries). We also compared Phobos spectra with a limited number of materials that are residues of the processing of various organic precursors. Such samples are analogs for the processed products of ultraprimative materials found in the outer solar system.

Despite the fact that the results can in principle point at any of the materials contained in the spectral libraries used for this effort (minerals, rocks, lunar soil, meteorites), only minerals are selected as good candidates. Among all the minerals contained the spectral libraries (carbonates, nitrates, borates, halides, oxides, phosphates, arsenates, vanadates, sulphates, chromates, molybdates and silicates), only silicates provide good spectral matches. In particular, the

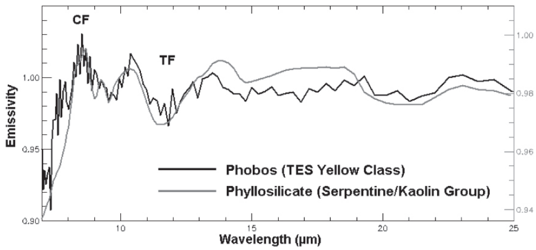

Fig. 2: Example of spectral match for TES spectra**.**

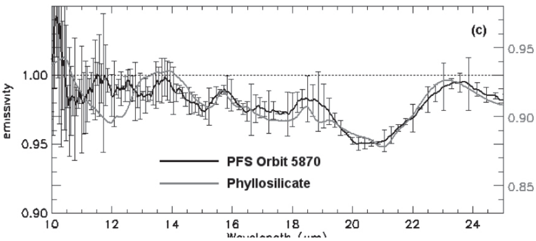

Fig. 3: Example of spectral match for PFS spectra.

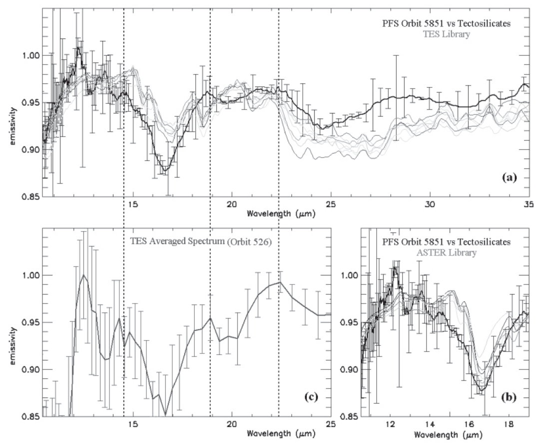

Fig. 4: Example of spectral match for PFS (orbit 5851) and TES (orbit 576) spectra in the "red" region defined by [1].

full wavelength analyses results are dominated by phyllosilicates.

The area northeast of Stickney has been observed by both instruments. It corresponds to the "blue" region as defined by Murchie et al [1]. Particularly in this area, both TES and PFS data suggest a phyllosilicate component (Fig. 2). Results for PFS orbit 5870 also suggest Phyllosilicates (Fig. 3). The PFS observation during orbit 5870 is in a region of transition between the red and the blue units defined by [1], and the analysis here is consistent with the presence of phyllosilicates (Fig. 3). Analysis of PFS (orbit 5851) and TES (orbit 576) observations in the "red" region defined by [1] are consistent with tectosilicates, especially feldspars (Fig. 4).

Conclusions: Visible and near-infrared spectra of Phobos lack of deep absorption features, making the compositional interpretation a tricky task. PFS/MEx and TES/MGS observations in the thermal infrared show several spectral features that can be used to investigate the composition of the surface. Our results show that the majority of the spectra are consistent with the presence of phyllosilicates, particularly in the area northeast of Stickney. This area corresponds to the "blue" region as defined by [1]. Analysis of PFS and TES observations in the "red" region defined by [1] are consistent with tectosilicates, especially feldspars. Two independent approaches of compositional analyses yield very similar results.

Comparison of the TES and PFS data to the meteorites shows that no class of chondritic meteorites provide significant agreement with the spectral features observed. The lack of consistency of the PFS and TES spectra to analogs of ultraprimitive materials (organic residues) suggests that an origin via capture of a transneptunian object is not supported by these observations. Derived surface temperatures from PFS and TES data are in very good agreement with brightness temperatures derived from Viking orbiter measurements, Earth-based observations, and values predicted by numerical models. Our results show that the surface temperature of Phobos varies with solar incidence angle and heliocentric distance, reconciling the different results.

Currently, the most likely scenario is the in-situ formation of Phobos, although a capture of achrondrite-like meteorites is not ruled out. A more definitive answer to the origin of Phobos will certainly benefit from in-situ measurements, or sample return. The future Russian Phobos-Grunt mission (Phobos Sample Return), to be launched in 2011, will certainly contribute to our understanding regarding the origin of Phobos.

References: [1] Murchie, S., et al.,, JGR, 104, 9069-9079, 1999. [2] Burns, J.A., in Mars, H. Kieffer et al. Ed., U.Az. Press, 1283-1301, 1992. [3] Craddock, R. A., 25th LPSC, 293, 1994. [4] Christensen, P.R., et al., JGR, 97, 7719-7734, 1992. [5] Christensen, P.R., et al., Science, 279, 1692-1698, 1998. [6] Formisano, V., et al., PSS 53, 963–974, 2005. [7] Giuranna, M., et al., PSS 53, 993–1007, 2005. [8] Lunine, J. I., et al., JGR, 87, 10297, 1982. [9] Lynch et al., Astron. J., 134, 1456-1463, 2007. [10] Kuzmin, R. O., and E. V. Zabalueva, Solar System Research, Vol. 37, No. 6, pp. 480–488, 2007.

PHOBOS OBSERVATIONS BY OMEGA/MARS EXPRESS HYPERSPECTRAL IMAGER

B. Gondet, J-P. Bibring, Y. Langevin, N.Manaud and the OMEGA Science team,
IAS/CNRS, Université Paris-Sud 91405 Orsay

OMEGA on board the ESA MarsExpress mission, has acquired hyperspectral images of Phobos in the visible and near infrared range (0.35 to 5.1 µm) down to a distance of 96 km, corresponding to a footprint of 120m (table1).

orbit	Altitude (kms)	Footprint (m)	Phase angle (°)
756_0	149	180	62.6
413_0	1882	2200	47.2
2747_0	1050	1200	95
2780_0	606	730	47.8
3769_3	776	900	65
3843_4	658	800	66
5851_2	96	120	50
7915_3	120	150	32
7926_3	287	350	40

Table 1: Omega observations list

We shall present an overview of results acquired, and discuss them in comparison to the pioneer observations of ISM and KRFM on board the Phobos 2 mission, and the recent CRISM/MRO ones (figures 1 and 2). The emphasis will be put on the seach for spectral signatures of mafic minerals, hydrated and carbonaceous phases.

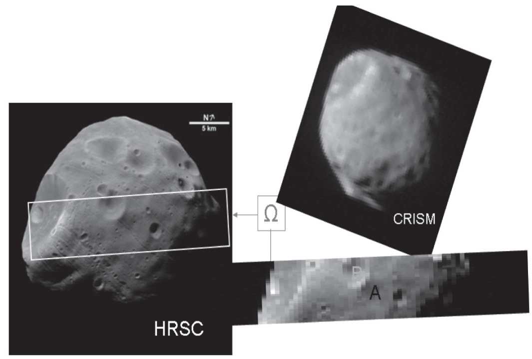

Fig. 1: OMEGA and HRSC images acquired simultaneously, and CRISM image with similar viewing conditions.

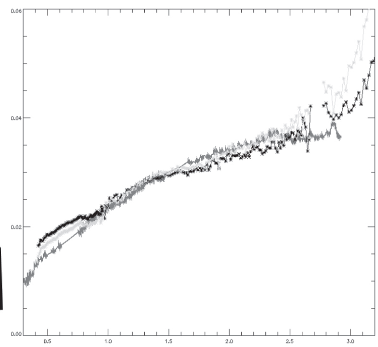

Fig. 2: OMEGA spectra acquired in A and B locations (see figure 1) superimposed on the KRFM/ISM Phobos 2 spectra (red).

References:
[1] Murchie, S. and Erard, S. Icarus, 123, 63–86, 1996.
[2] Rivkin, A. EPSC2009-723

ADVANCING TESTS OF RELATIVISTC GRAVITY VIA LASER RANGING TO PHOBOS

S.G. Turyshev[1], W. Farr[1], W. M. Folkner[1], A. R. Girerd[1], H. Hemmati[1], T. W. Murphy, Jr.[2], J. G. Williams[1], and J. J. Degnan[3], *[1]Jet Propulsion Laboratory, California Institute of Technology, 4800 Oak Grove Drive, Pasadena, CA 91109-0899, USA; [2]Center for Astrophysics and Space Sciences, University of California, San Diego, 9500 Gilman Drive, La Jolla, CA 92093-0424, USA; [3]Sigma Space Corporation,4400 Lottsford Vista Rd., Lanham, MD 20706, USA.*
Contact: turyshev@jpl.nasa.gov

Introduction: Interplanetary laser ranging may offer significant improvements in many areas space activities including planetary research, fundamental physics, and deep-space navigation. Recent progress in the development of active laser techniques could extend the accuracies characteristic of passive laser ranging to interplanetary distances. Technology is available to conduct such measurements, achieving single-photon time resolution measured in tens of picoseconds (ps). One millimeter of range corresponds to 3.3 ps; millimeter range precision can be statistically achieved with a few hundred photons in both uplink/downlink directions in ranging between the Earth and Mars. Interplanetary laser ranging has been demonstrated with the MESSENGER spacecraft that successfully established a two-way laser link over 24 million km of space, achieving 20 cm range accuracy (Smith et al., 2006). Achieving mm-level precision over interplanetary distances is within reach, thus opening a way to significantly more accurate (several orders of magnitude) tests of gravity on solar system scales.

We discuss deployment of pulsed laser transponders with future landers on Mars/Phobos. Highly-accurate time-series of the two-way travel times of laser pulses between an observatory on the Earth and an optical transponder on Mars/Phobos could lead to major advances in science investigations of Mars/Phobos. The resulting Phobos Laser Ranging (PLR) would benefit the study of Phobos and the Martian system and would allow major advances in the tests of fundamental gravity (Turyshev-2008).

The Phobos Laser Ranging Experiment: PLR is a concept for a space mission designed to advance tests of relativistic gravity in the solar system. PLR's primary objective is to measure the curvature of space around the Sun, represented by the Eddington parameter γ. A relativistic time delay of the laser signal passing through the Sun's gravity field in the immediate proximity of the Sun will deliver a high accuracy determination of this parameter. PLR will be able to do a measurement of the parameter g with accuracy of two parts in 10^7, thereby improving today's best result by two orders of magnitude (Turyshev et al., 2010).

Other mission goals include measurements of the time-rate-of-change of the gravitational constant, *G* and a search for a new long-range interaction via tests of the Yukawa forces violating the gravitational inverse square law at 1.5 AU distances – with up to two orders-of-magnitude improvement for each. In addition, PLR will test the EP looking for Jupiter-induced deviations in the Earth-Phobos range as these bodies orbit the Sun.

In addition to the primary astrophysics science, a variety of other scientific advances would be made by the PLR mission. For Phobos, these include detailed gravity and topographical maps, unprecedented orbital determination accuracy and knowledge of physical libration characteristics, an upper limit on tidal behavior, and local information about the landing site, such as rock distribution, regolith characterization, etc. For Mars, its overall body distortion and dissipation due to tides could be measured.

The science parameters will be estimated using laser ranging measurements of the distance between an Earth station and an active laser transponder on Phobos capable of reaching mm-level range resolution. A transponder on Phobos sending 0.25 mJ, 10 ps pulses at 1 kHz, and receiving asynchronous 1 kHz pulses from earth via a 12 cm aperture will permit links that even at maximum range will exceed a photon per second. A total measurement precision of 50 ps demands a few hundred photons to average to 1 mm (3.3 ps) range precision. Existing satellite laser ranging (SLR) facilities--with appropriate augmentation--will be able to participate in PLR. Since Phobos' orbital period is about 8 hrs, each observatory is guaranteed visibility of the Phobos instrument every Earth day. Given the current technology readiness level, PLR could be started in 2011 for launch in 2016 for 3 years of science operations (Turyshev et al., 2010).

We discuss the PLR's science objectives, instrument, and mission design. We also present the details of science simulations performed to support the mission's primary objectives.

Acknowledgements: The work described in this report was performed at the Jet Propulsion Laboratory, California Institute of Technology, under a contract with the National Aeronautics and Space Administration.

References: D.E. Smith et al., "Two-way laser link over interplanetary distance," Science **311**, 53 (2006)
S.G. Turyshev et al., "Advancing Tests of Relativistic Gravity with Laser Ranging to Phobos," *Experimental Astronomy* (2010), arXiv:1003.4961 [gr-qc].
S.G. Turyshev, "Experimental Tests of General Relativity: Recent Progress and Future Directions," Успехи физических наук 179(1) 3-34 (2009), [Physics--Uspekhi 52(1) 3-34 (2009)], arXiv:0809.3730 [gr-qc].

INVESTIGATIONS ON PHOBOS SAMPLE AND ITS ANALOGS: A MULTI-METHOD APPROACH

H. Rickman[1], E. Słaby[2], J. Gurgurewicz[2,1], M. Banaszkiewicz[1], J. Grygorczuk[1], M. Królikowska[1], M. Morawski[1], K. Seweryn[1], R. Wawrzaszek[1], *[1]Space Research Centre, Polish Academy of Sciences, Bartycka 18A, 00-716 Warsaw, Poland; [2]Institute of Geological Sciences, Polish Academy of Sciences, Twarda 51/55, 00-818 Warsaw, Poland. Contact: Hans.Rickman@fysast.uu.se*

Introduction: One of the most important goals of the Phobos Sample Return mission is to collect a soil sample from Phobos and deliver it to Earth. The sample will be collected from the surface of the satellite by the Polish penetrator CHOMIK, designed and manufactured at the Space Mechatronics and Robotics Laboratory, in Space Research Centre of the Polish Academy of Sciences (SRC PAS) in Warsaw. Apart from sampling, CHOMIK will perform thermal and mechanical measurements of Phobos' regolith. Planned experimental analysis using meteoritic material (i.e. carbonaceous chondrites) allows us to choose an adequate analysis framework for the Phobos sample. A combination of petrographical, mineralogical and geochemical characterization with radiometric dating, as well as development of new thermophysical models, should provide the means to read the history of Phobos, and perhaps to see during which period it was captured.

Phobos is assumed with some probability to be carbonaceous chondrite satellite of high diversity of geochemical composition [1]. Carbonaceous chondrites are amongst the most primitive materials from the solar system, and provide insights into early solar system formation processes. Hammond et al. study [2] offers an insight into volatile element depletion patterns in the carbonaceous chondrite groups, and a comparison between meteorite fall and find samples. Knowledge of the trace element chemistry of chondrite matrix is of value in understanding nebula conditions.

Geochemistry: On the basis of investigation on Kaidun meteorite, possibly originated from Phobos, Ivanov [1] supposed many processes to occur influencing the geochemical composition of single meteorite phases: *inter alia* condensation, agglomeration, transfer and precipitation of material, primordial magmatic differentiation, metasomatosis, aqueous alteration and others. Mineralogical characterization of carbonaceous chondrite phases is mainly linked petrographical description as well as to geochemistry, which can be best proved by whole rock composition testing or by in situ measurements. In the present abstract we want to concentrate at the latter possibility and combine it with thermal modelling.

The *in situ* geochemical characterization is precise. The collected by it data can give insight into series of complex processes causing the carbonaceous chondrite evolution. Everyone such a process (e.g. mentioned by Ivanov [1]) is characterized by different partitioning of trace elements between environment and being fed by this environment phase. All of the processes are complex phenomena, investigated and modelled with use of many geochemical tools, where data are provided *inter alia* by LA ICP MS. Within them trace elements play especially important role. The geochemical data retrieved from whole rock and from single phase (mainly collected *in situ* by LA ICP MS) composition have different and completive weights. The whole rock composition gives an average information on a sum of individual processes. The geochemical heterogeneity is better reflected in a complexity of a single phase growth morphology and composition then in a whole rock composition. Phase geochemistry registers all the nuances of the change of the element concentration of the environment, where its growth proceeds.

Among traces water as well as other volatiles can be incorporated into nominally hydrous and anhydrous minerals. The data on them are collected with use of FTIR and Raman spectroscopy. Hydrous species are incompatible in nominally anhydrous minerals. Many research work done on them within last years point to a growing interest in the pieces of information used for reconstruction of crystallization and further re-equilibration process. The investigation on water species in nominally anhydrous minerals (FTIR and Raman spectra) combined with data trace element composition (LA ICP MS on single phase) can give even more precious piece of information on the conditions of the phase formation as well as further changes provided by metasomatosis, aqueous alteration and others. In addition simultaneous information retrieved by LA ICP MS and FTIR/Raman on both compatible and incompatible trace elements and further data processing can give better insight into volatile role in all investigated processes.

As mentioned above three methods can be of preferential use: by LA ICP MS, FTIR and Raman spectroscopy. Previous studies [3,4] have illustrated that ICP MS analytical techniques provide both a precise and accurate way of measuring trace element abundances on small sample populations of meteorites. Bland et al. [5] have employed both laser ablation ICP MS and solution ICP MS to analyse the trace element composition of matrix in a range of carbonaceous chondrites. According to these authors LA ICP MS analysis appears to be an effective means of investigating matrix trace element abundance *in situ* in chondrites. Institutes of Polish Academy of Sciences have such an equipment. Both measurements are used to be done *in situ* on various parts of different minerals thus giving the possibility to retrieved all stages on the primary differentiation and to reconstruct the post-differentiation processes as well as to use the data sets for geochemical modelling. In particular geochemical modeling of magmatic phase crystallization is one of the subject practiced intensively in IGSci PASci. As usual the models can help in the recognition the origin of the material.

Thermal modelling: In the presented multi-method approach of sample investigations thermal modelling plays especially important role *inter alia* appending interpretation of geochemical data. Our knowledge of the bulk properties of comets and asteroids is fundamentally dependent on estimates of the thermophysical properties of their surfaces. The outgassing of H_2O from cometary nuclei, which drives their near-perihelion activity, is strongly conditioned by thenear-surface porosity and heat flow. This includes the directional pattern of gaseous outflow, which determines the jet effect on the nucleus and therefore is essential for mass estimates based on the corresponding orbital perturbations. In the case of asteroids and trans-neptunian objects, their sizes are generally inferred from thermal infrared observations, but this requires a good modelling of the surface temperature distribution.

While some thermophysical properties can be inferred at least roughly from independent observational constraints, it is noteworthy that the research community is still struggling with major uncertainties. A good example is the recent exploration of the nucleus of comet 9P/Tempel 1 by the NASA Deep Impact mission. The near-IR spectral mapping results have been modelled using two different approaches, leading to major differences in, e.g., the inferred thermal inertia. A major issue is the role of small-scale surface roughness and the associated beaming and self-heating effects. Moreover, current state-of-the-art thermal models of rough terrains have difficulties representing the observations, indicating that these are still too immature and that better tools are needed.

The surface of Phobos will likely provide a good analogue to asteroidal and cometary surfaces in general. Therefore, measuring the surface and near sub-surface temperatures using the lander of the Phobos Sample Return Mission may yield invaluable “ground truth” for the development of new-generation thermophysical models. The CHOMIK device will carry thermal sensors for these purposes, and a time series of measurements during the spin of Phobos coupled with knowledge of global and local topography from imaging may yield the thermal inertia. In addition, an active experiment will be carried out using a heater to measure the thermal conductivity. We expect the combination of these results to be extremely useful as a test case for thermal modelling.

References: Ivanov A. V. (2004) Solar System Research, 38, 97-107. [2] Hammond S. J. et al. (2008) LPSC XXXIX, Abstract #1786. [3] Wolf S. F. et al. (2005) Analytica Chimica Acta, 528, 121-128. [4] Friedrich
M. et al. (2002) Meteoritics & Planet. Sci., 37, 677-686. [5] Bland P. A. et al. (2003) LPSC XXXIV, Abstract #1750.

THE ROSETTA MISSION – EXPLORING SOLAR SYSTEM FORMATION

R. Schulz, *Research and Scientific Support Department, European Space Agency, Postbus 299, 2200 AG Noordwijk.The Netherlands. Contact: Rita.Schulz@esa.int*

Introduction: The Rosetta mission to comet 67P/Churyumov-Gerasimenko is one of the cornerstone missions of the European Space Agency. This space mission represents the next step into the improvement of our understanding of comet nuclei naturally following the successful comet nucleus fly-by missions carried out in the past. Rosetta is a rendezvous mission with a comet nucleus combining an Orbiter with a Lander. The Rosetta spacecraft will go in orbit around the comet nucleus when it is still far away from the Sun, and escort the comet for more than a year along its pre- and post-perihelion orbit while monitoring the evolution of the nucleus and the coma as a function of increasing and decreasing solar flux input. The Lander Philae will get down onto the surface of the nucleus at a time when the comet is still at a low state of activity and analyse nucleus material in-situ with the instruments on board. On its long journey to the comet rendezvous the Rosetta spacecraft performed close fly-by at two very different main-belt asteroids, namely (2867) Steins and (21) Lutetia.

Mission Overview: Rosetta is on its 10-year journey to rendezvous with Jupiter-family comet 67P/Churyumov-Gerasimenko. The spacecraft was launched with an Ariane-5 from Kourou / French Guiana on 2 March 2004, and has already successfully completed all four gravity assists (3 at Earth and 1 at Mars) that were necessary to acquire sufficient orbital energy for being able to rendezvous with its target comet and go in orbit around the nucleus. After the second and third Earth gravity assist Rosetta performed close fly-bys at main-belt asteroids. The first of these close encounters took place on 5 September 2008, when Rosetta flew by the 5-km sized asteroid (2867) Steins at a distance of 802.6 km. Then on 10 July 2010 Rosetta passed its main asteroid target, the 100-km sized asteroid (21) Lutetia, at a distance of 3162 km. The spacecraft is now moving into the outer solar system to rendezvous with its target comet at a heliocentric distance of $r = 4.5$ AU. It will reach the comet in May 2014 and go into close orbit in September 2014 at $r = 3.4$ AU and $\Delta = 2.8$ AU. Rosetta will start the global observation and mapping of the nucleus during which the spacecraft will fly down to distances of a few kilometres from the surface. The landing of Philae is planned for 10 November 2014 when the comet is about 3 AU away from the Sun. After a five day prime Lander mission, both, the Orbiter and the Lander will enter the routine scientific phase, escorting the comet to perihelion and beyond. The nominal mission ends on 30 December 2015.

Scientific Approach: Comets are believed to have stored information on the sources that contributed to the proto-solar nebula and on the condensation processes during the formation of the first planetesimals. Owing to their high content of frozen volatiles and organics they are particularly interesting in view to understanding solar system ices. However, it is these characteristics which make comets so difficult to study. Direct evidence on the volatiles in a comet nucleus is particularly difficult to obtain. Remote observations, even during fly-by missions, only cover species in the coma, which have been altered by physico-chemical processes such as sublimation and interactions with solar radiation and the solar wind. The Rosetta mission combines two strategies of characterizing the properties of a comet nucleus. A science spacecraft staying close to the nucleus along a major part of the orbit and performing comprehensive remote-sensing and analytical investigations of material from the nucleus and the coma, guarantees by design minimal perturbations of the comet material as analyses are performed in situ, at low temperatures, and in a microgravity environment. On top of this the Rosetta Lander Philae will get down onto the nucleus surface, before the comet is too active to permit such a landing (i.e. $r \sim 3$ AU) and examine in-situ the surface and subsurface composition of the comet nucleus as well as its physical properties.

The asteroids encountered during the long cruise phase were carefully selected through evaluation of the scientific significance of all reachable targets constrained by the available fuel budget. For each asteroid the fly-by strategy was arranged such that it allowed for continuous observations before, during and after closest approach ensuring that the spacecraft passes through phase angle zero during the encounter. Most of the scientific instruments on board Rosetta were switched on for investigations of the asteroid and its surrounding environment, obtaining imaging and spectral observations from the UV to radio wavelengths as well as particle and field measurements. Both targets have turned out to be extraordinarily interesting objects for close inspection.

VENUS EXPRESS: SCIENCE HIGHLIGHTS AND FUTURE PLANS

D.V. Titov[1], H. Svedhem[2] and the Venus Express Team, *[1]Max Planck Institute for Solar System Research, Katlenburg-Lindau, Germany, [2]ESA/ ESTEC, Noordwijk, The Netherlands (titov@mps.mpg.de)*

Since April 2006 Venus Express has been performing a global survey of the remarkably dense, cloudy, and dynamic atmosphere of our near neighbour. A consistent picture of the climate on Venus is emerging on the basis of the new data, which enables us to provide an overview of the global temperature structure, the composition and its variations, the cloud morphology at various levels, the atmospheric dynamics and general circulation, and near-infrared emissions from trace species such as oxygen in the mesosphere. Vertical profiles of atmospheric temperature in the mesosphere and upper troposphere show strong variability correlated with changes in the cloud top structure and many fine details indicating dynamical processes. Temperature sounding also shows that the cloud deck at 50-60 km is convectively unstable, in agreement with the analysis of UV images. Imaging also reveals strong latitudinal variations and significant temporal changes in the global cloud top morphology, which will inevitably modulate the solar energy deposited in the atmosphere. The cloud top altitude varies from ~72 km in the low and middle latitudes to ~64 km in the polar region, marking vast polar depressions that form as a result of the Hadley-type meridional circulation. Stellar and solar occultation measurements have revealed an extended upper haze of submicron particles and provided information on its optical properties. Solar occultation observations and deep atmosphere spectroscopy in several spectral transparency windows have quantified the distribution of the major trace gases H_2O, SO_2, CO, COS and their variations above and below the clouds, and so provided important input and validation for models of chemical cycles and dynamical transport. Cloud motion monitoring has characterised the mean state of the atmospheric circulation as well as its variability. Low and middle latitudes show an almost constant zonal wind speed of 100+/-20 m/s at the cloud tops and vertical wind sheer of 2-3 m/s/km. Towards the pole, the wind speed drops quickly and the vertical shear vanishes. The meridional poleward wind ranges from 0 to about 15 m/s and there is some indication that it may change its direction at high latitudes. Comparison of the thermal wind field derived from temperature sounding to the cloud tracked winds confirms the approximate validity of cyclostrophic balance, at least in the latitude range from 30 S to 70S. Non-LTE infrared emissions in the lines of O_2, NO, CO_2, OH originating near the mesopause at 95-105 km altitude were detected and mapped. The data show that the peak intensity occurs close to the anti-solar point, which is consistent with current models of the thermospheric circulation.

THE EUROPEAN ROBOTIC EXPLORATION OF THE PLANET MARS

A.F. Chicarro, *European Space Agency, Solar System Missions Division, ESTEC/ Code SRE-SM, Postbus 299, 2200 AG Noordwijk, The Netherlands.*
Contact: agustin.chicarro@esa.int

The ESA Mars Express mission was launched in June 2003 and has been orbiting Mars for over six years providing data with an unprecedented spatial and spectral resolution on the surface, subsurface, atmosphere and ionosphere of the red planet. The main theme of the mission is the search for water in its various states everywhere on the planet by all instruments using different techniques. A summary of scientific results is given below.

The High-Resolution Stereo Colour Imager (HRSC) has shown breathtaking views of the planet, pointing to very young ages for both glacial and volcanic processes, from hundreds of thousands to a few million years old, respectively. The IR Mineralogical Mapping Spectrometer (OMEGA) has provided unprecedented maps of H_2O ice and CO_2 ice in the polar regions, and determined that the alteration products (phyllosilicates) in the early history of Mars correspond to abundant liquid water, while the post-Noachian products (sulfates and iron oxides) suggest a colder, drier planet with only episodic water on the surface. The Planetary Fourier Spectrometer (PFS) has confirmed the presence of methane (also seen in ground-based observations), which would indicate current volcanic activity and/or biological processes. The UV and IR Atmospheric Spectrometer (SPICAM) has provided the first complete vertical profile of CO_2 density and temperature, and has discovered the existence of nightglow, as well as that of auroras over mid-latitude regions with paleomagnetic signatures and very high-altitude CO_2 clouds. The Energetic Neutral Atoms Analyser (ASPERA) has identified solar wind scavenging of the upper atmosphere down to 270 km altitude as one of the main culprits of atmospheric degassing and determine the current rate of atmospheric escape. The Radio Science Experiment (MaRS) has studied the surface roughness by pointing the spacecraft high-gain antenna to the Martian surface. Also, the martian interior has been probed by studying the gravity anomalies affecting the orbit, and a transient ionospheric layer due to meteors burning in the atmosphere, was identified by MaRS. Finally, results of the ionospheric and subsurface sounding radar (MARSIS) indicate strong echoes coming from the surface and the subsurface allowing to identify buried tectonic structures, as well as layers of water-ice and the very fine structure of the polar caps. Also, probing of the ionosphere reveals a variety of echoes originating in areas of crustal remnant magnetism. Mars Express is flying at the closest distance ever of Phobos (less than 100 km), allowing to determine the mass of Phobos with great accuracy, to sound its interior with a radar for the first time, to obtain the sharpest images ever, to observe the satellite in the visible, UV and IR, and to monitor the solar wind interaction with its surface.

Mars Express will be followed by ESA's new Exploration Programme, starting in 2016 with an Orbiter focusing on atmospheric trace gases and in particular methane. The ExoMars rover will follow in 2018 to perform geochemical and exobiological measurements on the surface and the subsurface. Later, potential missions may include a Network of 3-6 surface stations (possibly together with an orbiter), in order to investigate the interior of the planet, its atmospheric dynamics and the geology of each landing site. All these Mars Exploration missions will be carried out jointly with NASA.

Such network-orbiter combination represents a unique tool to perform new investigations of Mars, which could not be addressed by other means. In particular, i) the internal geophysical aspects concern the structure and dynamics of the interior of Mars including the state of the core and composition of the mantle; the fine structure of the crust including its paleomagnetic anomalies; the rotational parameters (axis tilt, precession, nutation, etc) that define both the state of the interior and the climate evolution; ii) the atmospheric physics aspects concern the general circulation and its forcing factors; the time variability cycles of the transport of volatiles, water and dust; surface-atmosphere interactions and overall meteorology and climate; iii) the geology of each landing site concerns the full characterization of the surrounding area including petrological rock types, chemical and mineralogical sample analysis, erosion, oxidation and weathering processes to infer the geological history of the region, as well as the astrobiological potential of each site. To complement the science gained from the Martian surface, investigations need to be carried out from orbit in a coordinated manner, such as i) global atmospheric mapping to study weather patterns, opacity and chemical composition; ii) a detailed map of the crustal magnetic anomalies from lower orbit (150 km); iii) study of these magnetic anomalies need to be studied in light of the magnetic field induced by the solar wind interaction with the upper atmosphere of the planet. The Network Mission concept is based on the fact that some important science goals on any given terrestrial planet can only be achieved with simultaneous measurements from a number of landers located on the surface of the planet (primarily internal geophysics, geodesy and meteorology) coupled to an orbiter.

The long-term goal of Mars robotic exploration in Europe remains the return of rock and soil samples from the Martian surface before Humans go to Mars. For further details on Mars Express science results: http://sci.esa.int/marsexpress/

BRIEF INTRODUCTION OF YINGHUO-1 MICRO-SATELLITE FOR MARS SPACE ENVIRONMENT EXPLORATION

WU Ji[1], ZHU Guang-wu[1], ZHAO Hua[1], WANG Chi[1], LI Lei[1], SUN Yue-qiang[1], GUO Wei[1], HUANG Cheng-li[2], HOU Jianwen[3], CHEN Changya[3], *[1]Center for Space Science and Applied Research, [2]Shanghai Astronomical Observatory, [3]Shanghai Academy of Space Technology*

Introduction: Replace these instructions with the text of your abstract. Do NOT delete the section break above. The text will appear in two columns (You'll have to switch to page layout view to see the two columns.) If you are including tables or figures, they MUST be imported into this file.

The Mars exploration of human beings has undergone several stages from the visual observation and the observation by ground-based telescopes, to the observation by telescopes aboard spacecraft and the observation by launching Mars probes orbiting Mars, until the landing exploration on the surface of Mars. At present, the main task of ground-based telescopic observations is to monitor, continuously or quasi-continuously, the variations on the Martian surface, such as the variation of the Martian atmosphere, including the formation and propagation of dust storms, and the variation of the polar ice cap, etc.

Since entering the space era, people have launched morethan30probestowardsMars, and about one half of them have entered Mars orbits. Aiming at the problem most concerned by human beings, namely the problem whether life exists on Mars, the exploration objectives of almost all probes are focused on the physical and chemical properties of the Martian surface, and the possibility that water exists in Mars. By the explorations of several recent programs, such as MGS and Mars Express, the evidence that there has been a large amount of liquid water has been found, even it can be concluded that underground water still exists now. Hence the major part of the planning Mars probes have their objectives concentrated on digging explorations, and try to discover the trace of life.

Even though for the explorations on the Martian surface, water and life have become hot points, but the atmospheric environment of Mars is still not well understood, particularly the high layers of its atmosphere and ionosphere. The fragmentary measured data of the atmospheric and ionospheric cross-sections are mainly obtained in the landing courses of landers above some limited locations. Another part of measured data, especially those of the ionosphere, are obtained from the occultation inversion of the refraction coefficients in the Martian atmosphere and ionosphere by using the telemetric signals sent back to the earth by Mars orbiters. As most of the orbiters for observing the surface features of Mars move in polar circular orbits around Mars, only the data at a height of about several hundred kilometers can be obtained, they are not very significant for analyzing the global features of the Martian atmosphere and ionosphere. Therefore, the human knowledge on the Martian high-layer atmosphere and ionosphere is very limited.

In recent years, people become more concerned about the Martian high-layer atmosphere and ionosphere, as well as the properties of the transition region of the interaction between the Martian high-layer atmosphere and the solar wind. This is because the sun as the source of energy supply for the planets in the solar system, its any variation will influence the planet environments. Being different from the earth, Mars does not have very strong intrinsic magnetic field, therefore it has no protection of the magnetosphere as that of the earth. Some local strong magnetic anomalies on the Martian surface make the distribution of magnetic fields around Mars become very complicated. Once a solar eruptive event happens, a great number of high-energy particles will impact on the Martian surface, particularly those areas with weak magnetic fields. This will bring serious threat to the future Mars landing. Besides, to study the composition and escape mechanism of Martian atmosphere is very important for the analysis and study on the evolution of Mars. How did the liquid water on the Martian surface disappear? What is its mechanism? The answers may be found from the composition of Martian atmosphere.

Yinghuo-1 (YH-1) is a microsatellite of 115kg. It will fly to Mars together with the Russian Phobos-Grunt probe. As soon as they enter in to the Martian gravitational field, YH-1 will separate with the Phobos-Grunt probe, and enter into a large elliptical orbit around Mars, with the apo-martian distance of about 80,000km, the peri-martian distance of about 800km, the orbit inclination of less than 5 degrees, and the orbital period of about 72h. Later, YH-1 will operate on its orbit for one year and carry out the explorations on the high-layer atmosphere and space environment of Mars to make contributions for a comprehensive knowledge about the features of the Martian space environment and the escape mechanism of the Martian atmosphere.

METNET- NETWORK MISSION TO MARS

A.-M. Harri[1], S. Alexashkin.[2], V. Linkin[3], H. Guerrero[4], H. Savijärvi[5], L. Vazquez[6], W. Schmidt[1], M. Uspensky[1], [1]*Finnish Meteorological Institute, Space Research Division, Helsinki, Finland. Contact: ari-matti.harri@fmi.fi ;* [2]*LA - Lavochkin Association, Moscow, Russia;* [3]*IKI - Russian Space Research Institute, Moscow, Russia;* [4]*INTA -Instituto Nacional de Técnica Aeroespacial, Madrid, Spain ;* [5]*HU – Helsinki University, Helsinki, Finland ;* [6]*UCM -Universidad Complutense de Madrid, Spain.*

We are developing a new kind of planetary exploration mission for Mars – MetNet in situ observation network based on a new semi-hard landing vehicle called the Met-Net Lander (MNL). The first MetNet vehicle, MetNet Precursor, slated for launch in 2011. The MetNet development work started already in 2001. The actual practical Precursor Mission development work started in January 2009 with participation from various space research institutes and agencies. The scientific rationale and goals as well as key mission solutions will be discussed.

The eventual scope of the MetNet Mission is to deploy some 20 MNLs on the Martian surface using inflatable descent system structures (Fig.1), which will be supported by observations from the orbit around Mars. Currently we are working on the MetNet Mars Precursor Mission (MMPM) to deploy one MetNet Lander to Mars in the 2011 launch window as a technology and science demonstration mission.

The MNL will have a versatile science payload focused on the atmospheric science of Mars. Time-resolved in situ Martian meteorological measurements acquired by the Viking, Mars Pathfinder and Phoenix landers and remote sensing observations by the Mariner 9, Viking, Mars Global Surveyor, Mars Odyssey and the Mars Express orbiters have provided the basis for our current understanding of the behavior of weather and climate on Mars. However, the available amount of data is still scarce and a wealth of additional in situ observations are needed on varying types of Martian orography, terrain and altitude spanning all latitudes and longitudes to address microscale and mesoscale atmospheric phenomena. Detailed characterization of the Martian atmospheric circulation patterns and climatological cycles requires simultaneous in situ atmospheric observations.

The scientific payload of the MetNet Mission encompasses separate instrument packages for the atmospheric entry and descent phase and for the surface operation phase. The MetNet mission concept and key probe technologies have been developed and the critical subsystems have been qualified to meet the Martian environmental and functional conditions. The flight unit of the landing

vehicle has been manufactured and tested. This development effort has been fulfilled in collaboration between the Finnish Meteorological Institute (FMI), the Russian Lavoschkin Association (LA) and the Russian Space Research Institute (IKI) since August 2001. INTA (Instituto Nacional de Técnica Aeroespacial) from Spain joined the MetNet Core Mission team in 2008.

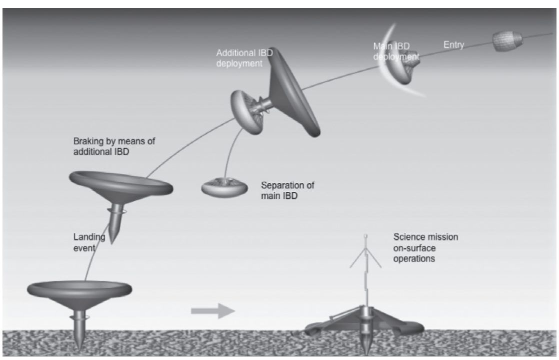

Fig. 1: The MetNet landing vehicle is decelerating its entry and descent by using inflatable systems. It will land to Mars with the velocity of 50 to 70 m/s.

NETWORKING STUDIES OF MARS CLIMATE AND INTERIOR IN THE PROJECT MARS-NET.

A.V.Rodin[1,2], V.M.Linkin[2], V.N.Zharkov[3], T.V.Gudkova[3], A.N.Lipatov[2], R.O.Kuzmin[4,2] and M.B.Martynov[5] *[1]Moscow Institute of Physics and Technology, Russia; [2]Space Research Institute, Russia; [3]Earch Physics Institute, Russia; [4]Vernadsky Institute for Geochemistry and Analytical Chemistry, Russia; [5]Lavochkin Science and Industrial Association, Russia. Contact: Alexander.Rodin@phystech.edu*

Introduction: Recent successful missions to the Red Planet have returned an extraordinary data set obtained by remote sensing instruments as well as from rovers and landers. Among few opportunities that have not yet been implemented in Mars exploration program, although being extensively discussed by different space agencies, is monitoring of transient events by means of network of continuously operating stations. Such a network may be employed for simultaneous meteorological observations, studies of seasonal changes in the upper soil layer, and the attempt to detect seismic activity on Mars.

International cooperation: The project implies deep international cooperation, first of all with Finnish Meteorological Institute, that have made a substantial contribution to the design and concept of Martian meteo station. At the same time, we envision wide participation of international partners in scientific instruments and coordination of the observation campaign with other contemporary Mars missions.

The project: Mars-NET mission implies the delivery to the surface of Mars up to 20 small stations, carrying meteopachage, seismic equipment and probes for sounding thermal and electrical soil properties. The principal design, scientific instruments and methods of delivery to the Martian surface have been inherited from earlier concepts of networking missions developed by IKI and NPOL in cooperation with European colleagues. For the moment, phase A of the project comes to its end and phase B announcement is achieved.

The number of stations and delivery locations must be constrained by mission requirements; however, from the point of view of climate studies, the optimum will be from 2 to 4 stations near equator from 3 to 6 stations at nearly same latitudes in North and South extratropics, and one in each polar region. The exact location of stations depends on their number, being connected with specific places on Mars, where the atmospheric circulation and hydrological cycle reveal most intense activity. Among such places one can mention Tharsis plateau, a region west from Syrtis Major characterized by intense water transport, the vicinity of Hellas and other.

The preliminary concept of science package includes:
meteo complex installed at all stations;
cameras and solar photometers for monitoring dust activity in the atmosphere;
seismometer, installed on 2 to 3 stations;

penetrating probe for measurements of soil heat and electric conductivity, installed at stations located in the areas with active water cycle.

The orbiter will carry instruments for Mars climate studies, including high resolution IR spectrometer and wide-angle hyperspectrometer that will provide observations of clouds, ices and frosts with broad coverage and high temporal resolution.

If implemented in reasonable term and continued with successive missions, this project not only promises to deliver the unique results, but also to become a pioneering step towards permanent human presence on the Martian surface.

MARS BALLOON REVISITED

M. J. Blamont, *CNES, 2 place Maurice Quentin 75039 PARIS cedex 01.*
Contact: jacques.blamont@cnes.fr

After the success of the NASA Mars rovers missions and high resolution images taken from ESA and NASA Mars orbiters, some unique domains of the research remain open for Martian ballooning. A list of scientific objectives and experiments for a Martian balloonmission will be proposed and a frame of international cooperation.

VENERA-D – THE FUTURE RUSSIAN MISSION TO VENUS

Zasova L.V.[1], Korablev O.I.[1], Zelenyi L.M.[1], Khartov V.V.[2], Martynov M.B.[2], Pichkhadze K.M.[2], Vorontsov V.A.[2], Elkin K.S .[3], Voron V.V.[4], Marov M.Ya.[5], Zakharov A.V.[1], Sanko N.F.[1], Basilevsky A.T.[5], Chukkov I.V.[1], Gavrik A.L.[6], Gerasimov M.V.[1], Gotlib V.M.[1], Grigoriev A.V.[1], Gromov V.[1], Ignatiev N.I.1, Khavroshkin O.B.[7], Klimov S.I.[1], Ksanfomaliti L.V.[1], Lipatov A.N.[1], Linkin V.M.[1], Liash A.[1], Mitrofanov I.G.[1], Moshkin B.E.[1], Nazarov Petrukovich A.[1], Skalsky A.A. [1], Tuchin A.[8], Vaisberg. O.L.[1], Zastenker G.N.[1], and the Venera-D team, *[1]IKI RAS, [2]NPOL, [3]TSNIIMASH, [4]Roscosmos, [5]GEOKHI RAS, [6]IRE RAS, [7]IFZ RAS, [8]IAM RAS. E-mail: zasova@iki.rssi.ru*

Venus was actively studied by Soviet and US missions in 60-80- th years of the last century. The investigations, carried out both from the orbit and in situ were highly successful. After a 15-years break in space research of Venus, the ESA Venus Express mission, launched in 2005, successfully continues its work on the orbit around Venus. In 2010 JAXA Akatsuki (Venus Climate Orbiter) was launched. However, many questions, concerning the structure and evolutions of planet Venus, which are the key questions of comparative planetology, very essential for understanding the evolution of the terrestrial climate, cannot be solved by observations from an orbit.

Now in Russia the new phase of Venus investigation begins: the mission Venera-D is included in the Russian Federal Space Program to be launched in 2016-2017. The conception of the mission is under discussion: descending probe(s) , orbiter., subsatellite. Proposed scientific instruments are aimed to solve the following scientific problems:

- investigation of the structure, chemical composition of the atmosphere, including noble gases abundance and isotopic ratios, structure and chemistry , microphysical properties of the clouds;
- study of dynamics of the atmosphere, nature of the superrotation, radiative balance, nature of an enormous greenhouse;
- study of structure, mineralogy and geochemistry of the surface, a search for seismic and volcanic activity, the lightening, interaction of the atmosphere and the surface;
- investigation of the upper atmosphere, ionosphere, magnetosphere and the escape rate.

Successful realization of the project Venera-D helps to solve the important scientific problems, in particular it may help to understand why do Venus and the Earth (sister-planets), being similar in many aspects, and formed at similar conditions in the protoplanet nebula evolve by such a different way.

“LUNA-GLOB” AND “LUNA-RESOURCE” MISSIONS

L.M. Zelenyi[1], V. Khartov[2], I. G. Mitrofanov[1], A. Skalsky[1], *[1]Institute for Space Research, Profsojuznaja 84/32, 117997 Moscow, Russia, [2]Lavochkin Assosiation, Russia. Contact: lzelenyi@iki.rssi.ru, imitrofa@space.ru*

Introduction: Two spacecrafts will head to the Moon in 2012 – 2013 time frame, which are landing segments of Russian mission “Luna-Glob” and joint Russian/India mission “Luna-Resource”/Chandrayaan-2. In accordance with directions of Roscosmos, these two Lunar Landers (Figure 1) will have practically identical package of scientific instruments. This decision allows to optimize the development, manufacturing and verification process of these instruments, as well as minimize funds for supporting this work.

Both Landers are designed for polar landing. Lunar Lander of “Luna-Recourse” will deliver Indian mini-rover on the lunar surface (see Figure 1). Lunar Lander of “Luna-Glob” will has boring system onboard. Both Landers have identical Manipulators for delivering samples to on-board analytic instruments.

In this talk the science program of two Landers will be presented, which will be based on capabilities of the selected package of the instruments. This talk will be done on behalf of Science Lead of the project, PIs of selected instruments and payload management in IKI and in Lavochkin association.

Scientific Task of investigations on the lunar surface: (1) To study content of volatiles in the polar regolith, processes volatiles transport and accumulation. To study the content of soil constituting elements for comparison with well-known samples from the middle latitudes. To measure the key isotopic ratios of lunar material.

(2) To study lunar exosphere at polar region, including dust and neutrals, and also to investigate the interaction of solar wind with the surface. To study dynamic diurnal processes at lunar poles, including thermal variations of subsurface.

Instrument package of Lunar Landers: (1) *Complex of instruments on Manipulator.* Three small instruments will be installed on the Manipulator arm: IR spectrometer LIS, Visual/UF spectrometer and Camera of Working Field (CWF). Total mass of this complex is about 2 kg.

(2) *Complex of instrument for in-situ analysis of samples.* The largest instrument of the mission is Gas Analytic Complex, which includes Thermal Differential Analyzer, Gas Chromatograph and Mass Spectrometer and has a mass about 10 kg. Second analytic instrument is Laser Mass Spectrometer (LASMA) (2.4 kg).

(3) *Instruments for remote sensing and contact measurements*. This complex includes nuclear instrument ADRON for active neutron and gamma-rays analysis of nuclear composition and layering structure, Radiometer-Thermometer (RT) will measure variations of subsurface temperature down to 1 meter with discreetness of 15 cm and accuracy of 1 degree. In parallel, Contact Thermometer (CT) will measure temperature on the surface and in the hole made by boring system of “Luna-Glob” Lander. Instrument PmL will measure dust flux on the lunar surface, and two instruments LINA and ARIES will measure charge particles and neutrals at landing site. Instrument SEISMO will monitor seismic activity on the Moon with ability for cooperation in future with another seismic instruments on the lunar surface.

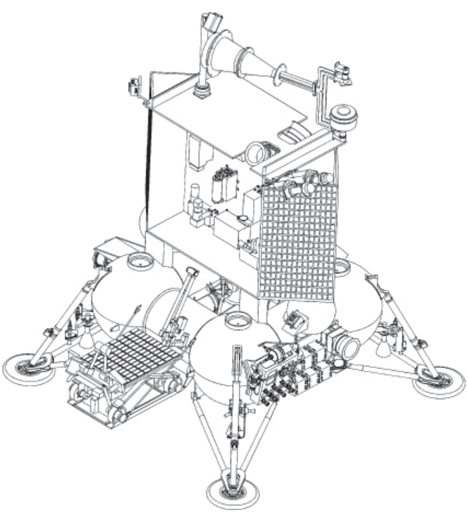

Fig. 1: Concept view of Lunar Lander for “Luna-Resource” mission. Indian mini-rover is also shown onboard this Lander, which is replaced by boring system onboard Lander of “Luna-

Scientific Groups of Lunar Landers: Scientific support teams will be created for scientific support of investigations on the lunar surface:

(1) Landing site selection Team (LSST). The team will suggest the best candidate sites for landing of “Luna-Glob” Lander.

(2) Team of surface operations (TSO): The team will develop the program of investigations on the surface by instruments of the Landers.

THE EUROPA JUPITER SYSTEM MISSION: INVESTIGATING THE EMERGENCE OF HABITABLE WORLDS AROUND GAS GIANTS.

D. Senske[1], R. Pappalardo[1], L. Prockter[2], J-P. Lebreton[3], R. Greeley[4], E. Bunce[5], A. Coustenis[6], M. Dougherty[7], O. Grasset[8], *[1]Jet Propulsion Laboratory/California Institute of Technology, 4800 Oak Grove Dr., Pasadena, CA 91109, USA; [2]Johns Hopkins University Applied Physics Laboratory, Maryland, USA; [3]RSSD, ESA/ ESTEC, The Netherlands; [4]Arizona State University, Arizona, USA; [5]University of Leister, United Kingdom; [6]Observatoire de Meudon, France; [7]Imperial College, United Kingdom; [8]University of Nantes, France. Contact: david.senske@jpl.nasa.gov*

Introduction: Jupiter is the archetype for the giant planets of the Solar System and for the numerous planets now known to orbit other stars. Jupiter's diverse Galilean satellites—three of which are believed to harbor internal oceans—are the key to understanding the habitability of icy worlds. The Galilean satellites are quite distinct with respect to their geology, internal structure, evolution, and degree of past and present activity. To place Europa and its potential habitability in the right context, as well as to fully understand the Galilean satellites as a system, the two internally active ocean-bearing bodies — Europa and Ganymede — must be understood. Thus, the Europa Jupiter System Mission (EJSM) is guided by the overarching theme: *The emergence of habitable worlds around gas giants* [1,2].

EJSM Mission Overview: The EJSM mission would consist of two major flight elements, the NASA-led Jupiter Europa Orbiter (JEO) and the ESA-led Jupiter Ganymede Orbiter (JGO). Aiming for an energetically very favorable launch opportunity in 2020, both spacecraft would arrive in the Jupiter system in 2026. Carrying eleven complementary instruments on each platform, the overall mission architecture provides opportunities for coordinated observations by JEO and JGO of the Jupiter and Ganymede magnetospheres, the volcanoes and torus of Io, the atmosphere of Jupiter, and comparative planetology of the icy satellites. Each spacecraft can and will conduct "stand-alone" measurements, including detailed investigations of Europa and Ganymede.

Science Goals and Objectives: The specific science to be achieved by this mission centers around three goals: (1) Explore Europa to investigate its habitability (JEO-focus); (2) Characterize Ganymede as a planetary object including its potential habitability (JGO-focus) and (3) Explore the Jupiter system as an archetype for gas giants (JEO + JGO) The last goal would be addressed primarily during a tour phase of the mission, lasting upwards of 2.5-years, whereby each spacecraft would perform multiple Galilean satellite fly-bys and make measurements of Jupiter and the Jupiter system.

Europa. Europa is believed to have a saltwater ocean beneath a relatively thin and geodynamically active icy crust and is unique among the large icy satellites because its ocean is in direct contact with its rocky mantle beneath. As such, the conditions could be similar to those on Earth's biologically rich sea floor. The discovery of hydrothermal fields on the Earth's sea floor suggests that such areas are excellent habitats, powered by energy and nutrients that result from reactions between the seawater and silicates. Consequently, Europa is a prime candidate in the search for habitable zones and life in the solar system. However, the details of the processes that shape Europa's ice shell, and the fundamental question of its thickness, are not well understood.

Ganymede. Ganymede is believed to have a liquid ocean sandwiched between a thick ice shell above and high-density ice polymorphs below, more typical of volatile-rich icy satellites. It is the only satellite known to have an intrinsic magnetic field, which makes the Ganymede-Jupiter magnetospheric interaction unique in the Solar System.

Io. The innermost of the Galilean satellites, Io is undergoing intense tidally driven volcanism. Io is important for understanding Europa because it illuminates Europa's own tidal heat engine and provides a window on Europa's silicate interior, and also because it is a potentially major source of contamination of Europa's surface. Io is also fascinating in its own right, as an extreme, readily-studied, example of interior, volcanic, atmospheric, and plasma processes that are important throughout the solar system.

Callisto. As the outermost large satellite of Jupiter, Callisto is the least affected by tidal heating and the least differentiated, thus offering an "endmember" example of satellite evolution for the Jovian system. Accordingly, assessing its internal structure, geologic history, compositional evolution, impact cratering history, and radiolysis of its surface are important to understanding the evolution of the Jovian satellites.

Jupiter System. Europa and Ganymede formed out of the Jovian circumplanetary disk and have evolved through complex interactions with the other satellites, Jupiter, and Jupiter's magnetosphere. To understand the potential habitability of Europa and icy moons in general, it is critical to understand how the intricately related components of the Jovian system originated and evolved, and how they currently operate and interact. This requires observations of the Jovian magnetosphere and particle environment, the planet Jupiter itself, and the minor satellites and ring system.

Conclusions: Operation of two spacecraft in the Jupiter system provides the unparalleled opportunity to address the high-priority science questions posed by the NASA Decadal Survey and ESA Cosmic Vision for exploration of the outer solar system. The EJSM mission concept represents a conservative and robust design approach to successfully answering these high-priority questions and making a major step forward in understanding the emergence of habitable worlds around gas giants.

References: [1] Jupiter Europa Orbiter, JPL Document, D-48297, 2008.
[2] Europa Jupiter System Mission, Joint Summary Report, JPL Document, D-48440, 2008.

EUROPA LANDER: MISSION CONCEPT AND SCIENCE GOALS.

L. Zelenyi[1], O. Korablev[1], M. Martynov[2], E.L. Akim[3], A.T. Basilevsky[4], N. Eismont[1], A. Fedorova[1], V.F. Galchenko[5], M. Gerasimov[1], O. Kozlov[1], L. Ksanfomality[1], I.V. Lomakin[2], G. Managadze[1], M. Podzolko[6], G.A. Popov[7], A.V. Simonov[2], A. Sukhanov[1], E. Vorobieva[8], Y. Agafonov[1], O. Prieto-Ballesteros[9], M. Blanc[10], J.P. Lebreton[11], R. Pappalardo[12] and the Europa Lander Team, *[1]Space Research Institute (IKI), Moscow, Russia; [2]Lavochkin Assosiation, Russia; [3]Keldysh Institute of Applied Mathematics; [4]Vernadsky Inst., Moscow, Russia; [5]Winogradsky Inst of Microbiology, Moscow, Russia; [6]Skobeltsyn Institute of Nuclear Physics, Moscow State University, Russia; [7]NII PME, Russia; [8]Moscow State University Soil Science Fac., [9]Centro de Astrobiología INTA, Spain, [10]Ecole Polytechnique, France; [11]ESA ESTEC, Netherlands, [12]JPL, USA.*
contact: lzelenyi@iki.rssi.ru, korab@iki.rssi.ru

Introduction: Starting from 2007 Russian Academy of Sciences and Roscosmos considers the possibility to include Europa surface element in the EJSM international mission to Jupiter system. The main scientific objectives of the Europa lander will be to search for signatures of possible present and extinct life, in situ studies of Europa internal structure, surface and environment. Clearly, remote investigations from the orbit around Europa would not be sufficient to fully address astrobiology, geodesy, and geology goals.

Science Goals of Europa Lander Mission and Possible Measurement Strategies: Scientific questions to be addressed by instruments on the surface of Europa and even by deep submarine expeditions were extensively discussed in the refereed literature (Chyba and Philips, 2001; Cooper et al., 2003; Gershman et al., 2003; Zimmerman et al., 2005; Langmaier and Elliott, 2008 and the references therein). We repeat some most obvious science goals, effectively addressed by surface science.

The main scientific questions of Europa exploration can be formulated as follows:

- Is there a liquid water beneath the ice crust of Europa?
- Does the global ocean really exist on Europa?
- What is the depth and distribution of the icy crust?
- Are environmental conditions on Europa suitable for life?
- Are there traces of extinct life on Europa?
- Are there evidences of life on Europa at present time?

Clearly, remote studies from the orbit around Europa would not be sufficient to fully characterize surface environment and to address astrobiology goals. Measurements on the surface are important for geodesy and geology, to study the Europa ocean and to characterize locally the ice crust. Laplace-Europa Lander project will tackle the fundamental questions of internal structure, surface environment, and habitability of Europa. The main objectives of the mission will be to softly land on the chosen location, to collect multiple samples from one or multiple nearby sites to provide access to the shallow subsurface (to reach unaltered by radiation material). The landing site will be selected using the most accurate remote imagery to land on geologically youngest area, and to probe the material as recently exposed to the surface as possible. The following science and measurement objectives are being considered:

- To corroborate the theory of the liquid ocean, to characterize of the thickness and stiffness of the icy crust, to study the internal structure by means of different geophysical measurements; to characterize the seismicity of Europa, and to measure the magnetic field on the surface
- To conduct a detailed study of surface material, characterize physical [electrical and heat conductivity, stiffness, etc.] and chemical [pH, redox potential] parameters, analyze the composition of ice and admixtures, including isotopic ratios by means of gas chromatography with mass spectrometry (GCMS) and other methods;
- To characterize environment with particular attention to its capability to support life, and to search the traces of extinct or extant life in the surface and shallow subsurface [organic components, anions, cations, salinity, elements relevant to primary biological productivity, e.g. N, O, P, S, Mg, potential metabolism products], isotopic composition [$^{13}C/^{12}C$, $^{15}N/^{14}N$, etc] at high sensitivity, by means of GSMS, Raman spectroscopy, other methods;
- To conduct observations and measurements in regional, local and micro scales, to study morphology and mineralogy of the surface and to validate remote orbital observations;
- To perform local measurements of radiation conditions, secondary ions, exosphere of the satellite and volatiles near the surface [CH_4, NH_3, CO_2, etc.].

A list of potential experiments to be considered on the surface of Europa, and their relevance to three major classes of science goals: Conditions, Composition, and Habitability is presented in Table 1. This list comprises many duplicating experiments, and should not be considered as a model payload, but rather as a long list of potential candidates to the model payload. Most of these methods contribute to the assessment of the habitability of Europa, and many chemical analysis experiments have a high potential for biochemical detection of life (see Table 1). Specific life-contrasting tests might include isotopic ratios (GCMS and TDLAS, but likely concentration needed); chirality (difficult detection by UV methods, Raman, could also be assessed by GCMS); wet chemistry set, and immuno-arrays.

A strategy to assess the feasibility of these experiments and a proper balancing between instruments proposed for a direct search of life and instruments for standard/advanced in-situ chemical and physical characterization of Europa is to be developed.

The most trustworthy experiments to be put on the surface of Europa identified so far are:

- seismometer, to estimate the thickness of the ice,
- a set of sensors for physical characterization
- chemical analytic package with high exobiology potential, based on GCMS
- IR spectrometer to link orbital and surface measurements
- a set of cameras, and microscopes

Three method to sample the surface, which are potentially compatible with the resources allocation of the lander are: the robotic arm/grinder, a drill to reach the depth of several tens of cm and to deliver the sample into the lander, and a melting probe with a mass of ~5 kg (1 kg instrument) to reach the depth of ~3 meters.

The science goals of the orbital element of the Laplace-Europa Lander mission are still to be considered. It is reasonable to duplicate some key investigations of NASA JEO, e.g., high-resolution imaging for landing site selection, lidar to characterize the figure of the satellite, near-IR mapping spectroscopy for surface composition, possibly a long-wave penetrating radar to map the thickness of the ice crust. A number of complementary measurements will be considered, to characterize in situ the ion and neutral composition of Europa environment, to measure the radiation dose, and to perform remote studies of Jupiter and other satellites.

Mission concept: The proposed space mission to Europa will include following basic stages: Interplanetary flight to Jupiter; Flight in the Jupiter-dominated zone; Insertion into an orbit around Europa and landing. A heavy-class launch vehicle “Proton” with upper stage booster “Breeze-M” is necessary to carry out the spacecraft (SC) to the escape trajectory.

In the vicinity of Jupiter a series of gravitational maneuvers near Galileo satellites will be conducted in order to minimize propellant mass during the insertion into the orbit around Europa. Any space mission to Jupiter system faces a considerable problem of radiation hazard. Lengthy approach to the planet is unacceptable due to enormous cumulative radiation dose, destroying the electronics of the spacecraft. The trajectory in the vicinity of Jupiter is chosen in order to minimize the duration of the trajectory within Europa orbit, and to exclude whenever possible entering within Io orbit. Estimations of charged particle fluxes and radiation doses under various shielding in different parts of the trajectory were made using different empirical models at each stage of the computations.

Following these basic considerations, the sequence of gravitational maneuvers in the vicinity of Jupiter has been chosen to be completed within less than two years. In the end of this stage the SC will be inserted into a circular polar orbit round Europa.

From this orbit remote studies of the surface will be conducted. The landing site meeting certain topography conditions will be chosen, also using the results of observations from EJSM Laplace Europa orbiter (JEO) led by NASA.

The landing module will be separated to perform an active soft landing onto the surface. The orbital module remains on the orbit and serves as a relay for the lander.

Preliminary estimations show that the mass allocation for scientific equipment on the orbital module is about 50 kg, and on the landing device – about 60 kg.

Phase 0 of the Europa Lander project has been started in 2009..

FAST FLIGHT TO THE BOUNDARY OF SOLAR SYSTEM FOR PRECISION MEASUREMENTS OF NOT GRAVITATIONAL INFLUENCES ON SPACECRAFT.

Linkin V. M, Gotlib V. M, Lipatov A.N., Manukin A.B., Ejsmont N.A., *Space Research Institute (IKI), Moscow, Russia*

The variant of fast flight to the boundary of Solar system for revealing of the reasons of anomalies in movement of spacecrafts the Pioneer-10 and the Pioneer - 11 is offered., The spacecraft project, the scenario of flight and a ballistic estimation, the possibilities of creation precision accelerometers with the permission 10-11 m/sec^2, possibilities measurement by radio engineering means of parameters of relative movement of the test masses which have been taken out from spacecraft are discussed. Possibility of realisation of the project with the general duration of flight less than 6,5 years is shown.

SCIENTIFIC PROGRAM OF THE PHOBOS-SOIL MISSION

L. Zelenyi, A. Zakharov, *Space Research Institute, Moscow, Russia.*
Contact: zakharov@iki.rssi.ru

Abstract: Phobos-Soil is a robotics mission to study a Martian moon Phobos under development now in Russia [Zelenyi et al. 2010]. The main goal of the mission is to deliver samples of the Phobos surface material to the Earth for laboratory studies [Galimov, 2010]. Other goals are studies of Phobos in situ and remote sensing during the spacecraft orbital motion, some experiments devoted studies of the Martian environment.

Remote sensing of the Phobos from the spacecraft orbiting at a very close to Phobos synchronous orbit will be directed to study global parameters of this body and to select a landing site for the spacecraft [Bazilevsky and Shingareva]. After landing of the spacecraft at the Phobos surface and take off the returned spacecraft with samples loaded in the returned capsule in situ science experiments will study chemical and mineralogy composition of the regolith near the landing place, study internal structure of this body, peculiarities of orbital and proper rotation.

The drive for Phobos investigation is strongly supported by the need to understand the basic scientific issues related to the Martian moons both as the representatives of the family of the small bodies in the Solar system and as principal components of the Martian environment: primordial matter of the Solar system (what many believe they are). The main goals of the mission are: (a) study physical and chemical characteristics of the Phobos regolith in situ and under laboratory conditions — these data can provide information on properties of primordial matter of the Solar system; (b) study of the origin of the Martian satellites and their relation to Mars — these data can help in our understanding of their evolution and the origin of satellite systems near other planets; (c) study of peculiarities of orbital and proper motion of Phobos, what is important for understanding their origin, internal structure, celestial mechanics applications; (d) study physical conditions of the Martian environment (dust, gas, plasma components) what is important to study of treatment processes of small body regolith under influence of external conditions and creation of engineering model of the Martian environment for future Martian missions; (e) monitoring of dynamic of the Martian atmosphere.

The science payload includes a number of science instruments: chromatograph, mass spectrometers, gamma and neutron spectrometers, IR spectrometer, radar, seismometer, dust sensor, plasma package. Scientific problems, goals and methods of Phobos study by the Phobos Sample Return mission payload are described in the paper.

References: L. M. Zelenyi, A. V. Zakharov, G. M. Polischuk, and M. B. Martynov, Project of the Mission to Phobos, Solar System Research, Vol. 44, No. 1, 15, 2010.
E. M. Galimov Phobos Sample Return Mission: Scientific Substantiation, Solar System Research, Vol. 44, No. 1, 5, 2010.
E. L. Akim, G. S. Zaslavsky, I. M. Morskoy, E. G. Ruzsky, V. A. Stepaniants, and A. G. Tuchin Primeval Substance Delivery from Phobos to the Earth —The Phobos–Soil Project: Ballistics, Navigation, and Flight Control, Solar System Research, Vol. 44, No. 1, 26, 2010.
A. T. Bazilevsky and T. V. Shingareva The Selection and Characterization of the Phobos-Soil Landing Sites, Solar System Research, Vol. 44, No. 1, 38, 2010.

SCIENTIFIC GOALS OF PHOBOS SAMPLES LABORATORY STUDIES (PHOBOS-SOIL PROGRAM)

E.M. Galimov, Yu.A. Kostitsyn, *Vernadsky Institute of Geochemistry and Analytical Chemistry*

Space mission to Phobos was suspended four times and now is planned to start in the fall of 2011. The main goal of the mission to the Mars' satellite is collection of soil samples from the Phobos surface and delivery them to Earth at 2013 for comprehensive laboratory studies. General success of the project depends on many technical and natural factors. However, the mission could be recognized as successful only in case if delivered material is studied and newly obtained scientific results are adequate to the great efforts spent for the space project realization. Our labs must be ready for the extensive studies of the Phobos material in advance.

Phobos is more useful then Moon for testing some long lasting important problems of satellites formation due to its small size, mass and especially its average density. Phobos specific gravity is only 1.85 g/cm^3 that suggests its high porosity (up to 1/3 of its volume) or high ice content, up to half of its mass. This implies that Phobos was not differentiated like planets or Moon and excluding some obvious surface alterations the material should preserve its pristine composition. This is a key point for resolving some important questions, particularly about genetic relations between Phobos and Mars.

Modern hypotheses of Phobos formation could be divided into two groups. Some of them relate formation of Phobos as well as another Mars' satellite, Deimos to catching of asteroids by Mars. Others explain the satellites origin in terms of processes of their common formation from the primary gas-dust cloud. Both groups of hypotheses have arguments both 'pros' and 'cons' and it is the Phobos samples study that could give us a solution to the problem. If Phobos is a captured asteroid then it could be close in composition to any known class of meteorites, probably to some group of ordinary or carbonaceous chondrites. If Phobos and Mars were formed from the same gas-dust source it should be close in composition to available SNC meteorites, which as supposed were knocked out from Mars by impact events. Thus, researches of Phobos material should give us an answer to a fundamental question, how planets' satellites were formed. Obviously the question directly concerns the Earth-Moon system formation. If, for example, Phobos material is close to SNC meteorites in terms of noble gases abundance pattern or by oxygen isotopic composition like this is the case for Earth and Moon, then the idea of contemporaneous formation of planets and their satellites from gas-dust cloud will get a very significant confirmation. If a compositional distinction between Phobos and Mars is found then a capture model will be more real for the satellite origin despite of small probability of such an event.

Beside the test of a genetic link between Phobos and Mars material there are other important questions, answers to which could be found during the study: to what extent the Phobos material is primitive, is it identical to any type of carbonaceous chondrites; does Phobos material contain relict components; what types of processes could have altered Phobos material; chronology of early events on Phobos; what kind of organic compounds (if any) does Phobos material contain, etc.

A general overview of demanded analytical equipment and techniques for these studies will be presented as well.

PHOBOS-SOIL MISSION CONCEPT AND CURRENT STATUS OF DEVELOPMENT

M.Martynov, V. Khartov, *Lavochkin Association, Khimky, Moscow region, Russia*

The Phobos-Soil project is under development now in Russia. The main goals of the mission are delivery of samples of the Phobos surface material to the Earth and in situ studies of Phobos and the Martian environment.

The presentation will display the Phobos-Soil spacecraft, what includes four main elements: a transfer-orbital module, a main propulsion system, a return module and a landing capsule. Results of the spacecraft development, its tests and the current status of the mission preparation will be done in the presentation.

THE PHOBOS–GRUNT PROJECT: BALLISTICS, NAVIGATION, AND FLIGHT CONTROL

E.L. Akim[1], G.S. Zaslavsky[1], I.M. Morskoy[2], E.G. Ruzsky[2], V.A. Stepanyants[1], V.A. Sishov[1], A.G.Tuchin[1], *[1]Keldysh Institute of Applied Mathematics, Russian Academy of Sciences, Miusskaya pl. 4, Moscow, 125047 Russia, [2]Lavochkin Research and Production Association, Khimki, Moscow oblast, Russia*

This paper is concerned with the problems of ballistics, navigation, and flight control of the spacecraft (SC) in the Phobos–Grunt mission. We consider an insertion into the Earth–Mars transfer trajectory, the strategy of corrections, and the accuracy of the insertion of the SC into Martian orbit. During the orbital maneuvering stage in the sphere of influence of Mars, we set up a scheme that allows for the insertion of the SC, with the prescribed accuracy, into a point 40-80 km above the Phobos surface over the theoretical landing area. We specify the sequence for a controlled landing and provide methods for solving the problems of navigation and control during a self contained landing. We also consider the liftoff from Phobos, insertion into the parking orbit, and the Mars–Earth transfer.

FOBOS-GRUNT LANDING SITE SELECTION.

A. T. Basilevsky, T.V. Shingareva, *Vernadsky Institute of Geochemistryand Analytical Chemistry, RAS, Kosygin Str., 19, 119991Moscow Russia.*
Contact: atbas@geokhi.ru

The main goal of the Fobos-Grunt mission is to return samples of material of the Martian satellite Phobos (Figure 1) to the Earth for studying in laboratories. For this, it is planned to land on Phobos, to collect samples within the reach of the robotic arm of the sampling unit, to load them into the return capsule, and to deliver them to the Earth.

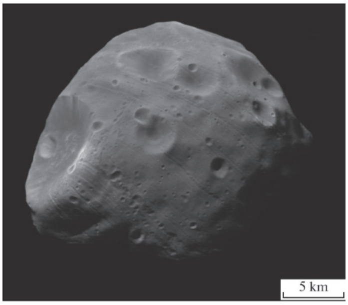

Fig. 1: The image of Phobos obtained with the Mars Express HRSC camera on August 22, 2004 from orbit 0756. ESA/DLR/FU Berlin (Neukum).

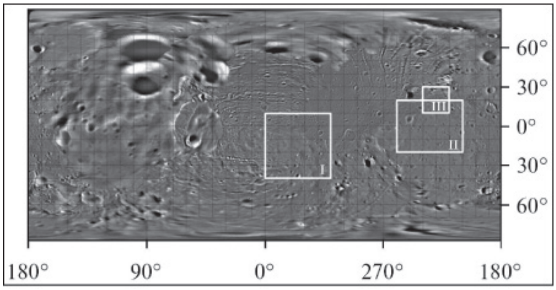

Fig. 2: The scheme of the prospective landing sites for the Fobos-Grunt spacecraft: the first (I), the second (II), and the suggested third (III) regions.

The region for the Fobos-Grunt landing site was selected on the basis of the ballistic and engineering requirements for landing security. The surface of the region should be of minimal roughness: without complicated relief structures (large craters and grooves), significant differences in altitude, and strongly rugged relief. When working on the Fobos-Grunt project, two regions on the surface of Phobos were recommended for the landing: the first one is on the side facing Mars, and the second one is on the far side (I and II in Figure 2).

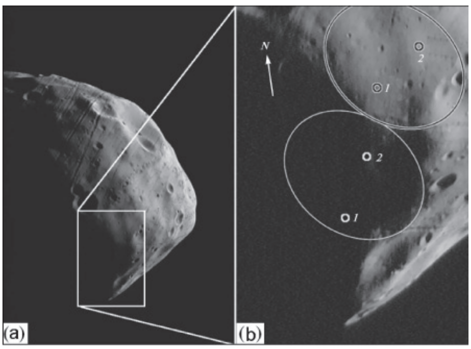

Fig. 3: (a) The image of Phobos taken from orbit 5851. (b) The blow-up of fragment of the same image, where the approved (the lower ellipse) and suggested (the upper ellipse) landing areas are shown. The white numbers indicate the planned landing sites in the approved region, and the black numbers, in the suggested region. ESA/DLR/FU Berlin (Neukum).

Since the available images of these regions of the surface of Phobos were made with a low resolution and under the conditions of the high Sun above the horizon, the authors and their colleagues suggested that the landing site should be shifted to the northeast of the last target area II, while remaining within the boundaries of the second approved landing region (III in Figure 2). The radius of the new target area (a circle) is 4 km, and the approximate coordinates of the center are 15°N, 230°W.

Characteristics of this new landing area have been studied through analysis of the HRSC images taken on July 23, 2008 from Orbit 5851 (Figure 3).

The Mars Express is planned to continue to flyby Phobos so new analyses of this new landing area are expected to be fulfilled. Meanwhile DLR Institute of Planetary Sciences, Berlin, Germany, and MIIGAIK Institute, Moscow, Russia are working on the precious determinations of the landing site coordinates.

Acknowledgments: We are grateful to G. Neukum for providing us the HRSC images; to B. Gilze and P. Thomas for providing the digital map of the Phobos surface; and to R.O. Kuzmin, E.V. Zabalueva, and V.P. Shashkina for their help in performing this study.

SCIENCE GROUND SEGMENT FOR PHOBOS-SOIL MISSION.

V. Nazarov[1], R. Nazirov[1], A. Zakharov[1], E. Larionov[1], A. Kruglov[2], A. Chebotarev[3], A. Shirshakov[4], Yu. Kazakevich[4], A. Kalyuta[5], *[1]IKI RAN, [2]RKS «Systema», [3]OKB MEI, [4]S.A. Lavochkin IA, [5]Space Forces, Ministry of Defense*

Science Ground Segment is intended for information support of all problems related to control of on-board science complex. Such tasks as telemetry processing, visualization, data archiving, user' access, information exchange with other system involved in the mission are covered by Science Ground segment as well as a set of other important tasks.

As Science Ground Segment is a one of the key component of the project and so it should be built on the base of modern information technologies from one side, and taking in account experience of development and maintenance of the similar systems created early from another one.

The article describes general principles of design of the Science Ground Segment, its basic functions and characteristics.

OVERVIEW OF THE YH-1 SCIENCE DATA SYSTEM

Ziming Zou, *Center for Space Science and Applied Research, Chinese Academy of Sciences, P.O.Box 8701, Beijing 100080, China. Contact: mzou@cssar.ac.cn*

Introduction: Yinghuo-1 Mars Mission is the first deep space exploration of China. This presentation firstly introduces the framework and components of the Ground Science Data System of YH-1 Mars Mission, including related software development and hardware deployment, and then represents the science data archiving work of the mission, which is in accordance with the NASA Planetary Data System, including data processing levels classifying, data archive organizing, naming and distributing, finally illustrates how to access the YH-1 science data archives of different payloads via the portal of the YH-1 Science Data Archiving System.

PDS ANALYST'S NOTEBOOK: SUPPORTING ACTIVE SURFACE MISSIONS AND ADDING VALUE TO NASA PLANETARY DATA ARCHIVES THROUGH INTEGRATION OF MISSION DATA AND DOCUMENTS

T.C. Stein[1], [1]*Washington University in St. Louis, One Brookings Drive, CB 1169, St. Louis, MO 63130, USA. Contact: tstein@wustl.edu*

The Planetary Data System (PDS) Analyst's Notebook (http://an.rsl.wustl.edu) provides access to the NASA Mars Exploration Rover (MER), NASA Mars Phoenix Lander, and NASA Lunar Apollo sur-face mission data archives. In addition, a Notebook is being developed for the NASA LCROSS mission.

Mars mission data are enriched by integrating se-quence information, engineering and science data, observation planning and targeting, and documenta-tion into web-accessible pages to fa-cilitate "mission replay." This provides context needed by scientists to understand observations made by these nondetermi-nistic surface missions. Historical data from the Apollo missions are presented along with associated documentation and links to external holdings.

Each Notebook contains data, documentation, and support files for a given mission. For MER and Phoenix, inputs are incorporated on a daily basis during the active mission phase into a science team version of the Notebook. The public version of the Analyst's Notebook is comprised of peer-reviewed, released data and is updated coincident with PDS data releases as defined in mission archive plans.

Apollo data are organized by mission, instrument, and station. Data are added to the Notebook as they are restored from original tapes, reports, and micro-film. Where data have not been restored the user is redirected to external data providers such as the Na-tional Space Science Data Center (NSSDC).

A number of methods allow user access to the Notebook contents. The feature set of each Note-book varies, depending on the types of input available. These include mission summary tables, timelines, maps, data and document searches, and additional resources (Fig. 1).

Work continues to incorporate additional Apollo missions within the Analyst's Notebooks framework. In addition, a Notebook is planned for the Mars Science Laboratory mission. For existing Notebooks, planned improvements include better accuracy of maps and easier data download. A number of Note-book functions are based on previous user sugges-tions, and feedback continues to be sought.

The Analyst's Notebook is developed through funding provided by the Planetary Data System Geosciences Node, the Mars Exploration Rovers Mission, and the Phoenix Mission. Cooperation of the MER and Phoenix science and operations teams is greatly appreciated.

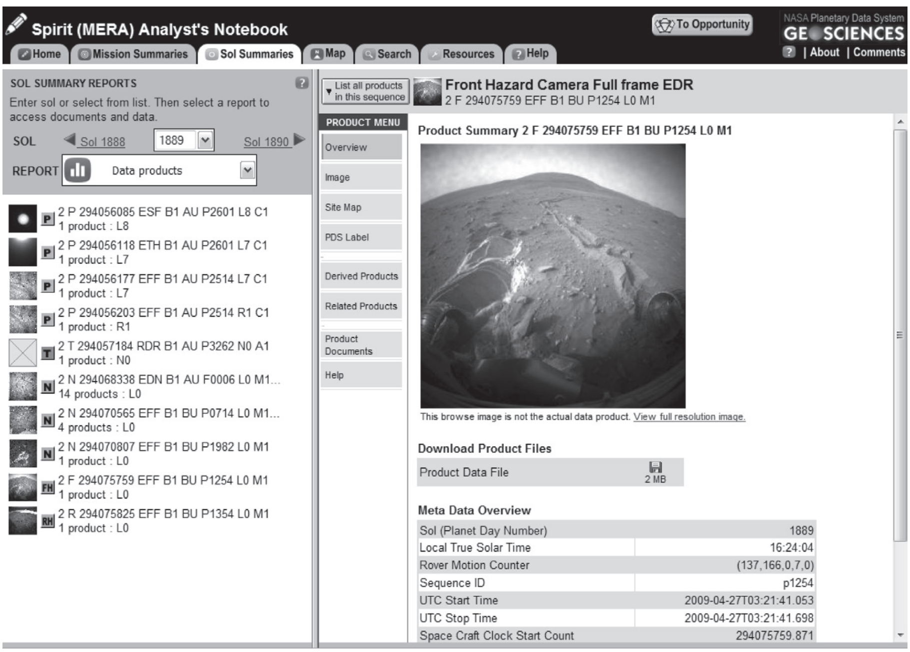

Fig. 1: Example MER Analyst's Notebook web page.

SOLUTIONS FOR PLANETARY PROTECTION ISSUES IN PHOBOS – SOIL EXPEDITION.

N.D. Novikova[1], O.I. Orlov[1], E.A.Deshevaya[1], V.N. Sychev[1], N.M. Khamidullina[2], S.N. Aleksashkin[2], M.B. Martynov[2], *[1]State Scientific Center of the Russian Federation – Institute for Biomedical Problems of the Russian Academy of Sciences, Moscow, Russia; [2]Lavochkin Association, Roscosmos, Khimki, Moscow region, Russia. Contact:novikova@imbp.ru*

The launch of a Russian spaceship to Phobos is being planned in 2011 as a part of the project “Phobos-Soil”.

Major goals and mission objectives of the project “Phobos soil” are:

- Landing of the orbital vehicle (transport module) on the Phobos surface, collecting soil samples for delivery to Earth in a sealed indestructible container;
- Exobiological experiments aimed to evaluate viability of dormant organisms-representatives of a variety of taxonomic groups after extended interplanetary trip.

According to COSPAR classification the orbital Mars spaceship flight is related to the category III and the mission of Phobos soil delivery to the Earth in a capsule on a descent vehicle is related to the category V to which any missions of return to the Earth are related. In order to supply Mars and Earth protection a number of actions is worked out:

- the probability of space craft destruction and its falling down on the Mars surface is limited, and that is proved by the calculations;
- the proposals to break the “chain of contact” with Earth of equipment used on the Phobos surface;
- preservation of tightness of the containers with Phobos soil and biological samples should be provided at all the stages of the mission up to the landing onto the Earth;
- Phobos soil and biological samples delivery to specialized organization licensed to carry out works with highly dangerous microorganisms should be organized.

So severe measures of the planet protection are based not only on the COSPAR demands, but also on the results of the Russian exobiological experiments, which proved that ability of survival in outer space was shown experimentally not only for spores of bacteria and microscopic fungi, but also for resting stages of higher organisms.

RADIO ASTRONOMY EXPERIMENTS WITH PLANETARY PROBES IN THE MARTIAN SYSTEM

L.I. Gurvits[1], S.V. Pogrebenko[1], G. Cimò[1], L.L.A. Vermeersen[2], T. Bocanegra Bahamon[2], G. Molera Calvés[3], D.A. Duev[4], V.M. Gotlib[5], A.S. Kosov[5], V.M. Linkin[5], A.N. Lipatov[5], I.A. Strukov[5], S.G. Turyshev[6], *[1]Joint Institute for VLBI in Europe, Dwingeloo, The Netherlands; [2]Delft University of Technology, Delft, The Netherlands; [3] Aalto University, Helsinki, Finland; [4]Moscow State University, Moscow, Russia; [5]Space Research Institute, Moscow, Russia; [6]Jet Propulsion Laboratory, Pasadena, CA, USA. Contact: lgurvits@jive.nl*

Radio astronomy experiments with planetary probes proved to be a powerful tool for multi-disciplinary scientific applications. We present scientific objectives, technical requirements and status of preparatory activities for the Planetary Radio Interferometry and Doppler Experiment (PRIDE) in adaptation for the Phobos Sample Return mission (PRIDE-Phobos). The science goals of PRIDE-Phobos are:

- Study of the internal mass distribution of Phobos;
- Precise estimates of the celestial mechanics parameters and their evolution for Phobos and Mars;
- Estimates of the parameters of the Areocentric dynamical system in ICRF;
- Gravitational physics experiments.

PRIDE-Phobos will be conducted with the Phobos landing vehicle and a network of Earth-based radio telescopes in the interests of multidisciplinary studies requiring precise estimates of the lander's state vector which in turn enables estimates of the orbital parameters of Phobos. The experiment will exploit the technique demonstrated recently in the Huygens VLBI Experiment and a number of other radio astronomy experiments with planetary missions conducted during the last few years.

The on-board instrumentation of the Phobos lander involved in PRIDE measurements includes an X-band (8.4 GHz) transmitter, Ultra-Stable Oscillator (USO) and medium-gain antenna. The Earth-based segment of PRIDE-Phobos includes deep space tracking stations, VLBI radio telescopes and data processing centres. The data measurements obtained with PRIDE-Phobos will be analysed in concurrence with data obtained with other on-board instruments, e.g. gravimeters and seismometers. PRIDE-Phobos will conduct measurements of three physical values:

- radial distance using the methods employed by the deep space navigation network;
- radial velocity using both a standard service two-way link radio system and a one-way (down-only) system based on the on-board USO;
- angular position relative to background radio sources using the VLBI technique.

The quality of scientific data obtained in PRIDE-Phobos will depend critically on the robustness and intrinsic accuracy of methods and algorithms of data processing, as well as the instrumental set-up of the network of radio telescopes. In order to verify and tune-up PRIDE-specific data processing pipeline, our group has conducted a number of preparatory observations of the ESA Venus Express and Mars Express spacecraft. In one of these test observations, three European VLBI Network stations (Metsähovi, Finland; Wettzell, Germany; and Yebes, Spain) observed the MEX spacecraft during its Phobos flyby on 2010 March 03. This test offered a very convenient opportunity to verify the PRIDE setup in the conditions practically coinciding with those of the Phobos Sample Return mission. The test confirmed that PRIDE-Phobos would meet requirements of high-precision characterisation of the spacecraft state vector required by the scientific objectives of the experiment.

The VEX and MEX PRIDE observations allowed us also to study phase fluctuations of the spacecraft carrier signal which provided information for characterization of the interplanetary plasma density fluctuations along the signal propagation line at different spatial and temporal scales and different Solar elongations. This type of scientific application of PRIDE-Phobos data will be exercised during the Phobos Sample Return mission in-flight operations in addition to the main objectives of the experiment.

The work described here was in part carried out the Jet Propulsion Laboratory, California Institute of Technology, Pasadena, California, under a contract with the National Aeronautics and Space Administration.

IN SITU MASS SPECTROMETRIC ANALYSIS IN PLANETARY SCIENCE.

P. Wurz[1], M. Iakovleva[1], M. Tulej[1], and G. Managadze[2], *[1]Physics Institute, University of Bern, Sidlerstrasse 5, 3012 Bern, Switzerland; [2]Space Research Institute (IKI), ul. Profsoyuznaya 84/32, Moscow, 117997, Russia.*
Contact: peter.wurz@space.unibe.ch

Introduction: Knowing the chemical, elemental, and isotopic composition of planetary objects allows the study of their origin and evolution within the context of our solar system. In the optimal case, such studies are performed in situ with dedicated mass spectrometer systems. Therefore, mass spectrometers have been part of the early lunar missions, have been successfully employed in Mars, Venus, Jupiter, Saturn, and comet missions, and are also foreseen for many planetary missions currently in planning.

Mass Spectrometric Investigation of Atmospheres: Mass spectrometric analysis of an atmosphere is relatively straight forward since the sample to investigate is already in the gas phase. Depending on the relative speed of the spacecraft with respect to the atmospheric gas specialised inlet systems might become necessary. Additionally, a gas-chromatographic column has been for sample preparation in same applications. Many different mass spectrometer types have been used in the past, with magnetic sector instrument and quadrupol analysers being used most often [e.g. Niemann et al., 2002]. Recently, high performance time-of-flight (TOF) systems became available, e.g. for cometary research [Scherer et al., 2006; Balsiger et al., 2007]. TOF systems have the advantage of a large mass scale, larger mass resolution, and larger sensitivity. The latter in part because TOF systems do not need to perform a mass scan, but measure the whole mass spectrum at once. For future mission these will be clearly the systems of choice, in particular when the object of interest can only be studied in a flyby mission scenario.

Mass Spectrometric Investigation of Surface Material on Planetary Bodies: Exploration plans in planetary research of several space agencies consider landing spacecraft for future missions. Although there have been successful landings of spacecraft in the past, more landers are foreseen for the Moon, for Mars and its moons, Venus, asteroids, and possibly even for some of the jovian moons. Furthermore, a mass spectrometer on a landed spacecraft can assist in the sample selection in a sample-return mission and provide mineralogical context, or identify possible toxic soils on Mars for manned Mars exploration. Given the resources available on landed spacecraft mass spectrometers, as well as any other instrument, have to be highly miniaturised. In recent years there has been an effort by several groups to develop highly miniaturised instruments [Managadze & Shutyaev, 1993; Brinckerhoff et al., 2000; Rohner et al., 2003, 2004]. These instruments are based on high intensity pulsed lasers removing material from a rock (or other solid), atomising and ionising the material and analysis of the ions by time-of-flight analysis. Such a system has been developed for the updoming Phobos-Grunt mission [Wurz et al., 2009].

References: H. Balsiger, K. Altwegg, P. Bochsler, P. Eberhardt, J. Fischer, S. Graf, A. Jäckel, E. Kopp, U. Langer, M. Mildner, J. Müller, T. Riesen, M. Rubin, S. Scherer, P. Wurz, S. Wüthrich, E. Arijs, S. Delanoye, J. De Keyser, E. Neefs, D. Nevejans, H. Rème, C. Aoustin, C. Mazelle, J.-L. Médale, J.A. Sauvaud, J.-J. Berthelier, J.-L. Bertaux, L. Duvet, J.-M. Illiano, S.A. Fuselier, A.G. Ghielmetti, T. Magoncelli, E.G. Shelley, A. Korth, K. Heerlein, H. Lauche, S. Livi, A. Loose, U. Mall, B. Wilken, F. Gliem, B. Fiethe, T.I. Gombosi, B. Block, G.R. Carignan, L.A. Fisk, J.H. Waite, D.T. Young, and H. Wollnik, “ROSINA - Rosetta Orbiter Spectrometer for Ion and Neutral Analysis,” Space Science Review 128 (2007), 745–801.
W B. Brinckerhoff, G.G. Managadze, R.W. McEntire, A.F. Cheng, and W.J. Green, “Laser time-of-flight mass spectrometry for space” Rev. Sci. Instrum. 71 (2000), 536-545.
Managadze, G.G., and I. Yu. Shutyaev (1993), in Laser Ionization Mass Analysis, Chemical, Analysis Series Vol. 124, Wiley, New York, Chapter 5.
H.B. Niemann, S.K. Atreya, S.J. Bauer, K. Biemann, B. Block, G.R. Carignan, T.M. Donahue, R.L. Frost, D. Gautier, J.A. Haberman, D. Harpold, D.M. Hunten, G. Israel, J.I. Lunine, K. Mauersberger, T.C. Owen, F. Raulin, J.E. Richards and S.H. Way, “The Gas Chromatograph Mass Spectrometer for the Huygens Probe” Space Sc. Rev. 104 (2002) 553–591.
Rohner, U., J. Whitby, and P. Wurz, A miniature laser ablation time-of-flight mass spectrometer for in situ planetary exploration, Meas. Sci. Technol., 14, (2003) 2159–2164.
Rohner, U., J. Whitby, P. Wurz, and S. Barabash, A highly miniaturised laser ablation time-of-flight mass spectrometer for planetary rover, *Rev. Sci. Instr.,* 75(5), (2004) 1314–1322.
S. Scherer, K. Altwegg, H. Balsiger, J. Fischer, A. Jäckel, A. Korth, M. Mildner, D. Piazza, H. Rème, and P. Wurz, “A novel principle for an ion mirror design in time-of-flight mass spectrometry,” Int. Jou. Mass Spectr. 251 (2006) 73-81.
P. Wurz, J.A. Whitby, and G.G. Managadze, “Mass Spectrometry in Planetary Science,” AIP Conf. Proc. CP1144 (2009) 70-75.

ON CHEMICAL ANALYSIS OF SOLIDS BY MINIATURE LASER -ABLATION TOF MS DESIGNED FOR SPACE RESEARCH

Marek Tulej, Maria Iakovleva, Andreas Riedo, and Peter Wurz, *Institute of Physics, Space Research & Planetary Sciences, Sidlerstr. 5, 3012 Bern, Switzerland. Contact: marek.tulej@space.unibe.ch*

The laser ablation time-of-flight mass spectrometry (LA-TOF MS) is a well established analytical method for investigation of chemical composition of solid materials. It is widely applied in various research fields where elemental and isotopic composition is of interest [Vertes et al, 1993]. Miniaturized mass analysers have been recently developed for space research [Brinckerhoff et al. 2000; Rohner et al., 2003, 2004] and are considered to be important part of the instrumentation dedicated to study planetary surfaces. Miniaturized LA-TOF mass spectrometer can be used for a rapid analysis of the entire elemental and isotopic composition of surface without its further preparation. Both lateral and vertical resolution can be achieved providing possibility for in-depth profiling and microanalysis. Microscopic mineral grains or non-altered material can be identified by means of elemental composition. The instrument can also measure trace and rare earth elements providing important data for studies of the nature of planetary differentiation and geological origin. The age dating of the material can be determined from isotopic patterns of radiogenic elements. The isotopic composition of bio-relevant elements is also of considerable interest to astrobiology. Bio-related isotopic anomalies have been well investigated in various terrestrial environments and their measurements on surfaces of other planets can provide important proves for the past and present live activities.

The performance of a laser ablation mass spectrometer (LMS) developed in our group for applications in space research will be demonstrated. The instrument is a small size reflectron-type time-of-flight mass spectrometer which can be coupled with various laser sources for ablation of the material. [Rohner et al., 2003]. The initial studies were conducted using IR output of Nd:YAG laser (λ = 1064 nm, τ=4ns) but the investigations involving other laser systems and wavelengths are underway. To establish quantitative capabilities of our instrument, NIST standard reference materials were investigated first. Initial measurement show that an effective dynamic range spanning seven decades can be achieved by combining spectra recorded in low and high gain channels. By using IR laser for the ablation, the method can be considered as a quasi-quantitative for the measurements of heavier elements (amu > 39), the quantitative detection of the lighter elements (e.g., C, P, S) is less accurate. The isotopic fractionation effects are small and typically do not exceed 1%. The mass spectra are measured with mass resolution exceeding (m/Δm) 600 and highly average spectra can be acquired. Measurements of minerals and meteoritic samples demonstrate potential of the mass analyzer for application to sensitive detection of elements in realistic samples. Figure 1 shows the mass spectrum of Galena (PbS) mineral (Kenguru, Congo) recorded in high gain (HG) channel. The quantitative detection of the isotopic abundances of Pb and S can be made with accuracy better than 1%. This implies that abundances of Pb isotopes can be used for age dating of the sample. A number of trace elements including Cu, Ag, Cr, Fe and Cd are also observed.

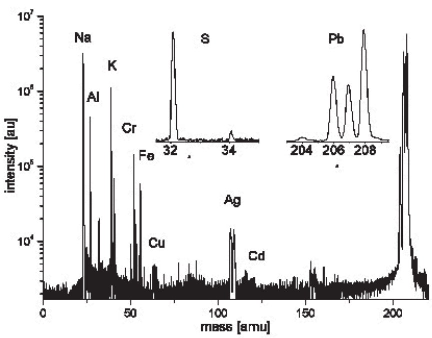

Fig. 1: HG mass spectrum of Galena. The spectra of the isotopic components of S and Pb are shown in the inserts. The effective dynamic range is ~6 decades.

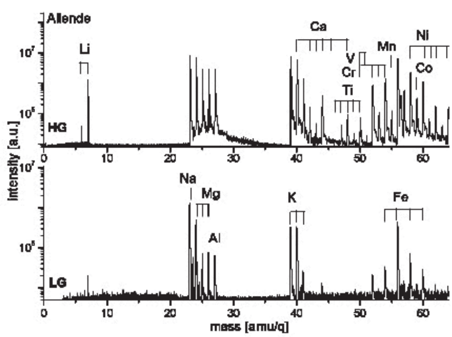

Fig. 2: Portions of the LG and HG mass spectrum of Allende meteorite (heterogeneous sample).

Figure 2 shows the HG mass spectrum of Allende meteorite. The spectrum can be analyzed in the effective dynamic range of 6-7. The studies demonstrate that measurements of elemental abundances can be used for identification of the meteoritic materials. High sensitivity and quantitative capabilities in measurements of the isotopic composition can be useful in studies of the isotopic anomalies caused by natural processes.

References: Brinckerhoff, W. B., G. G. Managadze, R. W. McEntire, A. F. Cheng and W. J. Green, Laser time-of-flight mass spectrometry for space, Rev. Sci. Instr., 71(2), 536–545, 2000.
Rohner, U., J.A. Whitby, P. Wurz, A miniature laser ablation time of flight mass spectrometer for in situ planetary exploration. Meas. Sci. Tech., 14, 2159-2164, 2003.
Rohner, U., J. Whitby, P. Wurz, and S. Barabash, A highly miniaturised laser ablation time-of-flight mass spectrometer for planetary rover, Rev. Sci. Instr., 75(5), 1314–1322, 2004.
Vertes, A., R. Gijbels and F. Adams, Laser Ionisation Mass Analysis, New York, Wiley, 1993.

DETERMINATION OF THE MARS GRAVITY FIELD FROM TWO SATELLITES' ORBITS DATA: A SIMULATION

C. L. Huang[1], M. Zhang[1], Z. Z. He[1], *[1]Shangha Astronomical Observatory, 80 Nandan Road, Shanghai, China. Contact: clhuang@shao.ac.cn*

Introduction: There are several models of the Mars gravity field published, mostly from the Doppler tracking data of the Mars Global Surveyor (MGS) spacecraft and partly from other spacecrafts around the Mars like Mars Odyssey and Mars Express (MEX), as well as the mission in the early age (Viking series). Unfortunately, most of these satellites are near-polar orbits, and due to the shortage of the method commonly used in the calculation of spherical harmonic coefficients of the gravity field, as a result, these spherical harmonic coefficients derived from one single orbiter or these similar orbits' data will suffer, more or less, from the so-called "lumped" phenomenon, i.e., the lower-degree coefficients are 'contaminated' from, or contain the influence of, higher-degree zonals.

The Chinese-Russian collaborated Mars mission is scheduled to be launched in Nov. 2011. In Chinese side, a satellite, YH-1, will run around the Mars for about 1 year. Thanks to the special characteristic of the orbit of YH-1, especially its low inclination, one can expect its radio tracking data to contribute the study of the Mars gravity field.

In this study, the radio tracking data of YH-1 is simulated. After integrating with other available Doppler tracking data, mostly of the MGS, we try to analysis how the YH-1 data help to improve the Mars gravity field, especially in the low latitude band zone in which most of the large-scale topographic characteristic area locate.

TO PROMOTE THE RADIO SCIENCE PROGRESS IN THE YH-1 MISSION

J. S. Ping, S.J. Zhang, T.T. Han, H.J. Yan, K. Shang, M.Y. WANG, *Shanghai Astronomical Observatory, CAS, Shanghai, Nandan Rd. 80.*
Contact: China pjs@shao.ac.cn

Introduction: China and Russia are planning to launch a joint Mars mission in 2011. In the joint mission, the 1st Chinese Mars Probe, Yinghuo-1 will explore the space weather of the Mars, and will test the deep space navigation techniques. Open-loop methods like DOR/DOD and 1-way Doppler are developed and applied to determine the s/c orbit and position.

Using the open-loop method, radio scientific experiments, like radio occultation (RO) and celestial mechanics (CM) will be study.

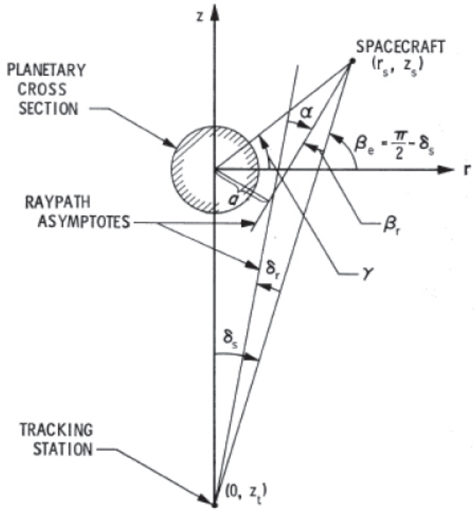

Fig.1: Ray path geometry of RO experiment

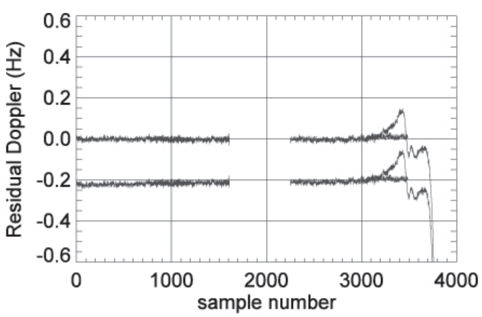

Fig.2: MEXMRS_0046 and X-band Doppler residuals before and after baseline correction.

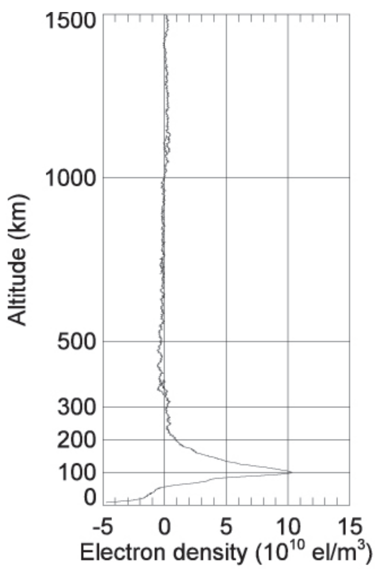

Fig.3: Derived ionosphere electron density profiles from MEXMRS_0046 X-band observation.

DEVELOPMENT OF SELENODETIC INSTRUMENTS FOR JAPANESE LUNAR EXPLORER SELENE-2

H. Hanada[1], H. Noda[1], F. Kikuchi[1], S. Sasaki[1], T. Iwata[2], H. Kunimori[3], K. Funazaki[4], H. Araki[1], K. Matsumoto[1], S. Tazawa[1], S. Tsuruta[1], , *[1]National Astronomical Oservatory, Oshu, Iwate 023-0861, Japan; [2]Institute of Space and Astronautical Science, JAXA, Sagamihara,Kanagawa 252-5210, Japan; [3]National Institute of Information and Communications Technology, Koganei, Tokyo 184-8795, Japan; [4]Iwate University, Morioka Iwate 020-8551 ,Japan. Contact: hanada@miz.nao.ac.jp*

Introduction: Japan will launch a lunar landing mission (SELENE-2) on the nearside of the moon, following the successful KAGUYA (SELENE). We propose instruments measuring lunar rotation and gravity field on board SELENE-2 and successors: iV-LBI (Inverse VLBI), LLR (Lunar Laser Ranging) and ILOM (In-situ Lunar Orientation Measurement). New observations with higher accuracy will contribute to improve the lunar gravity model and the lunar rotation model, and obtain new information related to properties of the lunar core and the mantle.

iVLBI (Inverse VLBI): Very long baseline interferometry (VLBI) is conventionally used for precise positioning of radio source. Radio signal transmitted from radio source, such as a quasar, is received at two separate ground VLBI stations, and the direction of the source is known from the time difference in arrival time of the signal. Inverse VLBI, on the other hand, measures the time difference in arrival times of radio signals transmitted from two radio sources. The radio sources are loaded on such as orbiter and lander, and radio signals transmitted from them are received at a ground VLBI station. These signals are cross-correlated and the difference of propagation times from vehicles to the ground station is measured.

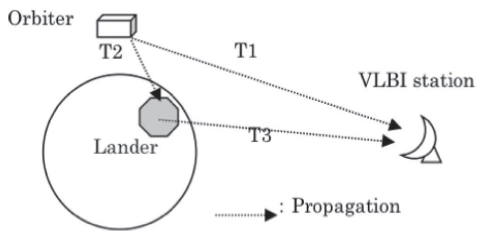

Fig. 1: The principle of inverse VLBI in the case of an orbiter and a lander.

The desired accuracy of the measurement is predicted to from several tens to several pico seconds. In the case of inverse VLBI for lunar observations, artificial radio sources are loaded on orbiters or landers on and around the Moon.

LLR (Lunar Laser Ranging): We are proposing to put a new retro-reflector on the Moon in order to expand the network of retro-reflectors and to make it possible for many ground stations to participate in the observations, and thus to improve the accuracy of LLR.

We started developing a single large CCR for better precision, and the following things are under consideration:

1. CCR type (a large single CCR; prism vs hollow)
2. Thermal design of CCR
3. Mount of CCR component (pointing toward mean-earth direction within ~2 degrees accuracy)
4. Domestic ground laser link station

ILOM: In-situ Lunar Orientation Measurement (ILOM) uses a kind of telescope for positioning astronomy on the Moon. A telescope of the photographic zenith tube (PZT) type set near the lunar pole determines the orientation of the axis of rotation of the Moon by positioning of several tens of stars in the field of view regularly for longer than one year. The PZT is suitable for a positioning telescope on the moon, since a mercury pool set at the middle point of the focal length compensates the tilt of the telescope caused by unequal thermal expansion. Star positions are recorded with a CCD camera and the center of the star image is measured with an accuracy of 1/1,000 of a pixel size.

We have already developed a BBM of the PZT and made some experiments in order to know the performance of the driving mechanism under the similar conditions to the lunar environment showing high vacuum, large temperature change and dusty condition. Optimization of the optical design of the PZT for attaining of such a high accuracy on the Moon is one of the most important and difficult problems.

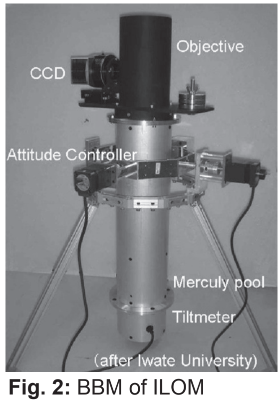

Fig. 2: BBM of ILOM

DEVELOPMENT OF THE SUBMILLIMETER INSTRUMENT ONBOARD JAPANESE MARTIAN ORBITER

Y. Kasai[1], T. Kuroda[2], H. Sagawa[1], P. Hartogh[3], D. Murtagh[4], MELOS SMM Sounder Team, *[1]National Institute of Information and Communications Technology, Koganei, Tokyo, Japan; [2]Institute of Space and Astronautical Science/JAXA, Sagamihara, Kanagawa, Japan, [3]Max Planck Institute for Solar System Research, Katlenburg-Lindau, Germany; [4] Chalmers University of Technology, Göteborg, Sweden. Contact: ykasai@nict.go.jp*

Introduction: Submillimeter remote sensing, in particular that employing the heterodyne technique, from the Martian orbit is a powerful and epoch-making tool for studying the Martian atmosphere. A number of strong spectral signals of key molecules to understand Martian atmosphere, such as H_2O, CO, HDO, H_2O_2, HO_2, OH, etc., are found in the submillimeter wavelength. The high frequency resolution of the heterodyne technique allows us to measure accurate line shapes of those molecular transitions. The pressure dependency of their line shape can be used to retrieve the vertical profiles of the temperature and molecular abundances from the measured spectra. Furthermore, the Doppler shift of the molecular transitions due to the winds on Mars can be also observed in the limb viewing geometry.

Another unique point of the submillimeter observation is that the Martian dust becomes almost transparent because of largeness of the observation wavelength compared to the dust particle size. Therefore, the submillimeter observations have an advantage in monitoring the Martian atmospheric state without being affected by the dust condition.

Such promising capabilities of the submilliemeter heterodyne observation for the Martian atmospheric research has been demonstrated by very recent successful Herschel/HIFI observations [e.g., Hartogh et al. 2009; 2010a, b]. Herschel/HIFI enables sensitive submillimeter observations from the space without being disturbed by the terrestrial atmosphere. However, one drawback of Herschel observations is that it cannot resolve the Martian disk because of rather large distance between Mars and Herschel (L2 point of the Sun-Earth-Moon system) and of limitation in the aperture size of the telescope. We consider the spatially resolved mapping from Martian orbit is the utmost priority for the next step of the submillimeter remote sensing of Mars.

Japanese Future Mars Mission: The Japan Aerospace Exploration Agency (JAXA) has started the pre-phase A study for the future Mars exploration mission. The mission is named MELOS which is an abbreviation of "Mars Exploration with Lander-Orbiter Synergy", a full explanation of how the mission looks like: it consists of one/two landers and one/two orbiters with different orbits. The launch is planned in 2020 or 2022. The scientific objective of one orbiter is the Martian meteorology, and we are now proposing a submillimeter instrument to this orbiter.

The draft design of our instrument is optimized to observe at the frequency band of 500 and 600 or 800 GHz. Such a dual band system enables us to observe multiple water vapor lines with different line strengths. Combination of the observations of weak and strong opacity lines improves the vertical sensitivity to the water vapor abundance: from the surface to ~100 km, depending on the orbit and the observation geometry. The current estimation for the mass and the power is 20 kg and 40 W, with leaving a high possibility of further miniaturization and power-saving.

Hartogh, P. et al. (2009), Planetary and Space Science, 57, 1596-1606.
Hartogh, P. et al. (2010), Astronomy and Astrophysics, in press, arXiv:1007.1301.
Hartogh, P. et al. (2010), Astronomy and Astrophysics, in press, arXiv:1007.1291.

FOUR-WAY DOPPLER MEASUREMENTS AND INVERSE VLBI OBSERVATIONS FOR MARS ROTATION OBSERVATIONS

T. Iwata[1], Y. Ishihara[2], Y. Harada[3], K. Matsumoto[2], F. Kikuchi[2], S. Sasaki[2],
[1]Institute of Space and Astronautical Science, Japan Aerospace Exploration Agency, Sagamihara, Kanagawa 252-5210, Japan; [2]National Astronomical Observatory of Japan, Oshu, Iwate 023-0861, Japan; [3]Shanghai Astronomical Observatory, Shanghai 200030, China. Contact: iwata.takahiro@jaxa.jp

Introduction: Variation of planetary rotation provides us information concerning both of an interior structure and surface mass redistribution. Such information is valuable for elucidating not only present condition but also evolution of a planet as a system. Precession and nutation of Mars reveal the core-mantle subsystem, besides length-of-day variation and polar motion of Mars show atmosphere-cryosphere subsystem

Precession and length-of-day variation have been measured by means of tracking data of Viking 1 and 2, and Mars Pathfinder (ex. Folkner et al., 1997). Results of the Love number k2 obtained by two Martian explorers, namely, Mars Global Surveyor (MGS) and Mars Odyssey, predict existence of a liquid core on Mars (ex. Yoder et al., 2003; Konopliv et al., 2006). Seasonal variation of the polar caps on Mars was estimated mainly based on the laser altimeter data on MGS in conjunction with gravity data (ex. Smith et al., 2001).

These measurements had, however, limitations in terms of accuracies within the framework of traditional technologies concerning space geodesy and astrometry. Thus, the new configurations of orbiterto-lander tracking have been proposed (ex. Yseboodt et al., 2003; Dehant et al., 2009). On the other hand, the Japanese research group has started to plan the new Martian explorer; MELOS (Mars Exploration with Lander-Orbiter Synergy). As one of the missions of MELOS, we are proposing areodetic observations using space geodetic techniques like as four-way Doppler measurements and inverse VLBI.

Four-way Doppler measurements: Four-way Doppler measurements (FWD) are ranging rate measurements of target spacecrafts via relay spacecrafts (ex. Iwata et al., 2010). Utilizing the heritage of FWD by SELENE (Namiki et al., 2009), we plan to track the MELOS Lander relayed by the MELOS Orbiter. The carrier links of the four-way are shown as a solid line in Figure 1. Two-way ranging and ranging rate (RARR) measurements for each spacecraft are executed simultaneously. The ranging signal links are dotted lines in Figure 1. The expected accuracies for these observations are almost in the same order as that in the case of satelliteto-lander tracking (Yseboodt et al., 2003).

Inverse VLBI: We also introduce the new technology called inverse VLBI (Kawano et al., 1999). One ground radio telescope, not a VLBI network, observes both the orbiter and the lander with same-beam or switching differential VLBI. The signals from the orbiter are coherently locked with those of the lander. Dashed lines in Figure 1 indicate these carrier links. One of the remarkable performances of inverse VLBI is that the theoretical accuracy of positioning depends only on the observation frequency and does not depend on the baseline length. Therefore, X-band observation of inverse VLBI will achieve the accuracy of 0.3 mm which is much better than that of FWD, RARR, and differential VLBI. Including the systematic phase noise, the accuracy for the rotation is estimated as less than 3 mas.

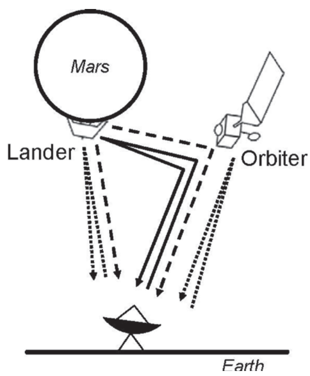

Fig. 1: A mission concept of Mars rotation observations proposed for MELOS. Solid, dotted, and dashed lines indicate the links for 4-way Doppler measurements, 2-way ranging and ranging rate, and inverse VLBI, respectively.

References: Dehant, V., et al., Planet. Space Sci., 57, 1050 (2009). Folkner, W. M., et al., Science, 278, 1749 (1997). Iwata, T., Transact. JSASS Spa. Tech. Japan, in press (2010). Kawano, N., et al., J. Geod. Soc. Japan., 45, 181 (1999). Konopliv, A. S., et al., Icarus, 182, 23 (2006). Namiki, N., et al., Science, 323, 900 (2009). Smith, D. E. et al., Science, 294, 2141 (2001). Yoder, C. F., et al., Science, 300, 299 (2003). Yseboodt, M., et al., J. Geophys. Res., 108, 12 (2003).

OPTIMISM (MARS-96) SCIENTIFIC EXPERIMENT REVIVAL

P. Schibler[1,2], P. Lognonne[1,3], J. Gagnepain-Beyneix[1], A. Anglade[1,2], T. Gabsi[1,2], T. Nébut,[1,2], *[1]Institut de Physique du Globe de Paris, 4 avenue de Neptune, 94100 Saint-Maur, France; [2]CNRS; [3]Université Paris Dide-rot. Contact: schibler@ipgp.fr*

Introduction: The objective is to realize, during three months, a seismic survey of Mars. For that, we will propose, on-board ExoMars EDL Demonstrator 2016 and on-board other possible Russian or US mission, to re-use a "on the shelf" model of the OPTIMISM seismometer which was launched by Russian Mars96 mission. This approach will minim-ize both coast and development/qualification time. Two models of OPTIMISM seismometer (Flight Model 3 and Engineering/Qualification Model) are still available at IPGP and are currently under tests. We will propose a "stand-alone packet" with its own energy and transmission devices.

Scientific objectives: The seismometer was de-signed to record long period waves. The seismic survey of Mars will allow,

- to confirm the level of μ-seismic noise;
- to detect about ten or more quakes (by P waves detection) and in a few cases (less than 5) to detect P and S waves to estimate epicentral distance;
- to better constraint global activity of Mars and so to prepare a future network mission;
- to detect some meteorites impacts.

The detection of thermo-elastic quakes should al-low to characterize the Martian conditions of propa-gation and to propose the first models of internal structure.

Although OPTIMISM's approach should be less efficient than the one based on a Very Broad Band Seismometer (as for Selene2 mission) the acquired data would be 100 times better than Viking data. So, OPTIMISM could be the first instrument to actually measure a Mars quake...

Instrument description: OPTIMISM was inte-grated inside the 2 Small Autonomous Stations of the Mars96 mission.

Seismometer specifications. The former instru-ment was composed by a seismometer and a magne-tometer. For this configuration, we propose to re-use only the OPTIMISM seismometer.

- Bandwidth: 0.02 – 2 Hz
- Volume: 9x9x9.5 cm
- Power: 67.5 mW under 15 V
- Sampling rates: 4, 1, ¼ sps
- Mass: 405 g
- Data: 1 Mbits/day expected

The half-sphere is locked in the landing situation. After landing, it levels itself by gravity with an accu-rancy better than 1°. Temperature sensors and tiltme-ters are added to the seismic outputs.

Seismic sensor is mounted inside the titanium half sphere. A leaf spring supports the pendulum. Detection of the seismic moving mass displacement is assumed by an inductive velocity sensor (sensibili-ty 0.2 nm/s) and by a capacitive position sensor (sen-sibility 0.3 nm). A motor allows the recentering of the moving mass.

Current status of OPTIMISM seismometer. More than 13 years after the launching of Mars96 mission, the different parts (sensors, hardware, software, do-cumentation, GSE) needed for integration and good working of the seismometer are still available at IPGP for a new mission. Hardware parts are the following:

Seismic sensors

- Flight Model 3: spare model of Mars96 mis-sion with a Martian spring. Qualification and delivery tests were done on this model

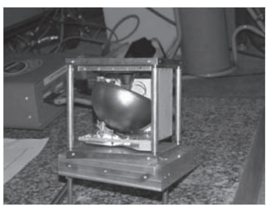

- Engineering and Qualification Model: with a terrestrial spring, qualification and delivery tests were done on this model and also shock tests (200 g, 20 ms)

Electronics parts:

- Spare Model: mounted in flight box with "savers" connectors. Tests with GSE were successful; flight EEPROM are accessible and can be easily updated

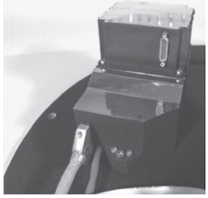

- Additional Model: for using at lab, with the same electronics boards as for the flight box

Tests for new operation of OPTIMISM seismo-meter. In December 2009, with the OPTIMISM GSE, we realized again "official and mandatory" tests and procedures, identical to those required for the delivery of the instrument to IKI at spring 1996. These two functional and environmental tests, Mod-eTest1 and Modetest2 were successful.

Then, in March 2010, FM3 sensor was installed during one week in our seismic vault nearby a terre-strial seismometer STS2 (on the same pillar) as ref-erence. We get two preliminary results: By using least square method and comparing with STS2, we get the direction of sensibility of FM3 Data recorded allowed also to retrieve, by com-parison with STS2, the amplitude answer of FM3. FM3 is still under tests in seismic vault. Further measurements will allow characterizing intrinsic noise of the instrument by cross correlation method.

Concept proposed on-board Entry, Descent and landing demonstrator Module (EDM) ExoMars 2016: To achieve the scientific objectives, OPTIMISM seismometer actually needs to work at least during 3 months on the surface of Mars. So, taking in account the constraints of science possibili-ties of the EDM, limited by the absence of long term power, we propose a concept of an "autonomous stand-alone packet", both in terms of energy and telemetry, without any specific deployment of the seismic sensor. For this, it is planned to benefit from CNES experience (batteries similar to those of Ro-setta lander, UHF transponder similar to the one proposed by CNES for ExoMars EDM 2016 and ExoMars Rover 2018).

This concept will minimize the interfaces (and the risks) with the lander. We just need that EDM would send a "wake-up signal" to "OPTIMISM re-vival" instrument before the end of EDM 8 sols life. Then "OPTIMISM revival" will start autonomously its 3 months working and should plan TM transmis-sion sequences when the orbiter will be ready to receive.

Available inputs. The 3 *i*nputs formerly used by the magnetometer in Mars96 configuration could be used by another instrument.
- 3 inputs +/-2.5V ; 100 kohms ; DC-10Hz ADC 16 Bits ; DU = 76µV
- 1 input PT1000, Acq : 1s/60sec

Energy. Prestudy with CNES expertise
- Saft LSH20 batteries (idem for Rosetta lan-der) are proposed
- 15V at -40°C, 297 Wh
- 2 strings of 5 serial mounted batteries
- 1100 g, 70x175x65 mm

OPTIMISM Data Processing Unit (ODPU). This electronics unit, dedicated to data storage and transmission is a simplified model of this devel-oped with an FPGA by ETH Zürich in the frame-work of SEIS-ExoMars and SEIS-Selene2 instrument.
- Emptying of ELEC-OPT internal memory (1 Mbits), 1 or 2 times per sol in mass memory of ODPU
- After 3 months, transmission of the whole data (90 to 180 Mbits) to the orbiter
- Working only a few minutes per sol during 3 months
- Negligible energy consumption during re-maining time

Organization/Responsibilities:
- Seismic sensor and its proximity electronics: IPGP
- OPTIMISM Data Processing Unit (ODPU), including telemetry management: ETH Zürich
- Energy: ETH Zürich
- Expertise for telemetry and energy: CNES

References: [1] B.Banerdt, Chicarro A.F., M. Cora-dini, F. Federico, R. Greeley, M. Hechler, J.M. Knudsen, C. Leovy, P.Lognonné, L. Lowry, D. Mc Cleese, C. McKay, R. Pellinen, R. Philipps, G.E.N. Scoon, T. Spohn S. Squyres, F. Taylor and H. Wänke. InterMarsnet, Phase A study report, ESA Pub, SCI(96)2, 1996. [2] P. Log-nonné, V.N. Zharkov, J.F. Karczewski, B. Romanowicz, M. Menvielle, G. Poupinet, B. Brient, C. Cavoit, A. De-sautez, B. Dole, D. Franqueville, J. Gag-nepain-Beyneix, H. Richard, P. Schibler, N. Striebig, The Seismic Optim-ism Experiment, *Planetary Space Sciences*, 46, *739-747*, ,doi : 10.1016/S0032-0633(98)00009-9, 1998. [3] Linkin, V., A.M. Harri, A. Lipatov, K. Belostotskaja, B. Derbuno-vich, A. Ekonomov, L. Khloustova, R. Krmenev, V. Ma-karov, B. Martinov, D. Nenarokov, M. Prostov, A. Pusto-valov, G. Shustko, I. Jar-vine,, H. Kivilinna, S. Korpela, K. Kumpulainen, R. Pellinen, R. Pirjola, P. Riihela, A. Sal-minen, W. Schmidt, T. Siili, J. Blamont, T. Carpentier, A. Debus, C.T. Hua, J.F. Karczewski, H. Laplace, P. Levach-er, P. Lognonné, C. Malique, M. Menvielle, G. Mouli, J.P. Pommereau, K. Quotb, J. Runavot, D. Vienne, F. Grun-thaner, F. Kuhnke, G. Mussman, R. Rieder, H. Wanke, T. Economou, M. Herring, A. Lane, C. McKay, A sophisti-cated lander for scientific exploration of Mars: Scientific objectives and Implementation of the Mars96 Small Sta-tion, *Planetary Space Sciences*, **46**, 717-737, doi:10.1016/S0032-0633(98)00008-7, 1998. [4] Gudkova, T., Lognonné, P. , Gagnepain-Beyneix, J., Seismic source inversion for Large impacts detected by the Apollo seis-mometers, Planet. Space. Science, in press, 2010

LIVING INTERPLANETARY FLIGHT EXPERIMENT (LIFE): THE FIRST DEEP SPACE TEST OF LIFE

L.D. Friedman[1], B.Betts[1], E Vorobyova[2], *[1]The Planetary Society. U.S.A. Contact: tpsldf@planetary.org, [2]Moscow State University, Russia*

Introduction: The Planetary Society has prepared a 95 gram small module containing 12 nonpathogenic, dormant, but living micro-organisms to ride aboard the Phobos-Grunt spacecraft on the round-trip Earth-Phobos-Earth trajectory. In addition a sterile mineralogical mixture inoculated by nonpathogenic methanogenic archae will be included in our capsule. Examining these micro-organisms and the soil sample after their return to Earth will provide new insight about the possibilities for transpermia (life travelling between the planets). The experiment will also provide experience for eventual handling of Mars sample returns on international missions.

The experiment samples include bacteria, animals, yeast, seeds, archaea and soil. The experiment team includes members from the United States, Russia, Germany, Turkey and Sweden. The experiment is privately funded by The Planetary Society.

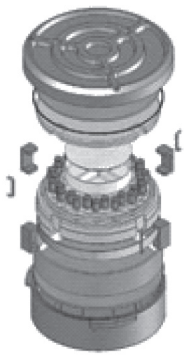

The Life Experiment Bio-Module

EXPERIMENT "BIOPHOBOS/ANABYOSIS" IN PROJECT 'PHOBOS-GRUNT"

O.I.Orlov[1], V.R.Alekseev[2], E.A.Vorobyeva[3], V.F.Galchenko[4], E.A.Deshevaya[1], A.V.Zakharov[5], M.A.Levinskikh[1], O.V.Muravenko[6], N.D.Novikova[1], S.V.Poddubko[1], N.A.Polykarpov[1], V.N.Sychev[1], *[1]SSC RF – Institute of Biomedical Problems RAS, Moscow, [2]Zoological Institute RAS, St.Petersburg, [3]Soil Science Faculty, Moscow State University, Moscow, [4]Institute of Microbiology RAS, Moscow, [5]Space Research Institute RAS, Moscow, [6]Institute of Molecular Biology RAS, Moscow*

"Phobos-Grunt" project provides a unique and the very first opportunity to estimate continues effect of deep space on survivability of resting forms or different organisms under conditions of lack of life parameters support systems. To achieve this goal, an experiment "BioPhobos/Anabiosis" was included in scientific program of "Phobos-Grunt" project.

Tasks for this experiment include:

- investigation of survival of resting stages of bacteria, fungi, animals and plants under conditions of interplanetary flights for estimation of damaging effect of factors of space environment on cryptobiotic stages of organisms and further development of technology of long-term preservation of organisms in conditions of biological resting;
- investigation of biological, biochemical and molecular-genetic changes in organisms after long-term spaceflight;
- estimation of risk related to possibility of transformation of microorganisms inhabiting the space object after their exposure to outer space with further return inside of the space object.
- comparison of survival under conditions of the spaceflight of resting stages with different level of survivability, including that of artificially induced be mean of cultivation with biologically active substances, for developing new biotechnological methods of investigations of resting stages for continuous space transportation.
- comparison of survival of resting stages of organisms under space flight conditions (BioPhobos/Anabiosis) and an orbital flight in control experiment on low Earth orbit on the outer side of RS of ISS (experiment "Biorisk-MSN")

For deposition of the biological objects in "Phobos-capsules" a methodology implemented in Russian part of "EXPOSE-R" experiment, currently being conducted on the outer side of RS ISS, will be used.

The experiment is conducted in the frame of Russian scientific program. For the experimentation, Workgroup on realization of the program of the biological investigations in the project "Phobos-Grunt" was organized by decision of "Space biology and physiology" section of RAS Council on Space Research. The Workgroup includes representatives of GSC RF – Institute of Biomedical Problems RAS, Space Research Institute RAS, Institute of Microbiology RAS, Moscow State University, Zoological Institute RAS and Institute of Molecular Biology RAS.

BIOFOBOS: INFLUENCE OF SPACE ENVIRONMENT ON SOIL MICROBIAL ECOSYSTEMS

E.A. Vorobyova, *Department of Soil Science, Lomonosov Moscow State University; Space Research Institute, Russian academy of sciences*

Microbial communities in natural habitats are protected from exposure to adverse factors. Interaction with the environment and interpopulation interactions have increased the various mechanisms of adaptation and protect cells. Therefore, undisturbed natural ecosystems should be considered among the most interesting of living objects in the study of issues of space anabiosis and transpermia.

A sample of soil, placed inside a sealed container (LIFE) will be displayed on the orbit of Mars outside the spacecraft and then delivered to Earth inside the returned capsule. The controls will be two other identical samples: one of them should be exposed to the conditions partially simulating those of the space flight (i), another one will be stored at normal conditions in the laboratory (ii). Sample of arid soil was selected in the desert Negev (Israel) and represents one of the terrestrial models of the soil of Mars.

Cultures of microorganisms isolated from the test sample will also be exhibited in the space inside another sealed container (experiment “BioPhobos / Anabiosis”), together with other cultures and biosamples. The isolated cultures will be presented by representatives of chemoautotrophic (methanogens, homoacetogens) and heterotrophic (Gram-positive and Gram-negative bacteria and eucaria) subsurface ecosystems. Control cultures will be stored under i-and ii-conditions in lyophilized and nonlyophilized state.

The following tests will be made with the initial soil samples: 1. Physico-chemical characteristics of the sample: granulo-metric composition, mineralogical analysis, pH, Eh, humidity, the content of organic matter and biologically significant ions. 2. Microbiological characterization of the sample: total count of microorganisms (bacteria, fungi) by direct microscopy (epifluorescent analysis); Direct in situ community composition studied by 16S-rRNA gene sequencing and cloning; lipid complex analysis. Diversity of methanogens will be investigated by analysing the MCR-functional gene coding the methyl-coenzyme M reductase, the key enzyme of methanogenic pathway. Micromorphological study of microorganisms in situ will be carried out by methods SEM, TEM and AFM microscopy. Metabolically active cells will be detected in situ by FISH with using oligonucleotide probes, specific for bacterial and archaeal communities. Microbial viability will be investigated studying the dynamics of in situ microbial activation and reproduction with the following isolation of pure cultures. The integral in situ biochemical activity of microbial communities as well as of isolated cultures by multi-substrate testing (ECOLOG, BIOLOG) will be evaluated. The experiments specified will be gone over with controls after finishing the space experiment.

Anaerobic microbial community will be activated by incubation on mineral medium supplemented with different substrates (peptone, glucose, acetate, trimethylamine, H_2 and CO_2) at 15°C. Enriched microbial cultures will be studied by following methods: 16S-rRNA gene analysis and cloning; Analysis of functional MCR-gens of methanogenic archaea; PCR-SSCP fingerprint analysis for investigating the community structure with detection of the key microorganisms after their activation; T- RFLP fingerprint analysis for determination of the main microbial clusters enriched their biomass after activation.

Microbial isolates should be identified, and biochemically tested. There will be a comparative analysis of viability, cyto-morphology and physiological properties of microorganisms in control and exposed soil samples (i, ii).

The Workgroup includes representatives of Lomonosov Moscow State University; Max-Planck Institute for Terrestrial Microbiology, Marburg, Germany; Technical University Braunschweig, Germany

UPDATING THE HIGH RESOLUTION PHOBOS ORTHOIMAGE MOSAIC FROM HRSC IMAGES

M. Wählisch[1], K. Willner[2], V. Schmidt[2], J. Oberst[1,2], K.-D. Matz[1], F. Scholten[1], T. Roatsch[1], H. Hoffmann[1], G. Neukum[3] *1German Aerospace Center, Rutherfordstrasse 2, 12489 Berlin, Germany; 2 Technical University Berlin, Department for Geodesy and Geoinformation Science, Straße des 17. Juni 135, 10623 Berlin, Germany; 3Freie Universität Berlin, Institute of Geographical Sciences, Malteser Strasse 74-100, 12249 Berlin, Germany. Contact: marita.waehlischr@dlr.de*

Introduction: A geometrically correct referenced global mosaic and an atlas of Phobos were published in 2008 (Wählisch et al. 2010; Willner et al., 2010) using images of the High Resolution Stereo Camera (HRSC) onboard Mars Express. This mosaic has a resolution of 16 pixel/degree or 12.010822 m/pixel relative to the reference sphere with a radius of 11.1 km. The results can be downloaded at [http://europlanet.dlr.de/Phobos].

New results: The preparation of the 2008 map was based on images of the Super Resolution Channel (SRC) of the HRSC and Viking orbiter images only. However, HRSC images, obtained recently, during various close flybys extend the coverage for different parts of Phobos' surface. This is also the case for regions of the anti Mars side that were, until now, only covered by images of the Viking orbiters. We were re-authoring the mosaic based on the additional HRSC images and modifying our mosaicing techniques. The resulting mosaic is much improved compared to the 2008 ones. Areas of overlapping images are less smeared and surface features are displayed more clearly. Our mosaic represents a planning tool for the Russian Phobos Grunt mission to be launched in 2011 (Basilevsky, 2010).

Basilevsky, A. T. and Shingareva, T. V.: The selection and characterization of the Phobos-Soil landing sites, Solar System Research, Vol. 44, pp. 38-43, Feb. 2010.

Wählisch, M., Willner, K., Oberst, J., Matz, K.-D., Scholten, F., Roatsch, T., Hoffmann, H., Semm, S., and Neukum, G.: A new topographic image atlas of Phobos, Earth and Planetary Science Letters, Vol. 294, pp. 547-553, 2010.

Willner, K., Oberst, J., Hussmann, H., Giese, B., Hoffmann, H., Matz, K.-D., Roatsch, T., and Duxbury, T.: Phobos control point network, rotation, and shape, Earth and Planetary Science Letters, Vol. 294, pp. 541-546, 2010.

MODELING OF STEREO IMAGE PROCESSING FOR CONTROL POINT CATALOGUE USING NEW DATA IN FRAME OF «PHOBOS – GRUNT» PROJECT

S. S. Dubov, D. M. Zhukov, K. M. Zel'kov, A. E. Zubarev, A. A. Konopikhin, B. V. Krasnopevtseva, I. E. Nadezhdina, I. Y. Rozhnev, K. B. Shingareva, *Moscow State University for Geodesy and Cartography, Moscow, 105064, Gorokhovsky per. 4, Russia. Contact: kirash1@yasenevo.ru*

Introduction: It is prepared the analyses of coordinate knowledge accuracy for spacecraft "Phobos — Grunt" landing site module by its coming to Mars satellite surface. It is shown that in order to provide large scale mapping on the landing site region it is necessary to develop the special global photogrammetric control point net, i.g. a new or renew catalogue. Till now a number of the images made from high orbits by different spacecrafts give us in general a possibility to create such a map. But it must be taken into account that large scale images on proposed landing site which can be used for this net were absent. It is possible to do such images only from quasisyncronised orbit by means of special cameras placed on spacecraft "Phobos-Grunt". In this case it will be very short time interval for information processing on the Earth and creation of large scale ortophotoplan for spacecraft module landing site. The details of proposed solution are discussed.

CLOSE ENCOUNTERS OF THE “PHOBOS-GRUNT” SPACE PROBE WITH INTERPLANETARY METEOR STREAMS

A.V.Bagrov, *Institute for Astronomy RAS,Moscow, Russia*

Meteor showers those are usual from the Earth observations, as they cross ecliptic plane at the distance of 1 a.u. from the Sun. Any meteoroid stream that exists in the Solar System and never crosses the Earth’s orbit cannot be observed at al. These streams may be indicated by observations of periodic comets. Comet’s evolution leads to eruption of meteoroid particles from comet core, which produce meteoroid swarm that remain on the parent comet orbit. So known comet orbits may be proposed as direct indicators of interplanetary meteoroid streams orbits. Positions of patches that indicate regions of crossing of ecliptic plane by proposed meteoroid streams are calculated. They must be viewed as regions of real meteor hazard for interplanetary space voyages along trajectories in the ecliptic plane. The number of old meteoroid streams, produced by nowadays totally decayed comets, has to be tens and hundreds times more then known comets. It seems reliable that they are homogeneously distributed over plane of interplanetary trajectories.

Any meteoroid stream that yearly encounters the Earth is permanently widened by its gravity by scheme of “gravitation maneuver”. The older is meteor stream the wider is pencil of its particles orbits. As for interplanetary meteoroid streams that never come close to large planet, they can be widen very slowly due to gravitation influence of giant planets that is weak at large distances to them. So the supposed width of interplanetary meteor showers is practically stable and equal to the initial one. We know example of young meteor shower that is observed from the Earth, but still is not noticeably widen by its gravitation. The famous star storm Leonides is only 200000 km across. At distances more than 100000 km from its axis, spatial dense of its particles became negligible. If we adopt this value as ordinary one for interplanetary meteor showers widths, we can estimate probabilities of dangerous encounters of space probes with meteoroid swarms for any planned orbit. It is strongly desirable to view out planned orbit of Martian probes to decrease risk of their breaking.

By the schedule of 2009 planned trip to the Phobos the probe had to cross the orbit of comet 9P/Tempel-1 at distance 0.00421 a.u. = $6{,}298 \cdot 10^6$ km or only at distance 63 times above radius of dense swallow. Taking in account that real position of meteoroid swallow may vary due to giant planets influence some tens million km, the risk of collision with killing meteor at the 300-th flight day was inadmissible. Newly planned mission has to be carefully examined for such risk.

ESTABLISHING OF FINE CO-ORDINATE FRAME FOR MARS AND ATMOSPHERE-LESS BODIES

A.V.Bagrov, *Institute for Astronomy RAS,Moscow, Russia*

Any co-ordinate frame must be based on fixing its null-points on the surface of a space body. For the Earth such points were positions of special Earth-based astronomical observatories as Greenwich, Paris or Pulkovo (today our geodesic frame uses Greenwich meridian as the null one). Nor Moon, nor Mars and nor any other body of the Solar system has astronomical observatory on their surfaces. Mapping of these surfaces may be detailed as fine as it is possible for mapping technique. But mapping does not mean establishing co-ordinate frame due to various aberrations of optical mapping systems and restriction to the accuracy of fixation null-point by their resolution power.

It is proposed to install on any point of Mars surface a lighthouse with millimeter-size light sours. If it will be based on bright light-diode with high efficiency, it will need very low power supply for operating, but it will be distinctively seen from orbiting probes. Existing mapping cameras will fix their rows of photos to the position of the lighthouse with accuracy respective to their resolution, but the more progressive technique will be used the more accurate co-ordinate will be achieved. The limiting accuracy for light-housing based co-ordinate frame would be comparative to the dimension of its light source. For example, LED as light source and optical interferometer for arcs measuring will provide sub-millimeter level of co-ordinate accuracy of planetary “kosmodesies” frame.

The low-mass lighthouses may accompany any landing device, and it will allow providing their works with best co-ordinate pointing, even when the device cannot be detected by TV orbital technique. Fine co-ordinates are especially desired for multi-station planetary seismometry.

INTERACTION OF METEOROIDS WITH PLANETARY ATMOSPHERES

Maria Gritsevich, *Institute of Mechanics, Lomonosov Moscow State University, Russia (gritsevich@list.ru), European Space Agency, Research and Scientific Support Department, Noordwijk, The Netherlands*

This study is devoted to description of the possible results that might accompany collisions of natural cosmic bodies with both a planet's atmosphere and surface. The methodology of the classification is based on the analytical solution of differential equations of meteor physics. These equations characterize the body's trajectory in the atmosphere, namely, the dependences of the body's velocity and mass on the flight altitude. The solution depends on two dimensionless parameters defining the drag rate and altitude, and the role of the meteoroid's mass loss when it moves in an atmosphere. The action of the collisions on the planet's surface essentially depends on values of these two parameters. Additionally we formulate recommendations for further studies of the important problem related to the interaction of cosmic bodies with planetary atmospheres.

CHEMISTRY OF METEOR EVENTS ON MARS

A. A. Berezhnoy, *Sternberg Astronomical Institute, Universitetskij pr., 13, 119991 Moscow, Russia. Contact: ber@sai.msu.ru*

Introduction: The Mars Express Orbiter Radio Science Experiment on the European Mars Express spacecraft observed a new ionospheric layer at altitude ranges of 65 to 110 km [1]. Its origin has been attributed to ablation of meteors and charge exchange of meteoritic Mg and Fe. A meteor event in Martian atmosphere was already detected during observations of the Martian atmosphere from the surface of the red planet by Spirit, the Mars Exploration Rover [2]. However, spectral observations of Martian meteors were not conducted yet. For preparation of such observations we need to know the chemistry of meteor events in the Martian atmosphere.

Calculations: Study of the chemical processes during meteor events in Martian atmosphere was performed based on approach [3] developed for the case of Earth's bolides. The elemental composition of the impact-produced fireball was taken to be that of a mixture of CI chondrites [4] and Martian atmosphere (0.03 wt% H_2O, 0.07 wt% CO, 0.13 wt% O_2, 1,6 wt% Ar, 2,7 wt% N_2, and 95.32 wt% CO_2). It was assumed that in impact-produced fireballs the mass of the matter of meteoroid origin is 30 times smaller than the mass of atmospheric origin. Thermodynamic calculations based on the quenching theory were conducted in order to estimate the chemical composition of the fireball. We consider fireball temperatures from 1500 to 6000 K with step of 500 K and pressures of 0.006 and 0.00004 bars.

Results: The pressure equal to 0.006 bar corresponds to the explosion of relatively big and slow meteoroids near the surface of Mars while the pressure of 0.00004 bars corresponds to majority of bolides exploded at altitude of 80 km in Earth's atmosphere. Thermodynamic calculations were performed with CHET program using standard methods of Gibbs free energy minimization. Our code allows calculations of equilibrium compositions for up to 102 species made from up to 15 elements. Thermodynamic properties of the considered species were taken mainly from the database [5].

Based on the quenching theory chemical reactions end when the chemical and hydrodynamic time scales became comparable. It was assumed that the quenching temperature is equal to 1500 – 2000 K for the train phase at 0.006 bar as for the case of Earth's bolides [2]. If equilibrium condensation takes place, the main Na-, Fe-, Ca-, Mg-, Al-, Si- bearing species at the quenching are Na, NaOH, FeO, Ca, Mg, AlO, and SiO, respectively (see Fig. 1).

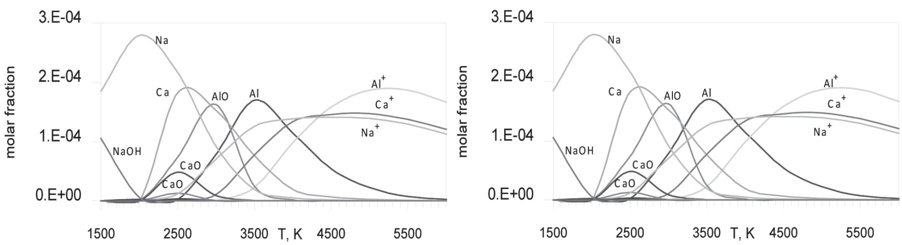

Fig.1: Equilibrium composition of Ca-, Al-, Na- (up), and Mg-, Si-, Fe- (down) bearing compounds in fireballs in Martian atmosphere at 0.006 bar as a function of temperature.

For Earth's bolides at 0.00004 bar the quenching temperature is about 2000-2500 K at the train phase while at the bolide phase chemical equilibrium between metal atoms and metal monoxides is not reached [3]. However, chemical equilibrium between atoms and ions is usually reached because ion-neutral reactions are fast. If equilibrium condensation takes place, the main Na-, Fe-, Ca-, Mg-, Al-, Si- bearing species at the quenching are Na, Fe, Ca, Mg, Al, AlO, and SiO, respectively (see Fig. 2).

Discussion: During the train phase chemical reactions occur until temperature falls below 1500 – 2500 K. At such low temperatures and 0.006 bar the abundances of molecules are relatively high for Na, Fe, Al, and Si. Decreasing of pressure leads to decrease of abundances of molecules and shift of maximal abundances of molecules to lower temperatures.

Let us note that spectra of Earth's meteoroids during bolide phase can be obtained easier than that during train phase. We expect that first spectra of Martian meteors will be obtained during bolide phase. The brightest lines in visible spectra of Earth's bolides are lines of Na, Fe, Mg, and Ca [6]. Let us consider the behavior of these elements in Martian meteors. At typical temperatures of Earth's bolides, 4000 – 5000 K, the main Na-, Fe-, Mg-, Ca-bearing compounds are Na^+, Fe, Mg, and Ca^+ at 0.006 bars and Na^+, Fe^+, Mg^+, and Ca^+ at 0.00004 bars, respectively (see Fig. 1 and 2). Equilibrium abundances of atoms and ions during bolide phase are almost the same with accuracy of about 10 % for Earth's and Martian meteors because in both cases the electron density is determined by the matter of meteoroid origin. It means that abundances of ions of atmospheric origin (O^+, N^+, C^+ and so on) are much smaller than abundances of ions of meteoroid origin (Na^+, Fe^+, Si^+ and so on). Thus, relative intensities of lines in visible spectra of Martian and Earth's meteoroids are comparable if the elemental composition of these meteoroids and fireball temperature and pressure are assumed to be the same.

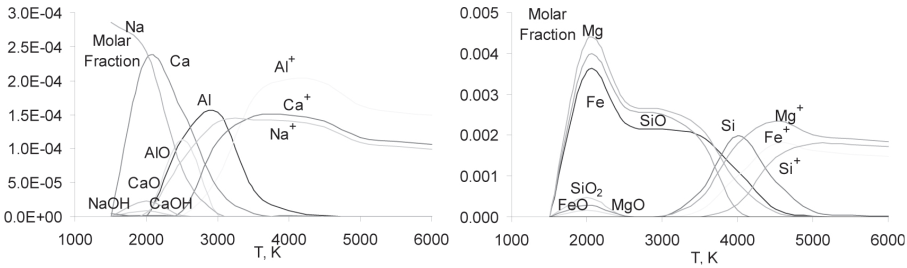

Fig. 2: Equilibrium composition of Ca-, Al-, Na-, (up), Mg-, Si-, Fe- (down) bearing compounds in fireballs in Martian atmosphere at 0.00004 bar as a function of temperature.

However, ions of atmospheric origin are the main sources of electrons at temperatures higher than 5200 K for Martian atmosphere and 6000 K for Earth's atmosphere. Ions of atmospheric origin must be taken into account for study of the composition and emission of the hot meteor component having temperature of about 10 000 K.

Conclusions: Chemical composition of impact-produced fireballs on Mars is estimated. The intensity of brightest atomic lines of meteoroid origin of Martian bolides is comparable to that of Earth's bolides because in both cases abundances of metal monoxides are comparable and the electron density is determined by the matter of meteoroid's origin. Similar chemical processes are expected to occur during meteor events in CO_2 – dominated upper atmosphere of Venus.

Spectral observations of Martian meteors will be useful for estimation of the elemental composition of meteoroid populations at the orbit of Mars.

The most intensive lines in visible spectra of Martian meteors are lines of Na, Fe, Mg, and Ca. It is desirable to search for Na 589 nm lines at night-time spectra of Martian atmosphere already obtained by OMEGA instrument onboard Mars Express mission.

Acknowledgments: The author would like to thank J. Borovička (the Czech Republic) and O.V. Tvorun (Ukraine) for helpful comments and suggestions and acknowledges the support of the Astronomical Institute of ASCR for his stay at the Ondřejov Observatory.

References: [1] Pätzold M. et al. A Sporadic Third Layer in the Ionosphere of Mars, Science, V. 310, p. 837-839, 2005
[2] Selsis F. et al. Extraterrestrial meteors: a Martian meteor and its parent comet, Nature, V. 435, p. 581-581, 2005
[3] Berezhnoy A.A., Borovička J. Formation of molecules in bright meteors, Icarus, accepted
[4] Lodders K. Solar system abundances and condensation temperatures of the elements, The Astrophysical Journal, V. 591, p. 1220-1247, 2003
[5] Gurvich L.V. et al. Thermodynamic Properties of Individual Substances, fourth ed. in 5 volumes. Hemisphere Pub Co., New York, 1989
[6] Borovička J. et al. A survey of meteor spectra and orbits: evidence for three populations of Na-free meteoroids, Icarus, V. 174, p. 15-30, 2005

MORPHOLOGY OF MARS' RELIEF IN THE AREAS OF PHOTOGRAPHIC SURVEY OF THE PLANET SURFACE BY THE SPACECRAFTS. NOTATION SYSTEM OF TOPOGRAPHIC OBJECTS.

S.G. Pugacheva[1], V.V. Shevchenko[1], K.B. Shingareva[2], O.V. Sakovnina[2],
[1]Sterberg Astronomical Institute, Moscow State University, Universitetsky 13, Moscow 119992, Russia, sve-pugacheva@yandex.ru; [2]Moscow State University for Geodesy and Cartography, 103064, Moscow. Contact: kirash1@yasenevo.ru

Introduction: The report considers the basic types of Mars' relief based on the materials of a television survey of the planet surface by the spacecrafts. For the first time the high quality color photographs of Mars surface were transmitted by Viking - 1 and Viking - 2 spacecrafts [1]. One can see an empty country with reddish ground dotted with stones in the pictures. There were identified the relief details and denominated the names in honor of men of science and culture. Later on the photographic survey of Mars' surface with the spacecrafts allowed to get pictures of relief detail surface with higher resolution [2]. Thus, an instrument Themis intended for multispectral photographic survey of Mars' surface in visible and infrared of spectrum was mounted at the spacecraft Mars Odyssey. The instrument's field of view was 4,6x3,5^{o} and 2,9x2,9^{o}, and a spatial resolution stood at 100 and 20 m in infrared and visible spectrum ranges respectively [3].

Mars' relief name system: For the time being, there are several name systems of topographical objects of Mars' relief. One of them is based on the results of ground measurements; other is built based on the data of photographic survey of the planet surface by orbital spacecrafts. The third system proposed and is used for naming of small planet's relief details, mainly craters of 10-100 km diameter. All systems of Mars's nomenclature names are interrelated and complement each other. The report gives the notation schemes of Mars's crater and extended relief objects according to different systems of name nomenclature [4].

Basic types of Mars' relief: The International Astronomical Union has approved 27 types of Mars' relief. Moreover, some types of relief were ascertained based on study results of large-scale pictures of the surface. The geomorphologic studies of Mars surface images enabled one to mark out the new types of relief unknown before. The following types of relief may be considered as the new types of Mars' relief: Collis, Fluctus, Labes, Lingula, Unda. Some types of relief named earlier, which were found out by their albedo specific features, were renamed later on and obtained the new geomorphologic status. The report shows the up-to-date types of Mars' relief and their extent. The pictures of Mars' surface are plotted with the orbits of spacecrafts and the relief parts where the photographic survey was made with high spatial resolution are marked [5].

Geomorphologic characteristics of the relief details: Some space pictures of Mars surface made with high spatial resolution were converted into stratigraphical schemes of linear and circle landforms. The schemes contain the geomorphologic characteristics of Mars relief details. Such as location, size, topographic height, surface slopes. The said characteristics were determined by photometric and statistic methods based on topographic maps of Mars' surface relief [6, 7].

Conclusion: The results of studies give an opportunity to compare scientific and technical information about the planet and make considerably easier the usage of space survey material in studying the surface geomorphology of Mars in view of outlooks of the planet learning.

References: [1] Ksanfomality L.V. Parade of the Planets. M. Science – PhysMathLit, 1997, page 92-138.
[2] Chicaro A.F. et al., 40th Lunar and Planetary Science Conference, 2009.
[3]http://Astrogeology.wr.gov/HotTopics/index/php?/archives
[4] International astronomical Union Working Group for Planetary System Nomenclature, (2008) Gazetteer of Planetary Nomenclature, http://planetarynames.wr.usgs.gov/.
[5] Annual Gazetteer of Planetary Nomenclature (Working Group for Planetary System Nomenclature), NASA (1986), page 270. http://planetarynames.wr.usgs.gov/rules/html
[6] Roach L.H. et al. Icarus, 2010, 206, page 253-268.
[7] Scuitz P.H. et al. Science, 2008, 322, page 1828-1832.

VARIOUS ICE DEPOSITS IN THE HELLAS BASIN RIM REGION, MARS.

V.-P. Kostama[1], M. A. Ivanov[2], H. Lahtela[1], J. Korteniemi[1], J. Raitala[1], *[1]Astronomy, Dept. of Physics, FIN-90014 Univ. of Oulu, Finlan; [2] Vernadsky Institute, Ul. Kosygina 19, RU-119991 Moscow, Russia. Contact: jouko.raitala@oulu.fi*

The eastern Hellas rim region has numerous fluvial systems, which were mainly active during the Hesperian period, with a few systems dating to the late Noachian and early Amazonian.

The major outflow channels Dao, Niger, Harmakhis and Reull Valles are the most prominent fluvial/water-related features in the area. These channels have been proposed to originate from melt water flows triggered by the late-stage effusive volcanism of Tyrrhena Patera or by the volcanic intrusions and the emplacement of Hadriaca Patera or by both. There are also a high number of smaller channels and channel networks on the highlands surrounding Hellas Basin. Our focus of this part of the study was on a particular extensive channel system and related interconnected paleo-lake craters.

The ice-deposits are important in many cases as the primary sources (both sub- and on-surface) for the different scale fluvial systems (larger outflow as well as smaller surface channels) and they also contribute widely to the later modification and embayment of the fluvial systems. This is seen, for example, as LVF and LDA formations on the valley and channel floors.

HOW MUCH CLAY IS ON MARS? LESSONS FROM VISIBLE/NEAR-INFRARED (VNIR) AND XRD STUDY OF HYDRATED SILICATE MINERAL ASSEMBLAGES IN ALTERED BASALTS FROM ICELAND

B.L. Ehlmann[1], J.F. Mustard[2], D.L. Bish[3], F. Poulet[1], *[1]Institut d'Astrophysique Spatiale, Université Paris-Sud, France; [2]Department of Geological Sciences, Brown University, USA, [3]Department of Geological Sciences, Indiana University,USA. Contact: bethany.ehlmann@ias.u-psud.fr*

Introduction: Recent orbital investigations have revealed distinctive assemblages of minerals that indicate aqueous alteration on early Mars took place in diverse environments [1], including low-temperature/pressure hydrothermal systems at neutral to alkaline pH [2]. We began study of the alteration of basalt lava flows in Iceland as a geochemical and mineralogic analog for Noachian Mars. Iceland has a variety of geothermal spring systems, which generate distinctive mineralogic assemblages, depending mostly on the temperature and sulfur content. Here we examine rocks collected from basalt flows that were in some places altered at the surface by pedogenesis and in other locations were hydrothermally altered by non-sulfurous groundwater circulation (low T, low S). We examine visible/near-infrared (VNIR) spectra of rocks and ground powders to make mineral identifications--such as is done for OMEGA and CRISM in Mars orbit--and compare to quantitative XRD data--such as will be collected by MSL's ChemMin instrument. We examine the limit to which VNIR spectra provide an accurate measure of hydrated mineral presence and abundance in natural samples.

Methods: VNIR spectra (0.4-2.5 μm) of rock samples were measured using an ASD portable spectrometer with a portable light source (contact probe). In the NASA/Keck RELAB facility, reflectance spectra from 0.4-25μm were acquired of dried particle-size separates (<25 μm, <150μm) derived from the bulk rock and from precipitated minerals extracted from vesicles and veins. Minerals were identified by examining the shape and position of absorptions, and band depths compared to similar prior mixtures of known composition [3]. Additionally, the 0.4-2.6 μm range will be used in radiative transfer modeling using the Hapke [4] and Shkuratov [5] models to estimate endmember abundances.

X-ray diffraction (XRD) data were measured on the <25μm size fraction from 2º to 70º 2θ with 0.02º 2θ steps. To verify the presence of smectite and check for possible interstratified or non-expanding clays (e.g., chlorite, kaolinite), oriented mounts of ethylene glycol-saturated samples were also measured. For untreated samples, areas of the most intense peaks from component minerals were measured, and the relative percentage of each constituent was determined using the reference intensity ratio (RIR) method [6], using literature RIR values. Rietveld refinement was also applied to de-

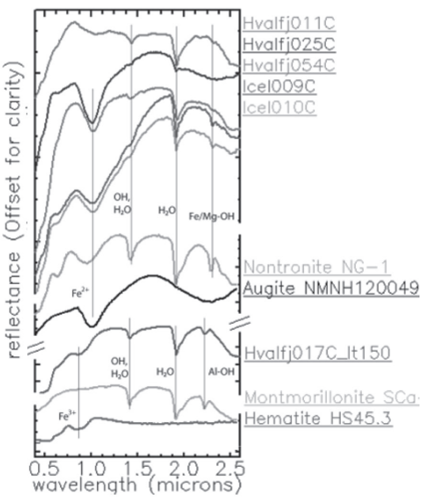

Fig. 1: VNIR spectra of <150μm samples from Iceland compared with laboratory spectra from USGS and CRISM spec-tral libraries.

Sample	Description	Inferred Miner., VNIR	Modal Mineral., XRD
Hvalfj011	gray friable rock near stream	HCP+Mg smectite	Smectite 16% Augite 54% Albite 24% Clinoptilolite 6%
Hvalfj025	host rock from rock with vesicles with blue-green precipitate	HCP+Fe-rich smectite/celadonite	Smectite 11% Anorth./Albite 49% Augite 39%
Hvalfj054	opaque white to cream precipitate in vesicle	HCP+Fe/Mg smectite	Smectite 17% Augite 66% Levyne 8% Hematite 5% Albite 3% Stilbite 1%
Icel009	brown rock with greasy feel	HCP+Fe/Mg smectite	Smectite 20% Anorth./Albite 59% Augite 21% Hematite <1%
Icel010	black rock with greasy feel	HCP+Fe/Mg smectite	Smectite 22% Anorth./Albite 59% Augite 18% Hematite <1%
Hvalfj017	reddish friable rock near stream	High-Ca Montmorillonite + Hematite	Smectite 79% Albite 9% Hematite 9% Epistilbite 2%

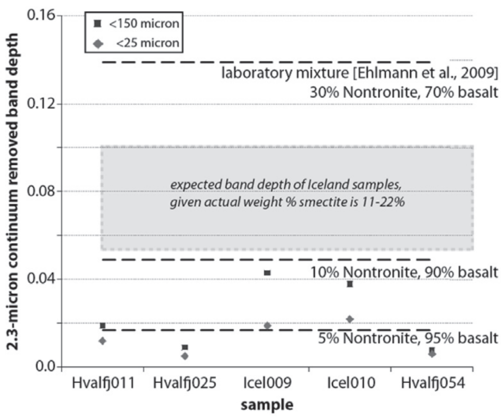

Fig. 2: Band strengths of the Fe/Mg-OH combination tone in Icel-and samples are weaker than expected compared to band strength from synthetic mixtures of nontronite and basalt (45-75 μm) made in the laboratory [4]

termine the relative abundance of the well-ordered (i.e., non-smectite) components. Final refined mineral abundances represent wt. % obtained from the Rietveld method scaled to include the RIR-determined smectite abundances.

First Results: VNIR spectra of all samples show evidence for aqueous alteration, including the 1.9μm combination tone from the stretch and bend of the H2O molecule (Fig. 1). OH and metal-OH overtones and combination tones are also visible near 1.4μm and over the 2.0-2.6μm region. Some minerals composing the sample, usually two or less, can be identified using the VNIR data (Table 1). Five samples have spectra consistent with high-calcium pyroxene and Fe/Mg smectite. The band depth at 2.3μm due to Fe/Mg-OH ranges from ~1-5%. One sample appears to be a mixture of hematite and montmorillonite, indicated by an Al-OH 2.2μm band (8% strength).

Results from XRD analysis confirm the findings of alteration minerals in all samples. Ground bulk rock samples have smectite as the dominant alteration mineral. Zeolites, SiO_2 phases, and other phyllosilicates are present in only minor amounts. Hvalfj017, likely from a paleosol horizon, is the most altered of all the samples, with nearly 80% smectite. Other bulk rock samples were dominated by the primary mafic components plagioclase and pyroxene (Table 1). Weight percent smectite ranges from 11-22%. Minor amounts of zeolite (<10%) are sometimes present. Modeling of the glycolated sample patterns with the NewMod program [7] showed that patterns are consistent with smectite with an interstratification of 0-10% chlorite and are not consistent with illitic layers.

Implications for hydrated minerals on Mars: In the Icelandic samples, the bulk rock is altered and smectite-bearing. Other alteration minerals such as zeolites, celadonite, and silica phases are concentrated in vugs or fractures. As little as ~10% smectite is observable in VNIR spectra of altered mafic rocks measured here; however, given the actual abundance of smectite, 2.3μm band depths are lower than expected based on comparison with band depths from artificial mixtures of basalt and nontronite [4] (Figure 2). Zeolites in <10% abundance also occur in the host rock, although their presence cannot be uniquely determined from VNIR. However, subtle differences such as a broadened 1.4 um band, strong 1.9 um band, and band near 2.5 m are consistent with zeolite presence.

All phases identified using VNIR spectroscopy were confirmed using XRD analysis. Nevertheless, VNIR spectroscopy does not fully capture the full amount or diversity of alteration mineral phases present, highlighting the importance of ground-truthing spectral data from Mars and improving techniques for quantitative remote determination of modal mineralogy.

The next step of this research is to apply radiative transfer modeling to both rock and particulate samples from these rocks to better understand the agreement (or not) between XRD quantitative mineralogies and estimates from Shkuratov and Hapke modeled abundances. Results from this modeling will be presented at the conference.

A key for future Mars exploration will be the synergistic use of these two technologies: VNIR spectroscopy for orbital mineral identification, mapping of key outcrops, and traverse planning coupled with in-situ XRD, for precise characterization of mineral assemblages, which is often necessary to determine past temperatures and aqueous geochemistry. The 2011 MSL mission will be the first to pair the use of these two technologies in operations planning, and these capabilities will also be important for future landed missions.

References: [1] Murchie et al., 2009, JGR 114 [2] Ehlmann et al., 2009, JGR 114 [3] Ehlmann et al., 2009, LPSC, #1771 [4] Hapke B. (1993) Theory of reflectance and emittance spectroscopy. Cambridge Univ. Press. [5] Shkuratov Y. et al. (1999) Icarus, 137, 235-246. [6] Chung, F.H., 1974, J. Appl. Cryst. 7 [7] Yuan and Bish, 2010, in press

COBBLES AND IRON METEORITES AT MERIDIANI PLANUM, MARS

I. Fleischer[1], G. Klingelhöfer[1], J. Brückner[2], J. Ashley[3] and C. Schröder[4], *[1]Institut für Anorganische und Analytische Chemie, Universität Mainz, Germany; contact: fleischi@uni-mainz.de. [2]Max-Planck-Institut für Chemie, Mainz, Germany. [3]Arizona State University, Tempe, AZ 85287, USA. [4]University of Bayreuth and Eberhard Karls University of Tübingen, Germany.*

Introduction: The landing site of the Mars Exploration Rover Opportunity at Meridiani Planum is characterized by frequent exposures of sulfate-rich outcrop rocks covered with basaltic sand and a lag deposit of hematite-rich spherules [1]. Since landing in January 2004, Opportunity has covered a distance of more than 20 km. Along the traverse, numerous loose, cm-sized rocks referred to as “cobbles” are present on the plains and in clusters close to craters, Fifteen of them were imaged with Opportunity’s Panoramic camera (Pancam) and investigated with the rover’s contact instruments, which provide information about elemental chemistry (Alpha Particle X-ray Spectrometer, APXS), iron mineralogy and oxidation states (miniaturized Mössbauer spectrometer, MIMOS II) and texture (Microscopic Imager, MI) [2, 3]. In addition to cobbles, Opportunity encountered four Iron meteorites, three of which were investigated with the rover’s contact instruments.

Cobbles: Based on APXS elemental chemistry and Iron mineralogy from Mössbauer spectra, cobbles can be divided into three distinct groups: Outcrop fragments are bright and indistinguishable from other outcrop rocks with regard to their texture, composition and Iron mineral content. All other cobbles are dark and referred to as “Barberton group cobbles” and “Arkansas group cobbles” after the first specimen of each group that was encountered by Opportunity.

Barberton group cobbles have high Ni contents and contain the minerals kamacite (Fe,Ni) and/or troilite (FeS), pointing to a meteoritic origin. Of examples in Earth-based collections, their overall composition is most consistent with that of mesosiderite silicate clasts [4-6]. However their textures suggest the possibility of either a new class of meteorite or an impact breccia that incorporates preserved fragments of the impacting body.

Arkansas group cobbles exhibit similarities to soil and Meridiani outcrop rocks. Their compositions and brecciated textures point to an impact-related origin. They are likely melt-bearing breccias derived from outcrop rocks and local soil [6]. Example Mössbauer spectra for the three cobble groups are shown in Figure 1.

APXS X-ray spectra were obtained on natural and brushed surfaces of the different cobbles. To infer their origin, they are also compared with SNC meteorites, which are believed to be Martian crater ejecta [7], and thus included in the composition plots.

The P-Al ratio is characteristic for most SNCs. These elements, incompatible in mafic systems, correlate for SNCs as a result of igneous fractionation. The Barberton group cobbles follow closely the SNC P-Al trend (Figure B1).

SNCs have variable olivine contents. Ni can be incorporated in olivine during crystallization, which is the cause of the SNC Ni-Mg correlation. The Ni and Mg contents are tightly clustered for most Meridiani Planum materials except for Barberton group cobbles. Their high Ni concentrations range up to 5000 μg/g. These high values and their deviations from compositions of SNC meteorites point to a meteoritic origin [6].

Iron Meteorites: Due to their metallic nature, Iron meteorites are susceptible to the presence of even trace amounts of water. They are therefore valuable probes to assess weathering conditions at their current site since their arrival [7].

Opportunity encountered the first Iron meteorite in January 2005. Informally named “Heat Shield Rock”, it was later classified as a IAB complex iron meteorite and given the approved official name “Meridiani Planum” after the location of its find [8]. Three other Iron meteorites, informally named “Block Island”, “Shelter Island” and “Mackinac Island”, were encountered between July and October 2009, separated less than 1 km from each other. Pancam images reveal the presence of a smooth, lustrous surface partially coated with a material that appears more purple compared to the uncoated surface in a false-colour image. Mössbauer spectra obtained on two of the meteorites show large amounts of kamacite (Fe,Ni), with contributions from cohenite ($(Fe,Ni.Co)_3C$) and / or schreibersite ($(Fe,Ni)_3P$). Iron oxides related to the discontinuous coating were detected in both of them, indicating a generally low degree of weathering through the interaction of the meteorites with small amounts of water [9, 10]. An example spectrum is shown in Figure 2. Cross-cutting relationships of the coating with kamacite-taenite lamellae differentially eroded by wind-blown sand confirm that the coating is not a fusion crust, supporting the weathering rind interpretation.

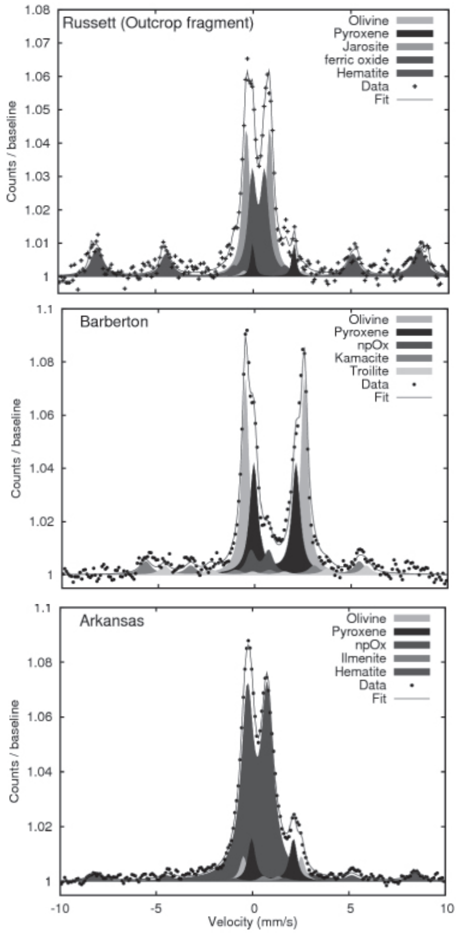

Fig. 1: Example Mössbauer spectra for specimens from each cobble group (npOx: nanophase ferric oxide).

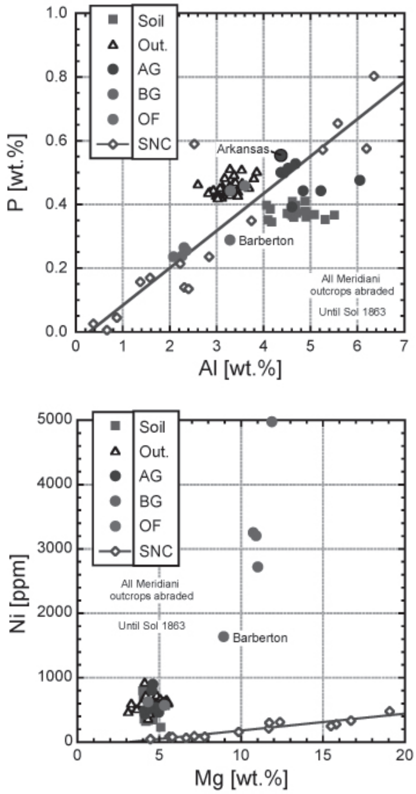

Fig. 2: Example of APXS concentration data of samples from Meridiani Planum (Out.= Outcrop, AG= Arkansas group cobbles, BG= Barberton group cobbles, OF= Outcrop fragments) and SNC meteorites.

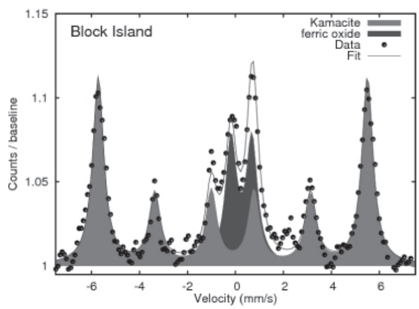

Fig. 3: Example Mössbauer spectrum from the "Block Island" meteorite with kamacite and ferric oxide.

References: [1] Squyres et al. (2006), *J. Geophys. Res.,* 111, E12. [2] Squyres et al. (2003), *J. Geophys. Res.* 108, E12.Squyres et al., 2003 [3] Klingelhöfer et al. (2003), *J. Geophys. Res.* 108, E12. [4] Schröder et al. (2008), J. Geophys. Res.113, E06S22. [5] Schröder et al. (2010), J. Geophys. Res., in review. [6] Fleischer et al. (2010), J. Geophys. Res., in review. [7] Treiman et al., Planet. Space Sci., 48, 1213. [8] Ashley et al. (2009), 2013-2022 Planetary Science Decadal Survey. [9] Connolly et al. (2006), Meteoritics & Planet. Sci 41, 90Connolly et al., 2006. [10] Ashley et al. (2010), J. Geophys. Res., in review. [11] Fleischer et al. (2010), Meteoritics & Planet. Sci., in review.

DEVELOPMENT OF LIMB-SCATTERING RADIATIVE TRANSFER MODELS FOR MARS REMOTE SENSING AND DATA ASSIMILATION

G. Uymin[1], J. Eluszkiewicz[1], J.-L. Moncet[1],1 D. Flittner[2], and M. Wolff[3,]
[1]Atmospheric and Environmental Research, Inc., [2]NASA Langley, [3]Space Science Institute

Measurements of the Martian atmosphere have experienced rapid growth during the past decade. As on Earth, remote sensing from orbit offers the advantage of nearly continuous, global coverage and a host of instruments have been employed for this purpose, including cameras [the Mars Orbiter Camera (MOC) and the Mars Color Image (MARCI)] and infrared sounders [the Thermal Emission Spectrometer (TES), the Mars Climate Sounder (MCS), and Compact Reconnaissance Imaging Spectrometer for Mars (CRISM)], as well as European instruments. The MCS is a dedicated atmospheric instrument, while the other instruments have yielded a wealth of information about the atmosphere in addition to their primary surface-studies focus. From the point of view of atmospheric studies, the dedicated limb-observing capability of the MCS, as well as the limb viewing “of opportunity” afforded by the TES, MOC, MARCI, and CRISM instruments offer significant advantages compared with the nadir-viewing mode. Chief among the advantages are the improved vertical resolution (particularly relevant to the studies of dynamic phenomena as reflected in the thermal structure) and the fact that observing against a cold space background (as opposed to a warm surface) offers the possibility of retrieving vertically resolved information about aerosols (including dust and H_2O and CO_2 ices) and minor gases (water vapor, carbon monoxide, methane, etc.). The main limitation to attaining the full scientific potential of limb measurements is the general lack of appropriate radiative transfer models. Such models must be capable, in a computationally efficient manner suitable for retrieval and radiance assimilation work, of accurately representing both gaseous absorption and aerosol scattering in a spherical geometry.

In this presentation, we will describe initial results from the development of efficient and accurate radiative transfer models for scattering and gaseous absorption in a spherical atmosphere. Our approach combines the Gauss-Seidel Spherical Radiative Transfer Model (GSSRTM) for scattering and the Optimal Spectral Sampling (OSS) model for gaseous absorption, employs a planetary version of the LBLRTM model as the line-by-line reference, and uses a realistic training set derived from the Mars Climate Database. The combined models will be used in validation, retrievals, and data assimilation from limb-sounding instruments, particularly MCS, TES, and CRISM, and future instruments for Mars and other planets. This work is very timely, as new instrument concepts employing limb viewing are likely to emerge from the upcoming NASA-ESA ExoMars mission opportunity dedicated to the detection of methane and other trace gases in the Martian atmosphere.

This work is funded by the NASA Mars Fundamental Research Program.

AN UNUSUAL FRESH IMPACT CRATER ON MARS: EVIDENCE FOR THE PRESENCE OF A RECENT ICE-RICH MANTLE

E. I. Schaefer[1,2], J. W. Head[1], and S. J. Kadish[1], *[1]Brown University Department of Geological Sciences, 324 Brook Street, Providence, RI 02912. [2]Colorado State University Department of Geosciences, 322 Natural Resources Building, Fort Collins, CO 80523. Contact: eis@rams.colostate.edu.*

Introduction: We document a 1.85 km diameter mid-latitude (38ºN) very fresh impact crater whose ejecta-related facies are perched ~20-30 m above the surrounding plains and whose proximal terrains are consistent with its emplacement on a tens of meters thick, regional ice-rich substrate.

On Earth, quasi-periodic changes in orbit and spin axis parameters significantly contribute to global climate change on scales of 10^4-10^5 years [1]. On Mars, similar cycles also affect climate but are far more severe, especially obliquity (spin axis inclination) [2,3]. During periods of high obliquity on Mars, most recently occurring ~100,000 years ago, ground ice was stable down to latitudes of ±~30º [4]. However, the mode of emplacement of this ice and the attendant potential for its relict preservation are debated [see 5-6].

One hypothesis proposes that vapor diffusion into regolith pore space alone is responsible for the deposition of ground ice [e.g., 4]. This mechanism could also produce isolated secondary ice lenses [7], but the latitudinal extent of the ground ice in the regolith would generally be in equilibrium with current conditions [5-7]. Conversely, a second hypothesis suggests that atmospheric precipitation of snow and codeposition of ice and dust emplaced a 10^0-10^1 meters thick mantle across the mid-latitudes that was subsequently preserved under a sublimation lag [6,8,9]. Evidence for this hypothesis includes the observation of mid-latitude surface textures that vary equator-ward from smooth and continuous to dissected to absent [8-11]. Topographic smoothing and concavity in the mid-latitudes is also consistent with such an ice-rich deposit [12], as is the observation of extensive layering in a mantle exclusive to the mid-latitudes [6]. Crater-proximal preservation of an ice-rich mantle coupled with regional removal has been suggested as a mechanism for producing craters that seem perched above their surroundings, including pedestal [13-16] and excess ejecta craters [17]. A third hypothesis interprets the mantle as dust, having contained isolated ice deposits only where dissection is now observed [5]. In this analysis, we study the crater's unusual impact-related facies and proximal terrains to assess these hypotheses.

Observations: The crater (Fig. 1) exhibits very few superposed craters on its associated facies. Importantly, there is also no compelling evidence for secondary craters out to a search distance of at least ~40 radii from the rim crest. The crater has minimal infilling, and the rim crest is sharp.

Seven approximately concentric geomorphic units can be identified in the crater vicinity, superposed on the background Hesperian ridged plains (Hr) [18] (Figs. 1-2). From the crater outward, these are unfilled crater interior (ci), crater rim (cr), lo-bate facies (lf), smooth facies (sf), radial facies (rf), and knobby terrain (kt).

Prominent tongues of radial facies (rf) extend outward from the smooth facies/radial facies (sf/rf) transition, which is topographically smooth in MOLA shot data. The radial facies (rf) is composed of radial, curvilinear ridge/trough couples. The high-albedo ridges and relatively lower-albedo troughs are each tens of meters wide and vary from continuous ridges to discontinuous ridges to disconnected knobs, generally becoming less continuous distally from the crater and toward the exterior boundaries of the unit.

Knobby terrain (kt) both laterally fringes rf and, in places, extends in tongues well beyond it. It is composed of polygonal to rounded knobs that range from equidimensional to elongate in planform. The knobs appear relatively low and flat-topped such that circular knobs approximately resemble coins. However, they are also frequently centrally pitted, then resembling looped ridges or rings. The knobs commonly range from ~25-60 m in width, but rare knobs may be as much as ~80 m wide. They have a moderate albedo and are always set in a relatively lower albedo background that is almost always darker (frequently much darker) than adjacent Hr. Knobby terrain (kt) can also be found in isolated craters up to ~41 km north of the fresh crater (Fig. 2).

MOLA shot data show that the radial facies (rf) is generally perched ~20-30 m above adjacent Hr, with interior facies perched equally high or higher relative to Hr. Where the knobby terrain (kt) fringes the radial facies (rf), it is always lower and slopes away from rf.

Interpretation: The low level of crater infilling, sharp rim crest, and paucity of superposed craters all indicate that this crater is very young. In addition, the knobby terrain (kt) and radial facies (rf) are distinctive and highly unusual.

The lobate facies (lf) is similar to common crater ejecta deposits [see 19], and the radial texture of rf clearly associates it with the impact. The smooth facies (sf) is also assumed to be impact-related, given its lateral position between lf and rf and its smooth topographic transition to rf. Conversely, the knobby terrain (kt) is unlike commonly observed ejecta morphologies, lacks any radial texture, and also occurs at great radial distances, suggesting that its formation is not impact-related.

The perched nature of the impact-related facies suggests that their initial emplacement occurred on a tens of meters thick substrate that has since been regionally removed, similar to hypotheses for the formation of pedestal [13-16] and excess ejecta [17] craters. The remarkable lack of secondary craters is also consistent with this explanation. Typically, the largest secondary craters have diameters 2-5% that of the primary crater [20-22], predicted to be ~37-92 m in this case. The depth/diameter ratio for martian secondary craters in this size range is ~0.11 [23], so the largest secondary craters would have been ≤~10 m deep and thus have been removed along with the tens of meters thick substrate.

The lower topographic and presumably stratigraphic position of knobby terrain (kt) suggests that it is a relict of this substrate. Further, the polygonal [e.g., 24] to rounded [25] knobs are similar in shape to thermal contraction crack polygons, which have been identified in many places on Mars and are associated with the thermal cycling of icy substrates. Although polygon widths are usually described as <2540 m [24,26], polygons 50-300 m wide have been identified in isolated areas of Mars, suggesting that microclimates and/or past climatic conditions might favor larger polygons [26]. Craters are also recognized as shelters for ablating ice on Mars [e.g., 27], and thus the knobby terrain (kt) seen in distal craters would be consistent with relict subsurface ice. For these reasons, the regionally removed substrate is interpreted to have been ice-rich and part of a more areally extensive latitude-dependent mantle [9]. Taken together, this evidence suggests the former presence of a regional ice-rich mantle tens of meters thick that is now locally preserved underneath and adjacent to the fresh crater. This geologic setting is identical to that suggested to account for pedestal and excess ejecta craters and thus offers further support for these models.

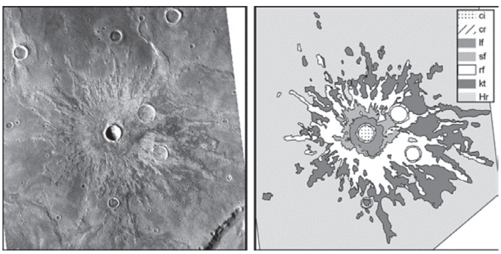

Fig. 1: Fresh crater at ~38.2°N, ~15.8° E. Left: Portion of CTX image P15_007057_2179. Right: Geomorphic map. Unit codes are defined in the text. Both figures are ~29 km wide. North is up.

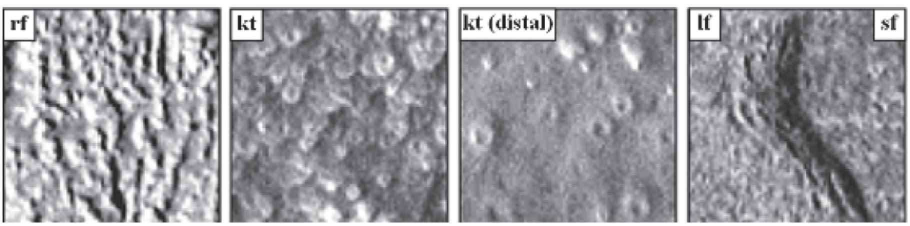

Fig.2: Geomorphic units as seen in CTX P15_007057_2179. Illumination is from the left. Each image is ~450 m wide. North is up.

References: [1] Hays, J.D. et al. (1976) Science 194, 1121-1132. [2] Laskar J. et al. (2002) Nature 419, 375 377. [3] Laskar, J. et al (2004) Icarus 170, 343-364. [4] Mellon M.T. and Jakosky B.M. (1995) JGR 100, 11,78111,799. [5] Searls, M.L. et al. (2008) LPSC XXXIX, Abstract #2376. [6] Schon, S.C. et al. (2009) GRL 36, L15202. [7] Mellon, M.T. et al. (2008) JGR 113, E3. [8] Mustard, J.F. et al. (2001) Nature 412, 411-414. [9] Head, J.W. et al. (2003) Nature 426, 797-802. [10] Milliken, R.E. and Mustard, J.F. (2003) Sixth Intl. Conf. on Mars, Abstract #3240. [11] Kostama, V.-P. et al. (2006) GRL 33, L11201. [12] Kreslavsky, M.A. and Head, J.W. (2002) GRL 29, 1719. [13] Barlow, N.G. (2006) MPS 41, 14251436. [14] Wrobel, K. et al. (2006) MPS 41, 1539-1550. [15] Meresse S. et al. (2006) MPS 41, 1647-1658. [16] Kadish, S.J. et al. (2009) JGR 114, E10001. [17] Black, B.A. and Stewart, S.T. (2008) JGR 113, E02015. [18] Skinner, J.A. et al. (2006) LPSC XXXVII, Abstract #2331. [19] Barlow, N.G. et al. (2000) JGR 105, 26,733-26,738. [20] Allen, C.C. (1979) GRL 6, 51-54. [21] Schultz, P.H. and Singer, J. (1980) LPSC XI, 2243-2259. [22] Melosh, H.J. (1989) Impact Cratering, Oxford Press. [23] McEwan, A.S. et al. (2005) Icarus, 351-381. [24] Levy, J.S. et al. (2009) JGR 114, E01007. [25] Levy, J.S. et al. (2006) Antarc. Sci. 18, 385-97. [26] Mangold, N. (2005) Icarus, 336-359. [27] Head, J.W. et al. (2008) PNAS 105, 1325813263.

PEDESTAL CRATERS ON MARS: EVIDENCE FOR THE PRESERVATION OF LAYERED PALEODEPOSITS

S. J. Kadish, J. W. Head, *Brown University, Providence, RI 02912, USA.*
Contact: Seth_Kadish@Brown.edu

Introduction: Pedestal craters (Pd) on Mars were first identified in Mariner 9 data [1], and have since been defined as an impact morphology characterized by a crater perched near the center of a plateau, surrounded by an outward-facing scarp [2,3]. Early studies implicated a formation mechanism based on armoring of fine-grained target material during an impact event, followed by prefe-rential eolian deflation of the non-armored intercrater ter-rain [1,2], yielding pedestals surrounded by marginal scarps. Our recent analyses, however, offer evidence that the target material from which Pd form must be ice-rich [4-6]. These studies highlight the latitude-dependent (poleward of ~35°) distribution of Pd [5,7], indicating a climate-related formation mech-anism, as well as key phys-ical attributes including sublimation pits in the marginal scarps of some Pd [6]. The resulting sublimation model for Pd formation proposes that impacts occur into ice-rich targets during periods of higher obliquity, when mid to high latitudes were covered by thick deposits of ice [8,9]. The impact armors the proximal surface of the ice-rich deposit. During return to lower obliquity, the deposit sub-limates, lowering the elevation of the intercrater terrain. Beneath the armored area around the crater, however, the ice-rich deposit is preserved, yielding a perched pedestal.

Supporting work from climate models [e.g. 10] has shown that the ice-rich material necessary to produce Pd can gradually accumulate (~10-20 mm/yr) at mid to high latitudes under certain atmospheric and orbital/obliquity conditions. The deposits ac-cumulate episodically on both short timescales, due to seasonal effects, and longer time-scales, due to obliquity cycles. Given this episodicity in accumulation, we would expect to see layers of dust and ice, similar to those in the polar layered deposits [e.g. 11], exposed along the marginal scarps of Pd.

Layered Pedestals: Our high-latitude survey has iden-tified 12 Pd with visible layers, five in the northern and seven in the southern hemisphere (Fig. 1). The presence of layering is usually established on the basis of albedo dif-ferences between adjacent layers. However, in some cases, layers are primarily expressed topographically, cre-ating stepped pedestal margins, without providing any signifi-cant albedo variations. The number of layers in a pedestal can range from three to more than thirty, with the thick-nesses of individual layers varying between two and more than twenty meters as measured from Mars Orbiter Laser Altimeter (MOLA) shot data. These layer thick-nesses are not constant in any given pedestal. Layers are often conti-nuous around the entire perimeter of the pedestal, although some are interrupted by material overly-ing the scarp, and may disappear for several kilometers.

There is a Pd (Fig. 2) on the south polar layered depo-sits (SPLD) that has armored the proximal surface. The surrounding terrain has since sublimated/eroded, exposing a clear sequence of layers along the pedestal's marginal scarp. The SPLD are known to be ice-rich, and possibly composed of nearly pure water ice [12]. The stratigraphi-cally lower layers in this pedestal are contiguous with surrounding layers of the SPLD, but the pedestal has pre-served some layers just beneath the armored surface which are no longer present in the proximal region. As such, this example offers empirical evidence of the ability of Pd to preserve ice-rich layers. The morphologic similarity and geographic proximity of this crater to other high-latitude Pd that also show layered exposures along their marginal scarps supports the interpretation that non-polar ped-estals are also capable of preserving ice-rich paleodeposits.

References: [1] J. McCauley (1973) JGR, 78, 4123. [2] R. Arvidson et al. (1976), Icarus, 27, 503. [3] N. Barlow et al. (2000), JGR, 105, 26733. [4] S. Kadish et al. (2008), GRL, 35, L16104. [5] S. Kadish et al. (2009), JGR, 114, E10001. [6] S. Kadish et al. (2010), Icarus, in press. [7] P. Moug-inis-Mark (1979), JGR, 84, 8011. [8] J. Head et al. (2003), Nature, 426, 797. [9] B. Levrard et al. (2004), Nature, 431, 1072. [10] J.-B. Madele-ine et al. (2009), Icarus, 203, 390. [11] S. Milkovich and J. Head (2005), JGR, 110. [12] J. Plaut et al. (2007), Science, 316, 92.

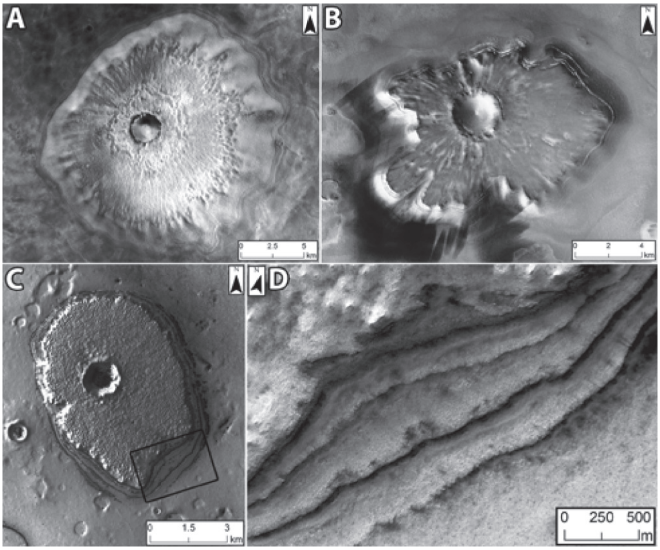

Fig. 1: Examples of layered Pd.

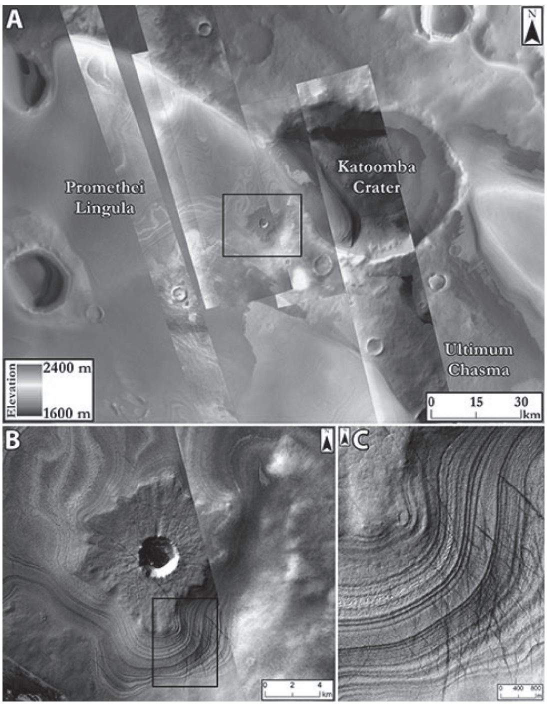

Fig. 2: The Pd located on the SPLD.

EVIDENCE FOR GLOBAL-SCALE NORTHERN MID-LATITUDE GLACIATION IN THE AMAZONIAN PERIOD OF MARS: DEBRIS-COVERED GLACIER AND VALLEY GLACIER DEPOSITS IN THE 30°-50°N LATITUDE BAND

J.W. Head[1], D.R. Marchant[2], *[1]Department of Geological Sciences, Brown University, Providence, RI 02912, USA; [2]Department of Earth Sciences, Boston University, Boston, MA 02215 USA. Contact: james_head@brown.edu.*

Introduction: Terrestrial cold-based glacial analogs [1,2] have recently been applied to the analysis of fan-shaped deposits on the NW flanks of the Tharsis Montes and Olympus Mons, interpreting them to represent extensive tropical mountain glaciers formed by enhanced snow and ice deposition during periods of high obliquity in the Amazonian [3-8]. Additional Earth glacial analogs have been used to develop criteria for the recognition of glacial deposits in various topographic and environmental settings on Mars [9]. These criteria have recently been applied to the assessment of the fretted terrain, one of the hallmark morphologies of the high-lowland boundary region in the northern midlatitude Deuteronilus-Protonilus Mensae area (30°-50° N and 10° -75° E). The fretted terrain [e.g., 10] consists of 1) lobate debris aprons (LDA) that surround many of the massifs and valley walls, and 2) lineated valley fill (LVF) that occurs on the floors of many of the valleys. We addressed the question of whether the accumulation of snow and ice, and resulting glacial activity, could account for some of the observed characteristics of the fretted terrain. In one area (Fig. 1; 1)(~37.5° N, 24.2° E) [11] evidence was presented that lineated valley fill formed in multiple accumulation zones in breached craters, alcoves, and tributary valleys and flowed laterally down-valley forming a major trunk system that was characterized by compression of ridges at constrictions, tight folds at converging branches, and a lobate, convex-upward terminus. In a second area (Fig. 1; 2)(~40.5° N, 34,5° E) [12] a single integrated system was documented covering ~30,000 km^2 and consisting of multiple, theater-headed, alcove like accumulation areas, converging patterns of downslope flow into several major valley systems, and broad piedmont-like lobes where the LVF extended out into the adjacent lowlands. The features and deposits in these two areas are interpreted to represent intermontaine valley glacial systems dating from earlier in the Amazonian.

Synthesis of criteria for recognition: Using the range of terrestrial analogs and the subset most likely to apply to the recent cold desert environment of Mars [e.g., 1,2,9], the following criteria have been developed to assist in the identification of debris-covered glacialrelated terrains on Mars; the interpretation of each is listed in parentheses: 1) alcoves, theater-shaped indentations n valley and massif walls (local snow and ice accumulation zones and sources of rock debris cover), 2) parallel arcuate ridges facing outward from these alcoves and extending down slope as lobe-like features (deformed flow ridges of debris), 3) shallow depressions between these ridges and the alcove walls (zones originally rich in snow and ice, which subsequently sublimated, leaving a depression), 4) progressive tightening and folding of parallel arcuate ridges where abutting adjacent lobes or topographic obstacles (constrained debris-covered glacial flow), 5) progressive opening and broadening of arcuate ridges where there are no topographic obstacles (unobstructed flow of debris-covered ice), 6) circular to elongate pits in lobes (differential sublimation of surface and near-surface ice), 7) larger tributary valleys containing LVF formed from convergence of flow from individual alcoves (merging of individual lobes into LVF), 8) individual LVF tributary valleys converging into larger LVF trunk valleys (local valley debris-covered glaciers merging into larger intermontaine glacial systems), 9) sequential deformation of broad lobes into tighter folds, chevron folds, and finally into lineated valley fill (progressive glacial flow and deformation), 10) complex folds in LVF where tributaries join trunk systems (differential flow velocities causing folding), 11) horseshoe-like flow lineations draped around massifs in valleys and that open in downslope direction (differential glacial flow around obstacles), 12) broadly undulating along-valley floor topography, including local valley floor highs where LVF flow is oriented in different down-valley directions (local flow divides where flow is directed away from individual centers of accumulation), 13) integrated LVF flow systems extending for tens to hundreds of kilometers (intermontaine glacial systems), 14) rounded valley wall corners where flow converges downstream, and narrow aretelike plateau remnants between LVF valleys (both interpreted to be due to valley glacial streamlining). Taken together, the occurrence of these features is interpreted to represent the former presence of debriscovered glaciers and valley glacial systems in the Deuteronilus-Protonilus region [11,12]. Snow and ice accumulating in alcoves, together with rock debris shed from adjacent steep walls, created debris-covered glaciers that flowed down-slope, merging with other ice lobes to form ever-larger LVF glacial systems.

Application to other parts of the Deuteronilus-Protonilus region: These criteria have been applied to detailed analyses of eight additional areas in this region (Fig. 1; 3-10) [13-20] and reconnaissance assessments of many other areas along the dichotomy boundary have been undertaken. Among the most important findings are: 1) Lobate debris aprons (LDA) can be subdivided into linear (along valley walls and degraded crater walls) and circumferential (around isolated massifs); 2) LDAs commonly form from numerous parallel individual flow lobes emanating from alcove-like indentations in massif and valley walls; 3) in some cases LVF glacial systems clearly merge with linear LDAs; 4) in some cases linear LDAs derived from opposite valley walls merge and flow down valley; 5) in massif clusters, circumferential LDAs often meet those from adjacent massifs, merge, and then flow downslope, forming piedmont-like lobate terminations in the adjacent lowlands; 6) the location and distribution of these features (Fig. 1) strongly suggest regional intermontaine valley glacial systems whose locations are dictated by topographic configurations (dichotomy boundary scarps, massifs, valleys and craters) conducive to accumulation and preservation of snow and ice and the formation of rock debris cover; 7) topographic and morphologic relationships suggest that some valley glacial systems may be partly fed from local plateau icefields. In summary, the Deuteronilus-Protonilus region (Fig. 1) was an area of active and very widespread glaciation during parts of the Amazonian.

Assessment of other regions in the 30°-50° N latitude range: The presence of valley glaciers could be due to local environmental conditions in which the accumulation of snow and ice was favored [e.g., 21]. The widespread distribution of these glacial systems in the Deuteronilus-Protonilus highland region (Fig. 1), however, suggests that conditions were much more regional, extending across a significant latitude band. To address the question of whether climatic conditions conducive to glacial activity extended beyond the Deuteronilus- Protonilus region, we undertook a systematic analysis of the remaining longitudes at these latitudes and found abundant evidence of local and regional Amazonian glacial deposits in the following areas (Fig. 1): 1) Elysium Rise: Hecates Tholus (Fig. 1; 11): A 45 km wide depression at the base of Hecates Tholus is host to a series of debris covered glacial deposits [22]. 2) Phlegra Montes (Fig. 1; 12): Debris-covered glacial deposits are located along the scarp of the montesas well as surrounding individual massifs there (e.g., 30o-50oN, 160o-167o E). 3) Arcadia Planitia (Fig. 1; 13): Degraded mountains in central Arcadia contain debris-covered glacial deposits (e.g., 35°-40° N, 185°-190° E). 4) Acheron Fossae (Fig. 1; 14): LVF and LDA of glacial origin are common in association with the graben and massifs [e.g., 23]. 5) Tempe Terra Region (Fig. 1; 15): LVF and LDA of glacial origin occur in numerous places in the graben and mountains (e.g., 45°-52° N, 280°-300° E).

Summary and conclusions: 1) an array of terrestrial analogs for glacial processes that are applicable to the range of conditions on Mars have been developed; 2) these have been used to test for the presence of deposits and sites of former valley glaciation and debriscovered glaciers (cold-based ice) in two specific areas of Mars; 3) from these analyses, general criteria for the recognition of debris-covered glacial deposits have been outlined; 4) application of these criteria to the northern mid-latitudes reveals the presence of widespread cold-based glaciation in valleys and mountains and along scarps, in the 30o-50o N latitude band; 5) the global-scale latitudinal distribution of these deposits (Fig. 1) suggests an extensive period in the Amazonian when ice was stable in this latitude band; 6) a plausible explanation for this configuration is an extended period of spin-axis obliquity at values higher than present, such that the mid-latitude band became the locus of deposition of ice mobilized from other latitudes (e.g., the poles) by the changing integrated insolation conditions [e.g., 24-26]. Specific global general circulation modeling (GCM) [27] shows that the climate in the mid-latitudes at ~35 obliquity with a moderately dustladen atmosphere can form ice-rich deposits in terms of net accumulation rates and the distribution of deposits. Further glacial flow modeling shows that lineated valley fill as observed can be produced by the accumulation rates predicted by the GCMs [28]. Further geological analysis helps to confirm local glaciatin [28], and updated syntheses show a coherent regional picture [29]. Recent analyses of the mid-latitude LDA and LVF show clear detection of buried ice below a layer of debris [29,30], as predicted by the synthesis of observations [28].

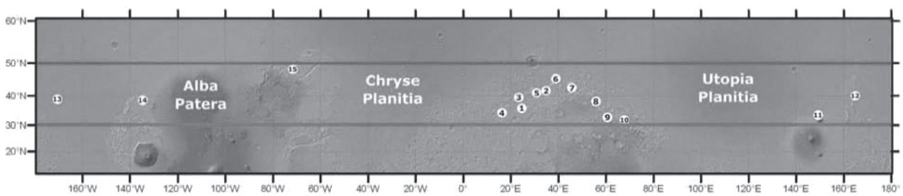

Fig. 1: Locations of areas showing evidence of glaciation discussed in this study. Red lines show 30°-50° N latitude band in which they occur.

References: [1] D. Marchant and J. Head, LPSC 34, 1361, 2003; [2] D. Marchant and J. Head, LPSC 35, 1405, 2004; [3] J. Head and D. Marchant, Geology, 31, 641, 2003; [4] D. Shean et al., JGR, doi:10.1029/2004 JE002360, 2005; [5] S. Milkovich et al., Icarus, 181, 388, 2006; [6] G. Neukum et al., Nature, 432, 356, 2004; [7] J. Head et al., Nature, 434, 336, 2005; [8] F. Forget et al., Science; 311, 368, 2006; [9] D. Marchant and J. Head, LPSC 37, 2006; [10] S. Squyres, Icarus, 34, 600, 1978. [11] J. Head et al., EPSL, 241, 633, 2006; [12] J. Head et al., GRL, 33, L08S03, 2006; [13] A. Kress et al., LPSC 37, 2006; [14] J. Head et al., LPSC 37, 2006; [15] G. Morgan et al., LPSC 37, 2006; [16] A. Nahm et al., LPSC 37, 2006; [17] D. Marchant et al., LPSC 37, 2006; [18] J. Dickson et al., LPSC 37, 2006; [19] M. Agnew et al., LPSC 37, 2006; [20] J. Levy et al., LPSC 37, 2006; [21] M. Hecht, Icarus, 156, 373, 2002; [22] E. Hauber et al., Nature, 434, 356, 2005; [23] J. Dickson et al., LPSC 37, 2006; [24] F. Forget et al., JGR, 104, 24155, 1999; [25] M. Mishna et al., JGR, doi:10.1029/2003JE002051, 2003; [26] R. Haberle et al., Icarus, I6I, 66, 2003; [26] J.-B. Madeleine et al., Icarus, 203, 390, 2009; [27] J. Fastook et al., LPSC LPSC 40, 1144, 2009; [28] J. Head et al., EPSL,10.1016/j.epsl.2009.06.041, 2010; [29] J. Holt et al., Science, 322, 1235, 2008; [30] J. Plaut et al., GRL, 36, L02203, 2009.

EARLY MARS: CONDITIONS, EVENTS AND SCENARIOS.

C. I. Fassett, J. W. Head, *Dept. of Geological Sciences, Brown University, Providence, RI 02912 USA. Contact: Caleb_Fassett@brown.edu*

Introduction: Spacecraft data indicate that the environment of early Mars differs from recent conditions in a variety of important ways. Mars appears to have had an intense magnetic dynamo [1], a wetter surface [2], neutral-pH aqueous alteration [3,4], a denser atmosphere [5], and higher impact and volcanic fluxes [6,7]. Moreover, direct evidence strongly favors the existence of lakes on the early surface, some of which were quite large [8]; more speculatively, there may have been an ocean in the northern hemisphere [9]. All of these conditions on were present in periods prior to the mid-Hesperian. Each of these factors (with the possible exception of a higher impact flux) is broadly consistent with Mars being more habitable early in its history than today. This has helped motivate an exploration strategy predicated on examining materials from this early period.

Given these different conditions inferred to exist, it has been common to assume that there is a discrete geological period (perhaps of some length) when all of these conditions were met simultaneously. Although such a scenario is possible, timing constraints suggest that it may not be probable. Here we review constraints on when these conditions existed and describe possible scenarios for the changes in the environmental conditions that may have occurred on Mars.

Valley Network Timing and Activity: Two independent studies [10,11] used slightly different variations of a 'buffered crater counting' approach to measure the superimposed crater population and timing of valley network formation. Large-scale valley formation on Mars appears to ended during or by the Early Hesperian, although most valley networks have dates that cluster near the Noachian/Hesperian boundary in the Late Noachian. (Note that certain, mostly small, valley systems are universally accepted as much younger [see discussion in 10, 12]). In [10], we suggested that two possible interpretations were consistent with our measurements: either global termination of valley activity near to the Noachian/Hesperian boundary (the view which we favored at the time), or persistence of some valleys into the Early Hesperian.

Recent evidence has strengthened the case for some of the largest valley network having continued to be active in the Early Hesperian, though some have argued for activity later [12], which is less consistent with the measurements in [10]. Younger ages seem to primarily result from differences in analytical choices, particularly: (1) how count regions are aggregated, (2) different stratigraphic interpretations and, most importantly, (3) the effective diameter used to compare observed crater populations with isochrons. These factors are coupled, since larger diameter craters require greater aggregation of area to achieve meaningful statistics, at the expense of ability to discern real local variation (if it exists) (as noted by [13]). Reliance on smaller craters commonly results in younger ages due to contrasting crater retention. In sum, data suggest that regionalto- global valley formation ended in Early Mars history, probably during the Early Hesperian.

Basin Sequence and Timing: Crater counts by Werner [14] and by us, on the visible crater record of Argyre, Isidis, and Hellas suggest that the sequence of the large, well-preserved impact basins was Hellas, Isidis, and then Argyre. These data imply that Hellas and Isidis formed in the Early Noachian, and Argyre in the Mid-to-Early Noachian. This sequence is also consistent with the fact that Argyre has the best preserved basin-related facies [15].

All of these basins have been incised by valley networks on their interior or near-exterior, implying that intense fluvial activity took place after their formation, consistent with crater counting of valley networks. Using current models of the declining cratering flux [7] to interpret the superposed crater populations of Argyre (the last basin larger than 500 km) and valley networks would imply a period of >50 Myr and possibly ~300 Myr between Argyre and the end of basin formation. Both the stratigraphy of valley networks and basins and their relative crater statistics preclude a simple causal relationship between basin formation and valley formation.

Timing of Magnetic Field: Observations from the Mars Global Surveyor magnetometer experiment demonstrated that there are crustal magnetic anomalies observed over much of the surface, with the strongest anomalies concentrated in the southern highlands [1]. These crustal anomalies likely imply an early core dynamo and global magnetic field. The existence of this magnetic field may have played an important role in arresting the loss of an early martian atmosphere by solar wind sputtering, as well as shielding the surface from energetic cosmic rays [e.g., 5].

The most important age constraint on the timing of the Mars magnetic field is the demagnetization (or non-magnetization) of certain basins and volcanoes. Magnetic anomalies are largely absent in Hellas, Argyre, Isidis, and Utopia, as well across most of Tharsis and volcanic edifices, with the exception of Hadriaca Patera [16,17]. The simplest explanation for the lack of magnetization on these basins and volcanoes is that they post-date the cessation of the magnetic field. If this interpretation is correct, the core dynamo must have ended during the Early Noachian, before the formation of Hellas [16,17]. Given this temporal relationship between the magnetic field and (younger) basins, and between basins and the valley networks, the magnetic field plausibly ended far before the end of valley network formation, as well as any hypothesized shift in mineralogical alteration on early Mars [3,4]. If a magnetic dynamo and/or atmosphere, the shield may have been removed well before water stopped was playing an important geomorphic role on the martian surface.

Summary: It has been hypothesized that the period when valley networks were formed early in the history of the planet is coincident with an early magnetic field that protected the atmosphere and that removal of this early shield ended clement surface conditions. As we describe here, this scenario appears unlikely (see Fig. 1). Furthermore, a causal relationship between formation of the largest basins and valley networks is not favored. If cratering helps contribute to valley formation, smaller craters must be invoked [see 10].

What does the sequence of events described here imply for the search for habitable environments? If a magnetic field was necessary for protecting life at the surface of Mars, valley sediments and phyllosilicate- bearing units that date to the Late Noachian/ Early Hesperian (e.g., at MSL landing sites such as Holden and Eberswalde]) may have been emplaced in conditions that had already become less favorable for life, since the dynamo may have terminated hundreds of millions of years before they were deposited.

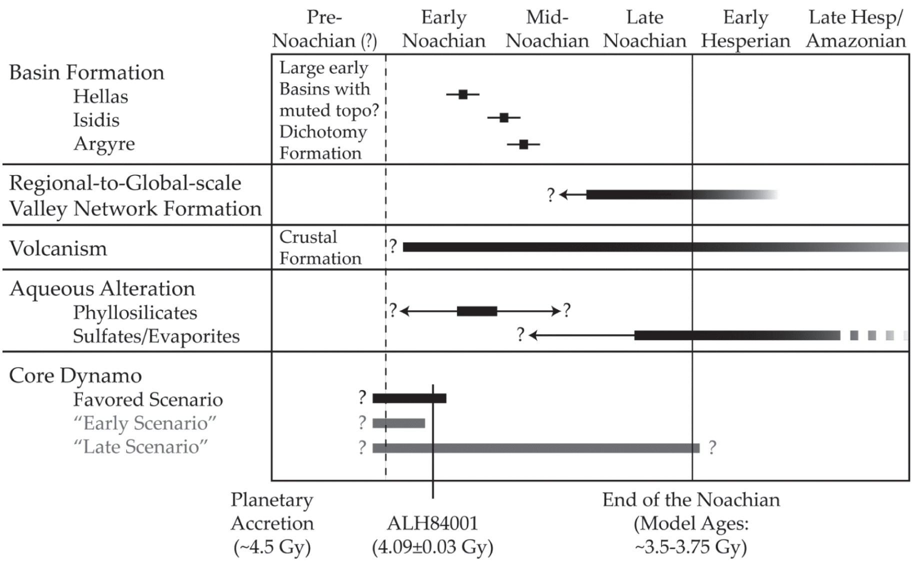

Fig 1: Schematic of various planetary conditions on Early Mars. Other important environmental conditions are: 1) The impact flux, which is probably declined over time, although the precise form of the flux is unknown; during the Noachian, there here may have been a peak during the period of basin formation (Late Heavy Bombardment) or simply a monotonic rise. 2) The atmospheric density, whose history is poorly constrained though evidence suggests that the atmosphere was denser during early periods than it is at present. The date for ALH84001 (our one sample from this time on Mars) comes from [18].

References: [1] Acuña, M.H. et al. (1999), Science, 284, 790-793. [2] Carr, M.H. (1996) Water on Mars. [3] Bibring, J-P. et al. (2006), Science, 312, 400-404. [4] Murchie, S.L. et al. (2009), JGR, 114, E00D06. [5] Jakosky, B.M, Philllips, R.J. (2001) Nature, 412, 237- 244. [6] Tanaka, K.L. et al. (1987), Proc. LPSC, 18, 665-678. [7] Hartmann, W.K., Neukum, G. (2001), Space Sci. Rev., 96, 165-194. [8] Fassett, C.I., Head, J.W. (2008), Icarus, 198, 37-56. [9] Clifford, S.M., Parker, T.J. (2001), Icarus, 154, 40-79. [10] Fassett, C.I., Head, J.W. (2008), Icarus, 195, 61-89. [11] Hoke, M.R.T, Hynek, B.M., (2009), JGR, 114, E08002. [12] Bouley, S. et al. (2009), PSS, 57, 982-999. [13] Bouley, S. et al. (2010), Icarus, 686-698. [14] Werner, S.C. (2008), Icarus, 195, 45-60. [15] Schultz, P., (1985), NASA TM-88383. [16] Lillis, R.P. et al. (2006), GRL, 33, L03202. [17] Lillis, R.P. et al. (2008), Icarus, 194, 575-596. [18] Lapen, T.J. et al. (2010), Science, 328, 347-351.

ANALYSIS OF THE ORIGIN OF AN ERODED CHANNEL IN AN ELYSIUM PLANITIA CRATER.

D. M. Hurwitz[1], C. I. Fassett[1], J. W. Head[1], and L. Wilson[2], *[1]Department of Geological Sciences, Brown University, Providence RI 02912, USA; [2]Lancaster Environment Centre, Lancaster University, UK. Contact: debra_hurwitz@brown.edu*

Introduction: Lava channels with a variety of morphologies have been widely observed on the surface of Mars (e.g., 1-4). Understanding the origin of lava chan-nels requires understanding the erosion regime (i.e., mechanical, [5] vs. thermal, [6-8]) present during channel formation. Detailed analyses of channel morphology can contribute to estimates of the flow velocity through the channel [e.g., 9]. These esti-mates can be used to determine the flow regime that was responsible for forming the channel and to de-termine the rates of erosion in both a mechanical and a thermal erosion environment [e.g., 7, 10-12]. When compared with predicted times of flow dura-tion, these estimates can be used to identify which erosion regime was responsible for the formation of the channel. We use this approach to infer condi-tions present during the formation of a lava channel observed in a crater within Elysium Planitia (Figure 1).

Local Geologic Description: The impact crater shown in Figure 1 is centered at 160.6°E, 0.9°N and lies within young Elysium Planitia lava plains (about 10-100 Ma, [13]) that originate in Cerberus Fossae [14]. These plains cov-er ejecta associated with the crater, flowing up the crater rim on all sides. The crater is a well-preserved complex crater with wall terraces and a prominent central peak visible in Figure 1. The crater rim is completely intact except in one location on the east-ern rim (c in Figure 1), where lava from the sur-rounding plains has breached the rim crest and flowed down the wall of the crater. This lava cut a channel into the wall of the crater (Figure 2) and flooded the crater interior, leaving hummocky flows in the crater interior with textures that are still visible on the crater floor.

Lava initially flowed into the channel at an angle of $\sim 6.2^{\circ}$ before getting diverted around and between terraces in the crater wall, decreasing the slope of the channel to $\sim 4.2^{\circ}$. The lava then flowed directly down-grade at a slope of $\sim 13.4^{\circ}$ and was deposited on the crater floor. Measurements of channel length, width, and depth indicate an approximate channel volume, and thus volume of eroded material, of 0.075 km^3.

Lava Channel Flow: These observations are used to define parameters required to determine lava flow velocity [9], erosion rate in both a mechanical [12] and thermal regime [10], and the duration of channel formation. Para-meters of interest include the volume flux of lava through the channel (Q) and the depth of the lava within the channel (d_{lava}). These parameters were varied iteratively within models of mechanical and thermal erosion until the eroded channel depth pre-dicted in the models matched the channel depths observed. Resulting erosion rates for each erosion regime are shown

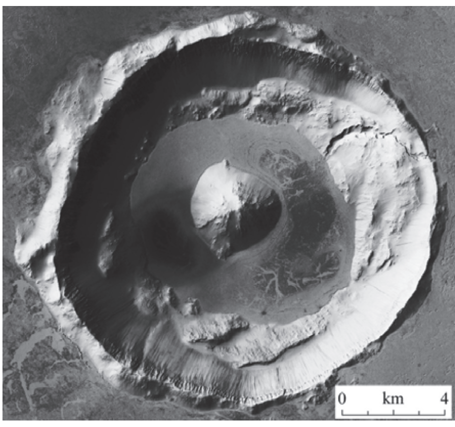

Fig. 1a: Impact crater (diameter, 15 km, depth, 1.1 km) within the lava plains of Elysium Planitia, Mars, centered at 160.6oE, 0.9oN. The crater has been completely embayed by the surround-ing lava plains. Lava breached the eastern crater rim and depo-sited lava in the crater interior, as shown in more detail in Figure 1b. CTX image P20_008713_1791_XN_00S199W, 8 m/pix resolution.

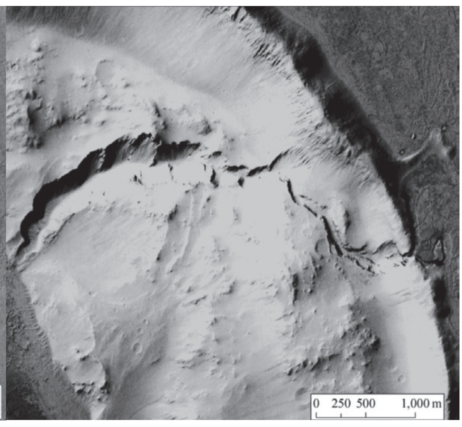

Fig. 1b: The channel cuts the wall of the crater within Elysium Planitia shown in Figure 1a. The channel has a length of 5.8 km, an average width of ~200m, and a depth of ~60 m. Hummocky lava deposits from the channel are observed at the base of the crater wall.

in Figure 2. Figure 2 indicates that erosion rates in the mechanical erosion regime are higher than those in the thermal erosion regime at slopes >4.3° such as those observed in the Ely-sium channel. These results imply that mechanical erosion is more likely to dominate the development of a channel that forms on a steep slope under the Martian conditions considered here.

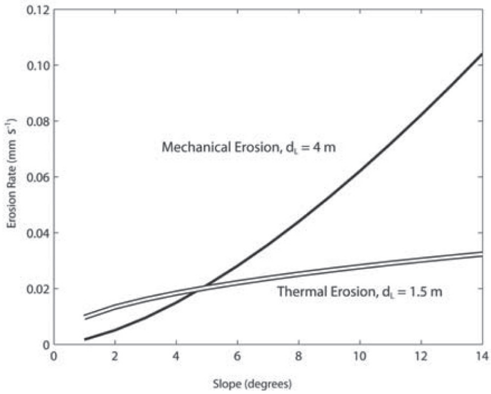

Fig. 2: Mechanical and thermal erosion rates predicted by [10, 12]. Mechanical erosion is more efficient than thermal erosion at slopes greater than ~4.5o under the considered conditions.

Conclusions: Our calculations indicate that the observed chan-nel formed as the result of mechanical erosion that occurred over ~30 Earth days at rates of 0.02-0.09 mm/s, as lava flowed at velocities of 17-25 m/s down slopes of 4.2°-13.4°. These results support previous analyses of the duration of the Cerberus Fossae eruption (1-6 Earth months [14]) that acted as the source for the observed channel.

References: [1] Mouginis-Mark, P. J., 2005, JGR, 110, E08007, [2] Bleacher, J. E., et al., 2007, JGR, 112, E04003, [3] Hauber, E. et al., 2009, JVGR, 185(1-2), p. 69, [4] Leverington, D. W., 2004, JGR, 109, E10011, [5] Rossi, M. J., 1997, Geomorph., 20, p. 95, [6] Hulme, G. & Fielder, G., 1977, Phil. Trans. Roy. Soc., 285, p. 227, [7] Williams, D. A., et al., 1998, JGR, 103, p. 27,533, [8] Oshigami, S. et al., 2007, LPSC 38, p. 1185, [9] Keszthelyi, L. & Self, S. 1998, JGR 103(B11), p. 27,447, [10] Hulme, G. 1973, Geophys. J. Int., 39, 361-383, [11] Wilson, L. and Head, J.W., 2010, LPSC 41, #1101, [12] Sklar, L. and Dieterich, W.E., 1998, Rivers over Rock, [13] Hartmann, W. K. & Neukum, G., 2001, Space Sci. Rev., 96, p. 165, [14] Jaeger, W.L. et al., 2010, Ica-rus, 205, 230-243.

THE SPECIFIC SIGNATURES OF THE SOLAR WIND-PHOBOS INTERACTION AS EVIDENCE OF THE PHOBOS MAGNETIC FIELD FROM THE PHOBOS 2 DATA

V. G. Mordovskaya, V. A. Styashkin, *Pushkov Institute of Terrestrial Magnetism, Ionosphere, and Radiowave Propagation, Troitsk, Moscow Region, Russia.*
Contact: valen@izmiran.ru

In this study we have considered the solar wind interaction with Phobos using the magnetic field and plasma data from the Phobos-2 mission during the closest fly-by on March 22–26, 1989. There are the specific magnetic field signatures in the fly-by data set when the spacecraft was located permanently in a vicinity of Phobos and the distances between them were 180--400 km.

These magnetic field enhancements in the regular part can be really attributed to the signatures of the solar wind - Phobos interaction because their appearance correlates strong with the S/C approaches to Phobos. They had disappeared when the S/C moved away from Phobos. The degree of the manifestation in the magnetic field signatures depends on the plasma parameters of the solar wind and is different for low and high plasma density. The enhancements of the magnetic field near Phobos are observed near the Phobos day-side if the solar wind density becomes significant and the proton skin depth(ω_{pi}) is comparable with the actual size of the Phobos obstacle. The actual size (L) of the Phobos obstacle is L ~c/ω_{pi} ~ 150--170 km.

The morphology of the magnetic field signatures observed during the time interval of March 22–26, 1989 is presented in Figs. 1–3.

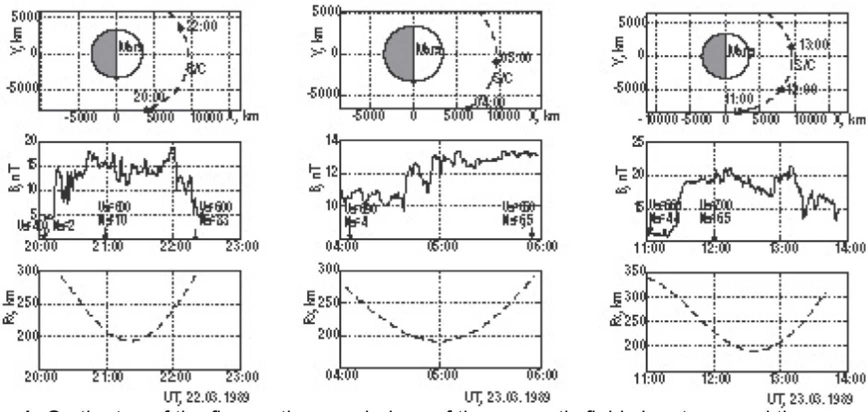

Fig. 1: On the top of the figures the morphology of the magnetic field signatures and the appropriate spacecraft trajectories in the projection onto the Mars ecliptic plane XoY are presented. The lower graphs correspond to the time history of spacecraft approaches to the dayside of Phobos inside the free solar wind. The data from 20:15 to 22:15 on March 22, 1989, the data from 04:00 to 06:00 on March 23, 1989 and the data from 11:00 to 13:45 on March 23, 1989.

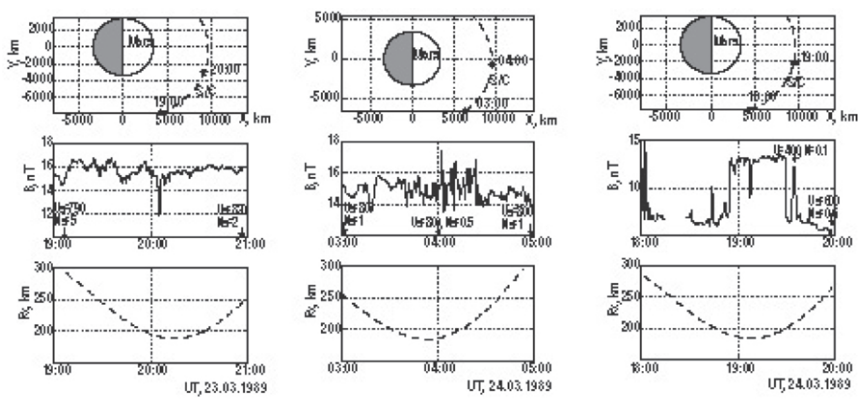

Fig. 2: Similar to Fig. 1 but the data from 19:00 to 21:00 on March 23, 1989, the data from 03:00 to 05:00 on March 24, 1989 and the data from 18:00 to 20:00 on March 24, 1989.

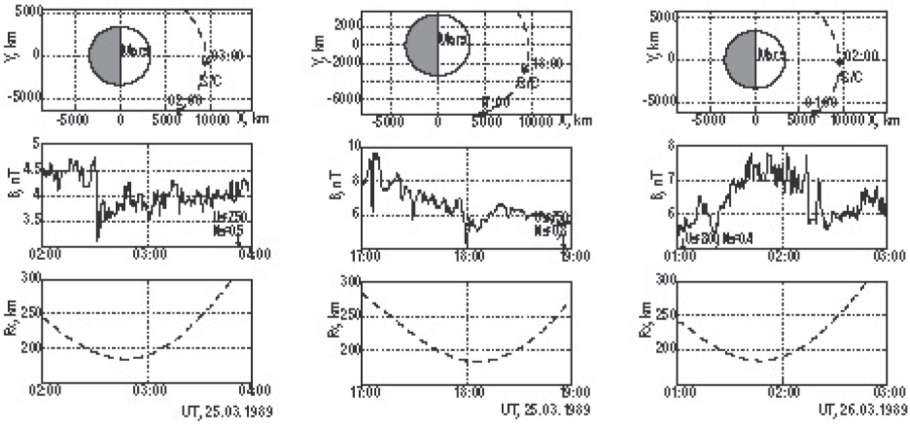

Fig. 3: Similar to Fig. 1, but the data from 02:00 to 04:00 on March 25, 1989, the data from 17:00 to 19:00 on March 25, 1989 and the data from 01:00 to 03:00 on March 26, 1989.

References: Mordovskaya, V.G., Oraevsky, V.N., Styashkin, V.A., and Rustenbach, J., Experimental Evidence of the Phobos Magnetic Field, JETP Lett., 74, pp. 293–297, 2001.
V. G. Mordovskaya, V. N. Oraevskii, and J. Rustenbach, Kosm. Issled. 39, 477 (2001).

THE EFFECTS OF VIEWING GEOMETRY AND TEMPERATURE ON OMEGA AND CRISM PHOBOS OBSERVATIONS

A. Fraeman[1], R. Arvidson[1], B. Gondet[2], J-P. Bibring[2], S. Murchie[3], T. Choo[3], D. Humm[3], N. Manaud[4], *[1]Washington University in St. Louis, MO, USA; [2]Institut d'Astrophysique Spatiale, Orsay, France; [3]The Johns Hopkins Applied Physics Laboratory, MD, USA; 4European Space Astronomy Centre, Madrid, Spain*
Contact: afraeman@wustl.edu

Introduction: The origin and composition of Phobos is still widely debated, making the Martian satellite an important target for scientific study. The Compact Reconnaissance Imaging Spectrometer for Mars (CRISM) aboard the Mars Reconnaissance Orbiter and the Observatoire pour la Minéralogie, l'Eau, les Glaces, et l'Activité (OMEGA) instrument on Mars Express have recently obtained hyperspec-tral, disk-resolved images of Phobos covering the wavelength range between 0.35-5μm. The spectral radiance from the moon within this wavelength range is controlled by surface properties and obser-vation viewing geometries (incidence, emergence, and phase angles), as well as thermal emission that becomes increasingly dominant towards longer wa-velengths (>~2.5μm). In this abstract we discuss methods for modeling all of the factors affecting the spectral radiance of Phobos, and then apply these models to compare regions of Phobos observed by CRISM and OMEGA under different lighting, view-ing, and thermal conditions.

Datasets: CRISM has acquired three hyperspec-tral images of Phobos between 0.362 – 3.92 μm [1]. These images were obtained at a spatial resolution of 350 m/pixel and phase angle of ~41˚. OMEGA has obtained six observations of Phobos covering a range between 0.35 – 5.1μm, and two observations from 0.35 – 1μm only [2]. The spatial resolution of the OMEGA data ranges from 2.2 km/pixel to 100 m/pixel, and the phase angles range from 47.2˚ to 95˚.

Two OMEGA observations (ORB0756_0 and ORB3769_3) have overlapping coverage with the CRISM data. Figure 1 demonstrates an example where CRISM data overlaps an OMEGA observa-tion, and I/F spectra from an area observed by both OMEGA and CRISM under different viewing and temperature conditions are shown in Figure 2.

Modeling Observation Geometries: The inci-dence, emergence, and phase angles for each pixel in the CRISM observations were determined using the shape model of Thomas (1993) [3] and the SciBox Toolkit developed at the Johns Hopkins Applied Physics Laboratory [4]. Figure 3 shows the resulting incidence and emergence angles calculated for FRT00002992_03. The photometric angles for the OMEGA data were computed using a prototype ver-sion of the Navigation and Ancillary Information Facility (NAIF) SPICE Toolkit that includes a Digi-tal Shape Kernel (DSK) system in conjunction with a Phobos DSK model (Figure 4).

The effects of lighting and viewing geometries on the spectral radiance measured by CRISM and OMEGA may be taken into account using a Hapke model for both solar and thermal contributions. Pa-rameters input into this model are related to surface properties and include the regolith single-scattering albedo (*w*), opposition surge angular width (*h*), op-position surge amplitude (*B0*), macroscopic rough-ness mean slope angle, and the asymmetry fac-tor used in the Henyey-Greenstein particle phase function (*g1*). For emission at longer wavelengths, the surface kinetic temperature is also important. Simonelli et al. (1997) [5] have determined global-average values of Hapke parameters for Phobos using Viking clear-filter images. This filter has ef-fective wavelength of ~0.54μm and a band-width of ~0.2μm [6].

Preliminary results indicate that there is a discre-pancy between the predicted I/F based on the best-fit model of Simonelli et al (1997) [5] and the OMEGA I/F data from ORB0413_0. Figure 5 shows that the OMEGA data appear to be systematically offset from the predicted I/F by a factor of ~1.5 at 0.54μm, and that this offset is even greater at longer wave-lengths; the modeled I/F value are off by a factor of ~4 at 2.0μm. The discrepancy may be due to a cali-bration difference between the Viking clear-filter and OMEGA data or to wavelength dependence in the Hapke parameters. The parameters reported by Simonelli et al (1997) [5] were derived using a wide-band filter, whereas the 0.54μm OMEGA data have a much narrower effective band width. If the Hapke parameters are wavelength dependent, the best fit values derived from the wide-band Viking clear-filter images will be different than those needed to model the narrow band, hyperspectral OMEGA data. The availability of several spatially overlapping OMEGA observations acquired at different phase angles allows us to independently investigate the best fit global-average Hapke-parameters across multiple wavelengths, and we will present the results of this investigation.

Thermal Contributions: As noted, in addition to the reflected solar component, thermally emitted radiation provides an increasingly significant contri-bution to the total observed radiance of the moons at wavelengths beyond ~2.5μm (Figure 3). The moon's surface temperatures control this thermally emitted contribution and must be known in order to analyze spectra at the longest wavelength ranges. We estimate surface temperatures using pairs of spectra from locations with the same emissivity but different temperatures. It is possible to solve for the emissivi-ty of one location in terms of its temperature and then substitute this value into the second location with similar properties to the first, allowing us to find a pair of temperatures that creates the best-fit model spectral radiances for both locations. Prelim-inary work with this method employing a simple Lambertian scattering model instead of the more complex Hapke function suggest the maximum tem-peratures in the CRISM Phobos observation are ~340K.

CRISM and OMEGA Comparisons: Phobos provides an excellent target for comparing observations from the OMEGA and CRISM instruments due to the absence of a spatially and temporally variable atmosphere and the availability of images with simi-lar spatial resolutions. A full model that can account for the effects of different observation and thermal conditions on the observed spectral radiance will allow us determine whether the differences in CRISM and OMEGA spectra from the same location (Figure 2) are due entirely to the different viewing geometries and surface temperatures of the observa-tions, or to differences in the calibrations of the two instruments.

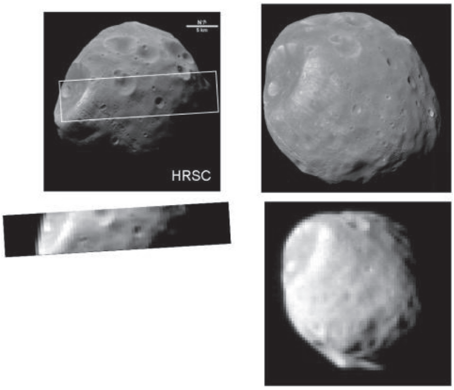

Fig. 1: HRSC observation (top left) overlain with the OMEGA track from ORB0756_0. This OMEGA observation is shown on bottom left and has a spatial resolution of ~200m/pixel and aver-age phase angle of 63˚. The HiRISE Phobos observation is shown in the top right and has approximately the same orientation as the CRISM Phobos observations (bottom right). CRISM has a resolution of ~350m/pixel and an average phase angle of 42˚. Both CRISM and OMEGA observations provide cover of Stick-ney and the area to the east.

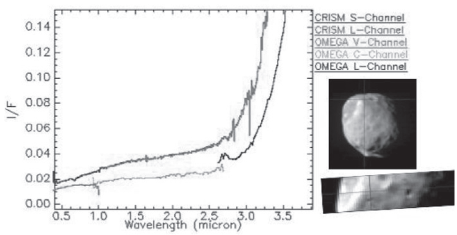

Fig. 2: Comparison between CRISM FRT0002992_03 and OMEGA ORB0756_0 observations of Phobos. Single pixel I/F spectra are from the region marked by red cross hairs in the cor-responding CRISM (top right) and OMEGA (bottom right) im-ages. The CRISM spectrum is from a pixel with an i,e, g of 65˚, 60˚, 41˚ respectively, and the OMEGA spectrum is from a pixel with an i,e,g of 62˚, 17˚, 64˚ respectively.

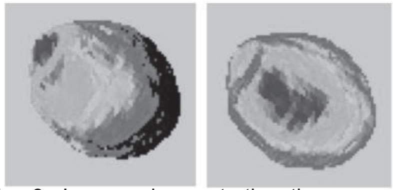

Fig. 3: Images demonstrating the range of incidence (left) and emergence (right) angles in Phobos CRISM observations. The angles range from ~0˚ (purple) to ~90˚ (red)

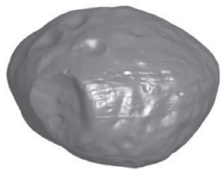

Fig. 4: Rendering of Phobos DSK used to calculate OMEGA observation geometries (ftp://naif.jpl.nasa.gov/pub/naif/misc/alpha_disk/data/phobos)

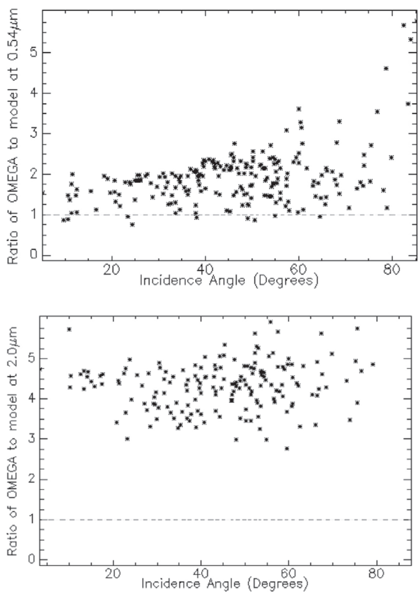

Fig. 5: Ratio between pixels in OMEGA observation and Simonelli et al, 1997 model [5] for ORB0413_0 at 0.54μm (top) and 2.0μm (bottom). This observation has an average phase angle of 42˚ and a spatial resolution of 2273m/pixel.

References: [1]Murchie, S. et al. 2008. MRO/CRISM Observations of Phobos and Deimos, LPSC XXXIX. Houston, TX.
[2]Gondet, B. et al. 2008. Phobos Observations by the OMEGA/Mars Express hyperspectral Imager, LPSC XXXIX. Houston, TX,
[3]Thomas, P. 1993. Gravity, tides, and topography on small satellites and asteroids: Application to surface features of the martian satellites, Icarus, 205, 326-344.
[4] Choos, T & Skura, J. 2004. SciBox: A Software Library for Rapid Development of Science Operation Simulation, Planning, and Command Tools. Johns Hopkins APL Technical Digest, 25, 154-162.

MODELLING OF REFLECTED HYDROGEN AND PROTONS SIGNATURES AT PHOBOS' ORBIT

F. Cipriani [1], R. Modolo[2] , F. Leblanc[2], and O. Witasse[1], *[1]ESA/ESTEC, Noordwijk, The Netherlands (fciprian@rssd.esa.int / Fax: +31-71-5654697), [2]LATMOS/IPSL, CNRS, Verrières Le Buisson, France*

Introduction and Purpose of the Study: Solar Wind protons are reflected by the Lunar regolith in proportion 0.1% to 1%, as suggested by MAP-PACE measurements onboard SELENE [1]. A similar process seems to lead to a significant emission of neutralized hydrogen (up to 20% of the impinging protons flux), as evidenced by SARA instruments measurements onboard the Chandrayaan-1 spacecraft [2]. As in the case of the Moon, Phobos' surface is weathered by micrometeoroids impacts and Solar Wind ions bombardment. Since a significant part of Phobos' orbit is exposed to the shocked Solar Wind, downstream of the Martian Bow Shock, a SW protons reflection process similar to that observed at the Moon is likely to occur, and was indeed observed (S. Barabash, private communication) in 2008. Following Phobos flybys by Mars Express in July 2008 and February 2010, the presence of reflected protons and neutral hydrogen populations can be investigated by instruments of the ASPERA3 package, namely IMA (Ion Mass Analyzer) and NPD (Neutral Particle Detector) sensors. In the present study we use a 3D Test Particle model to simulate reflection of SW protons both as ionized and neutralized hydrogen, in order to derive signatures of those populations in the Martian Environment.

Simulation / Expected Results: Our numerical model has been described and used in [3] to investigate physical characteristics of a putative neutral gas torus at Phobos' orbit for low solar activity conditions.

In the present study we set up the electromagnetic field values in the vicinity of Phobos' orbit given by a Hybrid simulation performed in minimum solar activity [4], in order to infer characteristics of the reflected proton population. As a first step we take energy distributions of the reflected populations consistent with those measured at the Moon.

Since Phobos' surface potential and charge state may significantly influence the protons reflection process and the charge state of ejected atoms, we also introduce a boundary condition at Phobos' surface in the simulation.

Trajectories of ejected neutral hydrogen atoms on the one hand, and protons on the other hand, are followed around Mars, where particles are subject to the Martian gravity and to the solar radiation pressure for the former, and to the Lorentz force for the latter. Particles can be lost into the Martian thermosphere, escape the system, become ionized when originating as neutrals, or neutralized when originating as protons.

Specifically, we describe neutralization of reflected protons through charge exchange reactions with exospheric oxygen atoms leading to an ENA signature on the one hand, and ionization of ejected neutrals through charge exchange reactions with SW protons leading to a proton signature on the other hand.

We will therefore present the results of our simulations and describe the morphologies of the reflected fluxes and their dependence on the IMF characteristics at low solar activity, regarding: 1) a reflected proton population, 2) a reflected neutral hydrogen population, 3) a neutralized hydrogen (ENA) component, and 4) an ionized hydrogen component.

References: [1] Saito, Y. et al, (2008) GRL, 35, L24205, doi:10.1029/2008GL036077.
[2] Wieser, D. et al, (2009), PSS, Extremely high reflection of solar wind protons as neutral hydrogen atoms from regolith in space, doi:10.1016/j.pss.2009.09.012
[3] Cipriani, F. et al (2010), PSS, A Model of Interaction of Phobos' Surface with the Martian Environment, submitted.
[4] Modolo, R. et al (2005), Influence of the solar EUV flux on the Martian plasma environment, Annales Geophysicae, 23, pp.433-444

NEW RESULTS FROM TES POLAR RETRIEVALS

J. Eluszkiewicz[1], T. Titus[2], K. Cady-Pereira[1], G. Uymin[1], J.-L. Moncet1, and E. Mlawer[1], [1]*Atmospheric and Environmental Research, Inc.,* [2]*U.S. Geological Survey*

The Thermal Emission Spectrometer (TES) aboard the Mars Global Surveyor (MGS) spacecraft has generated an unprecedented wealth of information about Mars. Although TES is primarily a surface-oriented instrument, analyses of TES spectra have also yielded abundant information about the Martian atmosphere, including its thermal structure, dust opacity, column abundance of water vapor, and optical properties of airborne dust and water ice particles. The focus of the TES retrieval and analysis work performed to date has been on the non-polar regions.

In a pilot study, Eluszkiewicz et al. [2008] performed simultaneous temperature and surface emissivity retrievals for a small sample of TES spectra collected over the northern seasonal cap and detected intriguing correlations between the atmospheric temperatures and surface emissivities. In this presentation, we will describe new results from this on-going work, performed in a “mapping mode” extending to larger geographical regions. We will also briefly describe Mars adaptations of AER’s radiative transfer codes employed in our work, particularly LBLRTM and OSS (Optimal Spectral Sampling). We expect these tools to be of interest to the wider community as new Mars sensors are planned for the next decade.

This work is funded by the NASA Mars Data Analysis Program.

PRIMERY RESULTS OF MARTIAN IONOSPHERE FROM MARSIS/MEX

J. S. Ping, M.Y. WANG, *Shanghai Astronomical Observatory, CAS, Shanghai, Nandan Rd. 80, P.R. China pjs@shao.ac.cn*

Introduction: The MARSIS mission in Mars Express has proven outstanding ability to detect both of the undersurface Martian structure, and the Martian ionosphere. We developed an self-adjust method to retrieving the ionospheric profile automatically from the down looking radio radar data. The primary result is introduced in this paper.

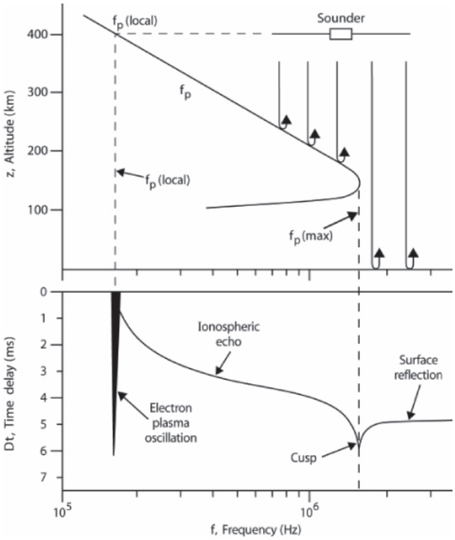

Fig. 1: Working Principle of MARSIS Mission

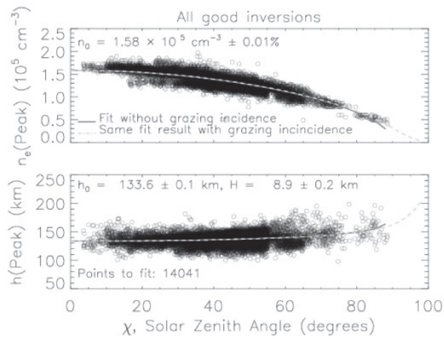

Fig. 3: Distributions of Martian Ionospheric-Chapman Model Parameters from MARSIS Ionospheric Profiles.

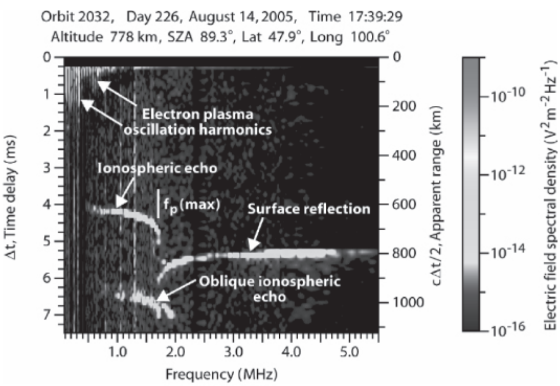

Fig. 2: Example of MARSIS Observation Image.

REMOTE POWER SUPPLYING OF EQUIPMENT FOR PLANETARY EXPLORATIONS

R. A. Evdokimov, V. Y. Tugaenko, A. S. Gribkov, V. V. Sinyavski, A. N. Bombin, A. A. Maslennikov *Korolev Rocket and Space Corporation "ENERGIA", 4-a, Lenin Street, Korolev, Moscow Region, 141070, Russia. Contact: evdokimovrom@yandex.ru*

Possible applications of the wireless energy transmission technology (WET) by the laser channel between spacecrafts for the planet explorations are considered in this paper. The WET present status and status of the space high power systems are represented.

Technology for remote power supplying of equipment in space and on surfaces of the Solar system bodies from space power stations by lase channel are developing in RSC "Energia|".

The theoretical system investigations and experimental works are conducting.

The main attention is paid for development of critical technology elements: sources of laser radiation, systems for narrow laser beam creation, special photovoltaic converters, control and prompting systems.

Now the ground based experiments with low power sources (tens – hundreds watts) are conducting with energy transmission on the distances from hundreds meters up to several kilometers. The purpose of these experiments is to confirm the main parameters of system elements, first of all – total efficiency of the WET channel.

In the near term perspective the space experiments with transmission of electric power from the board of International Space Station (ISS) to "Progress" cargo vehicle are planned. The power will be in the range of hundreds watts up to several kilowatts. The distance will be up to several kilometers.

Explorations in the area of the systems for power transmission on the distances from tens to hundreds kilometers (in far future – up to thousands kilometers and tens thousands kilometers) with high efficiency are conducting.

In present time the technology on the base of semiconductor IR lasers and special photovoltaic converters for receivers of monochromatic IR radiation is chosen. Semiconductor IR lasers have efficiency more than 50%, special PV receivers – up to 60% and higher.

This activity closely connected with large RSC "Energia|" experience in design and experimental development of high power space nuclear systems (SNS). SNS with electric power about 5 –15 Megawatts as energy sources for electric propulsion systems were designed for Mars manned expedition. The SMS with electric power 150 – 500 kilowatt were proposed for wide range of space applications including space transport system on the base of tugs with electric rockets engines. It was large program of SNS main elements experimental development including thermionic elements and heat rejection system.

These high power SNS can be used in space energy stations for consumers supplying with aid of wireless channel. For example, the possibility of development of high efficient interorbital transport system on the base of SNS and WET technology was studied. Also, the usage of the space energy stations with WET system for power supplying of near Earth infrastructure including future manned space stations is studied.

The equipment of the Mars manned expedition will include high power systems (nuclear or solar) without dependence from its concrete scheme.

The presence of the energy plants with power from hundred kilowatts to tens megawatts on the Mars orbit opens the possibility of centralized energy supplying of spread exploration infrastructure on the Mars surface and orbits. This exploration net, which potential could be essentially increased by additional energy supplying from the orbit, would include stationary and moving bases, piloted and automatic rovers, large system of small stations, balloons and light automatic planes in the Mars atmosphere and etc.

The same approach could be used in the large robotic missions (precursor of Mars manned missions).

This way could be fruitful for explorations of comets, asteroids and some satellites of outer planets (without thick atmosphere) by automatic spacecrafts with high power energy systems.

For example, spacecraft like JIMO could use its SNS not only for supply of electric propulsion system and a radar, but for energy support of the probes on Jupiter ice moons surfaces with aid of WET channel. This approach can essentially improve energy budget of probes and increase the program of science investigations.

The above described missions require high power energy plants (like SNS) and high level of WET technology development. However remote power supplying of spacecrafts could be used in science missions of middle term perspective too.

For example, the possibility of energy supporting of sub satellites and landers from the board of main spacecraft could be studied for missions to comets, asteroids and small planet's moons (missions like "Rosetta" or "Down").

In this case the effectiveness (life time, volume and quality of science experiments) of small landers could be seriously increased by transmission from orbiter only hundred watts from the distance about several kilometers or tens kilometers.

It is necessary to remark that development of WET elements could be closely connected with other important areas for planet explorations like laser sounding of planet's surfaces and atmospheres and laser communications.

THE MOESSBAUER SPECTROMETER MIMOS II ON THE PHOBOS SAMPLE RETURN MISSION

D. Rodionov[1,2], M. Blumers[1], G. Klingelhöfer[1], B. Bernhardt[3], J. Gironés Lopez[1], I. Fleischer[1], J. Maul[1], E. Evlanov[2], A. Shlyk[2], C. d'Uston[4], *[1]Institut für Anorganische und Analytische Chemie, Universität Mainz, Germany; contact: klingel@mail.unimainz.de. [2]Space Research Institute IKI, Moscow, Russia; [3]Von Hoerner & Sulger GmbH, Schwetzingen, Germany. 4 CESR, Toulouse, France.*

Introduction: Mössbauer spectroscopy is a powerful tool for quantitative mineralogical analysis of Fe-bearing materials. The miniaturized Mössbauer spectrometer MIMOS II [1] is a component of the Athena science payload on board of two Mars Exploration Rovers currently operating on the Martian surface. Both MIMOS instruments are operational after 6 years of work with a total integration time of more than 1 year. The MER mission has proven that Mössbauer spectroscopy is an important technique for the in-situ exploration of extraterrestrial bodies and the study of Fe-bearing samples [2-4].

The MIMOS II instrument is part of the scientific payload of the "Phobos-Grunt" mission (Russian Space Agency).

The "Phobos-Grunt" mission: Originally, "Phobos-Grunt" was scheduled for a launch in October 2009, but the launch was shifted to 2011/2012 for additional testing of the spacecraft and payload to ensure mission success. Mission goals are:

- Sample return. Laboratory analysis of Phobos substance delivered to Earth;
- In situ and remote studies of Phobos surface in cluding analysis of soil and regolith samples;
- Exploration of Phobos and its ambient space from orbiter.

MIMOS II is mounted on the robotic arm of the landing module (Fig.1). Scientific objectives are:

- Identification of iron-bearing phases (e.g., ox ides, silicates, sulfides, sulfates, and carbonates);
- Quantitative measurement of the distribution of iron among those phases;
- Quantitative measurement of the distribution of iron among its oxidation states.

MIMOS II for "Phobos-Grunt": The Mössbauer spectrometer for "Phobos-Grunt" is based on the MER version [1] with several modifications and improvements. The new design also comes with additional mass reduction. Instrument's firmware has been updated according to mission demands and experience from the MER mission.

Fig. 1: MIMOS II sensorhead mounted on the robotic arm of the Phobos Grunt lander module

A number of improvements were made to ensure optimal instrument performance at low temperatures (down to – 150 C). Fig. 2 shows the Mössbauer drive error signals in the temperature range 140 – 300 K demonstrating the expected functionality of the MIMOS instrument.

Additional temperature calibration of the detector system was performed to achieve optimal results at all temperature windows expected during the Phobos mission. The corresponding detector parameters are adjusted by firmware according to ambient temperature. Fig. 3 shows energy spectra of the 4 main detectors at ~ -130°C.

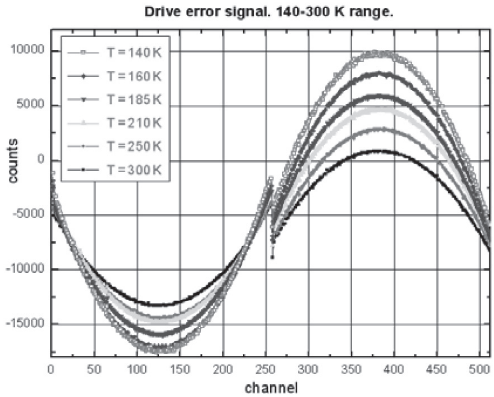

Fig. 2: MIMOS II drive error signals at different operating temperature windows.

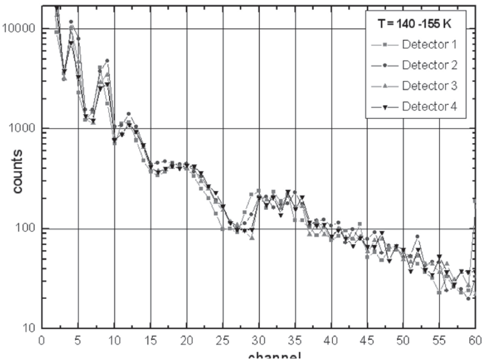

Fig.3: Energy spectra of the 4 main detectors at ~ -130°C. Clearly the 6.4 keV Fe-Xray line at about channel 4 and the 14.41 keV Mössbauer line at about channel 8 can be identified.

MIMOS II was thoroughly and successfully tested (vibration and shock tests) according to mission specifications (Fig.3). The thermal-vacuum tests were performed in a special chamber at the University Mainz.

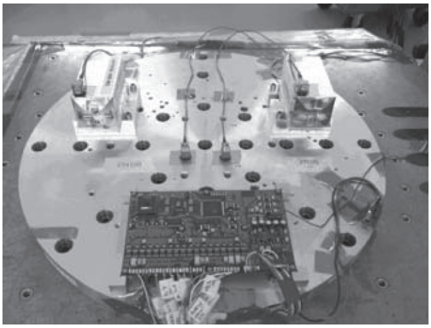

Fig. 4: MIMOS II test setup for vibration and shock tests. 2 sensor heads and 2 electronics boards were tested simultaneously.

Acknowledgments: Funded by the German Space Agency DLR under contract 50 QM 0703. Support by the Russian Space Agency is acknowledged.

References: [1] Klingelhöfer et al., JGR. 108(E12) (2003), [2] Morris et al., JGR111 (2006), [3] Morris et al., JGR 111 (2006) XXVII, 1344–1345, [4] Klingelhöfer et al., Science Vol.306 (2004) 1740-1745.

THE AOST MINIATURE FOURIER SPECTROMETER FOR SPACE STUDIES

O. I. Korablev[1], A. V. Grigoriev[1], B. E. Moshkin[1], L. V. Zasova[1], F. Montmessin[2], A. B. Gvozdev[1], V. N. Shashkin[1], D. V. Patsaev[1], V. S. Makarov[1], S. V. Maksimenko[1], N. I. Ignatiev[1], A. A. Fedorova[1], G. Arnold[3], A. V. Shakun[1], A. I. Terentiev[1], A.V. Zharkov[1], B. S. Mayorov[1], Yu. V. Nikolsky[1], I. V. Khatuntsev[1], G. Bellucci[4], K. V. Grechnev[1], R. O. Kuzmin[5], A. V. Rodin[1,6], *[1]Space Research Institute (IKI), 117997, 84/32 Profsoyuznaya Str, Moscow, Russia; [2]Laboratoire Atmosphères, Milieux, Observations Spatiales, CNRS, Saint-Quentin en Yvelines, France; [3]Institut fuer Planetologie, WWU, Muenster, Germany; [4]Istituto di Fisica dello Spazio Interplanetario INAF, Rome, Italy; [5]Vernadsky Institute of Geochemistry and Analytical Chemistry, Russian Academy of Sciences, Moscow, Russia; [6]Moscow Institute of Physics and Technology (State University), Moscow region, Dolgoprudny, Russia. Contact: korab@iki.rssi.ru*

Introduction: The AOST Fourier spectrometer being developed for the Phobos-Soil project is intended for remote probing in the 2.5–25 μm region. This spectral region includes not only reflected and transmitted solar radiation, but also the intrinsic thermal radiation of the celestial body being studied. The maximum spectral resolution, taking into account apodization, is 0.9 cm^{-1}, and the field-of-view angle is 2.5°. The device has its own thermal-stabilization and two-axis guidance systems, as well as an absolute-blackbody simulator for calibration. The time to record one interferogram ranges from 5 to 50 sec. The mass of the device is 4 kg, and its power requirement is as much as 10 W.

Scientific goals: The main scientific problem of the AOST experiment is to measure the methane concentration in the atmosphere of Mars with good SNR by observing the sun as it shines through the atmosphere of Mars (the “solar-eclipse” regime).

A more complete list of the scientific tasks includes the following:

1. Measuring the concentration of methane and other minor components, the height distribution of these gases and of the aerosol (in the solar-eclipse regime).

2. Measuring daily and seasonal variations in the atmosphere of the vertical profile of the temperature, the concentration of water vapor and of other minor components, and of aerosols (dust and condensation clouds). Study of the non-equilibrium atmospheric emissions.

3. Global mapping of the mineralogical composition of the surface of Phobos and determination of the thermophysical parameters of the regolith. Study of the spectrum of the surface at the landing site with a spatial resolution as good as several centimeters (from observations of Phobos).

Make-up of the device: Structurally, the device consists of two main parts: the base and the turret.

The turret contains the Fourier spectrometer proper (with interferometer of double-pendulum type), secondary supply sources, the microprocessor control and data-processing system, and also the aiming mechanism.

The base is a mechanical, electric, and information interface with the spacecraft.

Conclusion: The collection of parameters of the AOST device is unique - until now there have been no such space-based IR spectrometers. This becomes possible by using modern technical solutions. All subsequent modifications of the device have a good chance of being included in many future planetary missions.

GAS-ANALYTIC PACKAGE OF THE PHOBOS SAMPLE RETURN MISSION

M.V.Gerasimov, *Space Research Institute, Russian Academy of Science, Profsoyuznaya, 84/32, Moscow 117997, Russia. Contact: mgerasim@mx.iki.rssi.ru*

Introduction: Gas-analytic experiment is aimed on the comprehensive investigation of the volatiles inventory of the Phobos surface material. This information is valuable for understanding of the origin and differentiation of the Phobos. Chemical composition and abundance of volatile components in different types of meteorites is tightly connected with conditions of the meteorites origin in different regions of the protoplanetary cloud. The compositional difference of meteorites is present to a greater extent in the difference of the composition of volatiles. Information about the composition of the Phobos volatiles can give valuable information about the region of its origin in the Solar nebular and its relationship to Mars or any type of meteorites.

Information about isotopic ratios of key volatile elements (C, H, O, N, noble gases, …) is also of great importance for the discrimination between different models of the Phobos origin.

Tasks of the Gas-Analytic Package: The main tasks of the Gas-Analytic Package (GAP) are:

1. Detailed investigation of chemical composition and abundances of volatile compounds (H_2O, CO_2, N_2, H_2, noble gases, organics, etc.) in the solid surface material of the Phobos at the landing place;
2. Investigation of forms of incorporation of volatile components into the solid surface material;
3. Investigation of organic components in the surface material;
4. Measurement of isotopic composition of CHON elements ($^{13}C/^{12}C$, D/H, $^{17}O/^{16}O$, $^{18}O/^{16}O$, $^{15}N/^{14}N$) and noble gases
5. To constrain the mineralogical composition of the Pobos soil (with emphasis on the volatile-bearing minerals) on the basis of thermal and gas evolving experiments with the use of data from other experiments.

Description of the GAP: GAP consists of three individual instruments: 1) Thermal Differential Analyzer (TDA); 2) Gas Chromatograph (KhMS-1F); and 3) Mass-Spectrometer (MAL-1F).

Tasks of the TDA instrument are:

1. To measure exo- and endothermal reactions in the sample of soil to determine minerals with phase transitions at temperatures <1000°C;
2. To perform the release of volatile components into the gas phase and provide their transfer into GC and MS;
3. To perform pyrolysis of heavy organics (kerogens?) and provide their transfer into GC and MS.

Tasks of the KhMS-1F instrument are:

1. Accumulation of gases which are released from the sample during pyrolysis;
2. Redistribution of gases of different types (permanent gases, organics, etc.) between respective columns;
3. Separation of different gases by time of retention;
4. Measurement of abundance of each separate gas component;
5. Measurement of isotopic ratios of $^{13}C/^{12}C$, D/H, $^{17}O/^{16}O$, $^{18}O/^{16}O$, in CO_2 and H_2O using TDLAS.

Tasks of the MAL-1F instrument are:

1. Identification of gas components which are released from the gas chromatograph;
2. Measurement of isotopic ratios of volatile elements.

Method of analysis.

GAP receives a portion of soil from the Sample Acquisition Device of the manipulator. This portion is loaded into the SOil Preparation SYStem (SOPSYS) of the TDA instrument. SOPSYS provides milling of soil stones down to sub millimeter size and prepare a dose of the sample for load and sealing into pyrolytic cell (PC). PC perform programmed heating of the sample up to 1000ºC to do thermal analysis of the sample and to provides the release of volatiles into gaseous phase. Released gases are transported to the gas chromatograph by a flow of carrier gas (helium). Gases in time of pyrolysis are analyzed in KhMS-1F using tunable diode laser absorption spectrometer (TDLAS) to measure H_2O and CO_2 molecules and isotopic ratios $^{13}C/^{12}C$, D/H, $^{17}O/^{16}O$, $^{18}O/^{16}O$ in them. Afterwards gases are trapped in two absorption traps: one for permanent gases and another for high boiling components. Collected gases are analyzed than on two chromatographic capillary columns: one with carbobond for analysis of permanent gases; and the second with MXT-5 for analysis of high boiling components. Separated gases are transferred to mass spectrometer for mass spectrometric analysis.

Cooperation: Main partners of the Gas Analytic Package team are:
IKI RAS (Russia),
GEOKHI RAS (Russia),
LATMOS and LISA, University of Paris (France),
Max Planck Ins. for Solar System Res. (Germany)
Polytechnic University of Hong Kong (China)

COMPLEX OF SCIENTIFIC EQUIPMENT FOR ATTESTATION OF THE PLACE OF LANDING ON PHOBOS FOR THE SPACECRAFT "FOBOS-GRUNT"

E.M.Galimov[1], M.Ya. Marov[1], L.P.Moskaleva[1], A.G.Dunchenko[1], V.V.Visochkin[1], O.B.Khavroshkin[2], *[1]Vernadsky Institute of Geochemistry and Analytical Chemistry Russian Academy of Sciences, Kosygin Street, 19, 119991, Moscow, Russian Federation. Contact: geokhi.ras@relcom.ru, [2]Schmidt Institute of Physics of the Earth, Moscow D-242, B. Gruzinskaya str., 10, 123995. Contact: direction@ifz.ru*

In 2011, in accordance with Federal space program of Russia, there will be performed launching of FOBOS-GRUNT spacecraft.

The main task of this project is collecting and bringing to Earth from Fobos the samples of its soil. The studies of soil samples will permit to throw light on the process of formation of planets. This is first of all important for understanding of an early history of Earth, including beginning of life on Earth and this will permit to clear up the structure and composition of substance from which planets were formed. If Mars, Earth and Moon were smelted, differentiated and changed by secondary processes, then Fobos, as an "undercollected" material of Mars, is unique one for understanding of mechanism of planet formation.

At present, V.I. Vernadsky Institute developed, manufactured and delivered to Lavochkin Association a complex of scientific equipment for landing of spacecraft on Phobos attestation:

• **gamma-spectrometer FOGS** intended for determination of concentration of natural radioactive and main soil-forming elements: hydrogen, carbon, oxygen, magnesium, aluminum, silicon, potassium, calcium, titanium, manganese, iron, thorium and uranium in the soil layer with thickness of 1-2 meters in the place of landing of spacecraft.

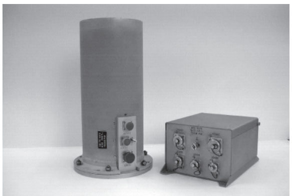

Fig.1: Gamma-spectrometer FOGS

The technical characteristics are present in Tabl.1.

That is measured	Gamma-ray energy, Thermal neutron flux
Range of measurements	Gamma-ray energy: 0,3 MeV - 9,0 MeV, Neutrons up to 0,4 eV
Resolution	1-2 wt.% for the maine rock forming elements
Mass of the instruments	5,4 kg

• **detector of space dust METEOR-F** intended for determination of density of meteor flow near Mars, for receiving of data about physic-dynamic properties of meteor particles, belonged to dusty cover of Mars, for evaluation of meteor danger for flights of spacecrafts.

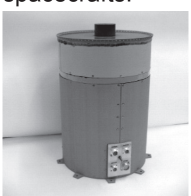

Fig.2: Detector of space dust METEOR-F

The technical characteristics are present in Tabl.2.

Mass of the instrument	3,5 kg
That is measured	Mass and velocity of the meteoric particles
Range of measurements	Velocity from 2 to 35km/s Mass from 10-14 to 10-5 g
Resolution	Mass– 30% Velocity: 10% - interval 3-10 km/s 30%- interval 11-35 km/s

• mass-spectrometer MAL-1 intended for investigation of composition of gaseous components of the soil in the region of landing. There are common works together with Ryazan State Radio-technical Academy.

Fig.3: Mass-spectrometer MAL-1

The technical characteristics are present in Tabl.3

Mass of the instrument	3,6 kg
That is measured	The mass of gas ions taken out of the Phobos' soil
Range of measurements	1 до 400 a.m.u.
Resolution	Better 1 a.m.u.

• **thermo-detector THERMOFOB** intended for thermo-physical measurements in the surface layer of Fobos soil in the place of landing of spacecraft. There are common works together with Institute of Applied Mathematics of Russian Academy of Science.

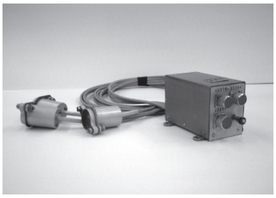

Fig.4: Thermo-detector THERMOFOB

The technical characteristics are present in Tabl.4.

Mass of the instrument	0,3 kg
That is measured	Soil temperature
Range of measurements	100 - 380 K
Resolution	0,25 of degree

• **seismometer SEISMO-1** intended for receiving of seismic data (seismograms) and recording of seismic noise data for solving of following fundamental and applied tasks: origin and internal structure of Fobos, gaseous-dust flows near Mars, structure and density of regolith, its mechanical properties. There are common works together with Physics of Earth Institute of Russian Academy of Science.

The are present the photos of scientific equipments, physical characteristics of the instruments, the physical scheme/method of measurements.

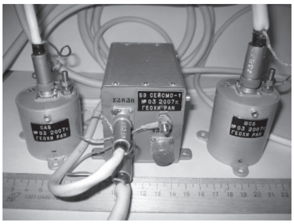

Fig.5: Seismometer SEISMO-1

The technical characteristics are present in Tabl.5.

Mass of the instrument	0,75 kg
That is measured	Acceleration, velocity, displacement
Range of measurements	No less than 100 db, $10^{-7} \div 10^{-12}$ m
Resolution	10%

Staff of the Vernadsky Institute, namely A.B.Andreenkov, V.V.Ivanov, A.S.Korotkov, A.G.Mityugov, V.I.Pogonin, V.I.Serbin participated directly in developing, manufacturing and testing of scientific equipment. Staff of the Vernadsky Institute, namely G.G.Smirnov, L.P.Tatsy, V.P.Kharyukova participated directly in developing design plans and specification, and technical documentation.

SEISMOLOGY OF PHOBOS: FROM GEOPHYSICS TO COSMOGONY

O. B. Khavroshkin, V. V. Tsyplakov, *Schmidt Institute of Physics of the Earth, Russian Academy of Sciences, Bol'shaya Gruzinskaya ul. 10, Moscow, 123995 Russia*

Abstract: Several of the most fundamental and feasible geophysical problems partially related to the Phobos Grunt mission have been analyzed based on the available works. The assumed results will form the informational basis for the development of the cosmogony of planets' small satellites and asteroids. Correspondingly, the aims of the experiment are to study the internal structure and energy state of Phobos; to analyze the manifestation of pulsed effects and fields, including the registration of seismic signals and wave fields of Phobos;and to measure the long_period oscillations on the surface of Phobos in the range of 10–5–10 Hz. Studying Phobos gives an example of specific problems peculiar to small bodies of the Solar System: specific features of cratering, grooves, and morphological structures. The registration of gas–dust streams extends the knowledge of the space–time structure of the Solar System and its objects and processes and will confirm that stellar systems can constantly interact. The physical principles of the registration of seismic fields and signals are briefly described, and the instrumental basis for cosmogonic seismology is comparatively presented. It has been indicated that the piezoelectric and electrodynamic systems of the desired signal registration complete each other, and it is desirable to use both systems if 2_ and 3_D registration systems are applied. The seismometric instrumentation of the Phobos spacecraft has been considered. The device's physical characteristics, block diagrams, energy consumption, and information content are presented. The seismoacoustic (HF) device unit and its advantages during the registration of very weak signals owing to the use of the mechanical transformer effect are described in more detail. The seismic system created can ensure the solution of the scientific problems of the mission to Phobos, including the study of the internal structure, origin, depth structures, and external impacts of the field, corpuscular, and micrometeorite types.

STUDY OF BASIC GEOCHEMICAL PROPERTIES OF PHOBOS REGOLITH USING LASER ABLATION TOF MASS-REFLECTRON

G.G. Managadze[1], P. Wurtz [2], R. Z. Sagdeev[1], A.E. Chumikov[1], M. Tulei[2], M. Yakovlevna[2], N.G. Managadze[1], A. L. Bondarenko[1], *[1]Space Research Institute, Russian Academy of Sciences, Russia, [2]Bern University, Switzerland, Contact: managa@bk.ru*

We analyze the features of LASMA onboard instrument meant to measure the isotopic and elemental composition of Phobos regolith via laser time-of-flight mass spectrometry. These measurements may confirm the hypothesis that Phobos material is the primordial substance with a composition close to that of carbonaceous chondrites, i.e., the substance from which the Earth formed. The results of measurements may also confirm the mechanism of anomalous absorption of Phobos regolith proposed in this paper. The elemental composition of regolith determined by our instrument may provide information about the conditions of the formation, origin, evolution, and age of Phobos.

We describe the research tasks of individual experiments and how to address them;

describe in detail the onboard instrument and the principle of its operation, as well as its analytical and technical data and design features. We also describe the most important functional units of the instrument, the procedure of the reduction of scientific data and its transmission to the Earth.

It is important that the mass spectra reported in the paper were obtained with onboard instruments during their laboratory tests and while choosing their operation mode.

We show the LASMA instrument to be the first version of a new-generation novel instrument developed at the Space Research Institute of the Russian Academy of Sciences and patented in Russia.

DETERMINATION OF THE SURFACE-AVERAGED COMPOSITION OF PHOBOS REGOLITH FROM SECONDARY ION FLUX MEASUREMENTS IN THE MANAGA-P EXPERIMENT OF THE “PHOBOS-GRUNT”

G.G. Managadze[1], R. Z. Sagdeev[1], A. E. Chumikov[1], V. T. Cherepin[2], G.Z. Saralidze[1], *[1]Space Research Institute, Russian Academy of Sciences, Russia, [2]Institute for Metal Physics, National Academy of Sciences of Ukraine, Ukraine, Contact: managa@bk.ru*

We describe the MANAGA-F onboard time-of-flight mass-reflectron meant for the measurement of the elemental and isotopic composition of the flux of secondary ions generated by the solar wind. We show that this instrument can be used to determine the composition of the surface layer of Phobos regolith averaged over a rather large area while the probe approaches the satellite. After the landing of the space probe lands on the surface of Phobos measurements will be conducted to study the local properties of regolith and the new mechanism of the synthesis of water in ion-impact processes. The instrument can reveal secondary molecular ions including organic ions produced as a result of various kinds of ion bombardment of the regolith.

We analyze the main research tasks to be addressed using this instrument. We describe the principle of operation of the instrument, its analytical and technical data, and design features. We also explain the range of its application for addressing a number of topical problems of modern science.

We show that MANAGA-F instrument is the first realization of a new-generation novel instrument invented, developed, and made at the Space Research Institute of the Russian Academy of Sciences.

SEISMO-GRAVIMETER "GRAS-F" FOR MEASUREMENT VARIATIONS OF THE GRAVITATIONAL AND INERTIAL FIELDS ON SURFACE OF THE FOBOS

Manukin A.B., Andreev O.N., Gorshkov A.N., Shlik A.F., *Space Research Institute, Russian Academy of Sciences, Profsoyuznaya ul. 84/32, Moscow, 117997 Russia*

In article problems of measurement of variations gravitational and inertial fields on the Fobos are considered, caused librational oscillations, tidal effects and seismic influences. It is shown that thermal equilibrium noise in mechanical oscillator, being a gage basis, define its limiting sensitivity at level of 8×10^{-9} m./s^2. Real sensitivity developed three-coordinate seismo-gravimeter which estimation is received by results of calibration, makes ~ 2×10^{-8} m/s^2 that allows to measure expected variations of a gravitational field and to receive the information on level of seismic noise with the resolution on amplitude of oscillations of a surface at level from $2{,}5\times10^{-7}$м on frequencies of 0,1 Hz to 10^{-10}м on frequencies more than 5 Hz.

LIBRATION CELESTIAL MECHANICS EXPERIMENT

O. N. Andreev, S. A. Antonenko, V. M. Gotlib, G. V. Zakharkin, V. M. Linkin, A. N. Lipatov, V. S. Makarov, B. K. Khairulin, and L. I. Khlyustova, *Space Research Institute, Russian Academy of Sciences, Profsoyuznaya ul. 84/32, Moscow, 117997 Russia*

Abstract: The exploration of planet moons and minor bodies (Avduevskii et al., 1996) is a basic task for comprehending the nature of the processes occurring in our Solar System. Knowing the current state of the moons, we can better describe their past and look into the future. This knowledge is important, first of all, for understanding the origin of the Solar System. Interest in the Martian moon Phobos has been displayed during recent decades. The interest is caused by some questions to which there have been no answers up until now (Sagdeev et al., 1988; 1989). For example, there is a question regarding the origin of the moon: whether it is an asteroid captured by Mars' gravitational field or it is an accumulated body in the Martian orbit. In connection with this, it is interesting to conduct studies aimed at answering this question. If Phobos appears to be an asteroid, then investigations regarding the chemical and isotopic compositions of the moon as the primary matter of the Solar System as well as its evolution are of great interest. As of today, we know that Phobos orbits 9400 km from the center of Mars, with the speed of its revolution being so great that it makes one revolution every one third of a Martian day (7 h 39 min), outrunning the daily spin of Mars. The strong tidal friction occurring due to the Phobos' position close to Mars reduces the energy of its motion. The moon is slowly approaching the planet's surface and will make impact with it eventually (this should happen over the course of 100 million years) if by that time Mars' gravitational field does not tear it to pieces (this should happen over the course of 50 million years). Phobos is an elongated body with dimensions of 27 × 22× 18.6 km. The measurements of the spectral characteristics performed during the Phobos_2 mission (Ksanformality, Moroz, 1995) have indicated that the reflection spectra of Phobos and Deimos differ substantially from those obtained in observations of Mars, as well as from the spectra of carbonaceous chondrites and other asteroid analogs. The latest scientific results demonstrate that the Martian moons most likely belong to class D asteroids, although the analogy is not perfect. The results of measuring the reflection characteristics display no bound water on the surface of the Martian moons. However, there are estimations, according to which the thermodynamic conditions on these moons are such that water may stay at a certain depth. Clarifying the issue regarding the presence of water (or hydrated molecules) on Phobos is very important not only from the scientific standpoint, but also from the practical one. Phobos is subject to a strong tidal effect by Mars; therefore, it always keeps the same side turned towards Mars. In connection with this, one of the most interesting characteristics of Phobos is libration. Phobos is a very amazing object among the known synchronously orbiting moons of the planets of the Solar System because it has a large amplitude of libration. The libration effect is always present in a several-bodies system.

TELEVISION SYSTEM FOR NAVIGATION AND OBSERVATION

G. A. Avanesov, A.A. Forsh, R. V. Gordeev, V. A. Grishin, E. V. Kolomeets, E. B. Krasnopevtseva, A. A. Krupin, M. I. Kudelin, V. M. Murav'ev, B. S. Zhukov, S. B. Zhukov, *Space Research Institute, 117997, 84/32 Profsoyuznaya Str, Moscow, Russia*

Introduction: The principal objective of the Phobos-Grunt mission is landing on Phobos and bringing back to the Earth samples of its soil. An important role in the project will be played by Television System for Navigation and Observation (TSNN) that will support the s/c orbital maneuvers as well as the landing on Phobos. It will also provide valuable information for scientific investigations of Phobos and its environment.

Scientific and navigational objectives of Phobos imaging:

The objectives of Phobos imaging can be summarised as follows:

Scientific investigations:

- high-resolution horizontal and vertical structure of craters and grooves,
- local photometry and regolith characteristics,
- center of mass location and density distribution inside Phobos,
- Phobos dust ring.

Orbital navigation tasks:

- imaging of Phobos and Mars to refine the parameters of the Phobos and s/c orbits,
- landing area selection.

Autonomous landing support:

- measuring the s/c altitude and horizontal velocity,
- autonomous landing site selection.

TSNN characteristics: TSNN includes two narrow-angle (NAC) and two wide-angle (WAC) cameras that are be located on the opposite sides of the s/c. The TSNN cameras are shown in Fig.1 and their principal characteristics are given in Table.1.

Table 1. Characteristics of TSNN cameras

Parameters	NAC	WAC
Focal length, mm	500	18
Relative aperture	1:7	1:2
Spectral band, µm	0.4-1.1	0.4-1.1
CCD element size, µm	7.4	7.4
Number of active CCD elements	1000 × 1000	1000 × 1000
Angular resolution, arc sec	3.05	84.8
Field of view, deg	0.85	23.3
Quantization, bits	10	10
Mass, kg	2.8	1.6
Power consumption, W	8	8
Number of sensors	2	2

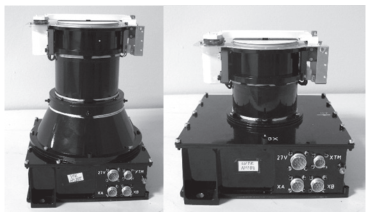

Fig.1: TSNN cameras: NAC (left) and WAC (right)

Orbital imaging: The resolution and the field of view of the TSNN cameras during Phobos imaging from the circular observation and quasi-synchronous (KSO) orbits are given in Table 2. At the observation orbit, the WAC will allow an initial capture of Phobos in its field of view during the navigation imaging, while the NAC resolution during the encounters with Phobos at 500 km will be comparable with the resolution of the best available images of Phobos.

Table 2. Resolution and field of view of the TSNN cameras during orbital imaging of Phobos

	NAC	WAC
Circular observation orbit (500 - 20000 km):		
resolution	7.5 - 300 m	200 - 8000 m
field of view	7.5 - 300 km	200 - 8000 km
KSO-orbit (30 -100 km):		
resolution	0.45 - 1.5 m	12 - 40 m
field of view	0.45 - 1.5 km	12 - 40 km

At KSO the NAC resolution of up to 0.45 m will be significantly better than the resolution of the currently available images of Phobos, while the WAC will allow referencing of high-resolution NAC images to the existing maps and digital models of Phobos. Apart from high-resolution cartography, these images will be used for landing area assessment and selection.

However, it can hardly be expected that it will be possible to find a sufficiently large landing area with the size corresponding to the scattering of the landing point (~1 km), which would be free from dangerous craters and grooves. Thus, the final landing site selection should be based on autonomous TSNN image processing during the descent.

TSNN operations during the landing: The landing on Phobos will start from a distance of ~30 km targeting at the center of the landing area selected on ground. During the descent images of Phobos will be taken by all four TSNN cameras. Up to 48 full-resolution images will be stored in the camera memories and transmitted to the Earth after the landing. About 25 images with a reduced resolution will be transmitted to the Earth in real time. The resolution and the field of view of the TSNN cameras during the landing are given in Table 3. Close to the surface the images will be smeared by defocusing.

Table 3. Resolution and field of view of the TSNN cameras during the landing

Altitude	NAC		WAC	
	Resolution	Field of view	Resolution	Field of view
30 km	52 cm	450 m	12 m	12 km
10 km	22 cm	150 m	4.1 m	4.1 km
3 km	12 cm	45 m	1.2 m	1.2 km
1 km	8.6 cm	15 m	42 cm	410 m
300 m	7.6 cm	4.5 m	13 cm	120 m
100 m	7.3 cm	1.5 m	5.0 cm	41 m
30 m	-	-	2.1 cm	12 m
10 m	-	-	1.3 cm	4.1 m

Apart from imaging, real-time processing of WAC data will allow autonomous landing site selection as well as estimation of s/c attitude and horizontal velocity to back up the corresponding LVV and DISD measurements.

S/c attitude will be estimated from the parallax measurements of 10 reference points in stereo images obtained by WAC cameras at a basis of 1.66 m. A reference point is characterized in terms of Hadamard transform coefficients that are transferred to the second camera and used to find the best match. The matching is performed using a hierarchical algorithm. The attitude measurement accuracy will be improving from ~7% at the distance of 300 m to within 1% at distances smaller than 30 m.

The s/c horizontal velocity can be estimated by measuring the displacement of a reference point in the consecutive images obtained by the same WAC camera. The displacement measurement algorithm is similar to the one used for the stereo measurements, however the processing is performed over a factor of 4 degraded image and only one reference point is traced in order to save the computation time. Image displacements due to variations in s/c attitude and image scale are corrected by the s/c computer. A sufficient accuracy of the horizontal velocity measurements is achieved already at the altitude of 1 km and is further improving while approaching the surface.

Table 4. WAC altitude and horizontal velocity measurement errors

Altitude, m	Altitude error, m	Horizontal velo-city error, cm/s
1000	210	28
300	20	8.4
100	2.5	2.9
30	0.32	1.0
10	0.07	0.4

Autonomous selection of a landing site will be performed by WAC starting from an altitude of 300-500 m, where the WAC resolution will reach 0.13-0.2 m. For this purpose, WAC will generate a 'landing suitability map', which will be used by the on-board computer to estimate the suitability of the surface around the forecasted landing point and in case it appears unsuitable to direct the s/c to the optimal landing site. The suitability map will be constructed by estimating the homogeneity of WAC images within moving windows. The homogeneity criterion is chosen to be a combination of statistical measures (relative radiance dispersion) to characterize the entire window and of radiance thresholding to exclude shadows, sky and strong non-homogeneities within the window. The non-homogeneity of the adjacent windows is also accounted for with a reduced weight. The window size is adjusted in the process of descending to keep the size of its projection on the surface close to 10 m until the s/c reaches the altitude of 100 m and then it will be gradually decreasing. The image resolution will also be gradually degraded during the descent to compensate the effects of fine regolith texture on image homogeneity. Fig.2 illustrates the optimal landing site selection in a test image.

The duration of the WAC imaging and image processing cycle during the landing is 6 s.

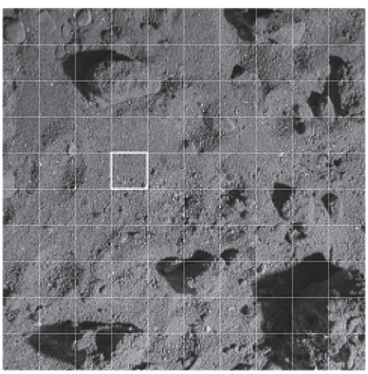

Fig.2:. Selection of the optimal landing site in a test image

SYSTEM FOR THE SCIENTIFIC PAYLOAD INFORMATION SUPPORT OF THE “PHOBOS-GRUNT” MISSION

V.Yu. Belov, T.Yu. Drozdova, I.Yu. Katasonov, M.I. Kudelin, V.M. Muraviov, A.A. Forsch, *Space Research Institute of the Russian Academy of Sciences, 84/32, Profsoyuznaya ul., Moscow, 117819, Russia e-mail: tatyana@nserv.iki.rssi.ru*

Abstract: Results of developing the “System for the Scientific Payload Information Support”, designed to control the data exchange flows (commands, scientific and telemetry data, onboard time code) between the onboard control system and the scientific payload of the Phobos-Grunt s/c. The problems solved by the System on board are described. The System functional diagram and destination of its modules are given.

To solve the variety of tasks of scientific space missions a large number of scientific instruments performing various experiments should be installed onboard any interplanetary s/c. These devices typically differ from each other for not only their functional purpose, but also the data, control, and telemetry interfaces.

For each mission the developers solve the problem of integrating such diverse in their interface characteristics scientific instruments in a single complex. This integration simplifies testing of the spacecraft hardware resources and reduces its duration. This provides an opportunity to work in parallel with the two functionally independent complexes: housekeeping systems and scientific instruments. This problem solution is to create a special instrument, which plays the role of an intellectual interface between the s/c command&control, information, telemetry systems, and the payload scientific instruments.

Development of a device or a system used to control scientific instruments being different in their functionality and purpose, as well as to obtain from them information transmitted via digital communication channels with these scientific instruments - is an independent task in designing s/c systems and instruments for scientific projects.

Within the framework of the “Phobos-Grunt” mission the both scientific payload and data storage control is fulfilled by the System for the Scientific Payload Information Support (SIOK). SIOK is a dubbed computer with an extended non-volatile memory and the two backup information and control interfaces in accordance with GOST R 52070-2003 (MILSTD-1553V).

Appearance of the SIOK flight model is shown in Fig. 1.

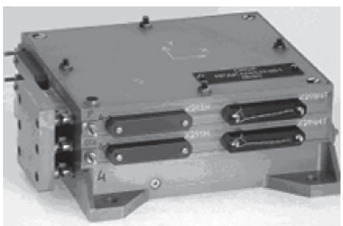

Fig.1 System for the Scientific Payload Information Support (SIOK)

SIOK receives and stores digital commands and onboard time code from the s/c onboard control system via data bus (s/c backbone serial interface). On this bus SIOK serves as the terminal device and the s/c control system – as the bus controller. SIOK transmits digital command controlling scientific instruments and onboard time code through the internal communication bus between SIOK and the scientific instrumentation (backbone serial interface of the scientific payload). On the data bus with scientific instruments SIOK serves as bus controller, and scientific instruments – as terminals.

SIOK also collects and stores in nonvolatile memory data received from s/c scientific instrumentation. This information SIOK stores up to receiving the request from the onboard control system. Then the control system transmits this data to a radio complex for broadcast to Earth.

By now three SIOK flight models has been manufactured and delivered to the customer.

MANIPULATOR COMPLEX OF THE PHOBOS-GRUNT SPACECRAFT

O. E. Kozlov, T. O. Kozlova, *Space Research Institute, Russian Academy of Sciences, Profsoyuznaya ul. 84/32, Moscow, 117997 Russia.*
Contact: o-kozlov@yandex.ru

The Phobos-Grunt automatic interplanetary station is designed for the delivery of samples of the soil of Phobos to the Earth and for an onboard examination of the physical and chemical characteristics of the soil. For solving scientific problems, on the Phobos-Grunt station a Manipulator complex is mounted whose main task is to take soil samples from the surface of Phobos and place them into a container to be returned to the Earth and into the soil collectors of scientific instruments (Fig.1).

The manipulator complex perform the following functions:

- to take samples of the regolith and consolidated fragments from the surface of Phobos;
- to transfer the taken samples into the container of the descent vehicle designed for their delivery to the Earth;
- to provide the instruments of the scientific apparatus complex with soil samples;
- to install the sensor unit of the Mossbauer spectrometer on the soil of Phobos;
- to support the guidance of the panoramic camera for taking a panoramic image of the surface of Phobos and for monitoring the sampling.

The Manipulator complex includes a manipulator, sampling device, Mossbauer spectrometer, panoramic camera, and a MikrOmega microscope.

The Sampling device (Fig.2) is mounted on the rotary platform of the manipulator. The manipulator is a two-link four-DOF mechanism rigidly fastened to the flying module bracket whose terminal link is the rotary platform where, in addition to the Sampling device, the panoramic camera and sensor unit of the Mossbauer spectrometer are installed.

Four DOFs are provided by four drives, which allow the manipulator to turn by the azimuth within the area allocated by the general configuration. The surface that can be explored by the manipulator is a 150° sector of a circle with a center at the manipulator's fastening point; it is confined by the manipulator length of about 900 mm. In the transport state, the manipulator is folded and fastened to the spacecraft at two points with the help of brackets and a system of pyrotechnic pins.

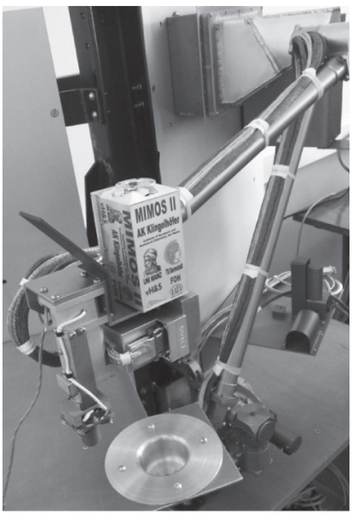

Fig.1: Manipulator complex.

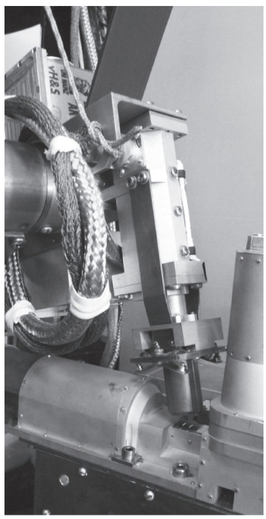

Fig.2: Sampling device.

PHPMS EXPERIMENT: PHOBOS PLASMA MAGNETIC SYSTEM ONBOARD THE PHOBOS SOIL MISSION

A.A.Skalsky[1],S.Barabash[2], K.Anufreychik[1], I.Chulkov[1], A.Grigoriev[1], I.Dobrovolsky[1], M.Emanuelsson[2], V.Korepanov[3], G Koynash[1], O.Vaisberg[1], P.Moiseev[1], *[1]Space Research Institute, Moscow, Russian Federatio, Contact: skalsky@iki.rssi.ru, [2]Swedish Institute of Space Physics, Kiruna, Sweden, [3]Lvov Center of Space Research Institute, Lvov, Ukraine*

Introduction: The PhPMS (Phobos: Plasma Magnetic System) experiment flown onboard the Phobos Soil spacecraft is aimed to investigate the solar wind –Mars interaction and physical processes resulting from the interaction of the Phobos-moon regolith with solar wind flow. It consists of:

- plasma (ion) sensors DI and DIM carrying out measurement of solar wind and planetary ions at energies between 1eV-15eV;
- magnetic field search coil and fluxgate sensors carrying out measurement of quasistatic field in a range of ±300nT and AC field at frequencies below 10KHz.

The DPU of PhPMS governs the sensor operations, onboard data preprocessing and their further handling. The experiment is developed in cooperation between institutes from Russia, Sweden and Ukraine.

SYSTEM OF TECHNICAL VISION OF THE MANIPULATOR COMPLEX SC «PHOBOS-SOIL»

A. Bondarenko[1], I. Dokuchaev[1], V. Kottsov[2], I. Sytenko[2], JP.Bibring[3], JJ Fourmond[3], *[1]Rastr Texnolodgy ltd, Russie, [2]Space Research Institute, Russie, [3]Institute Astrophisic Spatial, France*

Introduction: One of primary goals of "Fobos-grunt" mission is ground sampling in a place of landing and sample returning to the Earth, also samples are to be analysed by means of scientific devices onboard. The important role in all these tasks is taken away to system of technical vision of the manipulator complex. Vision the major source of the information about the world surrounding us. Images give representation about characteristic of observable object, its placing, interaction with an environment, optical (physical) properties.

Structure STV CM « Fobos-grunt » spacecraft includes a number of TV devices which carry out different functions:

The panoramic camera - is placed on last section of the manipulator. Panoramic camera - 12,4 mm, 70°. It is intended to control of a ground fence, shooting panoramas of Fobos surface and space vehicle.

The stereocamera consist of two television cameras (basis – 80 mm), which are placed on the case of the electronics block. It is intended for reception a spatial picture of a surface in front of the device, analysis of morphological characteristics, creation a digital model of the landing site and definition spatial coordinates of interesting objects for manipulator management.

The microscope-spectrometer, is placed on the manipulator basis. It is intended for detailed studying of ground samples microstructure. Reflective properties of ground samples are observed under different monochromatic illumination. Five groups of light-emitting diodes provide illumination in following parts of spectrum: 505 nm, 600 nm, 670 nm, 750 nm, 880 nm.

In infra-red range tunable acoustooptic filter is used to select monochromatic light from lamp emission.

LIULIN – F INSTRUMENT FOR RADIATION MONITORING DURING THE FLIGHT OF INTERPLANETARY PROBE PHOBOS – SOIL

Semkova J.[1], Maltchev S.[1], Tomov B.[1], Matviichuk Yu.[1], Dachev Ts.[1], Koleva R.[1], Benghin V. V.[2], Chernykh I.V.[2], Shurshakov V.A.[2], Petrov V.M.[2], Khamidullina N.M.[3], *[1]Space and Solar-Terrestrial Influences Institute, Bulgarian Academy of Sciences, Sofia, Bulgaria, jsemkova@stil.bas.bg, [2]Institute of Biomedical Problems, Russian Academy of Sciences, Moscow, Russia, benghin@pike.net.ru, [3]Lavochkin Association, Federal Space Agency, Russia, nmx@laspace.ru*

The main goal of the Liulin-Phobos experiment is the investigation of the radiation environment and doses in the heliosphere at distances of 1 to 1.5 AU from the Sun and in the near-Mars space. Measurements are planned during the cruise phase, on Mars orbit and on the surface of Phobos.

This research will be very important for assessment of radiation risk to the crewmembers of future exploratory flights including the Mars mission and can be used for evaluation of the radiation doses received by spacecraft components.

The Liulin – F instrument was developed for performing of these investigations. It permits to measure both the absorbed dose rate and the spectroscopic parameters of the radiation field along the flight trajectory. The instrument's detector is substantially the semiconductor telescope.

Liulin - F particle telescope will be mounted on the Descent Module of Phobos – Sample spacecraft.

It consists of two dosimetric telescopes - D1&D2, and D3&D4 arranged at two perpendicular directions. One of the detectors in every telescope measures the energy deposition spectrum in the range 0.1-10 MeV, and the other in the range 0.3 -70 MeV.

Every pair of telescopes consists of two 300 μm thick, 20x10 mm area Si PIN photodiodes, operating in coincidence mode to obtain Linear Energy Transfer (LET). The distance between the parallel detectors of every telescope is 28 mm. The entire package has a mass of 0.5 kg and consumes 1.4 W. The telemetry data rate is 250 kB/day.

The parameters featured by Liulin-F are:

- Absorbed dose rate in the range 0.04x10-6Gy/h - 0.1 Gy/h;
- Particle flux in the range 0 - 10^4 (cm^2/sec);
- Energy deposition spectra in the range 0.1-70 MeV;
- LET spectrum (in H_2O) in range 0.5–120 keV/μm;

Performance characteristics:

Construction – mono-block .

Dimensions – 172×114×45 mm,

Presently instrument was manufactured, tested and supplied for installing on the spacecraft.

EVALUATION OF PARAMETRS LAYERED GROUND ON MEASUREMENTS OF LONG WAVE ORBITER RADAR

V. M. Smirnov, O. V. Yushkova and V.N. Marchuk, *Fryazino Branch of the Institution of Russian Academy of Sciences Kotel'nikov Institute of Radio Engineering and Electronics of RAS, Fryazino, Russia. Contact: o.v.y@mail.ru*

The radar-tracking sounding of a space body surface by the orbital long-wave radar allows to estimate reflective ground properties as a whole and to reveal presence large subsurface inhomogeneities of the ground. The considerable contribution to practice a space subsurface radar-location was brought by researches of Mars surface by radar MARSIS («Mars-express») and SHARAD («Mars Reconnaissance Orbiter»). Both radar use signals with linear frequency modulation:

- MARSIS works in four frequency ranges with the central frequencies 1,8; 3; 4 and 5 MHz. Width of an impulse of 1 MHz [1];
- SHARAD – the central frequency – 20 MHz, width - 10 MHz [2].

On the difference of delay time of signals reflected from the surface and the internal borders, using a method of the optimum filtering, by the European and American colleagues have been constructed radarogramm extended layered formations. The traditional technique of processing of the reflected signals does not allow to evaluate parameters of the ground dielectric permeability and to specify ionosphere influence on the characteristics of reflected signal. For definition of these parameters the analysis of amplitude and a phase of accepted signals is required.

In the report results of modeling process of the MARSIS signals reflection taking into account their passage through ionosphere are presented at various zenith angles of the Sun. On the basis of the analysis of modeling results the following methods were developed:

- correction method of ionosphere influences on parameters of the reflected signal [3];
- method of the express analysis of the reflected signals for detection of reflection from subsurface borders, based on analysis of frequency dependence of reflection coefficient [4].

The square of the module of frequency dependence of reflection coefficient is used for restoration of dielectric parameters and a thickness of a reflecting layer [5].

The developed methods are approved at the analysis of the MARSIS radar signals received for a trace 1855, passed over polar areas of the Mars. The results of data processing for this trace are shown on figure: a) –Russian team, b) – ISA/JPL team

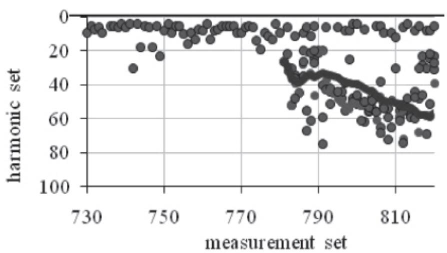

a)

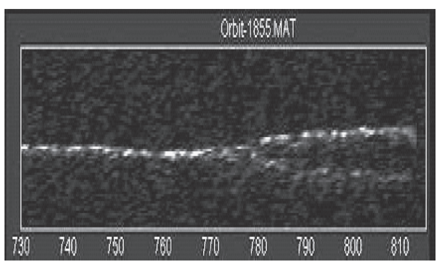

b)

References: 1. Picardi, G. Mars advanced radar for subsurface and ionosphere sounding (MARSIS)/ Picardi, G., Sorage S., Seu R., Fedele, Federico C., Orosei R. / Technical report N MNS-001/005/99,21/05/1999.

2. R. Croci et al. "SHARAD Design and Operation" / IGARSS 2007 Proceedings, Barcelona, 2007.

3. Кибардина И.Н., Юшкова О.В., Смирнов В.М., Марчук В.Н. Численное моделирование при интерпретации результатов радиолокационного зондирования грунта планет / Сборник статей «Фундаментальные космические исследования, 2009», Болгария, С.223-227.

4. Armand N. A., Smirnov V.M., Yushkova O.V. Method of Definition of Parameters Layered Ground on Measurements of Radiowave Reflection Coeffcient, Progress In Electromagnetics Research Symposium, August 18-21, 2009 Moscow, Russia, C.533

5. Yushkova O. V. Journal of communications technology and electronics / Vol. 55, No. 1, 2010, pp.35-39

CHOMIK SAMPLING DEVICE FOR RUSSIAN PHOBOS SAMPLE RETURN MISSION

J. Grygorczuk[1], K. Seweryn[1], H. Rickman[1], M. Morawski[1], S.N. Aleksashkin[3], M. Banaszkiewicz[1], M. Ciesielska[1], M. Dobrowolski[1], M. Drogosz[1], J. Gurgurewicz[1,4], O. E. Kozlov[2], T.O. Kozlova[2], M. Krolikowska-Soltan[1], E. Słaby[4], S. E. Sutugin[3], R. Wawrzaszek[1], L. Wisniewski[1], A.V. Zakharov[2], *[1]Space Research Centre, Polish Academy of Sciences, 18a Bartycka St., 00-716, Warsaw, Poland, [2]Russian Space Research Institute, Russian Academy of Sciences, 84/32 Profsoyuznaya St., 117997, Moscow, Russia, [3]Lavochkin Association, 24 Leningrad Hwy, Khimki-2, 141400, Moscow Region, Russia, [4]Institute of Geological Sciences, Polish Academy of Sciences, Twarda 51/55 00-818, Warsaw, Poland*

Measurements of physical properties of planetary bodies allow to determine many important parameters for scientists working in different fields of research. For example effective heat conductivity of the regolith can help with better understanding of processes occurring in the body interior. Chemical and mineralogical composition gives us a chance to better understand the origin and evolution of the moons. In principle such parameters of the planetary bodies can be determined based on three different measurement techniques: (i) in situ measurements (ii) measurements of the samples in laboratory conditions at the Earth and (iii) remote sensing measurements. Scientific missions which allow us to perform all type of measurements, give us a chance for not only parameters determination but also cross calibration of the instruments.

Russian Phobos Sample Return (PhSR) mission is one of few which allows for all type of such measurements. The spacecraft will be equipped with remote sensing instruments like: spectrometers, long wave radar and dust counter, instruments for in-situ measurements – gas-chromatograph, seismometer, thermodetector and others and also robotic arm and sampling device. PhSR mission will be launched in November 2011 on board of a launch vehicle Zenit. About a year later (11 months) the vehicle will reach the Martian orbit. It is anticipated that it will land on Phobos in the beginning of 2013. A take off back will take place a month later and the re-entry module containing a capsule that will hold the soil sample enclosed in a container will be on its way back to Earth. The 11 kg re-entry capsule with the container will land in Kazakhstan in mid-2014.

A unique geological penetrator CHOMIK dedicated for the Phobos Sample Return space mission will be designed and manufactured at the Space Mechatronics and Robotics Laboratory, Space Research Centre Polish Academy of Sciences (SRC PAS) in Warsaw. Functionally CHOMIK is based on the well known MUPUS instrument developed for Rosetta mission to the 67 P/Churyumov- Gerasimenko comet. One of the most important goals of the mission is to collect a soil sample from Phobos, Mars' moon, and deliver it to Earth. The sample will be collected from the surface of the satellite by the Polish penetrator and deposited in a container that is going to land in 2014 in Kazakhstan encased in the Russian re-entry capsule. The CHOMIK instrument is one of three instrument on the lander designated to collect sample from Phobos ground, specially design for sampling the stony surface. Apart from sampling the penetrator will perform thermal and mechanical measurements of Phobos' regolith. All these goals play an important role in the future exploration plans of the space bodies.

The work presented in the paper is focused on the presentation of CHOMIK instrument capabilities, scientific goals of the experiment and results from functional tests.

TRAJECTORY OF YH-1 AND MROE WITH PHOBOS-GRUNT FOR 2011 LAUNCH WINDOW

J.H. Zheng, X. Wu, *Center for Space Science and Applied Research, P.O. Box 8701, Beijing, P.R. of China. Contact: zhengjianhua@cssar.ac.cn*

Introduction: In 2011, Russia will launch the Phobos-Grunt Mission with the launcher of Zenit-2. YH-1 will fly to the Mars together with the Phobos-Grunt spacecraft. After 11 months flight, the joint spacecrafts will be captured by Mars. After 10 days flight in a big eclipse martian orbit, YH-1 will be separated from the Phobos-Grunt spacecraft and continue to fly in the martian orbit for one year. YH-1will explore the space environment of Mars and conduct the joint measurement with the Phobos-Grunt spacecraft.

In this presentation, the possible trajectory of YH-1 will be designed. The features of the martian orbit is also analysed. For example, the time for YH-1 to access ground stations, the time for YH-1 to fly in the shadow of Mars, the Doppler frequency shift for YH-1 relative to ground stations, etc.

Moreover, the Phobos-Grunt spacecraft will do the Mars radio occultation experimentation (MROE) with YH-1 in some orbit phases after YH-1 is separated from the Phobos-Grunt spacecraft. I would like show the possible chances for YH-1 to do the MROE with the Phobos-Grunt spacecraft. I also hope to talk about the experiment flow of MORE between two sides.

OVERVIEW OF SCIENTIFIC PAYLOADS SYSTEM OF CHINA-RUSSIA JOINT MARS EXPLORATION PROGRAM YH-1

SUN Yueqiang, DU Qifei, ZHANG Aibin,WANG Jingdong, GUO Wei, WU Ji, ZHU Guangwu, ZHAO Hua, WANG Chi, WANG Shijing, LI Lei, HU Xiong, *Center for Space Science and Applied Research, Chinese Academy of Sciences, Beijing, 100190*

Introduction: YH-1 is the first Chinese Mars exploration program collaborated with Russia. It is a micro-satellite mission focused on investigating the Martian space environment and the solar wind Mars interaction. YH-1 and Phobos-Grunt forms a two-point measurement configuration in the Martian space environment. FGM and Plasma package payloads Equipped on YH-1 will give coordinated measurement opportunities around Mars. MROE receiver equipped on YH-1 will receive radio signals from Phobos-Grunt making sc-sc occultation measurement of Martian ionosphere, particularly on the subsolar/middle night sides which cannot be done with s/c to Earth occultation measurement. In this presentation, the scientific objectives of YH-1 Payloads are reviewed, the scientific payloads and test results on the ground are also briefly described.

DUAL SPACECRAFT OBSERVATION OF THE MARTIAN PLASMA ENVIRONMENT

L. Li, Y. T. Zhang, H. Zhao, J. D. Wang, B. Zhou, *Center for Space Science Applied Research, The Chinese Academy of Sciences, China. Contact: lil@cssar.ac.cn*

Abstract: The Sino-Russian Joint Mars-Phobos Exploration program provides unique opportunity to investigate the global structure of the solar wind/Mars interaction region. Both spacecrafts in the program, Phobos-Grunt and YH-1, will carry plasma and magnetic field instruments aimed at monitoring the plasma environment of the planet. As the spacecrafts fly in different regions around the planet, there will be chances for dual space craft simultaneous investigation of solar wind- Mars interaction, by phenomena such as bow shock, MPB, and ion escape in the tail. Details about the program and related instrumentation are presented in the paper, while scientific topics of dual spacecraft observation are discussed as well.

YH1-PHOBOS GRUNT MARTIAN IONOSPHERE RADIO OCCULTATION EXPERIMENTAL RESEARCH

X. Hu, X. Wu, X. Gong, Q. Xu, J. Liu, Y. Sun, J. Wu, C. Wang, H. Zhao, *Center for Space Science and Applied Research, Chinese Academy of Sciences, China. Contact: xhu@cssar.ac.cn*

Abstract: The Martian YingHuo-1 Orbiter Radio Occultation experiments will be conducted (i) to firstly sound the martian ionosphere for deriving vertical ionospheric electron density profiles with their zenith angles greater than about 136 degree or less than about 44 degree, which have never be explored before with RO, (ii) to sound the neutral martian atmosphere to derive vertical density, pressure and temperature profiles.

The radio carrier links between the YH-1 and Phobos-Grunt (called satellite-satellite) and the links between the YH-1 orbiter and the Earth deep space stations (called satellite-ground) will be used for these investigations as depicted in Fig 1. For the sat-sat RO experiments, simultaneous and coherent dual-frequency links at 400 MHz and 800 MHz via the transmitter onboard the Phobos-Grunt and the receiver onboard the YH-1 will permit separation of contributions from the classic geometry effects and the dispersive media effects caused by the geometry between YH-1 and Phobos-Grunt and the propagation of the signals through the dispersive media, respectively. Unlike the sat-ground RO, the sat-sat RO will allow to explore the martian ionospheric electron density profiles with zenith angles greater than about 136 degree or less than about 44 degree.

For sat-ground RO, the single-frequency downlink at X-band (8.4 GHz) via the High Gain Antenna onboard the YH-1 will permit separation of contributions from the classical Doppler shift and the media effects caused by the motion of the spacecraft with respect to the Earth and the propagation of the signals through the media, respectively.

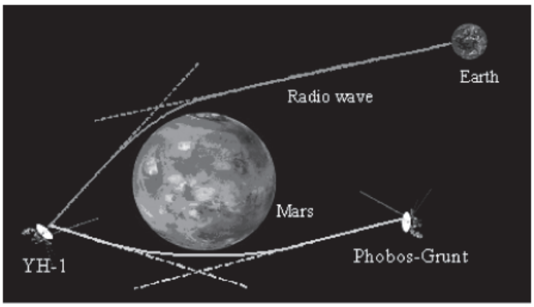

Fig. 1: Diagram of the YH-1 RO experiments

The investigation relies on the observation of the phase and amplitude of radio signals. The radio signals are affected by the medium through which they propagate (atmospheres, ionospheres, interplanetary medium, solar corona), and by the performances of the various systems aboard the spacecrafts and on Earth.

The two kinds of RO experiments will allow us to investigate further the martian ionosphere and neutral atmosphere, especially the night side ionosphere.

Acknowledgment: Thanks to the funding from Innovation project from Chinese Academy of Sciences and support from the Sino-Russian Joint Martian exploring project.

LUNAR PHYSICAL LIBRATION IN THE ILOM PROJECT (JAPAN): SIMULATING OF STAR TRACKS

N. Petrova[1,2], H. Hanada[3], T.Abdulmyanov[2], Nizamova G.[2], *[1]Kazan State University,18 Kremlevskaya str., [2]Kazan, Russia, Kazan Power Engineering University, Russia, [3]National Astronomical Observatory of Japan, Mizusawa, Ja-pan. Contact: nk_petrova@mail.ru*

Introduction: In the frame of the second stage of the Japanese space mission SELENE II [1] the placing of the tele-scope on the Lunar surface is planned, which is sup-posed to provide accuracy of 1 ms of arc for position detection of the star position on the CCD array. In situ Lunar Orientation Measurement (ILOM) [1] is an experiment to measure the Lunar physical libra-tions in situ on the Moon with a small telescope which tracks stars. Conditions of observations and parameters of the telescope will allow determining parameters of the Lunar physical libration with the accuracy, which was inaccessible nor from the ground based observations, nor from LLR.

Presented report describes simulating process of receiving “observed” selenographical polar distance of a star and “observed” time of its transition of the prime lunar meridian. We found the method which al-lows determining of libration angles in the node Iσ and in inclination ρ with certain accuracy. It’s shown that libra-tion in longitude τ cannot be determined from observation of polar stars, because polar distance of a star is not sensi-tive to longitudinal oscillation of a Lunar body.

Main stages of simulating: 1. The project ILOM proposes that polar distance will be measured for every star crossing lunar prime meridian. Stars were taken from various stellar cata-logues, such as the UCAC2-BSS, Hipparcos, Tycho and FK6. Stellar coordinates α_0, δ_0 were reduced from ICRF system to the ecliptical one λ, β at the epoch of observation [2]. Principal axes of inertia were taken as a frame for selenography system coor-dinates (Fig. 1) [3]. Reduction of the ecliptical coor-dinates to the selenography one (δ, α) were done using analytical theory of the physical libration. [6].

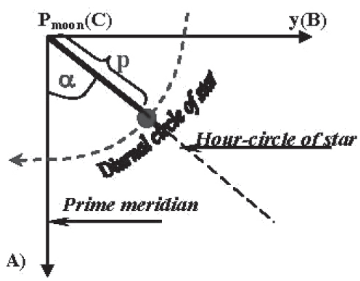

Fig. 1: Selenography coordinates of a star near the lunar pole.

2. From the observation we can measure polar distance of a star $p = \pi/2 - \delta$. We consider an ideal model, where the star is observed exactly in the prime meridian. In this case the selenography lati-tude $\alpha = 0$, and, as a consequence, $\cos\delta = p$.

3. As a result, in the system (1) the vector(p, $\sqrt{1-p^2}$, 0,)T — is a vector of observations.Us-ing it we need to find unknown values of libra-tion angles at the moment of observation *t*.

4. The Jacobian of the reduction equation system as appeared to be close to zero. As a result, the derived system is ill-posed. For described case we have found one of optimization methods – gradient method [5].

To start the iteration procedure we use as initial solu-tion the data, calculated by analytical theory of physical libration [4], [6]. We simulated observation error and followed its influence on the libration an-gles. At the Fig. 2 we can see that the errors in polar distance causes the same error in and. At the same time value of is independ-ent on polar distance and cannot be determined from polar stars.

Conclusion: We have found a suitable instru-ment for solution of “inverse problem” in the physi-cal libration of the Moon: if we can measure the po-lar distance of a star with a high accuracy, then we can obtain libration angles in ρ and in Iσ at the mo-ment of observation with the same accuracy. To im-prove accuracy of observations we suggest to meas-ure a polar distance of a star several time before and after crossing the prime meridian. Our simulating is done only for the case when error in time of merid-ian transition is equal to zero. The next stage of our simulating should study this kind of errors in obser-vation.:

Research is supported by the grant RFFI-JSPS 09-02-92113, (2009-2010)

References: [1] Hanada H., Noda H., Kikuchi F. et al., 2009. Proc of Astrokazan-2009, Kazan, Russia. p. 172-175
[2] Petrova N., Hanada H., Akutina M. (2009) EPSC, 2009, Potsdam. Berlin, Germany – EPSC2009-490, 2p.
[3] Petrova N.,Gusev.,KawanoN., Handa H. 2008. Ad-vances in Space Res., v 42, p. 1398-1404.
[4] Petrova N., Hanada H., 2010. EGU Assembly 2010, Vienna, Austria, 2010, vol 12., EGU2010-7054 , 2p.
[5] Demidovich B., Maron I, 2006. Basis of numerical mathematics, - the Book (in Russian) – 672p.
[6] *Petrova N., BarkinYu., Gusev A. and Ivanova T.,* 2010. Development of analytical theory, EGU Assembly 2010, Vienna, Austria, 2010, vol 12., EGU2010-12534 , 2p.

OPTICAL SOLAR SENSOR

T. Yu. Drozdova, Ye.V. Zaretskaya, M.I. Kudelin, A.V. Nikitin, A.A Forsh, *Space Research Institute of the Russian Academy of Sciences, 84/32, Profsoyuznaya ul., Moscow, 117819, Russia e-mail: tatyana@nserv.iki.rssi.ru*

Abstract: The optical solar sensor (OSD) as well as its destination, main characteristics and output data are presented. The instrument's functional design is briefly described. The optical solar sensor's software is considered.

Optico-electronic devices for attitude control by the Sun are the integral part of s/c motion control systems. The Sun is the most powerful source of radiant energy of the Solar System.

The static CCD-based optical solar sensor (OSD) with a CCD-line as a photosensitive element has been developed at the Optico-Physical department of the Space Research Institute. OSD is destined for determining parameters of direction towards the Sun in the instrument coordinate system. Optical solar sensor fixed on the transportation slab is shown in Fig 1.

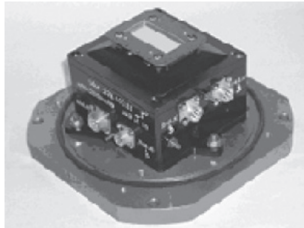

Fig. 1: Optical solar sensor

Technical characteristics of the optical solar sensor

Field of view, deg in the plane XOZ in the plane YOZ	 -60 – +60 -31 – +31
Ultimate total error of determining direction towards the Sun is less than (3σ), arcmin for the SC angular velocity less than 0.1°/s, stabilization angular velocity less than 0,0050/s,angular acceleration less than 0,060/s2 for the SC angular velocity less than 2.0°/s, stabilization angular velocity less than 0,20/s,angular acceleration less than 0,40/s2	 3 5
Mass, g	640
Dimensions, mm	120x112x72,5
Power consumption. W	3
Adapter operation temperature, °C	-10 – +45
Ambient pressure range, mercury	10-9 – 800
Lifetime, years	15

The OSD functional design consists of three modules:

1. Photoreceiver
2. Processor
3. Secondary power source.

Photoreceiver consists of coding mask (slit diaphragm) and linear CCD.

OSD operation is based on registering signal generating by CCD after the light having passed through the slit diaphragm falls on it.

The coordinates of vector of direction to the Sun are determined in the OSD internal coordinate system by the light strokes position on CCD. Then the obtained parameters are recalculated for the sensor's adapter coordinate system. This data is transferred to the onboard control system.

OSD operation is controlled by commands received from / transmitted to the onboard computer via data interface MIL-STD1553B. The sensor is switched on/off by the command from the computer. After switching on OSD is testing its hardware and outputs data about readiness for operation. Optical measurements are conducted after the command from a computer also. CCD analog signals are digitized at the 8-digit ADC and sent to processor. The calculations are fulfilled with the sensor's software developed at our department also.

Flight tests of four OSD were successfully fulfilled in 2008. Seven OSD (two engineering models, four flight models and one spare model) have been manufactured and delivered to the customer within the framework of the "Phobos-Grunt" mission.